

**MECHANISMS UNDERLYING THE METABOLIC AND  
VASODILATOR EFFECTS OF INSULIN**

By

**ANN ELIZABETH STRIDE**

A thesis submitted to the University of Birmingham for the degree of Doctor of  
Philosophy

School of Clinical and Experimental Medicine

The Medical School

University of Birmingham

Birmingham

B15 2TT

September 2012

UNIVERSITY OF  
BIRMINGHAM

**University of Birmingham Research Archive**

**e-theses repository**

This unpublished thesis/dissertation is copyright of the author and/or third parties. The intellectual property rights of the author or third parties in respect of this work are as defined by The Copyright Designs and Patents Act 1988 or as modified by any successor legislation.

Any use made of information contained in this thesis/dissertation must be in accordance with that legislation and must be properly acknowledged. Further distribution or reproduction in any format is prohibited without the permission of the copyright holder.

## **ABSTRACT**

Insulin causes uptake of glucose into cells and also causes increases in skeletal muscle blood flow by vasodilatation. In order for insulin to act at receptors on the skeletal muscle membrane, it must move through the capillary endothelium. In conditions associated with insulin resistance, insulin-induced glucose uptake and vasodilatation are often blunted and disordered transport across endothelium has been suggested.

Firstly, studies were conducted using the hyperinsulinaemic euglycaemic (HE) clamp in rats to assess the relationship between insulin-induced muscle vasodilatation and glucose uptake into skeletal muscle. Insulin-induced vasodilatation was abolished by nitric oxide (NO) synthase inhibition in Wistar rats, implicating NO. Nutritional status and hence availability of glucose also affected vasodilatation in Wistar rats, leading to the proposal that vasodilatation was linked to glucose metabolism.

Vasodilator response to insulin was significantly higher in lean versus obese Zucker rats. Nicotinic acid (NAc) did not decrease plasma FFA concentrations versus HE clamp, nevertheless, vasodilator response and glucose uptake were enhanced in lean and obese rats by some mechanism other than lowering FFA.

Optimisation of the microdialysis technique allowed measurement, for the first time, of interstitial insulin concentrations in lean and obese Zucker rats and showed a significant difference under basal conditions.

## ACKNOWLEDGMENTS

I would like to thank the following people for their contribution to the work presented in this thesis.

Ruth Macdonald whose guidance and support was fundamental to my completion of this thesis. I am extremely grateful.

Janice Marshall for her expert assistance in scientific writing, the discussion of scientific ideas and for dedicating so much time to my work in the last few years. Simon Poucher for his intellectual input, guidance, encouragement and patience. Anton Wagenmakers for discussions about the microvasculature and the opportunities for collaborations.

AstraZeneca and the BBSRC for financial support.

Janice's group for useful discussions throughout my studies. Clare Ray for the hours spent providing me with a sound knowledge of *in vivo* surgery and teaching me the importance of being organized during experimentation. Andy Coney for assistance with all things technical. Dave Hauton, Stuart Egginton, Prem Kumar and other staff from the Link Labs for guidance and interest in my work. BMSU staff for looking after my animals during my time in Birmingham. Anton's Group and Christopher Shaw for teaching me immunohistochemistry.

The IPG group at AstraZeneca, particularly Carina Ämmälä, Sue Loxham, Sue Birtles and Lorraine Gregory for helping me to learn a different way of working. The Analytical Group, Usha Chauhan, Gemma Convey and Dan Owen for assistance with the analysis of biological samples; special thanks to Julie Cook whose interest and expert knowledge was vital to my development of the chemical assays used in this thesis. AS & W staff 'Bertie' Burton, Kirsty Binnington, Dianne Tibbs, Bill Brown and Lisa Doar for their support during animal studies.

Gillian Douglas of Keith Channon's Group at the University of Oxford for HPLC analysis of tissue samples.

Will Rook, Fahima Syeda, Rumel Ahmed and Andy Holmes for sharing experiences and making me smile. Members of the BRAT club for friendship and escapism.

My family, whose continued support, interest and belief in me made it all worthwhile.

## LIST OF ABSTRACTS

### Posters

STRIDE, A. E., RAY, C. J., POUCHER, S. M., MARSHALL, J. M. 2009. Development of a model to investigate the relationship between endothelial dysfunction and insulin resistance in rats. Young Physiologists' Symposium, Dublin.

STRIDE, A. E., MACDONALD, R., WAGENMAKERS, A. J., MARSHALL, J. M., POUCHER, S. M. 2012. Effect of acute nicotinic acid treatment on insulin induced vasodilatation. *Diabetic Medicine*, 29 (Supp. 1), 54.

STRIDE, A. E., MACDONALD, R., COOK, J. D., WAGENMAKERS, A. J., MARSHALL, J. M., POUCHER, S. M. 2012. Effect of chronic tetrahydrobiopterin treatment on insulin access to the muscle interstitial fluid in obese Zucker rats. *Diabetes*, 61 (Supp. 1), A418.

### Oral communications

STRIDE, A. E., RAY, C. J., MACDONALD, R., WAGENMAKERS, A. J., POUCHER, S. M., MARSHALL J. M. 2010. Insulin increases hindlimb blood flow more in fed than in fasted Wistar rats. University of Manchester (2010) *Proc Physiol Soc* 19, C76.

STRIDE, A. E., RAY, C. J., MACDONALD, R., WAGENMAKERS, A. J., POUCHER, S. M., MARSHALL J. M. 2010. Insulin increases hindlimb blood flow more in fed than in fasted Wistar rats. Young Physiologists' Symposium, Manchester.

## TABLE OF CONTENTS

<b>CHAPTER 1 - GENERAL INTRODUCTION .....</b>	<b>1</b>
Over view .....	1
1.1 Metabolic effects of insulin .....	2
1.2 Diabetes.....	10
1.3 Animal models of diabetes.....	12
1.4 Methods of investigating action of insulin.....	14
1.5 Insulin-induced vasodilatation .....	18
1.6 Insulin-induced vasoconstriction.....	38
1.7 The endothelium as a barrier .....	40
1.8 Microdialysis.....	44
1.9 Mechanism of TET.....	45
1.10 Endothelial dysfunction .....	48
1.11 Aims.....	49
 <b>CHAPTER 2 - EFFECT OF INHIBITING NITRIC OXIDE SYNTHASE ON INSULIN- INDUCED VASODILATATION DURING HYPERINSULINAEMIC EUGLYCAEMIC CLAMP.....</b>	 <b>51</b>
2.1 Introduction .....	51
2.2 Methods.....	52
2.3 Results.....	59
2.4 Discussion.....	69
 <b>CHAPTER 3 - EFFECT OF NUTRITIONAL STATUS ON INSULIN-INDUCED VASODILATATION DURING HYPERINSULINAEMIC EUGLYCAEMIC CLAMP .</b>	 <b>85</b>
3.1 Introduction .....	85
3.2 Methods .....	87

3.3 Results.....	90
3.4 Discussion.....	100
 <b>Chapter 4 - Effect of acute nicotinic acid treatment on insulin induced</b>	
<b>vasodilatation.....</b>	<b>108</b>
4.1 Introduction.....	108
4.2 Methods.....	111
4.3 Results.....	121
4.4 Discussion.....	139
 <b>Chapter 5 - REFINEMENT OF THE MICRODIALYSIS METHOD.....</b>	
5.1 Introduction.....	149
5.2 Methods and Results.....	160
5.3 Discussion.....	201
 <b>Chapter 6 - Effect of chronic tetrahydrobiopterin treatment on insulin</b>	
<b>access to the muscle interstitial fluid in obese Zucker rats.....</b>	<b>207</b>
6.1 Introduction.....	207
6.2 Methods.....	212
6.3 Results.....	226
6.4 Discussion.....	249
 <b>Chapter 7 – General Discussion.....</b>	
References.....	274

## LIST OF FIGURES

Figure 1.1 Schematic showing gluconeogenesis. ....	5
Figure 1.2 Insulin receptor signaling involved in GLUT4 recruitment. ....	9
Figure 1.3 Worldwide prevalence of type 2 diabetes. ....	12
Figure 1.4 Insulin action at different levels of the arterial tree. ....	19
Figure 1.5 Insulin exposure versus per centage change in blood flow. ....	24
Figure 1.6 Insulin receptor signaling and control of vascular tone. ....	28
Figure 1.7 Graphical representation of the three compartment model .....	42
Figure 2.1 Representation of experimental protocol. ....	58
Figure 2.2 Effect of hyperinsulinaemic euglycaemic clamp (control) with or without L-NAME treatment on mean arterial blood pressure and heart rate. ....	64
Figure 2.3 Effect of hyperinsulinaemic euglycaemic clamp (control) with or without L-NAME treatment on change in femoral blood flow and femoral vascular conductance. ....	65
Figure 2.4 Effect of hyperinsulinaemic euglycaemic clamp (control) with or without L-NAME treatment on blood glucose and glucose infusion rate. .....	67
Figure 2.5 Effect of hyperinsulinaemic euglycaemic clamp on haematocrit, potassium and lactate. ....	68
Figure 3.1 Effect of hyperinsulinaemic euglycaemic clamp in fed and fasted animals on mean arterial blood pressure and heart rate. ....	95



<b>Figure 3.2 Change in femoral blood flow and femoral vascular conductance evoked by hyperinsulinaemic euglycaemic clamp in fed and fasted rats.</b>	<b>96</b>
<b>Figure 3.3 Effect of hyperinsulinaemic euglycaemic clamp in fed and fasted animals on integral of FBF.</b>	<b>97</b>
<b>Figure 3.4 Maximal change in femoral vascular conductance plotted against blood glucose concentration for fasted animals.</b>	<b>98</b>
<b>Figure 3.5 Effect of hyperinsulinaemic euglycaemic clamp in fed and fasted animals on blood glucose and glucose infusion rate.</b>	<b>99</b>
<b>Figure 4.1 Schematic diagram of the HE clamp experimental protocol.</b>	<b>114</b>
<b>Figure 4.2 Mean arterial blood pressure for lean and obese Zucker rats during hyperinsulinaemic euglycaemic clamp under different experimental conditions.</b>	<b>128</b>
<b>Figure 4.3 Heart rate for lean and obese Zucker rats during hyperinsulinaemic euglycaemic clamp under different experimental conditions.</b>	<b>130</b>
<b>Figure 4.4 Femoral vascular conductance (FVC) for lean and obese Zucker rats during hyperinsulinaemic euglycaemic clamp under different experimental conditions.</b>	<b>132</b>
<b>Figure 4.5 Effect of hyperinsulinaemic euglycaemic clamp with or without nicotinic acid on blood glucose in lean and obese Zucker rats.</b>	<b>133</b>
<b>Figure 4.6 Glucose infusion rate for lean and obese Zucker rats during hyperinsulinaemic euglycaemic clamp with or without nicotinic acid treatment.</b>	<b>134</b>

Figure 4.7 Rate of initiation of glucose uptake for lean and obese Zucker rats during hyperinsulinaemic euglycaemic clamp with or without nicotinic acid treatment. ....	135
Figure 4.8 Insulin data for lean and obese Zucker rats during hyperinsulinaemic euglycaemic clamp under different experimental conditions. ....	136
Figure 4.9 Insulin sensitivity of lean and obese Zucker rats exposed to hyperinsulinaemic euglycaemic clamp with or without nicotinic acid treatment. ....	137
Figure 4.10 Non-esterified fatty acid data for lean and obese Zucker rats during hyperinsulinaemic euglycaemic clamp under different experimental conditions. ....	138
Figure 5.1 Diagram of microdialysis probe insertion into tissue. ....	174
Figure 5.2 Schematic of protocol for Section 5.2.8. ....	175
Figure 5.3 FED analysis of <i>in vitro</i> recovery of insulin. ....	188
Figure 5.4 Initial inulin analysis using the Waugh method. ....	189
Figure 5.5 Adjustment of the standard curve used in the Waugh method. ....	190
Figure 5.6 Increased number of replicates using the Waugh method. ....	191
Figure 5.7 Additional spin steps added to the Waugh method. ....	192
Figure 5.8 Analysis of <i>in vivo</i> samples with the improved Waugh method. ....	193
Figure 5.9 Kinetics of inulin infusion <i>in vivo</i> . ....	194
Figure 5.10 Microdilaysis of inulin <i>in vivo</i> . ....	195
Figure 5.11 Inulin ELISA with provided BioPAL inulin and Inutest. ....	196

Figure 5.12 Comparison of 55 and 100 kDa cut-off probes <i>in vivo</i> .....	197
Figure 5.13 Reproducibility of standard curves of human insulin spikes in rat plasma.....	198
Figure 5.14 Protocol used for the measurement of insulin with microdialysis during hyperinsulinaemic-euglycaemic clamp. ....	200
Figure 6.1 Schematic representation of the hyperinsulinaemic euglycaemic clamp protocol.....	215
Figure 6.2 Mean arterial blood pressure and heart rate for lean and obese Zucker rats during hyperinsulinaemic euglycaemic clamp with microdialysis. ....	233
Figure 6.3 Blood glucose and glucose infusion rate for lean and obese Zucker rats during hyperinsulinaemic euglycaemic clamp with microdialysis. ....	234
Figure 6.4 Plasma and interstitial insulin concentrations for lean and obese Zucker rats during hyperinsulinaemic euglycaemic clamp with microdialysis. ....	235
Figure 6.5 Insulin sensitivity for lean and obese Zucker rats during hyperinsulinaemic euglycaemic clamp with microdialysis. ....	236
Figure 6.6 Mean arterial blood pressure and heart rate for lean and obese Zucker rats with or without BH <sub>4</sub> treatment during hyperinsulinaemic euglycaemic clamp. ....	237
Figure 6.7 Blood glucose and glucose infusion rate for lean and obese Zucker rats with or without BH <sub>4</sub> treatment during hyperinsulinaemic euglycaemic clamp. ....	238

<b>Figure 6.8 Plasma insulin and insulin sensitivity for lean and obese Zucker rats with or without BH<sub>4</sub> treatment during hyperinsulinaemic euglycaemic clamp. ....</b>	<b>239</b>
<b>Figure 6.9 Femoral vascular conductance for lean and obese Zucker rats with or without BH<sub>4</sub> treatment during hyperinsulinaemic euglycaemic clamp.....</b>	<b>241</b>
<b>Figure 6.10 BH<sub>4</sub> concentrations and BH<sub>4</sub>: BH<sub>2</sub> + B ratio in plasma and aorta samples from lean and obese rats with or without BH<sub>4</sub> treatment following HE clamp.....</b>	<b>242</b>
<b>Figure 6.11 BH<sub>4</sub> concentrations and BH<sub>4</sub>: BH<sub>2</sub> + B ratio in plasma and aorta samples from lean and obese rats with or without BH<sub>4</sub> treatment. ...</b>	<b>243</b>
<b>Figure 6.12 Mean arterial blood pressure and heart rate for lean and obese Zucker rats during hyperinsulinaemic euglycaemic clamp with microdialysis. ....</b>	<b>244</b>
<b>Figure 6.13 Blood glucose and glucose infusion rate for lean and obese Zucker rats during hyperinsulinaemic euglycaemic clamp with microdialysis. ....</b>	<b>245</b>
<b>Figure 6.14 Plasma insulin concentrations for lean and obese Zucker rats during hyperinsulinaemic euglycaemic clamp with microdialysis....</b>	<b>246</b>
<b>Figure 6.15 Interstitial insulin concentrations for lean and obese Zucker rats during hyperinsulinaemic euglycaemic clamp with microdialysis .....</b>	<b>247</b>
<b>Figure 6.16 Insulin sensitivity for lean and obese Zucker rats during hyperinsulinaemic euglycaemic clamp with microdialysis. ....</b>	<b>248</b>

<b>Figure 7.1 Proposed influence of insulin at different levels of the vascular</b>	
<b>tree.....</b>	<b>270</b>

## LIST OF TABLES

<b>Table 1.1 Animal models of type 2 diabetes.....</b>	<b>13</b>
<b>Table 2.1 Baseline values for femoral blood flow, femoral vascular conductance, blood pressure and heart rate.....</b>	<b>63</b>
<b>Table 2.2 Shows basal blood glucose concentrations for all experimental animals. ....</b>	<b>66</b>
<b>Table 3.1 Baseline values for blood pressure, heart rate, femoral blood flow, femoral vascular conductance, blood glucose and steady state glucose infusion rate.....</b>	<b>94</b>
<b>Table 4.1 Animal weights and group numbers.....</b>	<b>122</b>
<b>Table 4.2 Raw data with significance symbols for mean arterial blood pressure for lean and obese Zucker rats during hyperinsulinaemic euglycaemic clamp under different experimental conditions. ....</b>	<b>129</b>
<b>Table 4.3 Raw data with significance symbols for heart rate for lean and obese Zucker rats during hyperinsulinaemic euglycaemic clamp under different experimental conditions.....</b>	<b>131</b>
<b>Table 5.1 <i>In vitro</i> recoveries for insulin and inulin. ....</b>	<b>199</b>
<b>Table 6.1 BH<sub>4</sub> concentration in drinking water at 0, 18, 24 and 48 hours after the solution had been prepared. ....</b>	<b>240</b>

## ABBREVIATIONS

ABP	arterial blood pressure
ACh	acetylcholine
ANOVA	analysis of variance
BG	blood glucose
cAMP	cyclic adenosine monophosphate
CEU	contrast enhanced ultrasound
cGMP	cyclic guanine monophosphate
ECE	endothelin converting enzyme
EDL	extensor digitorum longus
eNOS	endothelial nitric oxide synthase
ET-1	endothelin-1
FBF	femoral blood flow
FFA	free fatty acid
FVC	femoral vascular conductance
G6P	glucose-6-phosphate
GIR	glucose infusion rate
Hct	haematocrit
HE	hyperinsulinaemic euglycaemic
HR	heart rate
IRS-1	insulin receptor substrate-1
IRS-2	insulin receptor substrate-2
ISF	interstitial fluid
L-NAME	nitro-L-arginine methyl ester
L-NMMA	NG-monomethyl-L-arginine
MABP	mean arterial blood pressure
MFBF	mean femoral blood flow
MSNA	muscle sympathetic nervous activity
NEFA	non-esterified fatty acid
NO	nitric oxide
NOS	nitric oxide synthase
O <sub>2</sub> -	superoxide
OCT	optimum cutting temperature
ONOO-	peroxynitrite
P <sub>O2</sub>	partial pressure of oxygen
RR	relative recovery
SNS	sympathetic nervous system
TA	tibialis anterior
VSM	vascular smooth muscle
VSMC	vascular smooth muscle cell

## **CHAPTER 1 - GENERAL INTRODUCTION**

### **Overview**

It is well established that insulin is released in response to an increase in plasma glucose concentration and causes uptake of glucose into cells where glucose is oxidised or stored as glycogen. There is also evidence that insulin can cause vasodilatation and increase skeletal muscle blood flow, the favoured mechanism for this being increased synthesis of the vasodilator nitric oxide (NO). Further, there is evidence that insulin can increase capillary recruitment in muscle, so increasing the capillary surface area and promoting glucose uptake from the plasma. Clearly, in order for insulin to act at receptors on the skeletal muscle membrane, it must move through the capillary endothelium, a process termed trans-endothelial transport.

In conditions associated with insulin resistance such as type 2 diabetes, insulin-induced vasodilatation is often blunted and it has been suggested there is disordered trans-endothelial transport of insulin as a result of the endothelial dysfunction. However, exactly how insulin transport from the blood to the interstitium of muscle may be altered in insulin-resistant states is not understood. Neither is it clear whether interventions may be made to improve glucose uptake by muscle.



Against this background, the overall aims of the present study were to use the hyperinsulinaemic euglycaemic (HE) clamp in rats to follow the relationship between insulin-induced muscle vasodilatation and glucose uptake into skeletal muscle and to determine whether they are NO-dependent. Particular aims were to establish whether this relationship is different in the fed and fasted states, in view of the fact that nutritional status may be important in the insulin-induced vasodilatation. Nicotinic acid (NAc) can decrease plasma free fatty acid concentrations and increase insulin sensitivity. Thus, studies were also undertaken to establish whether NAc infusion alters the relationship. Since the factors that regulate trans-endothelial transport (TET) are unclear, methodology was developed to enable interstitial concentrations of insulin to be followed during HE clamp by using the technique of microdialysis.

Given the obese Zucker rat provides a useful model of Type 2 diabetes, comparable experiments were performed on Zucker obese and lean controls and experiments were undertaken to test whether chronic administration of tetrahydrobiopterin a co-factor for NO synthesis, can improve muscle vasodilatation, transport of insulin into interstitium and glucose uptake.

The discussion below therefore deals with the background to these issues.

## **1.1 Metabolic effects of insulin**

In humans, blood glucose concentration is constantly maintained between 5.5-6 mmol/L (International Diabetes Nuttall et al., 2008, International-Diabetes-Federation, 2007). The brain almost exclusively uses glucose as a fuel; therefore any decrease in blood glucose concentration would restrict the brain of energy. Increases in blood glucose concentration are also detrimental as they cause tissue damage by glycosylation of proteins and oxidative damage (Nuttall et al., 2008). Several physiological processes operate to maintain glucose homeostasis, coordinating the appearance and disappearance of glucose in the blood with hepatic glucose output and glucose uptake into peripheral tissues.

Thus following an overnight fast, blood glucose concentrations are maintained by the endogenous production of glucose from the liver and kidneys. The liver is responsible for ~80% of endogenous glucose production following an overnight fast in healthy humans (Stumvoll et al., 1997). The liver produces glucose by two processes, glycogenolysis and gluconeogenesis.

### **1.1.1 Glycogenolysis**

Glycogenolysis involves the breakdown of liver glycogen stores; glycogen is a polymer of glucose monomers so breakdown enables the release of glucose monomers into the circulation. Glycogenolysis is regulated by glycogen phosphorylase which, by addition of inorganic phosphate, cleaves one monomer from glycogen to produce glucose-1-phosphate (G1P). Glucose-6-phosphate

(G6P) is then produced from G1P and is dephosphorylated by glucose-6-phosphatase (G6Pase) to produce glucose. The liver is the only tissue to release glucose into the circulation from glycogen as G6Pase is almost exclusively found in liver cells (Van Schaftingen and Gerin, 2002).

### **1.1.2 Gluconeogenesis**

Gluconeogenesis is the formation of glucose from noncarbohydrate precursors such as lactate, pyruvate, amino acids and glycerol. For an in depth review of the process see (Nuttall et al., 2008). Briefly, gluconeogenesis begins in the mitochondria where pyruvate is converted to oxaloacetate by pyruvate carboxylase. Oxaloacetate is then reduced to malate by malate dehydrogenase. Malate can be transported into the cytoplasm where it is oxidised to oxaloacetate. Oxaloacetate is then decarboxylated and phosphorylated by phosphoenolpyruvate carboxylase to phosphoenolpyruvate. The remaining steps in gluconeogenesis are a reverse of glycolysis. Phosphoenolpyruvate is converted to fructose-1,6-bisphosphate. Fructose-1,6-bisphosphate is converted to fructose-6-phosphate by fructose-1,6-bisphosphatase which is the rate limiting step in gluconeogenesis. Fructose-6-phosphate is then converted to glucose-6-phosphate which can be used in metabolic pathways or dephosphorylated to free glucose. Glucose-6-phosphate remains within the cell, whereas free glucose can be transported out of the cell.

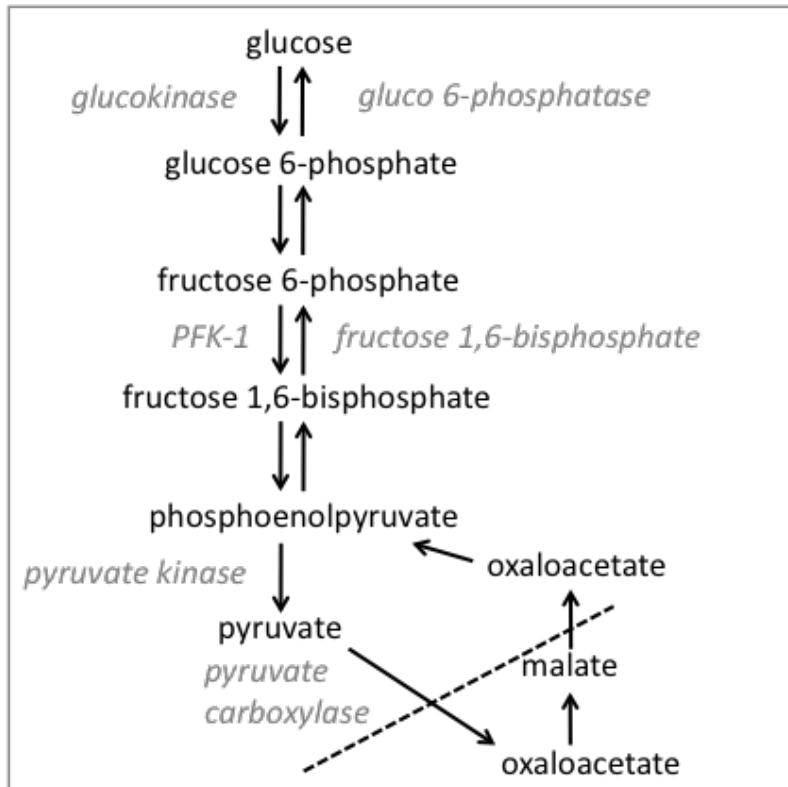


**Figure 1.1 Schematic showing gluconeogenesis.**

Schematic diagram of the processes involved in gluconeogenesis.

### 1.1.3 Hepatic glucose output

The contribution of these two processes to hepatic glucose output depends on the metabolic state. Following an overnight fast, the contribution of each is roughly 50%. Following prolonged fasting, however, the contribution of glycogenolysis is considerably less due to the depletion of liver glycogen stores; the contribution of gluconeogenesis is therefore increased (Nuttall et al., 2008). Hormones that increase hepatic glucose output are glucagon (released from the

$\alpha$  cells in the pancreatic islets of Langerhans) and cortisol (released from the adrenal gland) which are both released during short term and prolonged fasting respectively in response to a fall in plasma glucose concentration (Ruderman, 1975). In contrast, insulin, which is released from the pancreatic  $\beta$  cells plays an important role in the down regulation of hepatic glucose output. After an overnight fast, basal plasma insulin concentrations inhibit hepatic glucose output by ~50% whereas at higher physiological concentrations of insulin, such as those seen following a meal, hepatic glucose production is completely suppressed (Cherrington et al., 1978). Insulin's action on the pancreatic  $\alpha$  cells to decrease the release of glucagon also indirectly reduces hepatic glucose output. Thus, following a meal, the increase in glucose in liver cells and change in the ratio of insulin/glucagon in the blood stimulates glycogen phosphorylase and glycogen synthase, so increasing the storage of glucose as glycogen (Collier and Scott, 2004).

Following consumption of a mixed meal, glucose is released from the gut into the portal circulation, and raises blood glucose concentrations. As discussed above, many mechanisms prevent blood glucose concentrations from rising too high; in healthy individuals the peak is ~9 mmol/L. Under basal conditions most glucose uptake occurs into the brain as it requires constant delivery of glucose (Macdonald and King, 2007). However, following a mixed meal, glucose uptake into other tissues is stimulated and this decreases blood glucose concentrations and allows glucose to be stored as a source of energy. Insulin is released from pancreatic  $\beta$  cells in response to a rise in blood glucose and is able to stimulate the uptake of glucose into insulin-sensitive tissues. Its release is enhanced in

response to the release of gut peptides (incretins) following a mixed meal by them acting directly on the  $\beta$ -cell (Drucker and Nauck, 2006).

Insulin causes the uptake of glucose via glucose transporters (GLUT). GLUT4 is the predominant isoform in muscle and adipose tissue. Insulin causes the translocation of GLUT4 from intracellular stores to the plasma membrane in muscle and adipose tissue (Watson and Pessin, 2006). Under basal conditions, GLUT4 cycles back and forth from intracellular stores to the plasma membrane at a slow rate, but activation of the insulin signaling cascade within the cell as a result of insulin binding to its receptor, acts to increase the exocytosis and decrease the endocytosis of GLUT4 within the cell (Watson et al., 2004).

Following glucose uptake into cells by GLUT2 and GLUT4, in liver and muscle respectively, glucose is phosphorylated to G6P by glucokinase (GK) in the liver and hexokinase in the muscle. Depending on the energy status of the cell, G6P can be converted into glycogen by glycogen synthase or metabolized by glycolysis or oxidation (Rossetti and Giaccari, 1990).

Several molecules are thought to link insulin action to GLUT4 transport to the cell membrane. One of the key candidates is AS160, as described below. On binding to its receptor, insulin causes autophosphorylation of the transmembrane  $\beta$  subunits which results in increased tyrosine kinase activity (Bevan, 2001). This increased tyrosine kinase activity causes the tyrosine phosphorylation of insulin receptor substrate (IRS) 1 and 2. IRS1 and IRS2 are able to act as docking molecules for downstream regulators with Src homology 2

(SH2) domains. One such molecule is phosphatidylinositol 3-kinase (PI3-kinase). PI3-kinase consists of a regulatory p85 subunit and a catalytic p110 subunit. The subunit p85 allosterically regulates p110 which phosphorylates phosphatidylinositol 4,5-bisphosphate (PIP2) to produce phosphatidylinositol 3,4,5-triphosphate (PIP3). PIP3 recruits 3-phosphoinositide-dependent protein kinase-1 (PDK-1) and protein kinase-B (PKB/Akt) to the cell surface where they are able to elicit their actions. The signaling molecules downstream of PKB/Akt are able to communicate with the GLUT-4 containing compartments (see Figure 1.2).

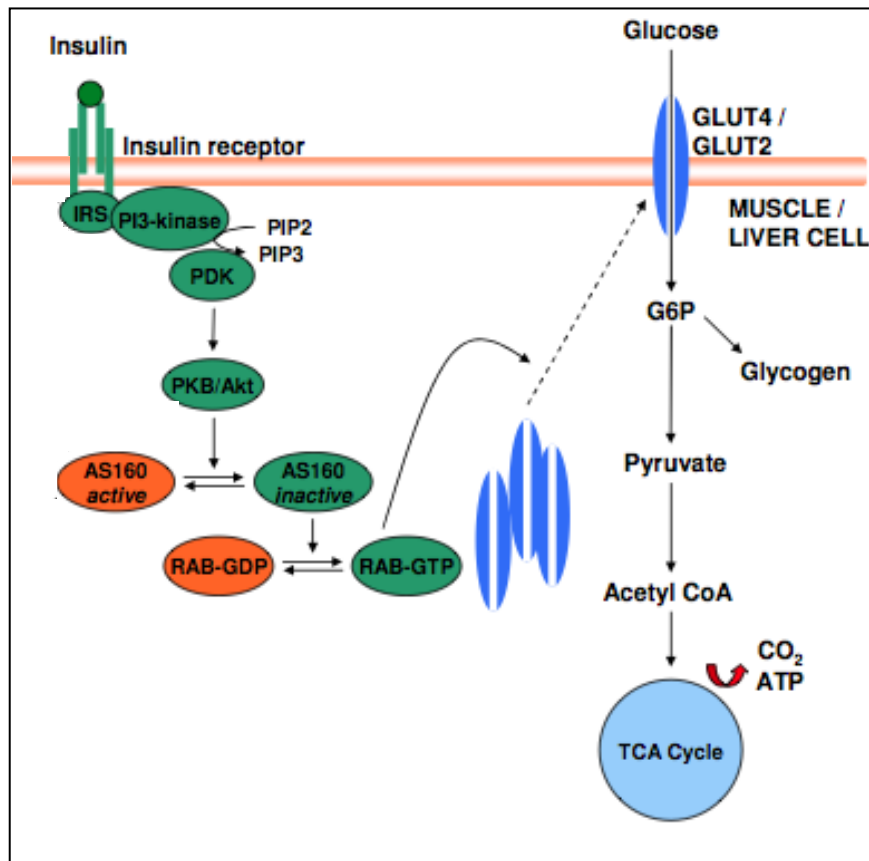


**Figure 1.2 Insulin receptor signaling involved in GLUT4 recruitment.**

Figure adapted from (Niswender and Schwartz, 2003).

Thus, as indicated above AS160 has been proposed as the link between the insulin-signalling cascade and GLUT4 translocation. AS160 contains a Rab GTPase-activating protein (GAP) domain which acts as a brake on GLUT-4 translocation; insulin stimulation relieves this inhibitory effect, resulting in GLUT4 translocation. Other processes must be involved as inhibition of the IRS-PI3-kinase pathway does not completely inhibit insulin-induced glucose uptake (Kanzaki, 2006).

On reaching the plasma membrane, the GLUT4 synaptic vesicle must dock in order to incorporate GLUT4 into the plasma membrane using SNARE proteins.



Thus, VAMP-2, the prototypical v-SNARE, on the GLUT4 vesicle membrane is able to associate with syntaxin 4, located on the plasma membrane. SNAP-23 also appears to be involved in GLUT4 docking and is associated with the plasma membrane. However removal of SNAP-23 does not inhibit GLUT4 docking but only slows it down suggesting that it is not a critical step (Foster and Klip, 2000).

## **1.2 Diabetes**

There are two main types of diabetes, type 1 and type 2. Type 1 diabetes (T1D) is an autoimmune T cell-mediated destruction of the  $\beta$  cells in the pancreatic islets of Langerhans. T1D usually has an onset of below the age of 40 and is thought to be mainly hereditary. By contrast, type 2 diabetes (T2D) has a more complex aetiology and is characterized by insulin resistance, hyperglycaemia, dyslipidaemia, hypertension, visceral obesity, high inflammatory cytokines, a prothrombotic state and changes in gene and protein expression. Insulin resistance is associated with elevated blood glucose concentrations as well as larger blood glucose excursions after a meal due to the inability of insulin to control blood glucose concentrations. Alternative names for T2D include non-insulin dependent diabetes mellitus (NIDDM) and diabetes (Shafir, 1996).

At the current time, humans have a much more sedentary lifestyle than ever before, with increases in Westernisation, industrialisation, mechanisation, computerisation and therefore an ever decreasing energetic output. In addition, there is now an increase in energy input associated with a higher availability of

fast foods, saturated fats and simple carbohydrates (Wagenmakers et al., 2006). This increase in overly rich nutrition has led to an increase in obesity, which is a key risk factor for T2D.

Thus, there is a global epidemic of diabetes. There has been an explosive increase in the past two decades in developed and developing nations alike. Diabetes is now one of the main threats to health in the 21<sup>st</sup> century, currently affecting an estimated 200 million people worldwide (International-Diabetes-Federation, 2007). It is projected that it will affect 366 million people worldwide by 2030 (see Figure 1.3; (Wild et al., 2004).

Diabetes represents a huge economic burden, costing the National Health Service around £1 billion a year, with over 5% of UK health care spending now dedicated to the diagnosis, monitoring and treatment of diabetes and associated morbidities (Department-for-Health, 2007).

As well as the insulin resistance and metabolic problems associated with diabetes, there is also significant vascular pathology. The risk of cardiovascular complications in T2D is two to four times greater than that of healthy individuals (Stumvoll et al., 2005). Major cardiovascular complications of diabetes are macrovascular and microvascular. Macrovascular complications, generally considered as hypertension, stroke, coronary artery disease and atherosclerosis, lead to cardiac insufficiency and eventually cardiac failure. Microvascular complications generally considered as retinopathy, neuropathy and nephropathy

lead to poor tissue perfusion and therefore to serious organ pathology (Klein, 1995).

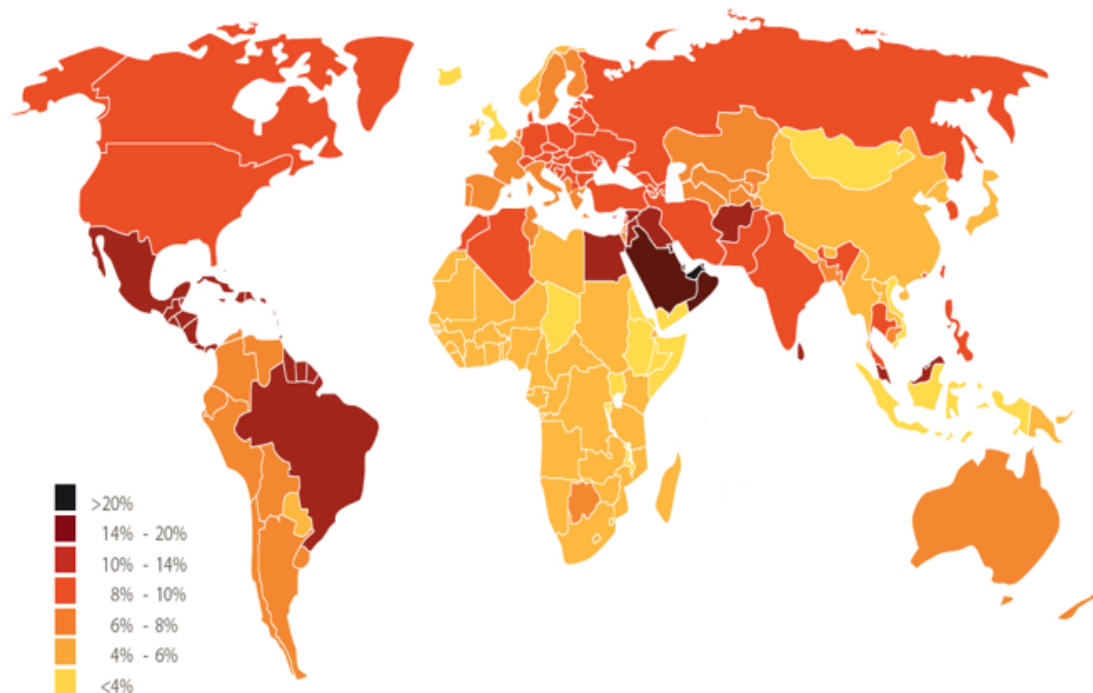


**Figure 1.3 Worldwide prevalence of type 2 diabetes.**

Figure from International Diabetes Federation 2007 (International-Diabetes-Federation, 2007).

### **1.3 Animal models of diabetes**

Following the observation in 1890 that removal of the pancreas in the dog induced T1D (von Mering and Minkowski, 1890), many studies of diabetes have involved pancreatectomised animals, including species that are now more commonly used such as rats and mice (Rees and Alcolado, 2005). However, streptozotocin has become the most common method to induce T1D in animals. Streptozotocin has direct toxic effects on the pancreas causing death of  $\beta$  cells, resulting in diabetes (Szkudelski, 2001). Fat-fed animals treated with

streptozotocin have also been used to study T2D by inducing diabetes in obese animals. There are however, numerous other animal models of T2D that can be used to study development and characteristics of the disease (see Table 1.1).

Ob/Ob mouse—monogenic model of obesity (leptin deficient)
db/db mouse—monogenic model of obesity (leptin resistant)
Zucker (fa/fa) rat—monogenic model of obesity (leptin resistant)
Goto Kakizaki rat
KK mouse
NSY mouse
OLETF rat
Israeli sand rat
Fat-fed streptozotocin-treated rat
CBA/Ca mouse
Diabetic Torri rat
New Zealand obese mouse

**Table 1.1 Animal models of type 2 diabetes**

Different animal models used in the study of T2D mellitus. Adapted from (Rees and Alcolado, 2005).

The three most commonly used animal models of T2D are the ob/ob mouse, the db/db mouse and the fa/fa rat. The ob/ob mouse which is leptin deficient, was discovered in 1949 in a laboratory in Maine and has been inbred to result in a strain of mice that are overweight, hyperphagic and insulin resistant (Lindstrom, 2007). The ob/ob mouse has been found to have a defect in the ob gene that codes for the protein leptin whereas both the db/db mouse and the fa/fa rat have been found to have mutations in the hypothalamic receptor for leptin (Rees and Alcolado, 2005). The db/db mouse is leptin resistant and exhibits profound obesity, diabetes and dyslipidemia (Sharma et al., 2003). The fa/fa (obese Zucker) rat (OZR) was a spontaneous mutant discovered by Lois Zucker in 1961 on crossing Merck M-strain and Sherman rats (Bray, 1977). The fa mutation is an

autosomal recessive mutation in the extracellular domain of the leptin receptor such that in homozygotes, the leptin receptor gene is not properly coded (Bray, 1977). Due to the defective leptin receptor, the animals lack a satiety reflex, are therefore hyperphagic and develop profound obesity in a similar way to the db/db mouse (Bray, 1977).

The OZR offers many advantages over other animal models as the development of metabolic syndrome is due to chronic hyperphagia, a similar aetiology to the development of metabolic syndrome in humans. As with T2D in humans, OZR experience prolonged hypertriglyceridaemia and insulin resistance prior to the development of T2D (Bray, 1977). Additionally, in a similar way to humans with T2D, the hypertension they develop is mild to moderate (Frisbee and Delp, 2006). The proinflammatory and prothrombotic state within OZR is also similar to humans (Bray, 1977). There are inevitably also disadvantages with the OZR as a model such as an inability to mobilize hepatic glycogen stores (Koubi et al., 1991) and the absence of basal hyperglycaemia (Mordes and Rossini, 1981). However, despite these disadvantages the OZR was chosen as the most appropriate animal model to investigate obesity induced diabetes in the experiments described in this thesis. The diabetic mouse models described above would also have been suitable but the size of animal and blood volume would have been prohibitive.

### **1.4 Methods of investigating action of insulin**

As discussed above, glucose homeostasis is a complicated process; a rise in plasma glucose concentration results in insulin release from pancreatic beta-cells which increases plasma insulin concentration, thus stimulating glucose uptake into tissues and decreasing plasma glucose concentration.

A number of different techniques have been employed in the study of insulin's action, for instance glucose tolerance tests (GTTs) and insulin tolerance tests (ITTs). GTTs assess the ability of the body to dispose of glucose following a glucose drink, this measures systemic insulin release and indirectly measures insulin action as it measures the response initiated to an acute increase in blood glucose concentration and the ability of insulin to decrease the blood glucose. Alternatively, ITTs use the rate of decline in blood glucose concentration following a known amount of insulin injection, as an estimate of insulin sensitivity (Muniyappa et al., 2008).

However, the steps in the process underlying glucose homeostasis are not sequential, but occur more or less simultaneously creating a feedback loop that must be interrupted if the aim is to make an assessment of tissue insulin sensitivity. It was with this in mind that DeFronzo developed the HE clamp to allow the investigator to break the glucose-insulin feedback loop by controlling plasma glucose concentration (DeFronzo et al., 1979).

The HE clamp offers significant advantages over the alternative ITT as it prevents the hypoglycemia induced by ITT and therefore reduces the possibility of counterregulatory neuroendocrine responses being mounted in response to hypoglycaemia. This increases the reliability of the measure of tissue sensitivity to insulin. The HE clamp also enables the investigator to assume endogenous insulin secretion is constant because factors, such as blood glucose concentration and activation of counterregulatory mechanisms that affect it are minimized (Sherwin et al., 1974). This ensures that both plasma insulin and glucose are entirely under the control of the investigator and thus the feedback loop between the two has been broken.

The HE clamp involves giving a constant insulin infusion that attains hyperinsulinaemia: an insulin concentration higher than normal ( $\sim 90$  pmol/L in humans (Manley et al., 2007) and  $\sim 200$  pmol/L in rats (Ross et al., 2007b)), that will increase glucose disposal and suppress endogenous glucose production. Hypoglycaemia is prevented by giving glucose by infusion at a gradually increasing rate at the beginning of HE clamp and a stable rate at the end of HE clamp; this clamps plasma glucose concentrations. Plasma glucose concentrations can either be clamped at the individual's basal plasma glucose concentration (euglycaemia) or a predetermined level (Muniyappa et al., 2008). Thus glucose concentration must be assessed at regular intervals. When there is no net change in glucose concentration for a set time period (normally  $\sim 20$  minutes), glucose is at steady-state and because endogenous production of glucose has been suppressed, glucose infusion rate (GIR) provides a measure of glucose uptake.

The HE clamp has become the reference gold standard for determining metabolic insulin sensitivity (Muniyappa, Lee et al. 2008). Insulin sensitivity is calculated as the ratio  $M/I$  where 'M' is the glucose disposal rate and 'I' is the plasma insulin concentration.  $M/I$  therefore allows quantification of the amount of glucose taken up by the tissue per unit of insulin in the plasma and so acts as a measure of tissue sensitivity to insulin (Sherwin et al., 1974). The measurements of change are all taken towards the end of the HE clamp when plasma insulin, blood glucose and GIR are all constant. As 80% of glucose uptake is thought to occur in the skeletal muscle (DeFronzo et al., 1981) 'M' is usually expressed per fat-free mass rather than body weight to generate normalised measures of insulin sensitivity that are assumed to relate to muscle (Muniyappa et al., 2008).

Several computer programs and algorithms have been developed to assist in controlling the glucose infusion rate (GIR) by controlling the glucose infusion pump so that plasma glucose concentration is maintained during an HE clamp (Muniyappa et al., 2008). However it is possible for an experienced investigator to control GIR efficiently. The main limitations of the HE clamp remain that it is time consuming, labour intensive, expensive and requires an experienced operator to manage the technical difficulties. Also the HE clamp uses steady-state insulin levels that are generally high physiological or supraphysiological levels which may reverse the portal to peripheral insulin gradient and thus not completely reflect physiological conditions (Muniyappa et al., 2008).



The HE clamp was used for experiments described in this thesis and in many of the studies discussed below. The HE clamp was chosen over the ITT as HE clamp allows both glucose and insulin to be held constant. The control of glucose concentration as well as insulin concentration ensures that the experimental observations are not as a result of hypoglycaemia induced by ITT.

### **1.5 Insulin-induced vasodilatation**

In addition to the above, well-characterized actions of insulin to control blood glucose concentrations by increasing glucose uptake via GLUT4 into skeletal muscle; there is a growing wealth of evidence to support insulin's ability to induce vasodilatation. This is discussed below.

Almost as soon as insulin started to be used in clinical practice, its apparent ability to increase muscle blood flow was documented (Abramson et al., 1939). This increase in blood flow can be seen as beneficial as Fick's principle dictates that the uptake of glucose by a tissue is the product of arterio-venous glucose gradient and blood flow. Thus, by acting on both variables, insulin would more rapidly increase glucose uptake.

Studies that have investigated the effects of systemic hyperinsulinaemia have consistently shown muscle vasodilatation in humans and experimental animals at a range of different insulin concentrations from physiological to supraphysiological (Tack et al., 1996a, Ueda et al., 1998, Vollenweider et al.,

1993, Utriainen et al., 1997, Laakso et al., 1990, Vincent et al., 2004). Also, intra-arterial infusions of insulin (Neahring et al., 1993, Ueda et al., 1998, Tack et al., 1996b) are able to cause an increase in muscle blood flow, which suggests that it is a local, as well as a systemic effect of insulin.

There is evidence supporting an action of insulin at all levels of the vascular tree (Barrett et al., 2011). This has particular physiological relevance because insulin resistance is known to be associated with pathological effects at all levels of the vascular tree (see figure 1.4).

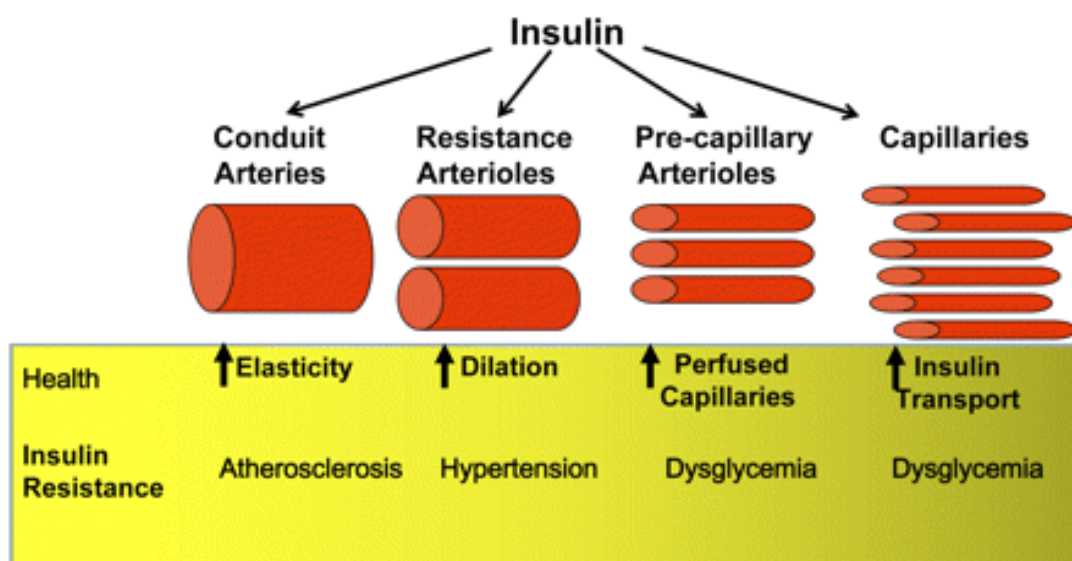


**Figure 1.4 Insulin action at different levels of the arterial tree.**

Figure taken from (Barrett et al., 2011).

Firstly, there is evidence that insulin is able to affect the compliance of conduit arteries as shown by Westerbacka et al., (1999) who used aplanation tonometry before and after HE clamp in aortas of healthy humans. In addition to this,

metabolic insulin resistance has been shown to increase vascular stiffness (Stehouwer et al., 2008).

Secondly, Baron and colleagues demonstrated by using thermodilution to measure blood flow, a link between the leg blood flow (controlled by resistance arterial vessels) and insulin-mediated glucose disposal (Baron, 1994, Laakso et al., 1990). These results indicated that insulin acts to enhance bulk flow to the muscle.

There are widely discussed inconsistencies in the reported magnitude of increase in muscle blood flow and glucose uptake in response to insulin; it has been suggested that these may be in part due to variations in the methodologies used, such as route of insulin administration, dose of insulin, time of exposure to insulin and subjects used. Studies demonstrating insulin-induced vasodilatation have used several different techniques. These include various techniques for assessing bulk blood flow: venous occlusion plethysmography (Tack et al., 1996a), thermodilution (Steinberg et al., 2000), or Doppler flow technique (Clark et al., 2001). Yki-Jarvinen et al., for instance, suggested that venous occlusion plethysmography gave significantly higher increases in blood flow than identical experiments using Doppler ultrasound as a measure of flow (Yki-Jarvinen and Utriainen, 1998).

Another possible reason for inconsistencies in measures of insulin-induced vasodilatation in the whole limb in response to insulin, is limb muscularity, which has been shown to vary from 24-81% in the human forearm (Utriainen et

al., 1995). In fact, in obese subjects when total flow to the limb is measured, size of the muscle vasodilatation may be underestimated or it may not be seen at all because of the increased proportion of fat being supplied.

Despite the bulk of evidence indicating that insulin acts to increase muscle blood flow there is also evidence that contradicts this. For example, experiments by Natali et al., (1994) on healthy human subjects showed a fourfold increase in forearm glucose uptake during HE clamp in overweight patients without a concomitant increase in forearm blood flow as measured by strain-gauge plethysmography.

Baron et al., were the first to show that insulin is able, in an NO-dependent way, to reduce precapillary arteriolar tone and vasomotion, so as to increase capillary flow and make it more homogenous, termed “functional capillary recruitment” (Baron, 1993, Baron, 1994). It was proposed that dilating terminal arterioles would increase microvascular perfusion and therefore enhance the endothelial surface area available for nutrient exchange and should enhance nutrient delivery, even in the absence of changes in bulk blood flow.

Behaviour of the microvasculature has also been assessed by various techniques: intravital microscopy of microvessel diameter in muscle preparations (McKay and Hester, 1996), 1-methylxanthine (1-MX) metabolism which measures 1-MX metabolism by xanthine oxidase on endothelial cells (Rattigan et al., 1997), contrast-enhanced ultrasound (CEU), which measures infused microbubbles to

asses microvascular volume (Vincent et al., 2002) and laser Doppler flowmetry (LDF) (Clark et al., 2001).

### **1.5.1 Time relationships**

In addition to inconsistencies in the reported magnitude of insulin-induced dilator effects, the time course of the increases in bulk flow, microvascular vasodilatation and glucose uptake have also been reported to vary.

Thus, the temporal relationship between glucose uptake and FBF was followed in detail by Vincent et al., (2004) who used 30 minute 3 mU/min/kg HE clamps in rats. They found that insulin recruited the capillary network of hindlimb muscle, as assessed by CEU imaging within 5 – 10 minutes and that this preceded changes in glucose uptake and bulk blood flow (measured by an ultrasonic flow probe) on the femoral artery.

Additionally, studies by Utriainen et al., (1995) showed that a 1 mU/kg/min insulin infusion in healthy humans rapidly increased the arterio-venous glucose gradient and increased the glucose extraction fraction by 10 fold within 60 minutes. However, the increase in muscle blood flow did not develop until after the first hour and continued to rise throughout the six hour infusion by which time the glucose uptake had plateaued. Similarly, Laakso et al., (1990) also observed that the insulin infusion had to be maintained for several hours before an increase in bulk blood flow was detected in the leg of healthy humans.

What is more, the study of McKay and Hester (1996) showed using *in vivo* microscopy of hamster cremaster muscle, that topical application of 200  $\mu$ U/ml of insulin caused vasodilatation within the fourth (terminal) order arterioles that occurred prior to dilatation of the second (proximal) order arterioles that contribute to changes in vascular resistance and therefore bulk flow.

Thus, it would appear that insulin is able to dilate terminal arterioles independently of, and before, proximal arterioles and that the time course for the microvascular actions of insulin is consistent with a role in glucose uptake. It would also appear that vasodilatation at the level of the microvasculature does not necessarily affect bulk blood flow.

### **1.5.2 Insulin exposure**

It is also possible that some of the differences in observed vasodilator response to insulin are due to the dose of insulin. It has consistently been shown that the time course for an increase in limb blood flow lags behind the insulin-induced increase in glucose uptake (Yki-Jarvinen and Utriainen, 1998). As indicated above it was observed that increases in limb blood flow were often only seen following long periods of insulin infusion or at supraphysiological insulin concentrations. This led Yki-Jarvinen and Utriainen to suggest some of the differences seen in insulin-induced vasodilator responses may be explained by calculating an arterial insulin exposure index (see Figure 1.5): Insulin dose (mU/kg/min) was multiplied by duration of exposure (hours). When this insulin exposure index was plotted against per centage increase in blood flow, there was

a significant positive correlation in both local intra-arterial infusion studies and systemic intravenous infusion studies (Yki-Jarvinen and Utriainen, 1998).

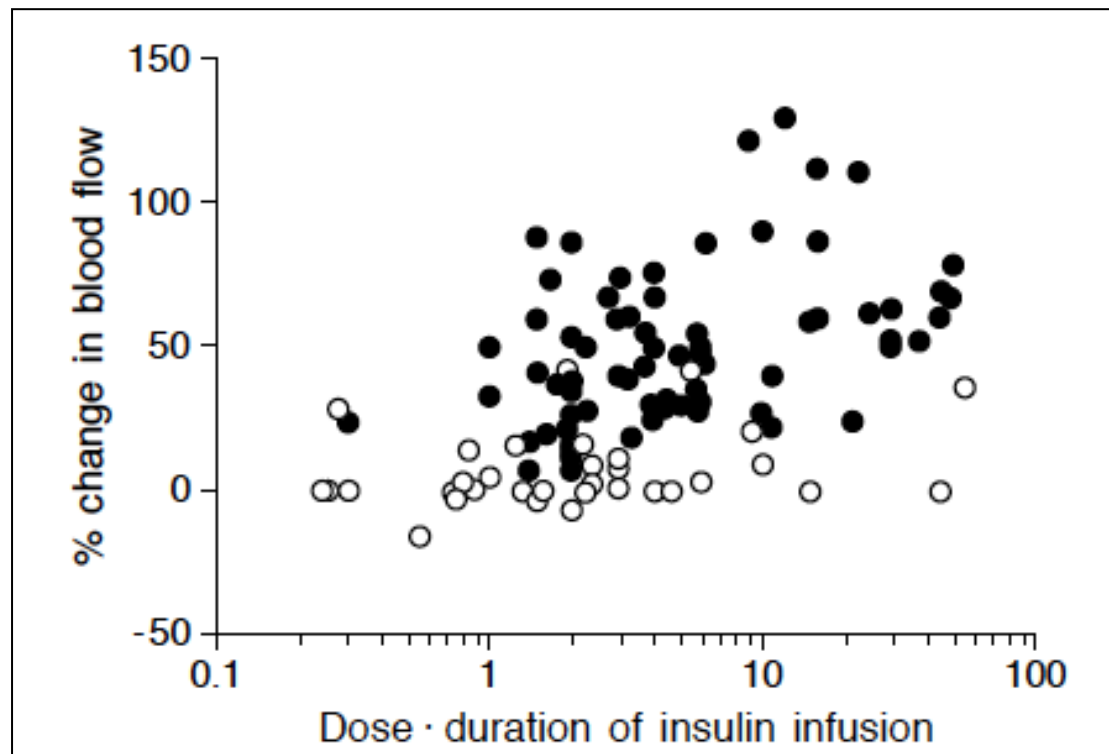


**Figure 1.5 Insulin exposure versus per centage change in blood flow.**

Figure from (Yki-Jarvinen and Utriainen, 1998). A summary of data taken from 75 different studies that tested the effect of intravenous insulin infusions on forearm or leg blood flow under normoglycaemic conditions in normal subjects. Studies in which flow increased significantly (solid symbols) or not (open symbols). Insulin exposure index calculated by multiplying the dose of insulin by the duration of the insulin infusion showed that it was significantly correlated with percentage change in blood flow ( $r = 0.5$ -,  $P < 0.0001$ ).

In agreement with this proposed insulin exposure index, Clark's group presented a set of experiments using HE clamps in rats at a range of concentrations of insulin. In the 3 mU/kg/min group, FBF was not significantly increased from baseline until 60 minutes from beginning of insulin infusion, whereas in the 10 mU/kg/min group FBF was significantly increased at 30 minutes and in the 30

mU/kg/min group, by as early as 20 minutes. Further, the maximal increase in FBF reached during the HE clamp increased in a dose-dependent fashion with insulin concentration (Zhang et al., 2004).

### **1.5.3 Influence of blood glucose concentration on insulin-induced vasodilatation**

Evidence has been presented that glucose uptake influences insulin-induced vasodilatation. Thus, Ueda et al., (1998) showed that in humans, in the fasted state, no change in blood flow occurred with an intravenous infusion of 1 mU insulin, whereas a weak forearm vasodilatation (~20%) did occur with an infusion of 5 mU of insulin. However, co-infusion of D-glucose with 5 mU of insulin potentiated the vasodilatation to an increase of 47%. Further investigations indicated that this effect is stereospecific for D-glucose as infusion of the inactive isomer L-glucose did not have the same effect. Furthermore, the increase in the vasodilatation was not just an osmotic effect as infusion of D glucose alone did not induce vasodilatation. Thus, they suggested that glucose acts as a positive feedback regulator of insulin-mediated vasodilatation and therefore that impaired glucose uptake in insulin resistance may impair the vasodilatation (Ueda et al., 1998).

Studies by Feldman et al., (1995) also showed that the glucose uptake and vascular effects of insulin are highly correlated in healthy subjects in which the sensitivity to insulin of dorsal hand veins was established by differential



transformer techniques and glucose tolerance to insulin was established using glucose tolerance tests with frequent sampling.

Further, in a study on patients with autonomic failure and therefore sympathetic vasoconstrictor failure, not only did intravenous insulin administration lower arterial blood pressure substantially, indicative of pronounced vasodilatation, but, administration of high concentrations of glucose (50%) to normalize the blood sugar concentrations in these patients, lowered the blood pressure further, suggesting the vasodilatation was even more pronounced (Mathias et al., 1987).

By contrast, Tack et al., (1996b) found that HE clamp induced a slow onset muscle vasodilatation that was preceded by an increase in glucose uptake, but a concomitant intra-arterial infusion of 5% glucose did not have any effect on the vasodilator response to insulin.

Considering the potential importance of glycemic status on insulin-induced vasodilatation, it is surprising that in studies performed on animals there is no general consensus on whether or not the animals were fed, or fasted when studied. This is even the case for studies from one laboratory, for instance the studies conducted by Clark et al., either seem to have fasted animals prior to experimentation (Vincent et al., 2003, Zhang et al., 2004) or allowed them access to food *ad libitum* (Ross et al., 2007b, Youd et al., 2000). In view of this, investigations described in this thesis were undertaken to look at the effect of

feeding or fasting of animals prior to experiments on insulin-induced vasodilatation evoked by HE clamp.

In addition to the metabolic actions of insulin to increase glucose uptake in skeletal muscle by recruiting GLUT4 to the skeletal muscle membrane (see Section 1.1), experiments conducted *in vitro* on endothelial cells have shown that insulin stimulates the insulin-signaling cascade in endothelial cells, with different end products. Thus, activation of the insulin-signaling cascade in endothelial cells results in the production of both NO and the potent vasoconstrictor endothelin-1 (ET-1) (Cardillo et al., 1999). As in skeletal muscle, stimulation of the insulin receptor phosphorylates insulin receptor substrate-1 (IRS1) which phosphorylates phosphoinositide 3 kinase (PI3K) which phosphorylates protein kinase B (PKB/Akt). However, in endothelial cells PKB/Akt is able to phosphorylate endothelial nitric oxide synthase (eNOS) to produce NO (see Figure 1.6). Conversely, the insulin receptor also phosphorylates insulin receptor substrate-2 (IRS2) which causes the activation of the adaptor protein src homology protein (Shc) initiating the extracellular signal regulated kinase 1/2 (ERK1/2) pathway and ultimately causing the endothelin-converting enzyme to produce endothelin-1 (ET-1). The balance of NO and ET-1 production by insulin is thought to help maintain vascular tone in healthy individuals with NO and ET-1 acting to decrease and increase vascular tone respectively (Bakker et al., 2009).

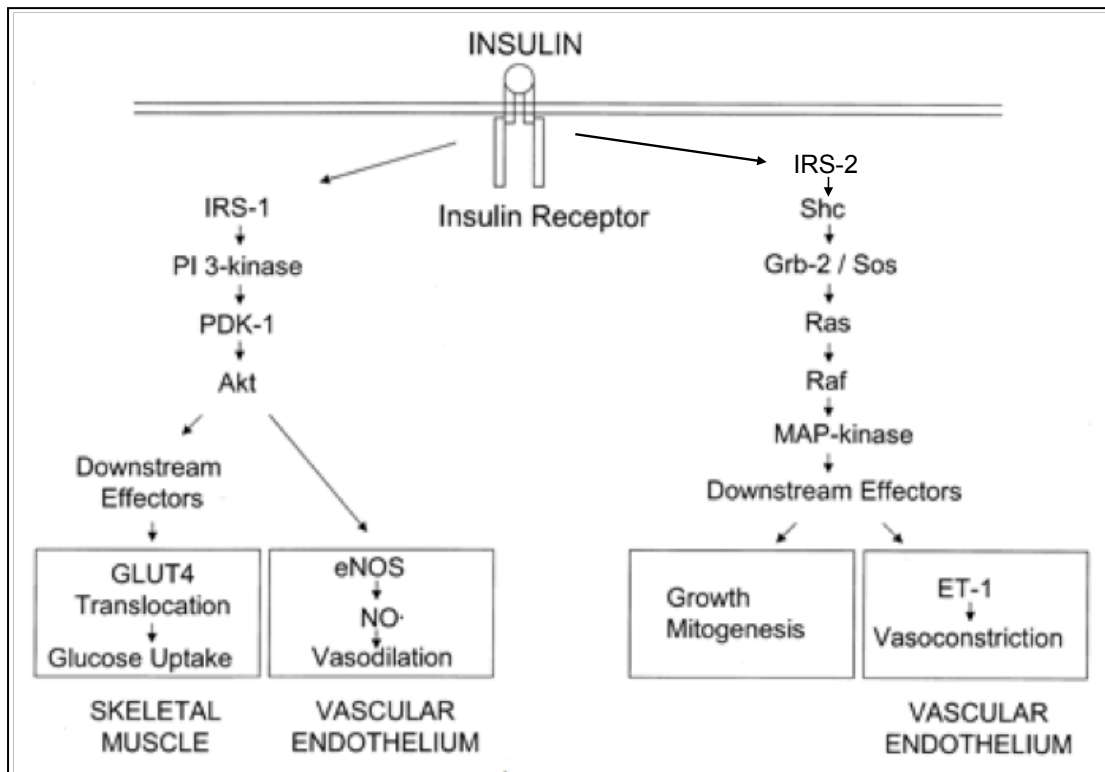


**Figure 1.6** Insulin receptor signaling and control of vascular tone.

Figure from (Kim et al., 2006)

#### 1.5.4 Insulin-induced vasodilatation and NO

The most extensively investigated mechanism for production of insulin-induced vasodilatation is NO. Much evidence has been gained for this from human studies. For example, Steinberg et al., (1994) conducted HE clamps in healthy subjects (120 mU/m<sup>2</sup>/min insulin, to achieve a plasma insulin concentration of ~1300 pmol/L) with or without the NO synthase competitive inhibitor L-NMMA infusion. They showed that 40 % of the increase in leg blood flow evoked by the HE clamp was NO-dependent. However, in the same year, Scherrer et al., conducted experiments using HE clamps in healthy subjects (1 mU/kg/min insulin, to achieve a plasma insulin concentration of ~450 pmol/L) and showed that L-NMMA infusion completely abolished insulin-induced vasodilatation in

the arm (Scherrer et al., 1994). These findings seem to indicate a different degree of involvement of NO in insulin-induced vasodilatation at different concentrations of insulin, ie NOS inhibition may completely inhibit vasodilatation only at low doses of insulin.

A few of the studies in humans on the NO-dependence of insulin-induced muscle vasodilatation also examined whether insulin-mediated glucose uptake is NO-dependent. For example, Sartori et al., (1999) used patients with regional thoracic sympathectomy to investigate the involvement of NO on insulin-induced vasodilatation in response to HE clamp (1 mU/kg/min insulin, plasma insulin concentration  $\sim 460$  pmol/L). They showed that forearm blood flow increased by  $\sim 30$  % during HE clamp, and only by 10 % when L-NMMA was given concomitantly, but this blunting of the increase in forearm blood flow was not associated with any change in whole body glucose uptake. However, Baron et al., (2000) conducted HE clamps with much higher insulin concentrations (300 mU/m<sup>2</sup>/min insulin, plasma insulin concentration  $\sim 1350$  pmol/L) in healthy individuals and showed that the increase in leg blood flow was attenuated by  $\sim 50$  % and the increase in leg glucose uptake by  $\sim 22$  % during L-NMMA infusion. It is difficult to directly compare the results of these studies as the condition of the subjects, the dose of insulin and therefore the plasma insulin concentration were so different. They certainly do not form a consensus on the contribution of NO to glucose uptake.

In addition, several studies have been carried out on animals to investigate the roles of NO in insulin-induced vasodilatation and glucose uptake. Thus, Baron et

al., conducted studies on awake rats and showed that L-NMMA caused a 20 % increase in baseline blood pressure and attenuated the increase in glucose uptake induced by HE clamp (12 microns/kg/min insulin; (Baron et al., 1995). They proposed that the acute hypertension induced by NOS inhibition caused insulin resistance as a result of a reduction in skeletal muscle perfusion and/or sympathetic nervous system activation. However, they did not actually record muscle blood flow or any index of sympathetic activity.

Vincent et al., (2004) investigated the importance of NO in insulin-induced capillary recruitment by using CEU and also measured glucose disposal in rats. They showed by using HE clamp (3 mU/kg/min insulin) that insulin infusion led to recruitment of capillaries as indicated by CEU beginning at 10 minutes, but did not substantially increase glucose uptake until 30 minutes: systemic L-NAME partially inhibited both capillary recruitment and glucose uptake (Vincent et al., 2004). Additionally, in experiments by the same group, L-NAME administered five minutes prior to and simultaneously with a 120 minute 10 mU/min/kg HE clamp completely blocked the insulin-induced hindlimb vasodilatation as determined from gross blood flow i.e. flow in the femoral artery and blunted glucose uptake by ~40% in Sprague-Dawley rats (Vincent et al., 2003). However, the only values of femoral blood flow provided were baseline and at the end of HE clamp. Thus, the effect of NOS inhibition on the time course of the vasodilatation and its relationship to glucose uptake were not apparent. In some contrast, in experiments using intravital microscopy of hamster cremaster muscle, McKay and Hester showed that L-NAME inhibited vasodilatation induced in secondary order (proximal arterioles), by topically applied insulin, but had no

significant effect on dilatation of fourth order (terminal arterioles). These results suggested that insulin-induced dilatation of proximal arterioles that determine bulk blood flow were partly NO-dependent but that dilatation of terminal arterioles was not. However, they did not assess glucose uptake, so gave no indication of the relationship between the timing of dilator responses and glucose uptake.

The relationship between the effects of NOS inhibition on, insulin-induced vasodilatation and glucose uptake were therefore explored in experiments presented in this thesis.

#### **1.5.5 How are the effects of glucose uptake and NO linked?**

McKay and Hester (1996) provided a possible link between increased glucose uptake, NO production and vasodilatation by demonstrating a role for adenosine in insulin-induced vasodilatation. In the experiments described above, using *in vivo* microscopy, they showed that an adenosine receptor antagonist abolished insulin-induced vasodilatation in proximal and distal arterioles of skeletal muscle and thus hypothesised that adenosine produced by the metabolic action of insulin on skeletal muscle is part of a feed forward mechanism that then facilitates insulin's action on skeletal muscle fibres by causing vasodilatation (McKay and Hester, 1996). They suggested that adenosine acts directly on vascular smooth muscle extraluminally and that the K-ATP channel is a possible mechanism of action given that the dilator action of insulin was attenuated by

the K-ATP blocker glibenclamide and given that adenosine is known to act via this channel (Nelson et al., 1990).

In further support of this hypothesis, Abbink-Zandbergen also provided evidence that adenosine is involved in insulin-induced vasodilatation in healthy humans as intrabrachial infusion of draflazine (an adenosine-uptake blocker) or theophylline (adenosine-receptor antagonist) increased and decreased respectively insulin-induced increases in forearm blood flow (Abbink-Zandbergen et al., 1999).

It is possible that the second messengers for NO and adenosine act in a synergistic manner. NO elicits vasodilatation by the production of cGMP, which relaxes vascular smooth muscle. Adenosine can cause vasodilatation by producing cAMP, which also relaxes vascular smooth muscle (Ralevic and Burnstock, 1998). There is evidence in the literature that cGMP and cAMP are able to act in a synergistic manner to cause vasodilatation (Wit et al., 1994): experiments using superfusion of hamster cremaster muscle showed a supra-additive vasodilator effect of substances that increase cAMP and cGMP versus the substances alone. It is plausible that the effects of NO and adenosine to increase the production of cGMP and cAMP respectively could be acting together to produce insulin-induced vasodilatation.

It may be that NO or some other mechanism acts rapidly to increase blood flow within the capillary network by dilating terminal arterioles (see Vincent et al., (2004), which occurs before the increase in bulk blood flow, whereas, the

dilatation of proximal arterioles, that takes a longer time to develop may be due to the production of metabolic products, such as adenosine, from the skeletal muscle fibers. However, there is undoubtedly overlap between these two effects as the experiments of McKay and Hester showed that an adenosine antagonist abolished insulin-induced dilatation in both proximal and terminal arterioles.

The insulin exposure index proposed by Yki-Jarvinen (1998) may also be explained by a link between the metabolic actions of insulin and the vasodilatation produced. Thus, greater exposure to insulin will presumably cause increased glucose uptake and therefore increased generation of metabolic products, which have the potential to act to produce vasodilatation.

#### **1.5.6 Insulin-induced vasodilatation and free fatty acids**

The demonstration in endothelial cells that increased FFA concentrations decreased insulin-dependent tyrosine phosphorylation of IRS-1 and thus attenuated the insulin signaling cascade (Kim et al., 2005), provides a possible link between FFA-induced insulin resistance and endothelial dysfunction as the insulin signaling pathway is shared by skeletal muscle and vascular endothelial cells (as discussed above). As such, FFA availability has the potential to affect insulin-induced vasodilatation by altering both glucose uptake (Randle, 1981, Roden et al., 1996) and endothelium-dependent dilatation (Steinberg et al., 1997, Pleiner et al., 2002).



There is an inverse correlation between FFA concentration and insulin sensitivity as FFAs act to decrease the uptake of glucose by skeletal muscle (Randle, 1981, Roden et al., 1996). Although there is agreement that this is the case, theories on the mechanisms behind this relationship vary. It was proposed by Randle et al., that a reciprocal relationship exists between the metabolism of glucose and FFA. Hence, they showed in preparations of rat heart that an increase in FFA availability caused by infusion of lipid and heparin which activates lipoprotein lipase on endothelial cells, increased the intracellular build up of G6P and glucose by inhibiting key glycolytic enzymes and therefore reduced glucose uptake (Randle, 1981). However, Shulman's group showed by using NMR in healthy humans that a decrease in glucose uptake caused by increased plasma FFA was associated with a decrease in G6P (Roden et al., 1996). This led them to postulate that FA may act directly on GLUT4 or affect upstream signalling.

FFAs have also been demonstrated to induce endothelial dysfunction. Lipid and heparin infusion into healthy humans for two hours to raise FFA levels to those seen in insulin-resistant subjects reduced muscle vasodilator responses to methacholine chloride, an endothelium-dependent dilator (Steinberg et al., 1997). Similarly, lipid and heparin infusion into healthy humans reduced the increase in femoral blood flow evoked by the endothelium-dependent dilator acetylcholine (Ach) by 55% (Pleiner et al., 2002).

Various studies have investigated the effects of increased FFA concentrations on the insulin-signaling cascade. In agreement with the results of Kim et al., on

endothelial cells in healthy individuals, lipid and heparin infusion followed by HE clamp resulted in a decrease in glucose transport and completely abolished the four fold increase in muscle PI3-K activity seen in glycerol and heparin infused individuals (Dresner et al., 1999). Further, lipid/heparin infusion for 5 hours prior to HE clamp in conscious rats resulted in blunting of insulin stimulated IRS-1 tyrosine phosphorylation and a 50% decrease in insulin-stimulated IRS-1 associated phosphorylation of PI3-K measured in muscle samples taken at the end of the clamp (Griffin et al., 1999).

Liu et al., (2009) demonstrated an effect of FFA concentration on both glucose uptake and vasodilatation. They showed that an increase in FFA in healthy humans for five hours induced by lipid and heparin infusion caused insulin resistance in the skeletal muscle, blunting both the recruitment of microvascular blood volume and glucose disposal seen in response to HE clamp and a mixed meal. Further, Clerk et al., (2002) demonstrated that lipid and heparin infusion prior to and during HE clamp in anaesthetized rats reduced hindlimb glucose uptake and capillary recruitment as compared with saline infusion and HE clamp.

In light of these results, experiments described in this thesis were performed to investigate whether acute lowering of FFA can improve insulin sensitivity and insulin-induced vasodilatation in lean and obese Zucker rats.

### **1.5.7 Other proposed mechanisms for insulin-induced vasodilatation**

Additional possible mechanisms of insulin-induced vasodilatation proposed in the literature are discussed below.

#### **Intracellular calcium**

Han et al., (1995) provide evidence that insulin acts in two ways to cause vasodilatation. Using isolated rat aorta, they firstly showed that endogenous insulin acts on the endothelium to increase endothelial calcium as measured using the fluorescent  $\text{Ca}^{(2+)}$  indicator fura 2, releasing NO which in turn decreases smooth muscle calcium and causes relaxation. But, insulin also acted directly on the smooth muscle of isolated rat aorta after endothelial removal to decrease intracellular calcium concentration (Han et al., 1995). It has also been shown that insulin acts on vascular smooth muscle to cause calcium efflux via  $\text{Ca}^{(2+)}$ -ATPase activity the decrease in intracellular calcium in vascular smooth muscle then induced relaxation (Zemel et al., 1992).

In conditions of insulin resistance such as hypertension, calcium metabolism in vascular smooth muscle can be abnormal, causing higher intracellular calcium concentrations, perhaps contributing to blunted relaxation in response to insulin (Baldi et al., 1996).

#### **Sodium potassium-ATPase ( $\text{Na}^+$ , $\text{K}^+$ -ATPase)**

To investigate whether  $\text{Na}^+$ ,  $\text{K}^+$  -ATPase on vascular smooth muscle contributes to insulin-induced vasodilatation, Tack et al., used the specific  $\text{Na}^+$ ,  $\text{K}^+$  -ATPase inhibitor ouabain in healthy individuals who were undergoing HE clamp.

Ouabain significantly inhibited insulin-induced vasodilatation when infused before or during HE clamp, indicating that  $\text{Na}^+$ ,  $\text{K}^+$  -ATPase activity is required for the response. In addition, L-NMMA produced blunted vasoconstriction when given in conjunction with ouabain which indicates  $\text{Na}^+$ ,  $\text{K}^+$  -ATPase is required for the action of NO, and by extrapolation for insulin-induced vasodilatation (Tack et al., 1996a).

$\text{Na}^+$ ,  $\text{K}^+$  -ATPase is a ubiquitous enzyme and has different effects in vascular smooth muscle cells and endothelial cells (Meharg et al., 1993). In both cell types,  $\text{Na}^+$ ,  $\text{K}^+$  -ATPase acts to cause hyperpolarisation of the membrane by exchanging three intracellular potassium ions for two extracellular sodium ones. In vascular smooth muscle cells, this hyperpolarisation causes the closure of voltage-dependent calcium channels, decreasing intracellular calcium concentrations and causing relaxation (Busse et al., 1989). By contrast in endothelial cells, the increase in electrogenic driving force causes a potential-dependent calcium influx and an increase in intracellular calcium because there are no voltage-dependent calcium channels in endothelial cells (Luckhoff and Busse, 1990). This increase in intracellular calcium stimulates eNOS and therefore NO synthesis (Palmer et al., 1988). Thus, the effect of ouabain on insulin-induced vasodilatation could be due to inhibition of the vascular smooth muscle, or endothelium-mediated component of dilatation or both.

Stimulation of  $\text{Na}^+$ ,  $\text{K}^+$  -ATPase may require translocation to the cellular membrane; it has been hypothesized that this process would take some time and may correlate with the slow-onset of insulin-induced vasodilatation (Tack et al.,

1996a). Indeed, Omatsukanbe and Kitasato showed that  $\text{Na}^+$ ,  $\text{K}^+$  -ATPase activity in the plasma membrane fraction of frog skeletal muscle is 1.8 times higher in insulin-stimulated muscle than control after 60 minutes. Studies performed to look at the proportion of  $\text{Na}^+$ ,  $\text{K}^+$  -ATPase at the plasma membrane and in the intracellular compartment indicate that insulin stimulation causes the translocation of  $\text{Na}^+$ ,  $\text{K}^+$  -ATPase from intracellular stores to the plasma membrane (Omatsukanbe and Kitasato, 1990). If the same is true for vascular smooth muscle then the timing correlates well with the time delay seen for insulin-induced vasodilatation of proximal arterioles.

### **1.6 Insulin-induced vasoconstriction**

As well as inducing vasodilatation, insulin also initiates processes that result in vasoconstriction. Thus, in addition to the production of NO, the insulin-signaling cascade is able to produce endothelin-1 (ET-1), which produces vasoconstriction (see above). It has also been suggested that insulin activates the sympathetic nervous system (SNS) to maintain arterial pressure during the peripheral vasodilatation it causes. Thus, inhibition of the vasodilator response to insulin by giving L-NMMA revealed a significant increase in blood pressure occurring in response to a subsequent infusion of insulin (Scherrer et al., 1994). Further, in patients with autonomic failure and therefore sympathetic vasoconstrictor failure, intravenous insulin administration lowered arterial blood pressure substantially indicative of more pronounced vasodilatation than occurs in people with intact sympathetic nervous system (Mathias et al., 1987).

More directly, Vollenweider et al., (1995) showed that hyperinsulinaemia in lean and obese subjects caused an increase in both muscle sympathetic nerve activity and noradrenergic outflow. Sympathetic activation as a result of insulin's action was also shown to increase release of noradrenaline into plasma in normotensive and hypertensive patients by Lembo et al., (1994).

Scherrer et al., found that sympathetic nerve activity is closely related to percentage body fat and BMI, indicating that body fat is a major determinant of resting sympathetic nerve activity (Scherrer et al., 1994). Indeed, they suggested that body fat accounted for roughly 50% of the interindividual variation in the rate of sympathetic firing to skeletal muscle. This is particularly pertinent considering the inter-individual variation seen in responses to insulin. They found that the rate of sympathetic firing was closely correlated with calf vascular resistance, with obese subjects having twice the sympathetic firing of lean subjects, irrespective of age. In this study, low dose insulin infusion in lean subjects to concentrations seen in obese fasting subjects was found to increase muscle sympathetic nerve activity (MSNA). They also found a positive correlation between lactate concentration and both body fat and MSNA.

In addition, there is evidence that as well as affecting the amount of neurotransmitter reaching the adrenoreceptors, insulin interacts with the downstream signaling processes. For instance, insulin has been shown to selectively *antagonise* the  $\alpha_2$ -adrenergic pathway (Lembo et al., 1994).

On the other hand, by increasing calcium efflux in vascular smooth muscle, insulin has been shown to blunt rises in intracellular calcium in vascular smooth muscle evoked by a range of agonists (angiotensin II, arginine vasopressin, and norepinephrine) and therefore attenuate their vasoconstrictor actions (Touyz et al., 1994). Thus, even though muscle sympathetic nervous activity is increased by insulin it is possible that insulin causes vasodilatation by attenuating the effects of sympathetic noradrenaline release.

However, there is also some controversy as to whether insulin is able to stimulate the sympathetic nervous system. Neahring et al., found that in obese hypertensive subjects, they could not attribute the increase in  $\alpha$ -adrenergic tone to impairment caused by local action of insulin to antagonize regional vascular reactivity to norepinephrine (Neahring et al., 1993).

### **1.7 The endothelium as a barrier**

Although insulin sensitivity is generally calculated as the ratio of glucose disposal to plasma insulin concentration (see Section 1.4 above), the concentrations of insulin in the blood may not actually reflect its concentration at the level of the muscle fibre or other cell where it acts. From the blood stream insulin must distribute through the capillaries, pass the endothelial barrier and diffuse through the interstitial space in order to access its receptors on the muscle and stimulate the insulin-signaling cascade. A significant number of

studies have been conducted to look at the distribution of insulin and try to elucidate the mechanism of movement of insulin through the endothelium.

Insulin's action to increase glucose uptake is significantly delayed, by ~ 20 minutes, compared to its release from the pancreatic  $\beta$  cells into the blood and correlates much more closely with glucose uptake rates (Castillo et al., 1994). One proposed reason for this time delay is the movement of insulin across the endothelium. Indeed, the notion that the body fluid is one "well-stirred space" was challenged in 1959 when Steele et al., performed studies using radiolabelled glucose and traced its distribution and showed that glucose equilibrated within three compartments. Concentrations of glucose were found to equilibrate most quickly within the plasma space (Compartment 1; see Figure 1.7). The second compartment (Compartment 2) was found to equilibrate rapidly with the plasma compartment and represent insulin independent tissues such as brain, splanchnic organs and renal medulla. The third compartment (Compartment 3), accounted for approximately half of the total pool and was found to represent the ISF (Steele, 1959). Sherwin et al., later demonstrated similarities in the way that insulin similarly equilibrates within these three compartments (Sherwin et al., 1974).



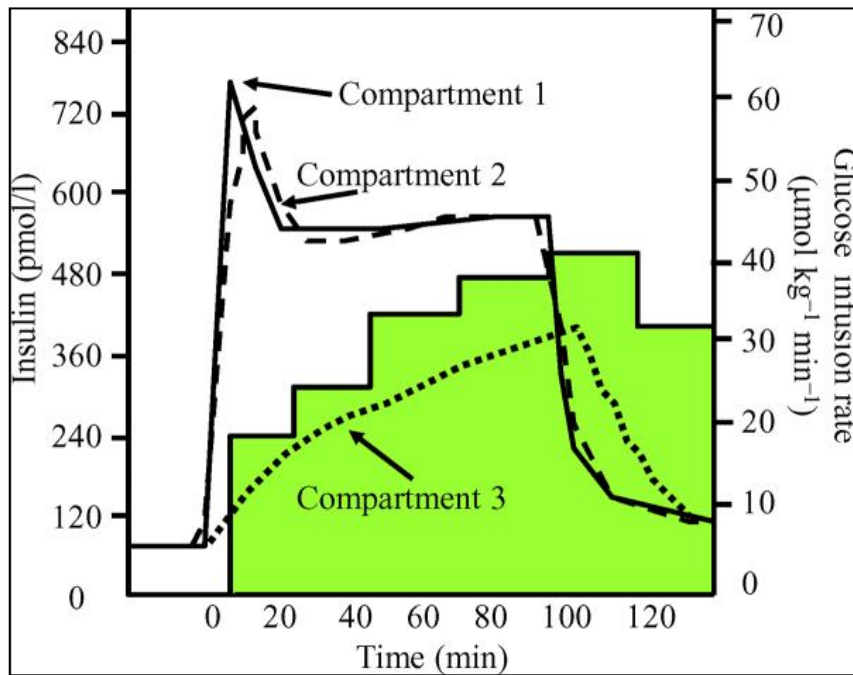


**Figure 1.7 Graphical representation of the three compartment model**

Graphical representation of the three compartment model for the distribution of insulin and glucose first proposed by Steele et al., in 1959. Compartment 1 represents the plasma space, Compartment 2 represents organs that equilibrate quickly with plasma (ie. heart, kidneys, gut and liver) and Compartment 3 represents the interstitial space. The area shaded green represents glucose infusion rate to maintain euglycaemia. Figure taken from (Barrett et al., 2011).

In accordance with the three compartment model, Yang et al., (1989) showed a significant delay between a rise in plasma insulin concentrations (compartment 1) and lymph insulin concentrations (compartment 2) during HE clamps in conscious dogs. In addition, they also showed that lymph insulin concentrations were much lower than plasma concentrations and correlated better with glucose uptake than plasma insulin concentrations (Yang et al., 1989). Castillo et al., (1994) confirmed these findings in lean humans showing lymph insulin concentrations to be significantly lower than plasma insulin concentrations and to correlate much more closely with glucose uptake.

Together these results strongly suggest that movement of insulin from the plasma into the interstitial fluid through the endothelium (TET) is the rate-limiting step in insulin's action. Additional evidence for this proposal has been presented by several other groups. Freidenberg et al., took muscle biopsies during HE clamps in normal male subjects and showed that there was a time delay between the rise in plasma insulin concentration and an increase in insulin receptor kinase (IRK) activity (stimulated by insulin reaching its receptor (Freidenberg et al., 1994). Likewise, Miles et al., demonstrated by using HE clamps in dogs that IRK activity in the muscle was directly correlated to lymph insulin concentration (Miles et al., 1995). In contrast to this, in the liver where the endothelium is fenestrated and more permeable to peptides the delay in IRK activity was only around 2-5 minutes (Miles et al., 1995). On the other hand, intramuscular injection of insulin into dog hindlimb, therefore by-passing trans-endothelial transport (TET), attenuated the delay in insulin-stimulated glucose uptake normally seen *in vivo* (Chiu et al., 2008).

As indicated above, several studies have used lymph insulin as a surrogate measure for ISF insulin concentration with the aim of assessing the movement of insulin into the ISF space (leg of humans (Castillo et al., 1994) and hindleg (Poulin et al., 1994) and thoracic duct of dogs (Yang et al., 1989)). Lymph can be used as a surrogate measure for interstitial (ISF) insulin concentrations because ISF drains into the lymph before it reenters the blood at thoracic duct. Indeed, as mentioned above that lymph insulin concentration correlated extremely well in time course with glucose uptake. However, whilst lymph drainage is a good

indicator of the concentration of interstitial insulin, lymph drainage is rarely derived selectively from skeletal muscle, but is a combination of lymph from many tissues including skin, adipose tissue and bone. Therefore it is not as accurate as direct sampling at the tissue of interest, as can be achieved using microdialysis.

## **1.8 Microdialysis**

Microdialysis, allows direct determination of ISF concentrations and therefore has enormous potential to aid investigations into the TET of insulin. However, very little work has been completed using the method due to the complexity of using the technique to measure insulin (for further discussion see Section 5.1).

Microdialysis has been used to measure ISF insulin concentration in diabetes (Wentholt et al., 2005). However, real discrepancies came to light when comparing arterial-interstitial insulin gradients between insulin sensitive and insulin insensitive subjects. Thus studies performed by Prager et al., (1986), Castillo et al., (1994) and Niklasson et al., (1998) show comparable arterial-interstitial insulin gradients in insulin sensitive and insulin insensitive subjects. By contrast, Holmang et al., (1997) reported higher insulin ISF concentrations in insulin resistant rats, with no gradient-between plasma and ISF. The possible reasons for these discrepant findings are explored in the introduction to Chapter 6. But, in brief, it seems likely that the disparities reflect at least in part, inaccuracies in the measurement of insulin. It should also be noted that the

majority of studies performed have attempted to measurement insulin in ISF at the plateau of HE clamp; very few have measured insulin ISF under basal conditions.

These controversies provided good reason to develop the microdialysis methodology so that it can be used accurately in the rat. Thus, experiments described in this thesis were performed to improve and validate the microdialysis technique for the measurement of insulin in ISF concentrations in lean and obese Zucker rats during hyperinsulinaemic euglycaemic clamp.

### **1.9 Mechanism of TET**

To investigate the mechanism by which insulin traverses the endothelium experiments were conducted by King and Johnson (1985) using bovine aortic endothelial cells (bAECs) grown in a confluent monolayer between two buffer filled chambers. It was shown that insulin transport is saturable as the addition of unlabeled insulin competitively inhibited  $^{125}\text{I}$ -insulin transport through the endothelium. This was subsequently confirmed by other groups (King and Johnson, 1985, Dernovsek and Bar, 1985, Bar et al., 1988, Wang et al., 2006). Saturability of insulin transport indicates that transport is receptor-mediated; this was confirmed in that addition of insulin receptor (IR)- anti-sera inhibited the transport of  $^{125}\text{I}$ -insulin across the bAECs (King and Johnson, 1985). In contrast to the results obtained with endothelial cells, when aortic smooth muscle cells were grown on the membrane between the chambers, the amount of both  $^{125}\text{I}$  labeled insulin and  $^{14}\text{C}$  inulin that was transported was increased 6-7

times and the addition of unlabeled insulin did not affect the transport. This suggested transport across vascular smooth muscle was distinct from the TET and is not saturable (King and Johnson, 1985). The possibility that an increase in TET of insulin shown was due to a general increase in permeability during experimentation was also addressed by showing that  $^{125}\text{I}$ -desoctapeptide (DOP) insulin (which has a lower affinity to the receptor) does not move through the endothelium (Bar et al., 1988); this further indicated that transport is an insulin specific process.

Receptor mediated transport of  $^{125}\text{I}$  labeled insulin *in vitro* across endothelial cells was found to have a lag time of about 15 minutes (King and Johnson, 1985). This was proposed to be due to transport across the cells, as evidence suggests that uptake by the endothelial cell is rapid. In fact, evidence has been presented that the endothelium not only transports, but stores insulin. Thus, in endothelial cells grown from both large blood vessels and capillaries, the association and dissociation of insulin was investigated. The initial insulin dissociation fraction was not affected by dissociating agent, indicating that there exists a non-receptor intracellular pool which may function to store insulin within the endothelial cell (Dernovsek et al., 1984). Likewise, in Langendorff heart experiments the intensity of labeling in the endothelial cell was >10 fold higher than that in the ISF, again suggesting that the endothelium can store relatively high concentrations of insulin (Bar et al., 1988).

Much evidence has been obtained suggesting that the movement of insulin across endothelial cells occurs via vesicles by the process of transcytosis. It is

proposed that vesicles bud off the luminal plasma membrane of the endothelial cell and migrate to the abluminal side. Thus, Wang et al., (2006) clearly showed the co-localisation of the main component of caveolae (caveolin-1) and IR in bAECs. Further, Schnitzer et al., (1994) who conducted *in vitro* experiments to follow the movement of insulin through microvascular cells cultured from epididymal fat pads, bovine lungs and bovine aortic endothelial cells (Schnitzer et al., 1994), found that insulin was not only internalized for degradative processes (in clathrin-coated vesicles), but also for transcytosis (in non-coated vesicles). They showed that the sterol binding agent filipin, which is able to disassemble endothelial non-coated vesicles associated with transcytosis, inhibited insulin transcytosis.

King and Johnson also provided evidence that TET of insulin across bAECs involves a non-degradative pathway as around 80% traversed the endothelium intact (King and Johnson, 1985). Similarly, very little degradation (< 98%) was also demonstrated in experiments using endothelial cells derived from bovine pulmonary arteries (Dernovsek and Bar, 1985).

More recently, Barrett et al., (2011) have proposed a mechanism by which insulin may act to promote its own uptake by both binding to its receptor and also through activation of the insulin signaling cascade. As noted above insulin acts via its receptor to increase the production of NO and it is proposed that this could act intracellularly to increase the transport of insulin through the cell in caveolae. Thus, in experiments observing the uptake of insulin into endothelial cells, inhibiting many parts of the insulin signaling cascade (PI3-kinase, ERK and

cSRC-kinase) individually inhibited the uptake of insulin by the endothelial cell (Barrett et al., 2011).

### **1.10 Endothelial dysfunction**

As discussed above, the endothelium undoubtedly plays a crucial role in the access of insulin to its receptors on the skeletal muscle membrane. Given this important role of the endothelium, it is interesting to consider the detrimental effects that endothelial dysfunction, seen in T2D, may have on the access of insulin to its receptors.

Healthy endothelium is able to adapt to stimuli including mechanical stress, oxidative and metabolic stresses, inflammation, hypoxia and many other stresses (Bakker et al., 2009). The endothelium produces anticoagulatory factors that contribute to haemostasis by ensuring continuity of blood flow. It also helps to regulate inflammation by inducing leukocyte adhesion molecules and other gene products and plays a role in angiogenesis which is important for the capillary perfusion of muscle (Bakker et al., 2009).

In endothelial dysfunction, seen in T2D, there is evidence of oxidative stress and an imbalance in the endothelial production of vasodilator factors such as NO and prostacyclin (PGI<sub>2</sub>) and vasoconstrictor factors such as ET-1 and Ang II (Mather et al., 2004) predisposing the vasculature to vasoconstriction, leukocyte adherence, platelet activation, impaired coagulation and atherosclerosis. This

imbalance is likely to be caused at least in part by the fact that  $O_2^-$  inactivates NO by forming  $ONOO^-$  (Agrawal et al., 2007).

Alterations in the insulin signaling cascade due to endothelial dysfunction are likely to affect both the metabolic and vascular actions of insulin as the signaling pathways leading to the metabolic and vascular actions of insulin show striking parallels (Vincent et al., 2003). Thus, it has been shown that in T2D patients PI3K-dependent insulin signalling is selectively impaired (Storgaard et al., 2001). Additionally, in studies using OZR as a model of T2D and obesity pretreatment of OZR with Saxagliptin for 4 to 8 weeks to improve their postprandial glucose control caused a decrease in peroxynitrite ( $ONOO^-$ ) production and therefore increased NO availability in aortic and glomerular endothelial cells ex vivo (Mason et al., 2011). Further, experiments that interfere with the NO pathway have been shown to improve both metabolic and vascular actions of insulin. Oral administration of tetrahydrobiopterin ( $BH_4$ ) improved endothelial function in the aortas of fructose-fed, insulin-resistant rats and improved their insulin sensitivity (Shinozaki et al., 2000). Therefore, it is possible that interventions that can offer an improvement in endothelial function may be able to restore both metabolic and vascular actions of insulin.

### **1.11 Aims**

The aims of the experiments in this thesis were therefore to, undertake a detailed time course investigation of the role of nitric oxide synthase in insulin-



induced vasodilatation using hyperinsulinaemic euglycaemic clamp. Experiments were then conducted to investigate the relationship between metabolic status of the animals and magnitude of insulin-induced vasodilatation. Subsequently, studies were undertaken to assess the involvement of FFAs in insulin-induced vasodilatation and glucose uptake using both insulin sensitive (lean) and insulin resistant (obese) Zucker rats. Additionally, improved methodology was developed for the accurate measurement of ISF insulin in rats and finally this methodology was used to assess the effects of BH<sub>4</sub> supplementation on endothelial function and access of insulin to the interstitium in lean and obese Zucker rats.

## **CHAPTER 2 - EFFECT OF INHIBITING NITRIC OXIDE SYNTHASE ON INSULIN-INDUCED VASODILATATION DURING HYPERINSULINAEMIC EUGLYCAEMIC CLAMP**

### **2.1 Introduction**

As discussed in the General Introduction (Section 1.5) there is general agreement in the literature that the vasodilatation induced in muscle by insulin and the insulin-induced increase in glucose uptake are NO-dependent to a greater or lesser extent. However, there is some evidence to suggest that the responses evoked by high concentrations of insulin are not wholly NO-dependent. The temporal relationships between the vasodilatation and glucose uptake that occur during an HE clamp have also not been fully established at high concentrations of insulin. Thus, a primary aim of the present study was to follow the time course of the muscle vasodilator response and the increase in glucose uptake that are evoked in the rat by an HE clamp at high physiological levels of insulin with or without blockade of NO synthesis. In order to test this, experiments were performed on rats in which MABP, HR and femoral blood flow were recorded continuously and blood glucose was determined at regular intervals, so that blood glucose could be maintained at a constant concentration during HE clamp.

The experiments in this chapter also allowed the development of a HE clamp protocol for use in the remaining studies described in this thesis. The

methodology used in the experiments of this chapter were an adaptation of the method used by (Ross et al., 2007b). The experiments also allowed detailed assessment of parameters such as haematocrit, blood potassium and lactate concentrations to test how they were affected by HE clamp.

One notable difference from the experiments of Ross et al., (2007b) is that the steroid anaesthetic Alfaxan (alfaxalone/alfadolone combination; Vétoquinol UK limited, Bucks, UK) was used as an anaesthetic for the present experiments. Anaesthesia achieved with this agent has been used for many published observations by Marshall's group (Marshall, 1987, Bryan and Marshall, 1999). It is a valuable anaesthetic for studies of cardiovascular responses in anaesthetized animals as it leaves autonomic control of the cardiovascular system more intact than other commonly used anaesthetics. As insulin is thought to have central as well as peripheral vascular effects (see General Introduction) Alfaxan seemed to be the anaesthetic of choice. Therefore the possibility of Alfaxan as an anaesthetic for studies when using HE clamps was also assessed.

Thus, the experiments of this chapter were performed to undertake a detailed time course investigation of the role of NOS in insulin-induced vasodilatation and glucose uptake using HE clamp under Alfaxan anaesthesia.

## 2.2 Methods

All experiments presented in this thesis were carried out in accordance with the Animals (Scientific Procedures) Act 1986. Experiments were performed on 18 male Wistar rats (weight  $238 \pm 9$ g; Charles River, Kent, UK). The rats had been housed in cages in the Biomedical Services Unit (BMSU) on a controlled 12 hour light-dark cycle and allowed standard rat chow and water *ad libitum*.

### 2.2.1 Anaesthesia

Anaesthesia was induced and maintained as described by (Bryan and Marshall, 1999). Anaesthesia was induced by passing the inhalation anaesthetic Isoflurane (3.5 % Novartis Animal Health UK Ltd., Herts, UK) in 4 L.min<sup>-1</sup> O<sub>2</sub> through a transparent box into which the animal had been placed. Lack of righting ability and loss of the pedal withdrawal reflex was taken as indicative of adequate anaesthesia. The animal was then placed in a supine position on an operating table and 3.5 % isoflurane in 4 L.min<sup>-1</sup> O<sub>2</sub> was delivered via a face mask. A vinyl cannula (Portex OD = 1.40 mm, ID = 0.63 mm) containing the steroid anaesthetic Alfaxan (Alfaxalone 10 mg.ml<sup>-1</sup> dissolved in cyclodextrin; Vétoquinol UK limited, Bucks, UK) diluted 1:2 with 0.9% saline was inserted into the jugular vein. Flow of Isoflurane in O<sub>2</sub> was then stopped and the respiratory rate was used as an indicator of depth of anaesthesia. Bolus doses of 0.05 ml Alfaxan were given to maintain an adequate level of anaesthesia as judged by respiratory rate of ~ 60 per minute and absence of withdrawal reflex during tracheotomy. The trachea was isolated and cannulated with a stainless steel T-shaped cannula so animals

could breathe room air spontaneously throughout the experiment and for patency. Anaesthesia was then maintained by a continuous infusion of Alfaxan ( $1.2 \text{ ml.hr}^{-1}$ ; dose of  $12 \text{ mg.kg}^{-1}.\text{hr}^{-1}$ ) via an infusion pump (Braun Perfusor Secura FT, Braun, Germany) through the jugular vein cannula (Bryan and Marshall, 1999); 0.05 ml boluses of Alfaxan were administered as necessary to ensure that somatic reflexes, tested at regular intervals by pinching the paw, gave no more than sluggish withdrawal of the paw, and that arterial pressure, heart rate and respiration were stable.

### **2.2.2 Surgical Preparation**

Several cannulae were then inserted (see below). As Heparin interferes with free fatty acid cycling and therefore potentially plasma insulin concentrations during HE clamp, all implanted cannulae were filled with saline containing sodium citrate (20mM; Tri-sodium citrate dihydrate; Merk, Darmstadt, Germany) as an anti-coagulant.

The right brachial artery was separated from the right brachial vein and nerve plexus and cannulated with polythene tubing (Portex, OD = 0.8 mm, ID = 0.4 mm). This cannula was used to obtain arterial blood samples throughout the experiment, for the determination of blood glucose concentrations and blood gases (see below).

The left brachial artery was isolated as above and cannulated with polythene tubing (Portex, OD = 0.8 mm, ID = 0.4 mm) and connected to a pressure

transducer (type 4-4222 Bell and Howell Ltd., UK) for the measurement of arterial blood pressure (MABP). The pressure transducer was calibrated before each experiment by using a mercury sphygmomanometer.

The right femoral vein was isolated and cannulated with vinyl cannula (Portex OD = 1.40 mm, ID = 0.63 mm) and the right femoral artery was cannulated with polythene cannula (Portex, OD = 0.96 mm, ID = 0.58 mm). The tips of both cannulae were advanced under the inguinal ligament towards the bifurcation of the vena cava and dorsal aorta and were used for the infusion of glucose and insulin (artery and vein respectively) during the experimental protocol (see below).

An incision was made into the left inguinal region and the abdominal muscle was retracted to allow the left femoral artery to be isolated. A perivascular flowprobe (0.7 V) attached to a flow meter (T106 small animal blood flow meter; Transonic Systems Inc., NY, USA) was placed around the artery proximal to the abdominal wall in order to measure femoral blood flow (FBF). Ultrasound gel (Henleys Medical, Herts, UK) was applied to the flowprobe to provide good acoustic coupling.

The animal was placed on a thermostatic blanket connected to a thermocouple (Harvard Bioscience Inc, Massachusetts, USA) that was used to measure rectal temperature; this allowed rectal temperature to be maintained at 37 °C ( $\pm$  0.5) for the duration of the experiment.

A MacLab/8s data acquisition system with Chart software (AD Instruments Ltd.) was used to collect the cardiovascular variables (MABP and FBF) at a sampling frequency of 100 Hz onto a Power Mac G5 computer (Apple Computers Inc.). MABP and FBF were recorded via a MacLab bridge amplifier (AD Instruments Ltd). Heart rate (HR) and mean ABP (MABP) were derived on-line by Chart from the MABP and mean FBF (MFBF) was derived from FBF. Femoral vascular conductance (FVC) was computed online by dividing FBF by MABP with a calculation frequency of 2Hz. As indicated above, continuous display of cardiovascular variables provided an additional means of assessing depth of anaesthesia, adequate depth being depth represented by stable traces for MABP and HR.

Following surgery and setting up the recording equipment, an equilibration period of one hour was allowed. Before the start of the experimental protocol, a 150µl arterial blood sample was collected in a heparinised capillary tube for determination of pH using a blood gas analyzer (Instrumentation Laboratory, xMA, USA). A 80µl arterial sample was similarly collected and centrifuged at 11,800 rpm for five minutes (Micro-haematocrit centrifuge; Hawksley and Sons Ltd., Lancing, UK) for determination of haematocrit (Hct). Hct was calculated by dividing the height of the cellular fraction by the height of the cellular fraction plus plasma. These measurements were repeated at the end of the protocol.

During the protocol (see below), blood glucose concentrations were measured at defined intervals in a small drop of arterial blood (~0.6µl) by using an AccuChek Aviva Glucose Meter (Roche Diagnostics GmbH, Mannheim, Germany).

On completion of each experimental protocol the tibialis anterior (TA) and extensor digitorum longus (EDL) muscles were excised and transverse sections of the mid portion of the muscle were cleanly cut, placed on labelled cork disks covered in Optimum Cutting Temperature (OCT) Embedding Matrix (Raymond A Lamb Ltd., East Sussex, UK) and immediately frozen in liquid nitrogen cooled isopentane ( $-170^{\circ}\text{C}$ ; Sigma Aldrich, Poole, UK). These samples were stored at  $-80^{\circ}\text{C}$  for later immunohistological analysis (see below).

At the end of each experiment the animal was humanely killed whilst under anaesthesia by anaesthetic overdose (Euthatal, Merial Animal Health, Harlow, Essex, UK) and cervical dislocation.

### **2.2.3 Experimental Protocol**

#### **Group 1 – hyperinsulinaemic euglycaemic clamp control (HE clamp control)**

In these rats ( $n = 10$ ) Insulin (Humulin®R; Eli Lilly, Indianapolis, USA) (Ross et al., 2007a) diluted in saline to a concentration of  $300 \text{ mU.ml}^{-1}$  was infused at  $30 \text{ mU.min}^{-1}.\text{ml}^{-1}$  for 120 minutes. Blood glucose concentration was measured five minutes before and approximately every five minutes for the first 30 minutes of insulin infusion and every 10 minutes thereafter. In each animal, glucose (30 % w/v; Sigma Aldrich, Poole, UK) was infused at a rate selected with the aim of maintaining blood glucose concentrations at  $\sim 4.8 \text{ mmol.l}^{-1}$  (Ross et al., 2007a).



To this end, glucose infusion rate (GIR) was generally increased to around 25  $\text{mg} \cdot \text{min}^{-1} \cdot \text{kg}^{-1}$ . See Figure 2.1 for representation of protocol.

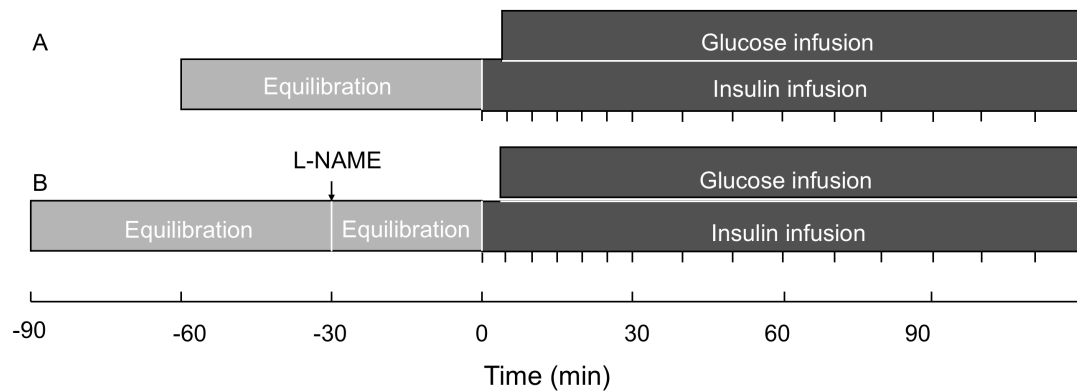


**Figure 2.1 Representation of experimental protocol.**

Surgery was followed by an equilibration period of 60 minutes. For control animals (A) insulin infusion was started following this equilibration period. Glucose infusion was started following a drop in blood glucose concentrations. For L-NAME treated animals (B) a bolus dose of L-NAME was given following the 60 minutes equilibration period and insulin infusion was started at 30 minutes after L-NAME treatment and conducted as for (A).

## **Group 2 – hyperinsulinaemic euglycaemic clamp + L-NAME (HE clamp + L-NAME)**

This protocol was carried out as described for Group 1 above ( $n = 8$ ) except that the NOS inhibitor L-NAME ( $10 \text{ mg} \cdot \text{kg}^{-1}$ ; Sigma Aldrich, Poole, UK) (Bryan and Marshall, 1999) was given at the end of the equilibration period and 30 min was then allowed before the HE clamp was conducted as above.

### **2.2.4 Analysis**

Data were extracted in 60 second intervals every 10 minutes from -10 to 110 minutes from the raw traces of MABP, HR, FBF and FVC in Chart and then

analysed in StatView. These data were used to calculate the mean  $\pm$  SEM for each group at each time point.

Blood glucose concentrations were not taken at set time points. Thus, the values measured were allocated to the nearest 5-10 minute time points so that mean and SEM values could be calculated.

ANOVA for repeated measures was applied to the continuously recorded variables to establish whether the variable changed and Dunnett's post hoc test was applied to determine the time at which the variable changed.

Factorial ANOVA was used to compare response between groups. Fisher's post hoc test was applied to determine the time at which the groups varied.

The baseline values of FBF, FVC and blood gases at the beginning and end of each of experimental protocols 1 and 2 were compared with a Student's *t*-test.

## **2.3 Results**

### **2.3.1 Cardiovascular variables during hyperinsulinaemic euglycaemic clamp**

Table 2.1 shows baseline values for MABP, HR, FBF and FVC in control and L-NAME treated animals. MABP was significantly higher in L-NAME group, whereas HR, FBF and FVC were significantly lower.

MABP was unchanged from baseline during HE clamp for both the control and L-NAME group. MABP in the L-NAME group was significantly higher than in controls at all time points during HE clamp ( $P < 0.05$ ; Figure 2.2 A). In the L-NAME group HR was significantly lower than in controls at time points -10, 0, 10 and 30 minutes ( $P < 0.05$ ; Figure 2.2 B) but not at 20 and 40 - 110 minutes. Towards the end of HE clamp (80-110 minutes), HR in the L-NAME group was raised significantly above baseline ( $P < 0.05$ ).

During the HE clamp FBF significantly increased from 30 minutes onwards in the control group, reaching a maximal increase at 60 minutes and then returning toward baseline. The FBF increased was from  $1.23 \pm 0.10$  to  $2.15 \pm 0.19$  ml/min (see Figure 2.3 A). The maximal change in FBF in the control group was  $0.92 \pm 0.14$  ml/min. Variability increased in the FBF data of the control group after FBF had achieved its maximal level (see Figure 2.3 A) because in some animals FBF waned towards baseline and in others there was a maintained increase. L-NAME treatment significantly decreased baseline FBF such that it was lower than baseline in control group ( $P < 0.05$ ;  $0.50 \pm 0.06$  vs.  $1.23 \pm 0.10$  ml/min). By contrast with the control group, FBF remained constant throughout HE clamp in L-NAME treated animals (Figure 2.3 A).

The FVC data are explained by the FBF data as there was no significant change in MABP in either group. Thus, the HE clamp caused an increase in FVC in the control group reaching significance from 40 to 90 minutes and a maximal increase at 60 minutes from  $0.011 \pm 0.001$  to  $0.020 \pm 0.002$  ml/min/mmHg (see Figure 2.3 B). The maximal change in FVC in the control group was  $0.009 \pm 0.001$

ml/min/mmHg. Mean FVC fell towards baseline from 60 – 110 minutes, with a concomitant increase in standard error reflecting the fact that some rats showed a maintained increase in FVC. By contrast, FVC was unchanged throughout HE clamp in L-NAME group (Figure 2.3 B).

### **2.3.2 Blood glucose and glucose infusion rate during hyperinsulinaemic euglycaemic clamp**

Table 2.2 shows baseline blood glucose concentrations for animals in control and L-NAME treatment groups. As can be seen they varied from 3.4 to 8.4 mM.

Blood glucose concentrations in each group were not significantly different from the intended concentration of 4.8 mmol/L from 15 minutes onwards of the HE clamp (see Figure 2.4 A). However, the two groups were significantly different during the early stages of the clamp blood glucose concentrations in L-NAME treated group being significantly lower than in the control group from 0-15 minutes. Figure 2.4 C gives an indication of the variability in the blood glucose concentration during the HE clamp in individual control animals.

The GIR required to maintain blood glucose at 4.8 mmol/L increased gradually in control animals from time zero reaching a plateau at ~20 mg/kg/min at ~ 90 minutes (Figure 2.4 B). Glucose infusion rates in L-NAME group were significantly greater than the control group from 10 minutes onwards ( $P < 0.05$ ),

GIR increasing much more steeply in the L-NAME group to reach a plateau at ~ 30 mg/kg/min at ~ 80 minutes.

### **2.3.3 Effect of hyperinsulinaemic euglycaemic clamp on blood components**

Figure 2.5 shows potassium and lactate concentrations for control and L-NAME groups before and after HE clamp. Haematocrit percentage is combined data for both (control and L-NAME) groups. Haematocrit was not significantly different from baseline following the HE clamp. Potassium concentration was however significantly decreased following HE clamp in both control and L-NAME treated groups ( $P < 0.05$ ), while lactate concentration was significantly increased following HE clamp in both control and L-NAME treated groups ( $P < 0.05$ ).

	<b>Control</b>	<b>L-NAME</b>
<b>Baseline MABP (mmHg)</b>	113.8 ± 0.10	147.3 ± 5.1*
<b>Baseline HR (bpm)</b>	404.7 ± 10.6	350.8 ± 10.7 *
<b>Baseline FBF (ml/min)</b>	1.23 ± 0.10	0.5 ± 0.06 *
<b>Baseline FVC (ml/min/mmHg)</b>	0.011 ± 0.001	0.003 ± 0.000 *

**Table 2.1 Baseline values for femoral blood flow, femoral vascular conductance, blood pressure and heart rate.** Table shows mean ± S.E.M for control (n=10) and L-NAME (n=8) treated animals at time point zero. \*  $P < 0.05$  all L-NAME baseline variables were significantly different from control.

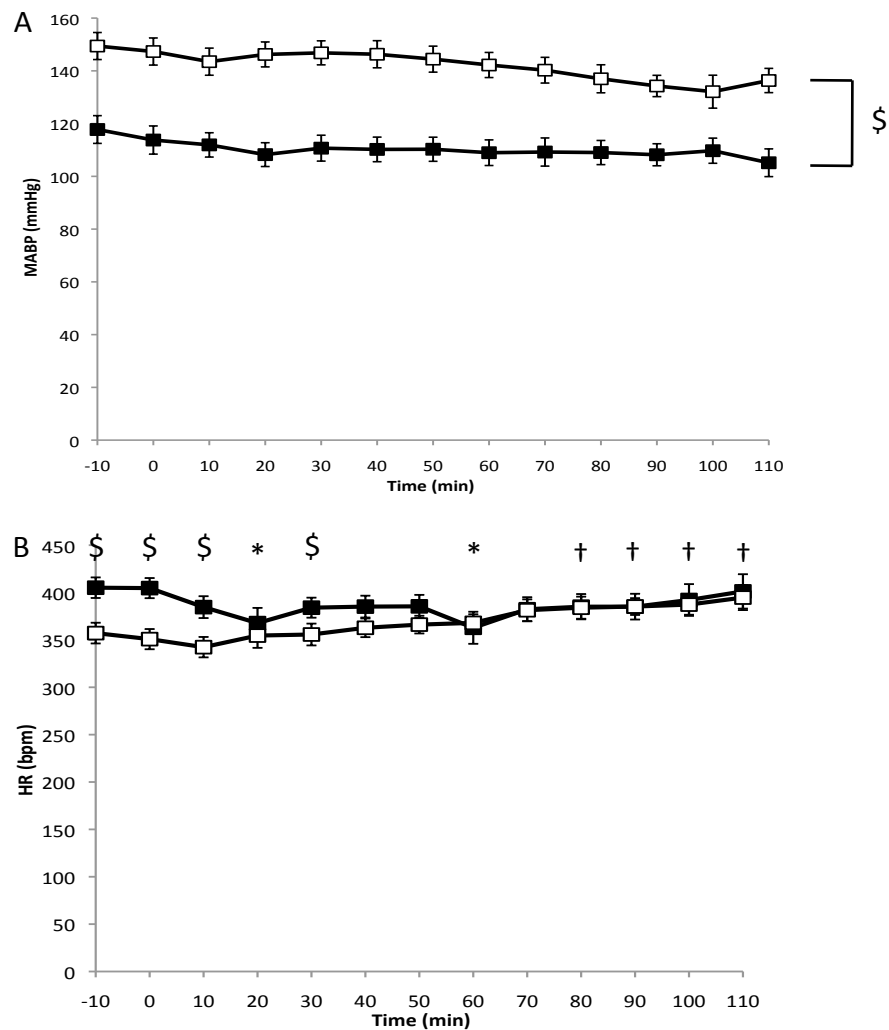


**Figure 2.2. Effect of hyperinsulinaemic euglycaemic clamp (control) with or without L-NAME treatment on mean arterial blood pressure and heart rate.** Graphs show mean  $\pm$  S.E.M MABP (A) and HR (B) for control (closed symbols;  $n=10$ ) and L-NAME treated animals (open symbols;  $n=8$ ) at each time point. L-NAME significantly increased baseline mean arterial blood pressure and significantly decreased baseline heart rate versus control ( $P<0.001$  and  $P<0.005$  respectively; not represented on the graph for simplicity). \*, †  $P < 0.05$  vs baseline (0 min) for control or L-NAME treated animals respectively (Dunnetts post hoc test). \$  $P < 0.05$  control vs. L-NAME treated animals.

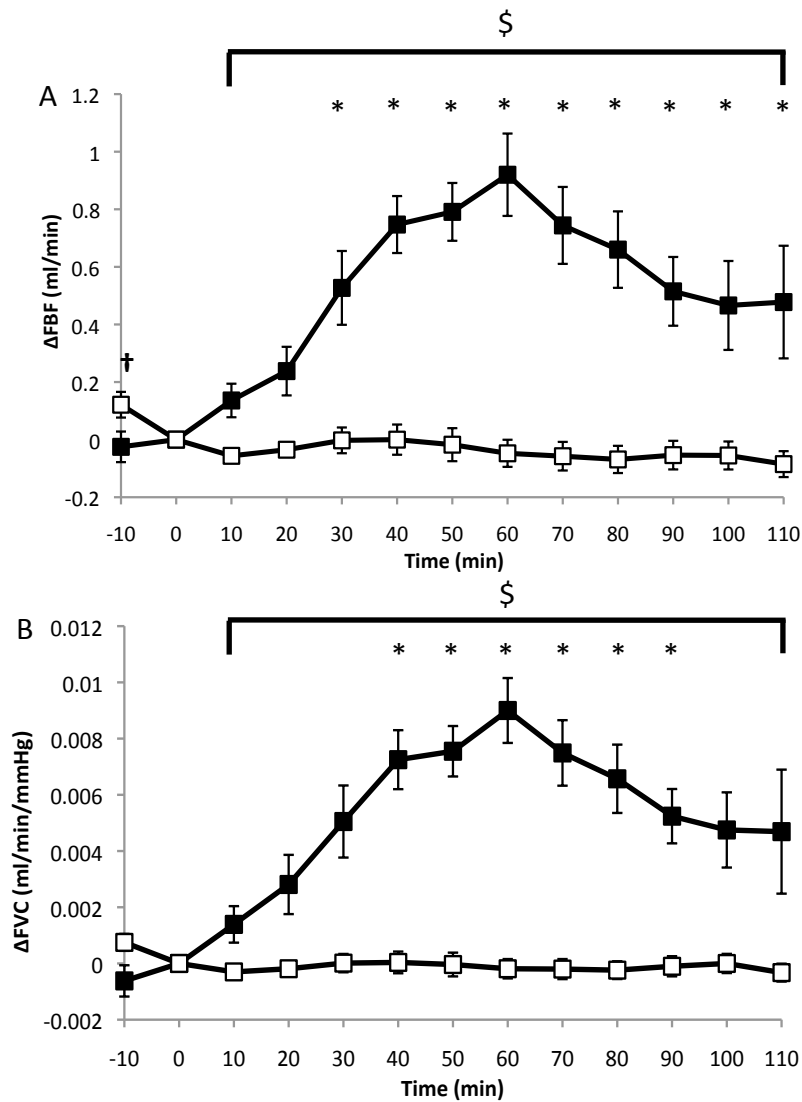


**Figure 2.3. Effect of hyperinsulinaemic euglycaemic clamp (control) with or without L-NAME treatment on change in femoral blood flow and femoral vascular conductance.** Graphs show mean  $\pm$  S.E.M for control (closed symbols;  $n=10$ ) and L-NAME treated animals (open symbols;  $n=8$ ) at each time point. \*,  $\dagger$   $P < 0.05$  versus baseline (0 min) for control or L-NAME treated animals respectively (Dunnetts post hoc test). \$  $P < 0.05$  control vs. L-NAME treated animals.



	Animal ID	Blood Glucose (mM)
Control	1	5.2
	2	5.5
	3	5.7
	4	5.2
	5	4.8
	6	5
	7	5.9
	8	4.1
	9	7.4
	10	6.8
L-NAME	11	3.4
	12	7.8
	13	8.4
	14	5.6
	15	5.6
	16	6.5
	17	6.4
	18	6.2
	Mean $\pm$ SEM	5.9 $\pm$ 0.3

**Table 2.2 Shows basal blood glucose concentrations for all experimental animals.** Values show the baseline blood glucose measurement taken for control animals (1-10) and L-NAME treated animal (11-18).

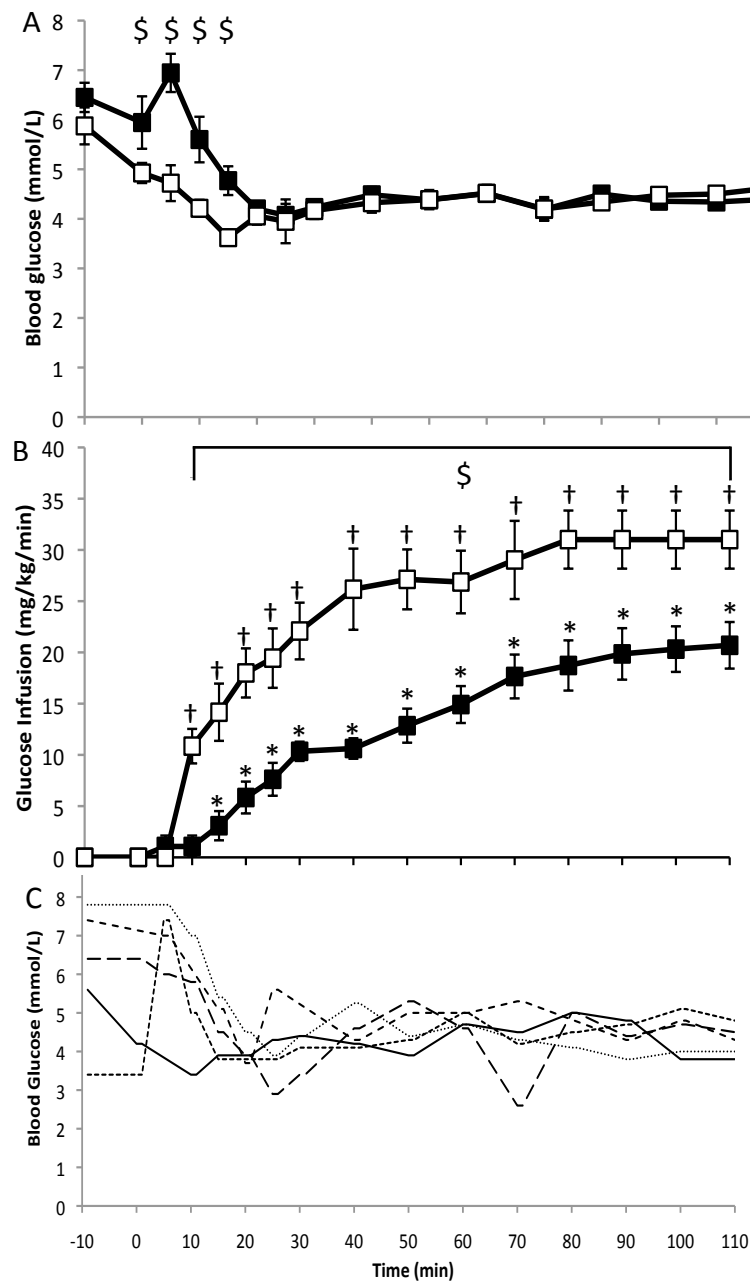


**Figure 2.4. Effect of hyperinsulinaemic euglycaemic clamp (control) with or without L-NAME treatment on blood glucose and glucose infusion rate.** Graphs show (A) blood glucose concentrations and (B) glucose infusion rate for control (closed symbols; n=10) and L-NAME treated animals (open symbols; n=8). Graph (C) shows blood glucose concentrations for five control animals. \*, †  $P < 0.05$  vs baseline (0 min) for control or L-NAME treated animals respectively. \$  $P < 0.05$  control vs. L-NAME treated animals.

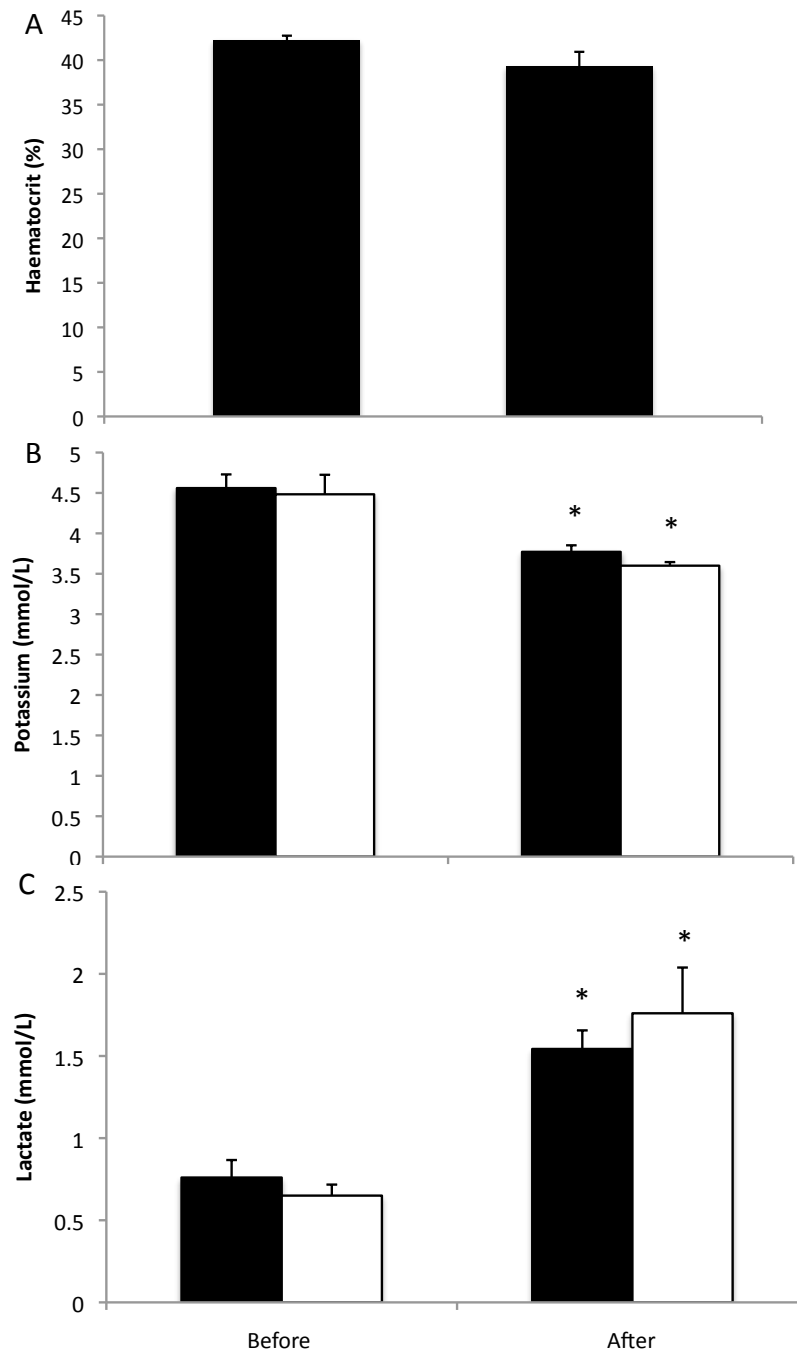


**Figure 2.5. Effect of hyperinsulinaemic euglycaemic clamp on haematocrit, potassium and lactate.** Bars show mean  $\pm$  S.E.M for before and after hyperinsulinaemic euglycaemic clamp (n=11) for (A) haematocrit, (B) potassium and (C) lactate. Bars in (B) and (C) represent HE clamp with (white) or without (L-NAME) \*  $P < 0.05$  versus before for control for after clamp time point (Student's  $t$ -test).

## 2.4 Discussion

The main findings of the experiments presented in this chapter were as follows. HE clamp in Wistar rats anaesthetised with Alfaxan that were allowed food *ad lib* until they were used for the acute experiments, did not significantly affect MABP or HR. However, HE clamp caused vasodilatation in the hindlimb with the maximal increase in FVC attained at 60 minutes from the beginning of HE clamp. During the HE clamp there was also a significant increase in the GIR required to keep blood glucose constant at 4.8 mM that plateaued at ~ 90 minutes; the increase in GIR began at ~ 15 minutes and before the increase in FVC which did not begin until 40 minutes. Administration of L-NAME prior to HE clamp and thus NOS blockade, significantly increased baseline MABP and significantly decreased HR versus control at baseline. L-NAME also completely abolished the insulin-induced increase in FVC, but significantly increased GIR required to maintain blood glucose concentration at 4.8 mM.

### 2.4.1 Cardiovascular variables during hyperinsulinaemic euglycaemic clamp

The finding that in rats under Alfaxan anaesthesia, HE clamp did not affect MABP is consistent with previous work by other investigators who showed MABP to be maintained during HE clamp in rats anaesthetised with sodium pentobarbital (Vincent et al., 2003, Zhang et al., 2004).

Heart rate was also unchanged during the HE clamp in the control group as has previously been reported (Vincent et al., 2003, Zhang et al., 2004). Heart rate in anaesthetised animals is partly a reflection of depth of anaesthesia and thus its stability also indicates stable anaesthesia throughout the protocol.

The finding that in the control group FBF began to increase after 30 minutes and reached a maximal increase of  $0.92 \pm 0.14$  ml/min at 60 minutes in response to insulin infusion at 10 mU/kg/min is consistent with the findings of Zhang et al., (2004) who reported a maximum change in FBF of  $\sim 1$  ml/min with the same dose of insulin in Wistar rats. Not surprisingly, FVC (calculated as FBF/MABP) followed the changes in FBF because there were no significant changes in MABP. In other words, there was a substantial muscle vasodilator response to insulin that reached significance from baseline at 40 minutes and until the end of the HE clamp the maximal increased being at 60 minutes.

The finding of no change in MABP during the HE clamp, but a significant muscle vasodilatation is somewhat surprising for it can be assumed that the increase in vascular conductance occurred in all muscle. This would be expected to have a large effect on total peripheral resistance as muscle vasculature accounts for about 20% of total peripheral resistance and therefore reduce MABP. As discussed by Clarke et al., (2003) there must either have been a counter-regulatory increase in cardiac output (CO) or vasoconstriction in organs, such as the gastrointestinal tract, kidneys and/or the skin. The lack of change in MABP or HR in the present chapter suggests that CO was not changed (although this was not directly measured). Hence, it seems more likely that there was a

redistribution of blood flow between organs. Indeed, it is likely that the maintenance of MABP was due to increased sympathetic nerve activity. For example, Vollenweider et al., showed that the absence of a drop in MABP during insulin-induced vasodilatation was associated with increased muscle sympathetic nerve activity and plasma noradrenaline (Vollenweider et al., 1995). Additionally, in patients with autonomic failure and therefore sympathetic vasoconstrictor failure, intravenous insulin administration lowered arterial blood pressure substantially (Mathias et al., 1987). The counteracting vasoconstriction could therefore have been the result of a baroreceptor-mediated reflex increase in sympathetic nerve activity in vascular beds other than the muscle, such that MABP was maintained constant.

The marked time delay between the beginning of insulin infusion and the beginning of the increase in FVC such that it began at ~40 minutes, after the increase in GIR, raises the possibility that the dilatation was secondary to the increase in GIR and was therefore secondary to a metabolic effect on skeletal muscle (for further discussion see below). The latter finding is consistent with the results of Yang et al., (1989) who showed a 20 minute time delay between insulin appearance in the plasma and appearance in the lymph.

It is also interesting that in the present study, the insulin-induced increase in FVC, decayed after maximal vasodilatation at 60 minutes, despite the maintained HE clamp conditions until 110 minutes. Thus, the plasma insulin concentrations, plasma glucose concentrations and glucose uptake were all consistent during the period of decline in FVC from 60 minutes onwards. This was not the case in the

results presented by (Zhang et al., 2004) who used the same infusion dose of insulin but found that FBF remained raised. It is important to note that the variability in the FVC data following the maximal vasodilatation at 60 minutes (see Figure 2.3) which reflects the fact that some animals showed a maintained increase in FVC and FBF while others showed a decline in both variables. Thus, it was only some animals of the present study that contrasted with the mean behaviour of the data shown by Zhang et al., (Zhang et al., 2004).

A possible explanation of the decline in FVC or relative vasoconstriction seen in the second half of the HE clamp in some animals is the production of endothelin-1 (ET-1) by insulin and the MAP kinase pathway, as discussed in the General Introduction (Section 1.8). However it is surprising if, in healthy rats, in which there was tonic production of NO (see below) ET-1 had such a profound effect on the vasodilator response. Firstly, NO inhibits the conversion of Big ET-1 to ET-1 by endothelin converting enzyme (ECE) thus limiting the release of ET-1 (see review by (Vanhoutte, 2000)). Secondly, although ET-1 acts on ET<sub>A</sub> receptors on the vascular smooth muscle to produce vasoconstriction, ET-1 also acts on ET<sub>B</sub> receptors on endothelial cells, which increases the synthesis of NO; this effect of ET-1 normally limits the vasoconstrictor response (Vanhoutte, 2000). It therefore seems unlikely that ET-1 caused the secondary vasoconstriction seen in some of the control group, particularly as blockade of NOS did not reveal or enhance the vasoconstrictor response (see Figure 2.3 and below). The involvement of ET-1 could be tested in further experiments using an endothelin receptor antagonist (such as PD145065) in conjunction with an HE clamp.

Another possible explanation for the secondary vasoconstriction relates to the use of Alfaxan as an anaesthetic. As mentioned in Section 2.1, Alfaxan preserves autonomic control of the cardiovascular system when compared to pentobarbital anaesthesia (Marshall, 1987). Thus, it is possible that the waning of the increase in FVC towards the end of HE clamp resulted from increased activation of the sympathetic nervous system evoked by insulin, which does not occur when using pentobarbital as an anaesthetic. Consistent with this idea, Scherrer et al., showed that there is a significant time delay of at least 60 minutes between maximal increases in plasma insulin concentration and maximal increases in muscle sympathetic nerve activity in non-anaesthetised human subjects (Scherrer et al., 1993). If this is the explanation, it substantiates the proposal made above that the baroreceptor reflex also helped to counterbalance the vascular responses evoked by insulin under Alfaxan anaesthesia. Otherwise MABP would not only have been expected to fall in association with the increase in FVC but also to rise from 60 minutes onwards when FVC returned towards baseline.

#### **2.4.2 Blood glucose concentration and glucose infusion rate**

As Figure 2.3 demonstrates, in the fed rats of the present study blood glucose concentration initially fell in response to insulin infusion in the control group and glucose had to be infused at a variable rate in individual animals in order to achieve blood glucose concentrations at  $\sim 4.8 \text{ mmol.l}^{-1}$ . In fact there was variability within and between animals in blood glucose concentration during the beginning of the clamp (Figure 2.4 A) and throughout the protocol (Figure 2.4 C). This variability probably reflects the fact that the decision was taken to



maintain blood glucose at a pre-determined concentration (4.8 mM) as described by Ross et al., (Ross et al., 2007b). Thus, some animals were forced to higher and some to lower blood glucose concentrations than their own physiological concentration in order to maintain 4.8 mmol.l<sup>-1</sup>. The variability seen in the present study raises the question as to whether this aspect of the protocol is appropriate if the aim is to carry out detailed investigations of the relationship between vasodilatation and glucose uptake.

Despite the fluctuating glucose concentrations at the beginning of the HE clamp, blood glucose was successfully maintained at ~4.8mmol by adjusting GIR, during the later stages of insulin infusion, from 25 – 110 minutes. Unfortunately, plasma insulin concentrations were not measured in these experiments. However, given the supraphysiological infusion rate of insulin (30 mU/kg/min) during these experiments and the fact that insulin exposure is considered to be the product of both dose of insulin and period of exposure (Yki-Jarvinen and Utriainen, 1998) it is reasonable to assume that plasma insulin concentration was raised well above physiological concentrations (~200 pmol/L). It should be noted that, in experiments conducted by Zhang et al., (2004) insulin infusion of 30 mU/kg/min for 120 minutes raised plasma insulin concentrations in fed Wistar rats from 337 ± 31 to 9,667 ± 660 pmol/L.

Since glucose infusion rates during the HE clamp were significantly increased versus baseline from 15 minutes onwards, whereas the increase in FVC did not reach significance until 40 minutes, it seems likely as argued above, that the arterial resistance vessels that contributed to the increase in FVC dilated as a

consequence of metabolic products produced by muscle following the increase in GIR. In other words they did not respond to insulin *per se* but their metabolic products. Nevertheless, it is possible that dilation of terminal arterioles that increase distribution of blood flow to capillary beds did occur prior to, or with the onset of the increase in GIR (Rattigan et al., 1997), and that their dilatation did not significantly affect FVC. In accord with the evidence discussed in the General Introduction the substance that links muscle metabolism with vasodilatation could have been adenosine (see Section 1.5.5). This would be interesting to test in future experiments.

#### **2.4.3 Effects of L-NAME**

As expected baseline MABP was significantly higher in animals treated with L-NAME than in the control group; inhibition of NO synthase (NOS) L-NAME removed the tonic vasodilator effects of NO on the vasculature. This outcome is consistent with many previous studies (eg. (Bryan and Marshall, 1999)). Further, in the L-NAME group baseline HR was lower than control until 30 minutes onwards. The initial fall in HR could be attributed to the fact that the baroreceptor reflex response to raised MABP results in bradycardia (Bryan and Marshall, 1999).

As in the control group, MABP was maintained throughout the HE clamp after L-NAME. It was suggested above that the maintenance of MABP during insulin infusion despite muscle vasodilatation in the control group was a result of insulin acting to increase baroreceptor-induced modulation of sympathetic

nerve activity and sympathetic output . In experiments on humans, Scherrer et al., (1994) showed that after systemic administration of L-NMMA at concentrations that did not alter baseline blood pressure, but inhibited forearm insulin-induced vasodilatation, insulin infusion then caused a significant increase in blood pressure suggesting that the effect of insulin on sympathetic nerve activity was preserved. In the present study, the increase in baseline MABP and fall in baseline FVC induced by L-NAME may have masked any insulin-induced increase in blood pressure and decrease in FVC evoked by insulin's action on SNA. However, it can not be excluded that the L-NAME acted at least in part via the CNS. For, it has been shown that intracerebroventricular administration of L-NMMA (500 µg) in rats prevented insulin-induced increases in glucose uptake, muscle blood flow and microvascular perfusion induced by HE clamp (10 mU/kg/min), suggesting that NO acts centrally as well as peripherally to modulate insulin's vasodilator and metabolic effects (Bradley et al., 2010). Thus, it may be that in the present study L-NAME also acted centrally to inhibit the action of insulin on sympathetic nerve activity.

It should be noted that towards the end of HE clamp, HR in the L-NAME group was raised significantly above the original baseline. This could be a result of reduced effectiveness of a single bolus of L-NAME being given prior to the HE clamp to inhibit tonic vasodilatation and therefore raise MABP over time. In accord with this suggestion, the MABP did fall slightly over the course of the protocol in the L-NAME group which would have been expected to reduce the baroreceptor-mediated bradycardia effect. This suggestion does not however indicate a lack of effectiveness of L-NAME on the hindlimb vasculature with time

as the increase in FVC evoked by HE clamp in the control group was absent throughout the HE clamp in the L-NAME group.

Considering the effects of L-NAME on femoral vasculature in more detail, L-NAME given 30 minutes before beginning HE clamp significantly decreased baseline FBF and FVC compared to control animals (Table 2.1) indicating significant NO-induced tonic vasodilatation that was removed. At -10 minutes before the HE clamp began the FBF was significantly increased above baseline at 0 minutes, which indicates that the HE clamp was started before FBF had reached a new baseline after L-NAME infusion. Nevertheless, L-NAME completely blocked insulin's ability to increase FBF and FVC above baseline which agrees with previous reports by Clark's group in experiments in which only 10 mU insulin was used (see (Ross et al., 2007b)). Thus, the present study indicates that the insulin-induced increase in FVC is completely NO-dependent even, at supraphysiological doses of insulin.

Rather unexpectedly, glucose infusion rate was significantly higher at the end of the HE clamp in the L-NAME group versus control from 10 – 110 minutes. Therefore the present results indicate an increase in glucose uptake in response to insulin following inhibition of NO synthesis, amounting to ~50% increase from ~ 20 up to ~ 30 mg/kg/min.

This finding contrasts with results of previous studies on anaesthetised rats or humans that showed L-NAME to decrease (Baron et al., 1995, Vincent et al., 2003), or not affect (Scherrer et al., 1994) respectively, insulin-induced glucose

uptake. The increase in GIR in response to HE clamp after L-NAME is particularly surprising because the loss of vasodilatation in the muscle would be expected to decrease the access of glucose for uptake into the muscle. It is possible that the increased glucose uptake was directly linked to the decrease in NO availability (Baron et al., 1995, Baron et al., 2000, Sartori et al., 1999). Thus, Kapur et al., (1997) showed in skeletal muscle *in vitro* that both the NO donor GEA 5024 and sodium nitro-prusside induced dose-dependent inhibition of insulin-stimulated glucose uptake. However, most studies have demonstrated that NO donors increase glucose uptake and that NOS inhibitors reduce glucose uptake by direct effect on the muscle. Additionally, if the model put forward by Barrett et al., (2011) is correct and intracellular insulin signalling involving NO is able to increase transendothelial transport of insulin then one would expect a decrease in glucose uptake in response to L-NAME.

A possible explanation for the increase in glucose infusion rate seen in the present study, and thus presumably the increase in glucose transport into the skeletal muscle is the ability of NO to negatively regulate the mitochondrial respiratory chain by inhibiting cytochrome *c* oxidase (the terminal enzyme in the mitochondrial respiratory chain) therefore limiting respiration (Brown, 2001). However, the increase in plasma lactate (indicative of anaerobic respiration) does not support this argument. Likewise, it is unlikely that an increase in respiration and therefore ATP production could operate for ~ 3 hours without removal of the excess glucose.

The decrease in baseline blood flow and the lack of vasodilatation in response to insulin after L-NAME may have potentiated the accumulation of adenosine evoked by insulin's action on muscle fibres, particularly as intracellular acidosis facilitates adenosine accumulation (Tu et al., 2010a). Vasodilatation evoked by adenosine in muscle is attenuated by NOS inhibition with L-NAME (Ray and Marshall, 2009). Thus, it is not surprising there was no increase in FVC but adenosine may have acted on receptors on muscle to increase GIR (Thong et al., 2007).

The increase in GIR in response to HE clamp after L-NAME treatment in the present experiments warrants further investigation, but is not within the scope of this thesis. It is also important to note that the GIR measured was for whole body glucose disposal, but that vascular responses were recorded only in the hindlimb. Thus, if there are large changes in hepatic response then these will manifest as disconnection between the FVC and GIR results.

#### **2.4.4 Effect of hyperinsulinaemic euglycaemic clamp on blood parameters**

There was no significant difference in haematocrit following HE clamp when control and L-NAME groups were considered together. This was an important finding as despite the fact that the HE clamp described above was taken from an established protocol (Ross et al., 2007a), it has not previously been conducted during intravenous infusion of an infusion anaesthetic. In the current experiments in which ~6 mls were infused with the anaesthetic during the experiment and ~2 mls were removed for analysis, it was important to test

whether there was significant haemodilution. In fact, the combination of infusions and blood sampling used in the protocol had no such effect

Plasma potassium concentrations were significantly decreased following HE clamp in both groups which is consistent with insulin's known effects to cause hypokalaemia (Natali et al., 1993). However, the decrease was less than 1 mM and not sufficient to have a significant cardiovascular effect (Wilson et al., 1994). The increase in plasma lactate in both groups is indicative of an increase in anaerobic glucose metabolism and may be explained excess pyruvate production by the muscle was converted to lactate.

#### **2.4.5 Limitations of hyperinsulinaemic euglycaemic clamp protocol**

The methodology used for the HE clamp in the present study was based on the experimental methods described in the study of (Ross et al., 2007a). However as a consequence of performing the present study it became clear that there are several ways that the method could be improved to make results more physiological, consistent and reliable. These limitations are outlined below.

As indicated above, control of blood glucose concentration at the onset of insulin infusion in the experimental animals was poor. There was significant variation in blood glucose in individual animals and between animals in the same experimental group. It was vital for future experiments that much better control of blood glucose is achieved. It also seems better that blood glucose should be kept at euglycaemia for each animal so that the effects of hyperinsulinaemia can

be assessed without the confounding effects of changing the animals blood glucose concentration. This is of particular importance because if the clamped blood glucose is set too far from euglycaemia (3.4 – 8.4 mmol/L; see table 2.3), then the possibility of acute changes in glycaemia during HE clamp is enhanced, increasing the coefficient of variation for blood glucose and affecting estimations of insulin sensitivity (Muniyappa et al., 2008).

In the present experiments, the blood glucose concentration was measured every 5 for the first 30 minutes of HE clamp and every 10 minutes thereafter. To improve glucose control in future experiments, particularly during the dynamic first half of clamp, it would be better to take a sample to measure blood glucose concentration every 3 minutes from 10 min to 50 min of HE clamp and at every 5 minutes before and after this period. This should allow for closer monitoring of blood glucose concentration and reduce oscillations in glucose concentration due to the time lag in adjustment of glucose infusion rate. This is vital if GIR is to be used as an accurate representation of glucose uptake in muscle.

In the present experiments, glucose was infused at a concentration of 30 % (w/v) and the rate was adjusted in  $\text{ml}\cdot\text{hr}^{-1}$  in whole integers. In order to achieve finer control of blood glucose in future experiments, it would be better if glucose were infused at a lower concentration of 20 % (w/v), with the rate being adjusted in  $\text{ml}\cdot\text{min}^{-1}$  by using an infusion pump accurate to two decimal places; both adjustments would allow much finer control of the GIR.



Apart from natural variation between animals, an additional source of variation in blood glucose concentrations throughout the HE clamp was likely to have been the fact that the rats were allowed to feed prior to experimental intervention. Thus, the prevailing blood glucose concentrations would have been high in some animals due to food intake, but lower in those who chose not to feed. The present experiments were conducted on animals that were allowed food due to the observation of (Zhang et al., 2004) that insulin-induced vasodilatation was greater in fed, than fasted animals. In order to test this further, the relationship between metabolic status of the animal and magnitude of insulin-induced vasodilatation was directly explored in the experiments of Chapter 3 with groups of rats that were either fed or fasted.

In the present study, insulin was administered using plastic syringes. As insulin is a peptide, the plastic may have bound a significant amount of insulin (DeFronzo et al., 1979). This may have reduced the concentration of insulin that was actually administered below that intended (Kraegen et al., 1975). This could be overcome in future by using Hamilton glass syringes to administer the insulin solution so as to reduce the binding of insulin and allow greater accuracy. Insulin also binds avidly to the salts in saline solution and this reduces its availability in the tissue. To avoid this insulin can be diluted in the plasma expander Haemaccel, which is commonly used as a carrier for insulin.

As discussed above, in L-NAME-treated rats HR was significantly decreased at baseline versus control animals but rose from 30 – 40 minutes during the HE clamp protocol. The L-NAME was given as a single bolus before the HE clamp as

described previously in this laboratory (Bryan and Marshall, 1999), in order to limit infusion volumes given in conjunction with the infusion of anaesthetic. However, this may have resulted in reduced effectiveness of NOS blockade towards the end of the protocol. Thus in future experiments, L-NAME could be given as a bolus followed by an infusion or a repeat bolus dose could be given.

Additionally, it is important to note that in the experiments presented in this chapter there is a change in baseline values of MABP, HR and particularly FBF and FVC following L-NAME infusion. This is because NOS inhibition removes the tonic vasodilator effect of NO by decreasing cGMP concentrations in the vascular smooth muscle. With cGMP concentrations low, insulin may not be able to cause dilatation by any mechanism, whether or not this is normally via an increase in NO synthesis (Wit et al., 1994). Thus, ideally the experiments would be repeated with a NO clamp: NO donor infusion to re-establish basal NO tone. Thus the effects of inhibiting new insulin-induced NO synthesis via eNOS would be seen, in the absence of a change in basal NO-induced dilator tone. This experiment has not been conducted by other investigators and would give significant insight into the NO dependence of insulin-induced vasodilatation.

#### **2.4.6 Conclusions**

The experiments described in this Chapter showed that HE clamp in Alfaxan anaesthetised Wistar rats that must have produced supraphysiological concentrations of plasma insulin, does not affect mean arterial blood pressure or heart rate, but induces an insulin-induced increase in FVC (vasodilatation) in the

hindlimb beginning at 30 minutes, achieving a maximal increase at 60 minutes and then waning. The HE clamp also caused a rapid and significant increase in glucose infusion rate beginning at 10 – 15 minutes and therefore prior to the increase in FVC. L-NAME administration, and thus NOS blockade, completely abolished insulin-induced the vasodilatation evoked even by supraphysiological doses of insulin showing it is NO-dependent, but significantly increased glucose infusion rate; the mechanisms underlying this are not clear.

## **CHAPTER 3 - EFFECT OF NUTRITIONAL STATUS ON INSULIN-INDUCED VASODILATATION DURING HYPERINSULINAEMIC EUGLYCAEMIC CLAMP**

### **3.1 Introduction**

In Chapter 2, the difficulties encountered in controlling blood glucose concentration at a constant concentration at the beginning of HE clamp in fed rats, and the associated variability in insulin-induced glucose uptake and the variability in the muscle vasodilator responses towards the end of the HE clamp were discussed. It was proposed that this variability was due in part to the relatively high, but variable intrinsic concentrations of insulin and glucose at baseline. Thus, in the experiments described in the present chapter, additional steps were taken to improve control of blood glucose concentration throughout the HE clamp and blood glucose was controlled at each rat's own basal concentration rather than at a pre-determined concentration of 4.8 mM.

Additionally, as discussed in the General Introduction (see Section 1.5.3), there is a lack of consistency between published studies as to whether or not animals were fasted prior to investigation of insulin-induced vasodilatation. This was even the case in studies from one laboratory, for instance, Clark's group seem to have either fasted rats prior to experimentation (Vincent et al., 2003, Zhang et al., 2004) or allowed them access to food *ad libitum* (Ross et al., 2007b, Youd et al., 2000) but did not discuss this issue when considering their results. On the other hand, Zhang et al., (Zhang, Vincent et al. 2004), who conducted dose

response curves to insulin in both fed and fasted rats, reported significantly different responses in hindlimb blood flow between the two groups, dilatation being much greater in the fed group. However, these experiments were conducted in different strains of rat the fed rats being Wistars and the fasted being Sprague Dawleys. Thus, these results were not conclusive on the effect of feeding. The experiments described in this chapter therefore directly compared insulin-induced muscle vasodilatation to the same dose of insulin in fed and fasted Wistar rats.

Although it is well established that the vasodilator actions of insulin are NO-dependent (see Chapter 2), given the immediacy of NO's action, it is not clear why, if the dilatation is NO-mediated, the onset of the vasodilator effects of insulin and maximal vasodilatation are delayed compared to the rapid action of insulin on glucose uptake. It is possible that glucose uptake stimulated during the initial stages of HE clamp has a secondary effect to cause insulin-induced vasodilatation; that is, metabolites produced as a consequence of glucose uptake may act to cause the vasodilatation. Indeed it was suggested by Ueda et al., (1998) that the blood glucose concentration has a direct effect on insulin's action. Thus, they showed that insulin has a relatively minor vasodilator effect when infused alone, but a much more pronounced effect when infused in conjunction with D-glucose (Ueda et al., 1998). Moreover, several other studies have provided evidence that blood glucose concentration affects insulin-induced vasodilatation (Ueda et al., 1998, Feldman et al., 1995, Mathias et al., 1987). Thus, a major aim of the experiments in this chapter was to compare insulin-induced muscle vasodilatation in fasted animals, when plasma insulin and glucose

concentrations are low and in fed animals when plasma insulin and glucose concentrations are high, the hypothesis being that dilatation would be greater in the latter.

### **3.2 Methods**

Experiments were performed on 15 male Wistar rats (weight  $222 \pm 14$ ; Charles River, Kent, UK) that had been housed in cages on a controlled 12 hour light-dark cycle. Fed animals were allowed standard rat chow and water *ad libitum* until the time at which they were taken from the cage for the acute experiment. Fasted animals were fasted in a wire bottomed cage for 16 hours prior to experimentation but were allowed water *ad libitum*.

#### **3.2.1 Anaesthesia**

Induction of anaesthesia and tracheotomy were performed as detailed in section 2.2.1 except that the jugular vein was cannulated with three vinyl cannulae (Portex OD = 0.8 mm, ID = 0.4 mm superglued inside Portex OD = 0.96 mm, ID = 0.58 mm) (Oakes et al., 2001). Cannulae were used for the administration of insulin, glucose and the steroid anaesthetic Alfaxan (Alfaxalone 10 mg.ml<sup>-1</sup> dissolved in cyclodextrin; Vétoquinol UK limited, Bucks, UK) diluted 1:2 with 0.9% saline.

#### **3.2.2 Surgical Preparation**

Surgical preparation was carried out as in section 2.2.2 with the following

exceptions.

The polythene tubing inserted into the right brachial artery was adapted to allow the continuous infusion of 20mM sodium citrate ( $10 \mu\text{l} \cdot \text{min}^{-1}$ ) as well as the withdrawal of arterial blood samples with a Y tubing adapter (Small Parts, Inc., Seattle, USA). The right femoral artery and vein were not cannulated because the additional cannulae used in the experiments of Chapter 2 were inserted in the jugular vein (see above). Heart rate (HR), mean arterial blood pressure (MABP), femoral blood flow (FBF), femoral vascular conductance (FVC) and blood glucose (BG) were recorded or derived as detailed in Section 2.2.2.

At the end of each experiment the animal was humanely killed whilst under anaesthesia by anaesthetic overdose (Euthatal, Merial Animal Health, Harlow, Essex, UK) and cervical dislocation.

### **3.2.3 Experimental Protocol**

#### **Group 1 – fasted hyperinsulinaemic euglycaemic clamp**

Blood glucose concentrations were measured at defined intervals in a small drop of arterial blood ( $\sim 0.6 \mu\text{l}$ ) by using an AccuChek Aviva Glucose Meter (Roche Diagnostics GmbH, Mannheim, Germany). Basal blood glucose concentration for each rat was averaged from three basal blood glucose samples at (-20, -10 and 0 minutes before insulin infusion). Blood glucose concentration was then

measured at predetermined time points, every 2 – 4 minutes from 0 – 50 minutes of the protocol and every 5 minutes thereafter. In these rats (n=7) human recombinant insulin (Humulin®R; Eli Lilly, Indianapolis, USA; as described by (Ross et al., 2007) was infused at a constant rate of 10 µl/min to achieve a dose of 30 mU/kg/min for 120 minutes. In each rat, glucose (20 % w/v; Sigma Aldrich, Poole, UK) was infused at a variable rate in order to maintain blood glucose concentrations at the rats' basal concentration (i.e. isoglycaemia although this will still be described as euglycaemia due to the maintenance of a 'normal' blood glucose concentration).

Insulin and glucose were both infused using gas tight Hamilton syringes (Harvard Bioscience Inc, Massachusetts, USA) in order to reduce the binding of insulin to the equipment.

### **Group 2 – fed hyperinsulinaemic euglycaemic clamp**

In fed rats (n=8), the protocol was undertaken as detailed above for fasted animals.

#### **3.2.4 Analysis**

For all cardiovascular variables, data were extracted for 60 second periods every 10 minutes from the raw recordings in Chart and then analysed in StatView. ANOVA for repeated measures was applied to the continuously recorded variables in both groups to establish whether the variable changed and Dunnett's post hoc test was applied to determine the time at which the



variable changed.

Factorial ANOVA was used to compare response in  $\Delta$ FBF and  $\Delta$ FVC between fed and fasted groups. Fisher's post hoc test was applied to determine the time at which the groups varied.

Integrated FBF was also calculated in Chart as FBF during HE clamp minus baseline and also expressed as a two phase response due to the observation that FBF reached a peak at  $\sim$  70 minutes in the fed group and then fell towards baseline (see Figure 3.4). Whole response and the two phases were compared between groups by using an unpaired Student's *t*-test.

Glucose infusion rate (GIR) at steady state and baseline values of FBF, FVC, MABP, HR and blood glucose in fed and fasted experimental groups were compared using an unpaired Student's *t*-test.

### **3.3 Results**

#### **3.3.1 Cardiovascular variables during hyperinsulinaemic euglycaemic clamp**

Table 3.1 shows baseline values for MABP, HR, FBF and FVC in fed and fasted animals. Baseline MABP, HR and FVC were not significantly different between groups at baseline, although there was a trend for FVC to be greater in fasted than fed. Baseline FBF was significantly higher in the fasted rats versus fed rats

( $P < 0.05$ ). Both Baseline BG and steady state GIR were significantly higher in the fed rats ( $P < 0.05$ ).

Figure 3.1 shows MABP (A) and HR (B) during HE clamp for fed and fasted animals. MABP and HR were not different between fed and fasted animals at any time point. Moreover, MABP was unchanged versus baseline for both fed and fasted rats throughout the HE clamp. HR was also unchanged versus baseline for both fed and fasted animals.

HE clamp in fed rats significantly increased FBF from baseline, from 40 to 70 minutes with a maximum increase versus baseline at 60 minutes (see Figure 3.2 A; from  $1.10 \pm 0.14$  to  $1.54 \pm 0.20$  ml/min;  $P < 0.05$ ). The maximal change in FBF in fed animals was  $0.44 \pm 0.14$  ml/min. By contrast, in fasted rats FBF was not significantly changed from baseline throughout the clamp. FVC reflected FBF and thus, HE clamp significantly changed FVC from 30 to 70 minutes with a maximum increase versus baseline at 60 minutes (see Figure 3.2 B) in fed rats. FVC was not significantly changed from baseline in fasted rats throughout the HE clamp.

Area under curve (integrated FBF) was calculated to further analyse the different responses in the fed and fasted rats. FBF was chosen rather than FVC as it reflects the delivery of blood (and therefore insulin and glucose) to the muscle, which is of physiological relevance for the hypotheses being tested. Integrated FBF for the duration of HE clamp (0-110 minutes) was significantly higher in fed rats (see Figure 3.3 A;  $P < 0.05$ ). The FBF response was split into two sections for

both groups (0 – 70 and 70-110 minutes) to correspond to the point where FBF began to wane and was no longer significantly different from baseline in the fed animals. Fed rats showed an overall increase in AUC over the time course of the HE clamp with a large increase in AUC from 0 – 70 minutes (17.2 AU) and a smaller increase in AUC from 70 – 110 minutes of clamp where the vasodilatation was waning (6.4 AU). This manifests as a monophasic vasodilatation, with a slow onset vasodilatation from 0 – 70 minutes of the clamp and then a waning of the dilatation from 70 – 110 minutes of the clamp. AUC was not significantly different from baseline at either time point in fed rats. In contrast, in fasted rats, there was an overall small decrease in AUC (-3.0 AU) with a small increase in AUC from 0 – 70 minutes (4.0 AU) and a decrease in AUC from 70 – 110 minutes (-7.0 AU; see Figure 3.3 B). This shows a monophasic response where there is very little change in blood flow in the first half of the clamp and a vasoconstriction in the second half. AUC was not significantly different from baseline at either time point in fasted rats. AUC was not significantly different between fed and fasted animals for 0 - 70 minutes of clamp, but was significantly different for 70 - 110 minutes ( $P < 0.05$ ; Figure 3.3).

Interestingly the two fasted rats that showed the largest increase in blood flow were the two that had the highest basal blood glucose concentration (see Figure 3.4; blood glucose 4.1 and 3.8 mmol/L in comparison to group averages of  $3.5 \pm 0.2$  and  $6.4 \pm 0.2$  mmol/L for fasted and fed animals respectively) and presumably the highest plasma insulin concentrations at baseline.

### 3.3.2 Blood glucose concentration and glucose infusion rate

Table 3.1 shows baseline blood glucose concentrations and steady state glucose infusion rate for fed and fasted animals. Basal blood glucose concentration in fed animals was significantly higher than fasted animals ( $6.4 \pm 0.2$  vs.  $3.5 \pm 0.2$  mmol/L;  $P < 0.05$ ). Blood glucose concentrations for fed rats were significantly higher than for fasted rats at all time points during HE clamp ( $P < 0.05$ ; see Figure 3.4).

Blood glucose concentration fell significantly below baseline in fed rats from 10-24 minutes of the HE clamp (Figure 3.5 A;  $P < 0.05$ ), but then was well maintained at euglycaemic concentrations throughout the clamps. By contrast, in fasted rats, blood glucose concentration was successfully maintained at euglycaemic concentration throughout HE clamp.

Glucose infusion rates increased at a similar rate in fed and fasted animals at the initiation of clamp changing from baseline within 10 minutes. Steady state glucose infusion rate was then significantly higher in fed rats than fasted rats from 24 – 110 minutes ( $P < 0.05$ ) thus maintaining blood glucose concentrations at their respective euglycaemic concentrations (Figure 3.5 B and Table 3.1).

	Fed	Fasted
<b>Baseline MABP (mmHg)</b>	111.1 ± 3.1	110.3 ± 3.4
<b>Baseline HR (bpm)</b>	429.7 ± 9.7	431.9 ± 11.8
<b>Baseline FBF (ml/min)</b>	1.10 ± 0.14	1.57 ± 0.24 *
<b>Baseline FVC (ml/min/mmHg)</b>	0.010 ± 0.001	0.014 ± 0.002
<b>Baseline blood glucose (mmol/L)</b>	6.4 ± 0.2	3.5 ± 0.2 *
<b>Steady state GIR (mg/lbmkg/min)</b>	39.1 ± 3.2	24.3 ± 2.3 *

**Table 3.1** Baseline values for blood pressure, heart rate, femoral blood flow, femoral vascular conductance, blood glucose and steady state glucose infusion rate. Mean ± S.E.M values for fed (n=7) and fasted (n=8) animals at time point zero (baseline) or steady state. \*  $P < 0.05$  fed vs. fasted animals.

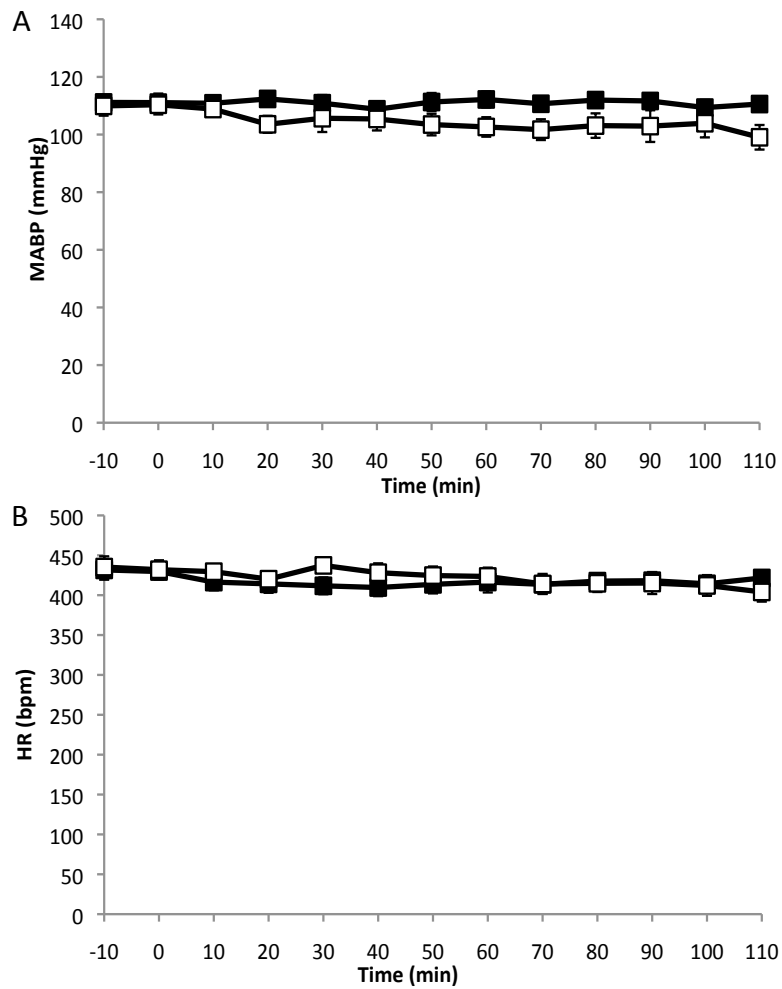


**Figure 3.1 Effect of hyperinsulinaemic euglycaemic clamp in fed and fasted animals on mean arterial blood pressure and heart rate.** Graphs show mean  $\pm$  S.E.M MABP (A) and HR (B) for fed (closed symbols; n=7) and fasted animals (open symbols; n=8) at each time point.

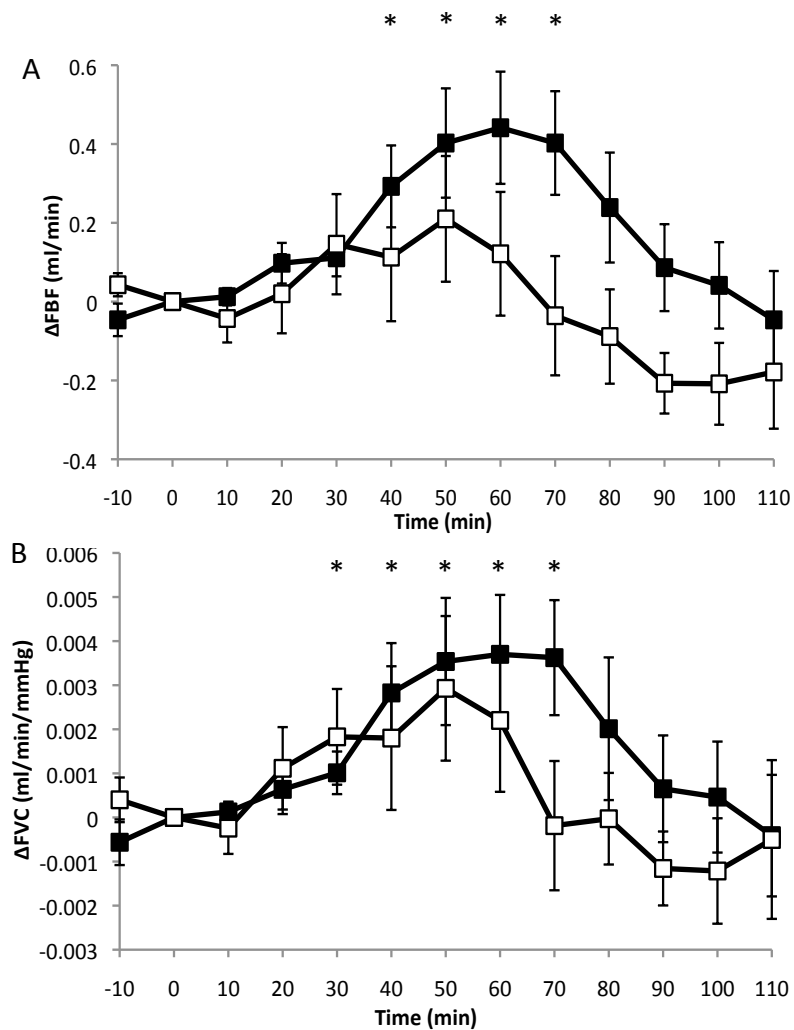


**Figure 3.2 Change in femoral blood flow and femoral vascular conductance evoked by hyperinsulinaemic euglycaemic clamp in fed and fasted rats.** Graphs show mean  $\pm$  S.E.M for fed (closed symbols;  $n=7$ ) and fasted animals (open symbols;  $n=8$ ) at each time point. \*  $P < 0.05$  versus baseline (0 min) for fed animals (Dunnetts post hoc test).

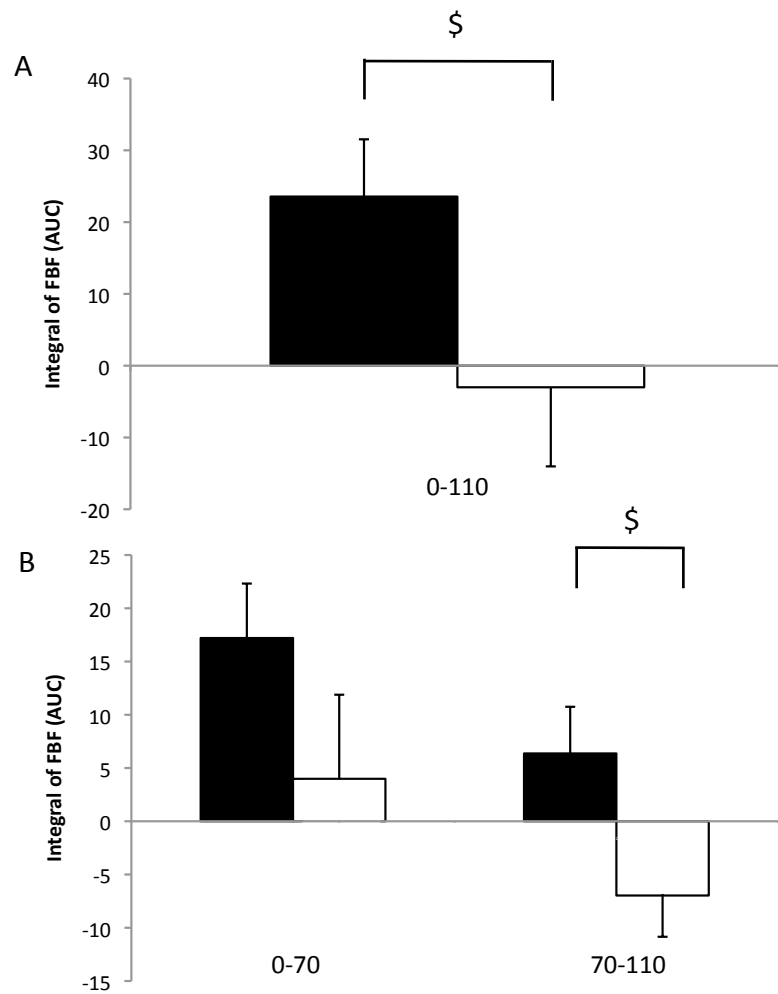


**Figure 3.3 Effect of hyperinsulinaemic euglycaemic clamp in fed and fasted animals on integral of FBF.** Graphs show (A) integral of FBF for duration of HE clamp and (B) integral of FBF for 0-70 and 70-110 minutes for fed (solid bar; n=7) and fasted animals (open bar; n=8). \$  $P < 0.05$  fed vs. fasted animals.



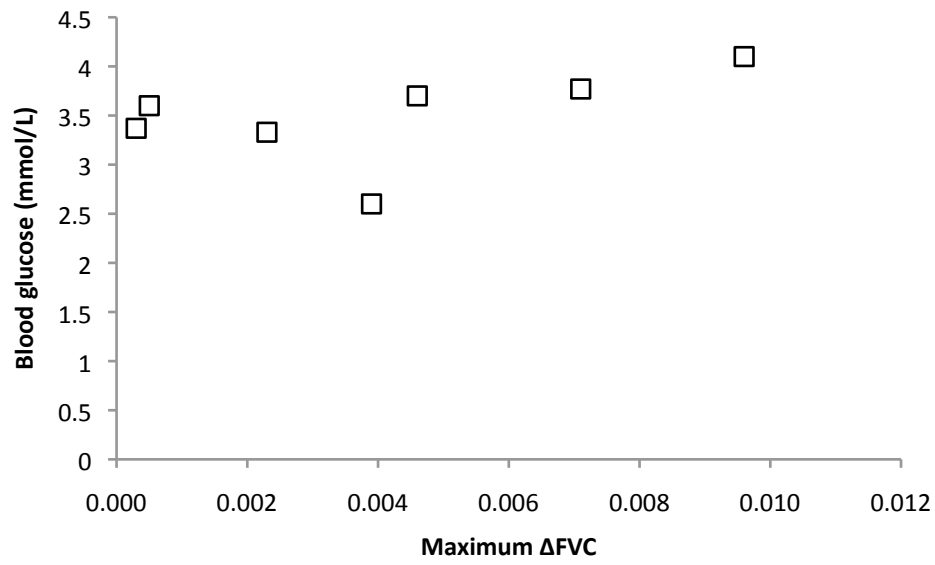


**Figure 3.4 Maximal change in femoral vascular conductance plotted against blood glucose concentration for fasted animals.** Graph shows maximum change in femoral vascular conductance for each animal relative to each animal's individual blood glucose concentration for fasted animals.

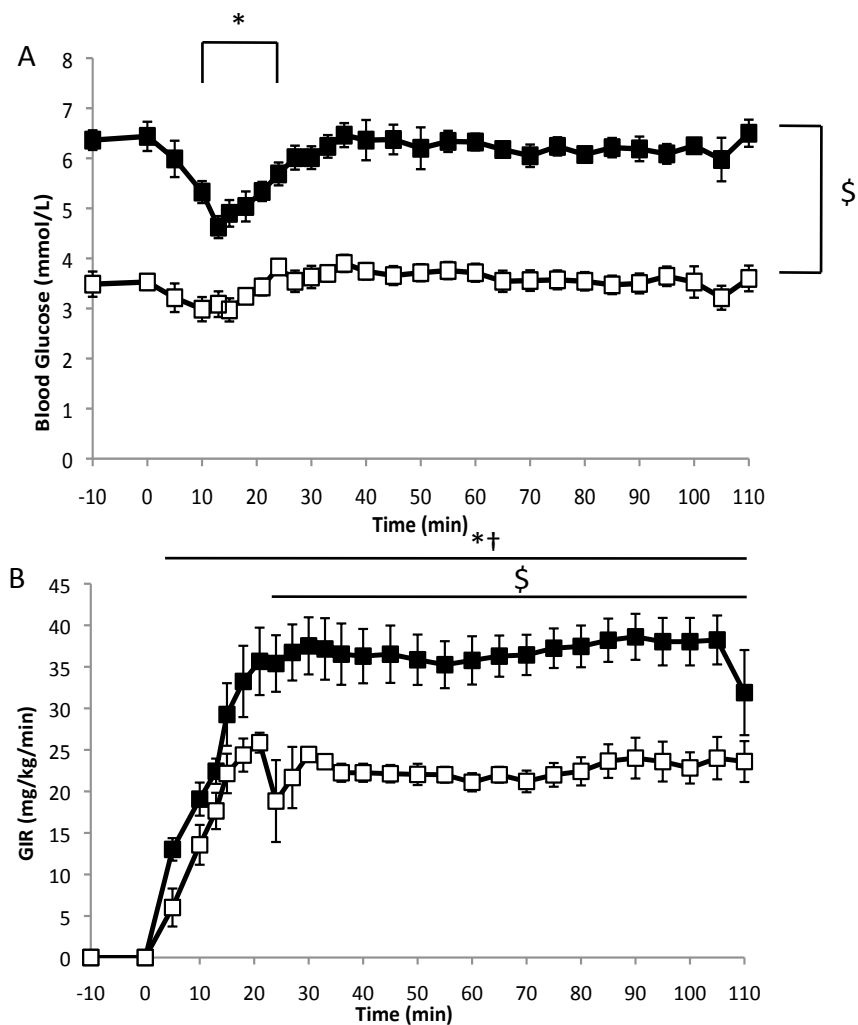


**Figure 3.5 Effect of hyperinsulinaemic euglycaemic clamp in fed and fasted animals on blood glucose and glucose infusion rate.** Graphs show (A) blood glucose concentrations and (B) glucose infusion rate for fed (closed symbols;  $n=7$ ) and fasted animals (open symbols;  $n=8$ ).  $\$ P < 0.05$  fed vs. fasted animals.  $*, \dagger P < 0.05$  versus baseline (0 min) for fed and fasted animal respectively (Dunnetts post hoc test).

### **3.4 Discussion**

The main findings of the experiments presented in this chapter were as follows. HE clamp did not affect mean arterial pressure or heart rate in either fed or fasted rats. Fed rats exhibited a muscle vasodilatation that peaked at ~ 60 minutes and then waned for the rest of the HE clamp. By contrast, fasted rats exhibited a late muscle vasoconstrictor response to HE clamp, with no change in FVC in the first half of the clamp, loss of vasodilatation that began at ~ 70 minutes of the clamp. Basal blood glucose concentration and glucose infusion rate were significantly higher in the fed animals versus fasted. Control of blood glucose in the initial stages of the HE clamp (0 – 30 minutes) was much tighter in the fasted animals, but glucose concentration was well maintained from 30 – 110 minutes in both fed and fasted rats. The increase in GIR evoked by the HE clamp began at ~10 minutes in both fed and fasted rats and thus preceded changes in FVC in both groups.

#### **3.4.1 Cardiovascular variables during hyperinsulinaemic euglycaemic clamp**

Baseline FBF was significantly lower in the fed, than fasted rats (Table 3.1). This is most likely due to a redistribution of blood flow away from muscle and towards to the gastrointestinal tract in fed animals in association with absorption (Zacho et al., 2012). Baseline MABP and HR were comparable in the fed and fasted groups indicating that the higher FBF in the fed rats, must have been balanced by vasoconstriction in the gastrointestinal tract and/or by

increased cardiac output. Due to the difference in the basal FBF values, the *changes* in FBF and FVC in the two groups are considered below.

Throughout the HE clamp, HR and MABP were not affected by insulin infusion in either fed or fasted group (see Figure 3.1). This is consistent with previous work that shows MABP to be maintained even when muscle vasodilatation is associated with HE clamp (Vincent et al., 2003, Zhang et al., 2004) as discussed in Chapter 2. Indeed as HR and MABP remained constant in the present study, an increase in muscle blood flow as occurred in fed group represents vasodilatation in skeletal muscle as shown by an increase in FVC.

When the changes in FBF were analysed as the integral of the change in FBF in the first 0 – 70 minutes and the second 70 – 110 minute period of the HE clamp, it became very clear that during the first half of the HE clamp, there was a net increase in FBF in fed rats and very little change in the fasted rats. Further, in the second half of the clamp, when the effects of insulin on glucose infusion rate had plateaued there was a waning of the increase in FBF in the fed animals and a trend for a decrease in FBF from baseline in the fasted animals indicating a vasoconstriction; the responses in the fed and fasted animals were significantly different from each other from 70 – 110 minutes ( $P < 0.05$ ). For a full discussion of the loss of vasodilator response to insulin during HE clamp see Section 2.4.1. Briefly, it is most likely that insulin caused a delayed increase in sympathetic nerve activity that would be expected to cause a vasoconstriction. Given this and the fact that the fed and fasted groups were dosed with the same concentration of insulin, it is interesting that the magnitude of the fall in FBF from peak seen in

the fed group of the present study and in the rats of Chapter 2 that were allowed food ad lib was very similar ( $\Delta$  FBF  $\sim 0.4$  ml/min). What is more the decrease in FBF from baseline in the fasted group of the present chapter was also  $\sim 0.4$  ml/min. Further, these decreases in FBF all began at  $\sim 70$  minutes. It therefore seems likely that insulin infusion evoked a vasoconstriction mediated by an increase in sympathetic nerve activity that was not affected by the metabolic status of the animal.

The fact that the change in GIR occurred before the increase in FVC in the fed rats and that there was no increase in FBF in the fasted rats is consistent with the ideas of Cleland et al., (1999) that vasodilatation is caused by some by-product production of skeletal muscle glucose metabolism. In fasted animals, endogenous concentration of glucose was low and presumably endogenous insulin was therefore also low. Thus, it can be argued that glucose uptake into the muscle was much lower (versus fed) and that this results in the production of only small amounts of metabolic products capable of producing vasodilatation. The opposite would have been true in the fed animals: a greater amount of metabolic dilator products would have been produced. In agreement with this idea, it is interesting to note that the two rats that showed the largest increase in blood flow in the fasted group were the two that had the highest basal blood glucose concentration (blood glucose 4.1 and 3.8 mmol/L in comparison to group averages of  $3.5 \pm 0.2$  and  $6.4 \pm 0.2$  mmol/L for fasted and fed animals respectively) and presumably the highest plasma insulin concentrations.

The proposal that vasodilatation of proximal arterioles that contribute to the increase in FVC is mediated by metabolic byproducts is consistent with the findings of McKay and Hester (1996) who showed by using *in vivo* microscopy of hamster cremaster muscle, that an adenosine receptor antagonist-inhibited insulin-induced vasodilatation induced in proximal and distal arterioles of skeletal muscle. Their hypothesis was that adenosine produced by the metabolic action of insulin on skeletal muscle is part of a feed forward mechanism that then facilitates insulin's action (McKay and Hester, 1996). Abbink-Zandbergen also provided evidence that adenosine is involved in insulin-induced vasodilatation in healthy humans as intrabrachial infusion of drafazine (an adenosine-uptake blocker) or theophylline (adenosine-receptor antagonist) increased and decreased respectively insulin-induced increases in forearm blood flow (Abbink-Zandbergen et al., 1999). The absence of an increase in FBF of similar time course in the fasted rats may be explained if relatively low concentrations of adenosine were produced in the fasted rats due to their lower rate of metabolism of glucose, such that they only acted back on terminal arterioles to affect distribution of blood flow in the capillary network and were not sufficiently high to dilate the proximal arterioles that regulate muscle blood flow.

An alternative possibility is that the Na<sup>+</sup>, K<sup>+</sup>-ATPase pump was a common link between glucose uptake and insulin-induced vasodilatation in the present study. The Na<sup>+</sup>, K<sup>+</sup>-ATPase channel is ATP driven and so would be expected to be powered by glucose metabolism (Sowers, 1996). Thus, activation of the Na<sup>+</sup>, K<sup>+</sup>-ATPase pump by insulin on vascular smooth muscle and endothelial cells could

enhance hyperpolarisation of vascular smooth muscle cells and stimulation of eNOS in endothelial cells, both contributing to relaxation of blood vessels. It is also possible that translocation of the Na<sup>+</sup>, K<sup>+</sup>-ATPase pump to vascular smooth muscle and endothelial cell membrane induced by insulin could correlate with the slow onset of insulin-induced vasodilatation (Tack et al., 1996a).

Whether adenosine is involved in the vasodilator response to insulin could be tested in future experiments by performing the HE clamp with or without an inhibitor of adenosine such as DPSPX. Likewise, the involvement of the Na<sup>+</sup>, K<sup>+</sup>-ATPase channel could be tested by using the Na<sup>+</sup>, K<sup>+</sup> -ATPase inhibitor ouabain.

It is interesting to compare the results from fed animals in this chapter to the control (fed) group in the previous chapter as the protocols are similar except for a few amendments. The maximal increase in muscle blood flow seen in the fed animals of the present experiments was lower than in the rats of Chapter 2 that were allowed food ad lib, the maximum increase being ~0.4 ml/min in the present chapter and ~0.9 ml/min in the experiments of the previous chapter.

Thus, although the results of the present chapter are consistent with a relationship between glucose uptake and muscle vasodilatation, it is intriguing that in the present experiments when both blood glucose and glucose infusion rate were higher than in the experiments of Chapter 2 (~6 mmol/L and ~35 mg/lbmkg/min versus ~4.8 mmol/L and ~20 mg/lbmkg/min) the vasodilatation was smaller. Given the improvements made to the protocol it is surprising that the change in FBF seen in the present experiments was smaller than others reported in the literature (~0.4 ml/min in the present study

compared to ~1 ml/min reported by (Zhang et al., 2004) following the same infusion of insulin).

It is possible that the improvements made to the protocol explain the differences. It could be that the smaller muscle vasodilatation was due to better control of blood glucose. For instance, the initial increase in blood glucose seen in the rats of Chapter 2 at the onset of HE clamp may have facilitated vasodilatation by a metabolic mechanism. Another possibility is that the fluctuations in blood glucose concentration at the onset of the HE clamp seen in the experiments in Chapter 2 caused release of adrenaline which facilitated the vasodilatation. This seems unlikely as preliminary investigations using the  $\beta_2$  adrenoceptor antagonist ICI 118, 551 indicated that insulin-induced vasodilatation during HE clamp was not caused by adrenaline. In experiments on eight fed rats, the increase in FBF evoked by a 30 mU/kg/min HE clamp was  $0.69 \pm 0.11$  ml/min and so not significantly different from the control response.

### **3.4.2 Blood glucose concentrations and glucose infusion rate**

Figure 3.2 shows that control of blood glucose was improved in experiments of the present chapter compared with those of Chapter 2, from the onset of insulin infusion and that steady state glucose infusion was reached much quicker. Thus, the adjustments made to the methodology – finer adjustment of infusion rate of more dilute glucose, clamping to each animal's own blood glucose concentration and more regular assessment of blood glucose concentration were effective. However, the control of blood glucose concentration was much tighter at the



onset of infusion in rats that had been fasted than in those that had been fed prior to experimentation. This was most likely due to lower basal glucose and presumably lower insulin concentrations in the fasted rats. There was a much greater drop in blood glucose concentration in the fed animals at the onset of the clamp versus that in the fasted animals, and thus presented a greater challenge of controlling blood glucose concentrations in fed rats.

As expected, basal blood glucose concentration was significantly higher in the fed animals versus the fasted animals throughout the protocol (Figure 3.2). As a result of this, to maintain the raised blood glucose concentration, GIR was also significantly higher in fed animals from 15 minutes onwards (Figure 3.2).

Unfortunately, plasma insulin concentrations were not measured in the experiments in this chapter and so it is not possible to compare plasma insulin concentrations between the groups and or calculate insulin sensitivity in fed and fasted rats. It was decided therefore that in order to be able to draw safer conclusions in future experiments, plasma insulin concentrations would be measured from arterial blood samples taken at various time points throughout the HE clamp.

Higher blood concentrations of glucose and endogenous insulin in the fed rats would be expected to mean that insulin infusion increases drive in glucose uptake from the unabsorbed nutrients in the gut towards the skeletal muscle. This may therefore result in more variable blood glucose concentrations in these rats as the amount of glucose uptake from the gut will vary. For future experiments described in this thesis it was essential that this initial drop in blood

glucose reduced in order that a reliable and reproducible HE clamp could be obtained. Control of blood glucose concentration was also key to measurements of insulin sensitivity (M/I) that were planned for future experiments, for assessment of M/I requires that the glucose infused (GIR) is being taken up into the muscle: endogenous concentrations of glucose and therefore insulin must be low. Therefore, on the basis of the results of the present experiments, future experiments described in this thesis were performed on rats that were fasted.

### **3.4.3 Conclusion**

In conclusion I have, for the first time, directly compared the vascular actions of insulin in skeletal muscle during HE clamp in fed and fasted rats of the same strain. Thus, I showed that the vasodilator actions of insulin are dependent on the nutritional status of the animal; fed rats show a muscle vasodilatation that waned whereas fasted animals show muscle vasoconstriction.

## **CHAPTER 4 - EFFECT OF ACUTE NICOTINIC ACID TREATMENT ON INSULIN INDUCED VASODILATATION**

### **4.1 Introduction**

As discussed in the General Introduction FFA have been shown to decrease both glucose uptake (Randle, 1981, Roden et al., 1996) and responses to endothelium-dependent dilators (Steinberg et al., 1997, Pleiner et al., 2002). Briefly, increased FFA concentrations have been shown to decrease insulin-dependent tyrosine phosphorylation of IRS-1 and thus limit the insulin signaling cascade in endothelial cells (Kim et al., 2005). In obesity, the increased fat mass and resistance to insulin-mediated inhibition of lipolysis results in day long exposure to FFA (de Jongh et al., 2004). It is therefore possible that FFAs contribute to the impaired insulin-mediated capillary recruitment and glucose uptake that is seen for example in obese Zucker rats (Wallis et al., 2002). Indeed, insulin-induced PI3-K activation was decreased in arterioles taken from obese Zucker rats during HE clamps (Jiang et al., 1999).

Although many studies involving FFA have involved long time courses, insulin resistance may also be induced by FFAs acutely (Boden et al., 1994); lipid and heparin infusion into healthy human subjects caused a decrease in glucose uptake after 200 minutes when HE clamp and lipid and heparin infusion were started simultaneously. Additionally, lipid and heparin infusion commencing at the same time as HE clamp in healthy humans completely abolished the insulin-mediated increase in glucose oxidation (Bonadonna et al., 1989).

Nicotinic acid (NAc) has been used clinically as a treatment for dyslipidaemia for over 50 years. Acutely, it acts as an antilipolytic agent inhibiting the hydrolysis of triglycerides in adipose tissue and therefore decreases plasma free fatty acid (FFA) concentrations. Chronically, it exerts its beneficial effects on lipid profile by decreasing total cholesterol and low-density lipoprotein (LDL)-cholesterol concentrations whilst increasing high-density lipoprotein (HDL)-cholesterol concentrations. NAc acts via its G<sub>i</sub>-coupled receptor (GPR109A) to inhibit adenylyl cyclase activity, limiting accumulation of cAMP so leading to reduced PKA activity and decreased phosphorylation of hormone-sensitive lipase, thereby decreasing lipolysis. The GPR109A is found mainly in adipose tissue (Wise et al., 2003) but also in the spleen as well as monocytes, Langerhans cells, neutrophils (Maciejewski-Lenoir et al., 2006), keratinocytes (Hanson et al., 2010) and macrophages (Soga et al., 2003).

Despite the potential beneficial effects of NAc to decrease non-esterified fatty acids (NEFA) concentrations, improve lipid profile and so increase insulin sensitivity and glucose tolerance in diabetic patients (Grundy et al., 2002), concerns have been raised about its use. NAc has a relatively short half life and when blood concentrations of NAc decrease, a rebound increase in FFA concentrations can occur, resulting in decreased insulin sensitivity. Further, NAc is known to produce facial flushing, although it has been suggested that this vasodilatation is localised to the skin (Morrow et al., 1992). Thus, the NAc analogue Acipimox (a long acting derivative of NAc) is preferred due to its slower absorption after oral administration and significantly longer half life

(Gille et al., 2008). Several doses of Acipimox given to obese subjects decreased plasma FFA concentrations and increased skeletal muscle glucose uptake and capillary recruitment, as observed by nailfold capillaroscopy on the following morning (de Jongh et al., 2004).

Despite the limitations in the use of NAc clinically, it was decided to use NAc in the present study as a means of causing a rapid pronounced decrease in plasma NEFA concentrations within minutes (Plaisance et al., 2009). The investigations were designed to investigate whether acute lowering of FFA at the onset and throughout HE clamp by infusion of NAc would 1) improve insulin sensitivity by increase insulin-stimulated glucose uptake and 2) increase insulin-induced vasodilatation in both lean and obese Zucker rats. The working hypothesis was that NAc would be able to increase both insulin-induced glucose uptake in the skeletal muscle and NO production and therefore NO-dependent vasodilatation by facilitating the same signaling pathway.

## 4.2 Methods

### 4.2.1 Animal groups

The experiments in this chapter were performed at AstraZeneca. Experiments were performed on 16 lean and 20 obese Zucker rats (Charles River France, France) that had been housed in cages on a controlled 12 hour Light/Dark cycle.

There were six experimental groups in the present study. Firstly, lean and obese rat groups that underwent HE clamp with vehicle (0.9 % sodium chloride) infusion. Secondly, lean and obese rat groups that underwent HE clamp with NAc (64 nmol/kg/min) treatment. Finally, lean and obese rat groups that underwent a sham HE clamp (no insulin or glucose infusions but instead their vehicles, Haemaccel® and 0.9 % sodium chloride respectively) with NAc (64 nmol/kg/min) treatment.

In contrast to the fasted rats in Chapter 3 that were fasted for ~ 15 hours (ie. from 4 pm on the previous day) resulting in basal blood glucose concentrations of ~ 3.9 mmol/L; rats used in these experiments received a fixed ration of diet of 10 or 16 g (lean and obese respectively) at 16:00 on the day before the experiment. These amounts of food were based on previous in-house measurements of food consumption in Zucker rats (Cardiovascular and Gastrointestinal Group, AstraZeneca, Alderley Park). The intention was to provide sufficient food until approximately midnight ~eight hours before the experiment began; the animals can then be considered post absorptive rather

than fasted. This shorter fasting period should reduce the chance of continuing glucose uptake in the gut relative to a fed animal, whilst avoiding the counter-regulatory mechanisms when starvation responses begin to activate.

#### **4.2.2 Anaesthesia**

In contrast to the experiments of Chapter 2 and 3, animals were anaesthetised with an intra-peritoneal injection of sodium-thiobutabarbital (Inactin®, Sigma-Aldrich Ltd, UK). Animals received an initial intra-peritoneal dose of 160-190 mg/kg. Supplementary doses were given via a cannula placed in the jugular vein (see below). This decision was taken so that results could more easily be compared with those of previous studies on rats, which have generally used pentobarbital anaesthesia.

#### **4.2.3 Surgical Preparation**

The cannulae used in this study were not the same as in Chapter 2 and 3 and so the details are given below. All catheters were made from Intramedic™ polyethylene medical grade tubing (Becton, Dickinson and Company, US) and filled with 20mM sodium citrate solution to prevent clotting within catheters.

The right jugular vein was isolated for cannulation. Three catheters (PE10 connected to PE50) were placed into the jugular vein for infusions of insulin, glucose, and compound/vehicle. A fourth catheter (PE10 connected to PE50) was placed in the same vein for periodic bolus doses and infusions of anaesthetic

as required. A fifth catheter (PE10 connected to PE50) was placed in the same vein to ensure a tight seal when the catheters were secured.

A tracheotomy was performed using PE240 tubing rather than the stainless steel cannula used in Chapters 2 and 3. The cannula was used to facilitate breathing during the experimental procedure. Additionally, a stream of Medical O<sub>2</sub> was directed through a water filled cylinder and over the opening of the tracheotomy, with the aim of maintaining arterial PO<sub>2</sub> Levels within physiological range even if respiration was depressed.

The left carotid artery was isolated and separated from the vagus nerve for cannulation. One catheter (PE50) was placed into the carotid artery and secured. This catheter was attached to an adapted sampling system consisting of a modified 3-way stop-tap to allow minimal sample volumes (15µl/sample) and a four way adaptor. This system allowed for blood sampling, recording of MABP, infusion of anti coagulant and a syringe to pull blood back through the system. Carotid artery patency was maintained from shortly after cannulation until the conclusion of the experiment using a continuous infusion (10 µl/min) of 20mM sodium citrate solution via the carotid artery catheter using a 5ml Hamilton syringe and digital syringe pump (Model KDS101, KD Scientific Inc, US).

In addition a perivasular flowprobe was placed on the right femoral artery as described in Chapters 2 and 3 to allow recording of FBF.



Body temperature was monitored and maintained at 37°C using a rectal probe thermo-coupled to a heat blanket (Harvard Apparatus Ltd, UK).

4.2.4 Experimental Protocol

Following surgery, animals were given a 60 minute stabilisation period before commencement of the HE clamp. Details of the protocol are summarised in Figure 4.1.

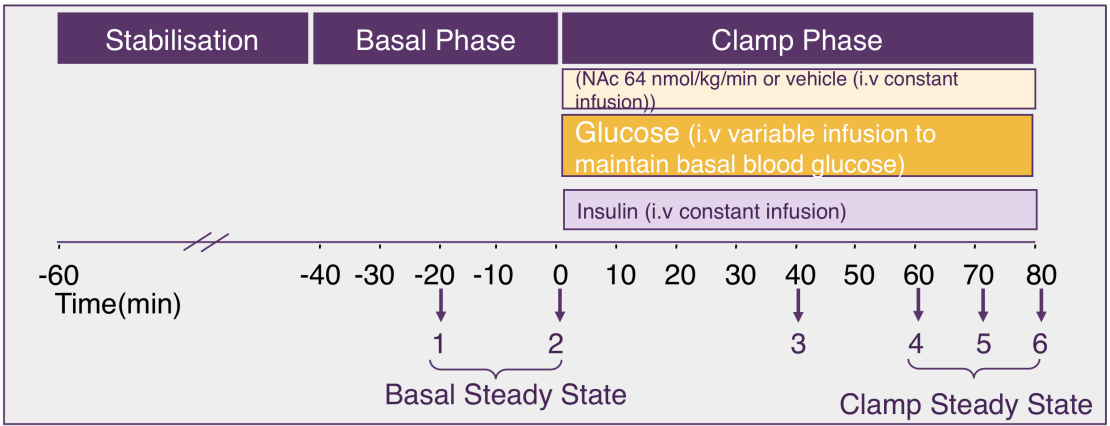


Figure 4.1 Schematic diagram of the HE clamp experimental protocol.

Downward arrows represent time points for arterial blood sampling. Various combinations of NAc, glucose and insulin infusion were used in the three experimental groups (see text). The stabilisation period immediately followed surgery.

4.2.4.1 Basal phase

In each group, arterial blood samples (200 µl) were collected via the carotid catheter at -20 and 0 min for determination of blood glucose concentration by using a Roche Accu-chek® monitor and for plasma glucose concentration by using an YSI 2700 Clinical Analyser (YSI Inc, US). An additional sample was taken

at -10 min for determination of blood glucose concentration using a Roche Accu-chek® monitor only. In addition to the protocols described in Chapter 2 and 3, remaining sample was frozen in 30 µl aliquots for subsequent analysis of plasma insulin concentrations (see below). This also allowed post experimental calculation of insulin sensitivity (M/I) from the hyperinsulinaemic euglycaemic clamp.

The blood glucose concentrations at -20, -10 and 0 minutes were measured and the average of these values was used as the target blood glucose concentration for the HE clamp. The plasma glucose concentrations at -20 and 0 minutes were used to define plasma glucose concentration and the average of these values was the subsequent plasma glucose concentration used for the clamp. Plasma glucose concentration is established during the basal phase so that the ratio of plasma to blood glucose concentration can be monitored during the experiments. If the ratio changes due to haemodilution or other factors, plasma glucose is used as a more accurate measure of glucose concentration as it is not affected by the concentration of red blood cells in the sample. In practice however the ratio did not change and so blood glucose in basal phase was used as target concentration.

#### **4.2.4.2 Clamp phase**

The Lean and Obese NAc Sham received NAc infusion, Lean and Obese NAc Clamp groups received NAc infusion with HE clamp and Lean and Obese Vehicle Clamp groups received vehicle infusion with HE clamp. The HE clamp phase began after collection of the 0 min sample.

Vehicle or NAc was infused via a dedicated jugular vein catheter using a 10 ml Hamilton glass syringe and digital syringe pump (Model KDS101, KD Scientific Inc, US). NAc was prepared by making a stock concentration of 0.788 mg/ml and then diluted in 0.9% sodium chloride to administer 64 nmol/kg/min, at a constant rate of 10  $\mu$ l/min. Vehicle (0.9% sodium chloride) was also administered at 10  $\mu$ l/min.

Human insulin (Actrapid®, Novo Nordisk, Denmark diluted in 10 ml of Haemaccel®) was infused via another dedicated jugular vein catheter using a 5 ml Hamilton syringe and digital syringe pump (Model KDS101, KD Scientific Inc, US). It was infused at a fixed volume infusion rate of 10  $\mu$ l/min so as to deliver a final insulin infusion rate of 10 or 20 mU/kg<sub>LBM</sub>/min in the lean and obese animals respectively. The dose used for the lean rats of the present study was less than used in the experiments of Chapters 2 and 3 (30 mU/kg/min). Obese animals were given twice the concentration of lean animals for several reasons. Firstly, in order to calculate insulin sensitivity 'M/I' of the animals accurately, insulin infusion rates that correspond to the linear part of the insulin sensitivity curve (glucose infusion rate plotted against insulin infusion rate) should be used; otherwise potential differences in insulin sensitivity may be missed (Muniyappa, Lee et al. 2008). Due to the decreased responsiveness of the tissue to the metabolic actions of insulin and to the inhibition of hepatic glucose production, higher insulin infusion rates are required in obese animals in order to target the linear part of the curve. Secondly, as discussed in the General Introduction, obese animals are insulin resistant and therefore require a higher dose in order to elicit

an effect. Thirdly, plasma insulin concentrations are so high in the obese animals that a greater amount of insulin must be given in order to significantly increase plasma concentrations.

Thereafter, arterial blood glucose concentration was determined every 3 to 5 min (Roche Accu-chek) using a modified 3-way stop-tap to allow minimal sample volumes (15µl/sample). Blood glucose was clamped at the basal concentration (see above) by infusing 20% (w/v) glucose via a third jugular vein catheter by using a 10 ml Hamilton syringe and digital syringe pump (Model 22, Harvard Apparatus Ltd, UK).

During NAc sham experiments, Haemaccel® and 0.9% sodium chloride were infused in place of insulin and glucose respectively: Haemaccel® at 10 µl/min and 0.9% sodium chloride at 12 µl/min.

During the clamp period, additional (200 µl) samples were taken at 40, 60, 70 and 80 minutes. 200 µl samples were collected for determination of plasma glucose (using the YSI Clinical Analyser), plasma non-esterified fatty acids (NEFA) concentration (using NEFA-HR(2) ACS-ACOD Method (Wako)) and plasma insulin concentration (using Mercodia Human and Rat Insulin ELISA kit, Mercodia, Sweden, see below). All blood samples were collected into potassium-EDTA coated tubes (Microvette®, Sarstedt Ltd, UK), and were centrifuged (13,000rpm, 5 min, 4°C) immediately for plasma separation. Plasma glucose concentration was determined using the YSI Clinical Analyser and remaining plasma was aliquoted into 0.5 ml Eppendorf tubes, and the samples stored at -

20°C for later determination of endogenous rat insulin, human insulin and NEFA concentration.

At the end of the experimental protocol, animals were humanely killed whilst under anaesthesia by overdose of sodium-thiobutabarbital via the jugular vein and death was confirmed by cervical dislocation.

#### **4.2.5 Calculation of insulin sensitivity**

Insulin sensitivity (M/I) is a measure of tissue responsiveness to a given plasma concentration of insulin. Due to the assumptions made during HE clamp, glucose infusion rate (GIR) is used as an index of skeletal muscle glucose uptake (Muniyappa et al., 2008). Insulin sensitivity was calculated as:

$$M/I (\mu\text{mol/kg/min per pmol/L}) = \text{GIR } (\mu\text{mol/kg/min}) / \text{Plasma insulin (pmol/L)}$$

where GIR is the steady state glucose infusion rate (at the end of HE clamp) and plasma insulin concentrations represent measurements taken at corresponding time points.

#### **4.2.6 Analytical methods**

##### **4.2.6.1 Insulin (Endogenous Rat & Human)**

Individual concentrations of rat insulin and human insulin were determined in plasma samples containing both rat insulin and human insulin using two

Mercodia Insulin ELISA kits. Human insulin was determined using one ELISA (Mercodia Human Insulin ELISA kit, Mercodia, Sweden). In this assay, there was no cross-reaction with rat insulin (as specified in Directions for Use and confirmed by the Analytical Group, AstraZeneca, Alderley Park). Therefore, samples containing both rat insulin and human insulin yielded a measured concentration for human insulin only.

Although the Mercodia Rat Insulin ELISA kit employed antibodies raised against rat insulin, the assay is not specific for rat insulin and cross-reacts with human insulin by 148% (established by running rat insulin standards on the human ELISA during analysis). Therefore, samples containing both human and rat insulin yielded a measure of total insulin concentration i.e. endogenous rat insulin plus human insulin. Endogenous rat insulin (ERI) concentration was determined from the difference in immunoreactive insulin concentrations obtained from the two assay systems using the following equation:  $ERI = (HI / 1.48) - RI$  where HI is the concentration of human insulin obtained from the human insulin assay; RI is the concentration of total insulin obtained from the rat insulin assay and 1.48 is the crossreaction factor for human insulin in the rat insulin assay. ERI is not presented in the Results section but was calculated to confirm the suppression of endogenous rat insulin secretion. Endogenous insulin concentration was significantly decreased versus baseline in all groups ( $P = 0.02$  by Student's paired t-test). Insulin concentrations represented in the Results section are a measure of total insulin concentration.

#### **4.2.6.2 Non-esterified fatty acids (NEFA) concentration**

NEFA concentrations were determined using an enzymatic colorimetric assay (NEFA-HR(2) ACS-ACOD Method (Wako Diagnostics, Virginia, USA)). The assay was carried out according to the kit protocol. Briefly a standard curve was prepared by serially diluting Oleic acid (Sigma-Aldrich Ltd, UK) in bovine serum albumin diluted in phosphate buffered saline (100 mg/ml) (BSA/PBS). 10 µl of standards, quality controls and plasma samples were added to the assay plate. 150 µl of R1 solution (Alpha Labs, Hampshire, UK) was added to each well and incubated for 10 minutes at 37°C. Samples were read at an absorbance of 550 nM using a SoftMaxPro (Molecular Devices, California, US) to provide a “pre-read”. 80 µl of R2 solution (Alpha Labs, Hampshire, UK) was added to each well and incubated for 10 minutes at room temperature. Samples were read at an absorbance of 550 nM using a SoftMaxPro (Molecular Devices, California, US) to provide a “final-read”. Pre-read is then subtracted from final-read to produce a standard curve from which unknowns can be calculated.

#### **4.2.7 Data analysis**

Glucose infusion rate (GIR) shown in Results section was corrected for lean body mass, and is expressed as mg/kg<sub>LBM</sub>/min. Lean body mass (LBM) was estimated from empirical linear regression formulae relating LBM to total body weight (BW). These formulae were derived from body composition analysis of Zucker rats performed at AstraZeneca (Cardiovascular and Gastrointestinal Group, AstraZeneca, Alderley Park). The equation for the Obese Zucker rat is:

$$\text{LBM (g)} = 59 + 0.50 \times \text{BW (g)}$$

The equation for the Lean Zucker rat is:

$$\text{LBM (g)} = 31 + 0.77 \times \text{BW (g)}$$

Femoral vascular conductance (FVC) was calculated as  $\text{FVC} = \text{Femoral blood flow (FBF)} / \text{Mean arterial blood pressure (MABP)}$ . Change in FVC was calculated as change from time point zero.

The rate of initiation of glucose uptake in arbitrary units (AU) was calculated as the gradient of a linear line of best fit for time points 5, 10, 13, 15 and 18 minutes of GIR for each group and then meaned in groups.

All results are expressed as mean  $\pm$  standard error of the mean. Differences between treatment groups were evaluated using factorial ANOVA. Differences from baseline within the group were analysed using a repeated measures ANOVA with Dunnett's post hoc test.

### **4.3 Results**

The body weights and numbers in experimental groups are shown in Table 4.1.

The mean body weight of the lean animals was significantly different from that of the obese animals ( $P < 0.05$ ).



Group	Weight (g)	Number
Lean Vehicle Clamp	303.8 ± 7.7	5
Obese Vehicle Clamp	430.2 ± 19.4 *	7
Lean NAc Clamp	296.0 ± 9.5	5
Obese NAc Clamp	435.5 ± 19.5 *	7
Lean NAc Sham	339.0 ± 8.5	6
Obese NAc Sham	447.6 ± 14.5 *	6

**Table 4.1 Animal weights and group numbers.**

Weights are mean ± SEM. Lean and Obese Vehicle Clamp animals received vehicle infusion with HE clamp. Lean and Obese NAc Clamp animals received NAc infusion with HE clamp. Lean and Obese NAc Sham animals received NAc infusion with sham clamp.

Lean and obese group GIR cannot be directly compared as the insulin infusion used to achieve hyperinsulinaemia was different for the two groups (10 and 20 mU/kg<sub>LBM</sub>/min for lean and obese animals respectively).

#### **4.3.1 Cardiovascular variables during hyperinsulinaemic euglycaemic clamp**

There were no differences between MABP values at baseline between the three lean and the three obese groups. MABP gradually fell throughout the protocol in all groups. In the lean vehicle clamp group, MABP was significantly different from baseline at 30-80 minutes (see Figure 4.2 A;  $P < 0.05$ ). There was no significant change in MABP throughout the protocol in the lean NAc sham group (see Figure 4.2 A) but MABP fell from baseline in the lean NAc clamp group being significantly different at 30-80 minutes (see Figure 4.2 A;  $P < 0.05$ ).

There was no significant change in MABP in the obese vehicle clamp animals or the obese NAc sham groups (see Figure 4.2 B). However, MABP fell significantly from baseline by 50-80 minutes in the obese NAc clamp group ( $P < 0.05$ ).

Heart rate showed a tendency to fall from baseline in all groups but any change only reached statistical significance in the obese NAc clamp group in which HR was significantly lower than baseline values at 40 and 50 minutes (see Figure 4.3 B).

The HE clamp alone caused muscle vasodilatation in the lean vehicle clamp group FVC gradually increased from baseline and was significantly different from baseline from 30 - 80 minutes ( $P < 0.05$ ; see Figure 4.4 A). However, in the lean NAc clamp group there was a greater increase in FVC than in the lean vehicle clamp group, FVC being significantly different from FVC in the lean vehicle clamp group at 50 - 70 minutes ( $P < 0.05$ ). In the lean NAc sham clamp group there was no change in FVC (Figure 4.4 A).

By contrast, in the obese vehicle clamp group, HE clamp alone did not increase in FVC (see Figure 4.4 B). However, in the obese NAc clamp group, FVC was significantly different from baseline from 50 - 80 minutes ( $P < 0.05$ ) and was significantly different from FVC in obese vehicle clamp group from 50 minutes ( $P < 0.05$ ; see Figure 4.4 B). In the obese NAc sham clamp group there was no change in FVC (Figure 4.4 B).

Comparison of Figures 4.2 and 4.4 suggests a direct relationship between the increase in FVC, and therefore vasodilatation in the muscle, and a decrease in MABP within groups, both occurring in the lean vehicle clamp and lean NAc clamp groups and in the obese NAc clamp group.

#### **4.3.2 Blood glucose and glucose infusion rate during hyperinsulinaemic euglycaemic clamp**

Blood glucose concentrations in the lean vehicle clamp group were significantly lower than in the obese vehicle clamp group throughout ( $P < 0.05$ ). Blood glucose concentrations of the lean NAc clamp group were also significantly lower than the obese NAc clamp group, except at 27 minutes ( $P < 0.05$ ; cf Figure 4.5 A and B).

Blood glucose concentration was significantly higher in the lean NAc clamp, than lean vehicle clamp group at 0, 13, 40, 43, 65, 70 and 75 minutes ( $P < 0.05$ ; see Figure 4.5 A). By contrast, blood glucose concentrations were not significantly different between obese vehicle clamp and obese NAc clamp groups at any time point. Infusion of NAc did not significantly affect blood glucose in either lean or obese animals.

Glucose infusion rate was not significantly different between lean vehicle clamp and lean NAc clamp groups at basal or end of HE clamp (see Figure 4.6 A).

However, during the dynamic phase of the clamp, the GIR required to maintain euglycaemia in the lean NAc clamp group was significantly greater than in the

lean vehicle clamp group, between 24 and 40 minutes ( $P < 0.05$ ; see Figure 4.6 A). However, calculation of the rate of initiation of glucose uptake (from 5, 10, 13, 15 and 18 minute GIR values) showed no significant difference between lean vehicle clamp and lean NAc clamp groups (see Figure 4.7).

The GIR for obese vehicle clamp and obese NAc clamp groups were also not significantly different under basal conditions or at the end of HE clamp (see Figure 4.6 B). There was a tendency for GIR to be greater during the dynamic phase (from 15 – 25 minutes) of the clamp in the obese NAc clamp group, than vehicle clamp group but any difference was not statistically significant (Figure 4.6 B). However, the rate of initiation of glucose uptake was significantly greater in obese NAc clamp than obese vehicle clamp, by almost 100% ( $P < 0.05$ ; see Figure 4.7).

#### **4.3.3 Plasma Insulin and insulin sensitivity**

During the HE clamp human insulin was administered as a constant rate of 10 or 20 mU/kg<sub>LBM</sub>/min (in lean and obese animals respectively); with the intention of increasing circulating insulin to hyperinsulinaemic concentrations. Plasma insulin concentrations measured in the basal phase were significantly lower in all the lean versus the obese groups (Figure 4.8). Plasma insulin concentrations were not different in the vehicle clamp groups versus the NAc clamp groups at 40 or 80 minutes, although there was a tendency for plasma insulin to be lower in both lean and obese NAc clamp groups than in the respective vehicle clamp groups at 40 minutes (Figure 4.8).

Plasma insulin was significantly raised from baseline at both 40 and 80 minutes in the lean vehicle clamp and lean NAc clamp group ( $P < 0.05$ ) but did not change from baseline in the lean NAc sham group (see Figure 4.8 A). Plasma insulin was significantly greater at 40 and 80 minutes in the lean vehicle clamp group versus the lean NAc clamp group ( $P < 0.05$ )

Similarly, plasma insulin was significantly raised from baseline at both 40 and 80 minutes in the obese vehicle clamp group and obese NAc clamp group ( $P < 0.05$ ; see Figure 4.8 B). Plasma insulin concentrations did not differ from baseline in the obese sham clamp group (see Figure 4.8 B).

Insulin sensitivity (M/I) a measure of tissue responsiveness calculated from GIR (see Methods), was  $\sim 5$  times greater in the lean vehicle clamp and lean NAc clamp groups than in the corresponding obese groups ( $P < 0.05$  in each case). Insulin sensitivity was not affected by NAc infusion alone in either the lean or obese groups (see Figure 4.9).

#### **4.3.4 Plasma Non-Esterified Fatty Acid Concentration**

Plasma NEFA concentrations were significantly lower in the lean groups than in obese groups at all time points ( $P < 0.05$ ; see Figure 4.10 A). Surprisingly, at baseline, NEFA concentration in the obese NAc sham group was significantly lower than in both the obese vehicle clamp and obese NAc HE clamp groups whereas there was no difference in the leans ( $P < 0.05$ ; see Figure 4.10 B).

As expected NEFA decreased significantly in the lean NAc sham group following infusion of NAc. As insulin inhibits lipolysis there was also a significant decrease in plasma NEFA concentrations in the lean vehicle clamp group. NEFA concentrations were also decreased in the lean NAc clamp group. NEFA concentrations were decreased further in both the lean vehicle clamp and lean NAc clamp groups than in the lean NAc sham group ( $P < 0.05$ ; see Figure 4.10 A) but there was no significant difference between the two groups lean vehicle and lean NAc clamp groups. NAc in combination with HE clamp was therefore no more effective at lowering NEFA than NAc alone.

HE clamp decreased NEFA concentration significantly below basal concentrations in the obese vehicle clamp group, at 80 minutes ( $P < 0.05$ ; see Figure 4.10 B). NEFA concentration in the obese NAc sham group was not different to that of the obese NAc clamp or lean vehicle clamp. However, there was a tendency for NEFA in the obese NAc clamp group to be lower than in the obese vehicle clamp group.

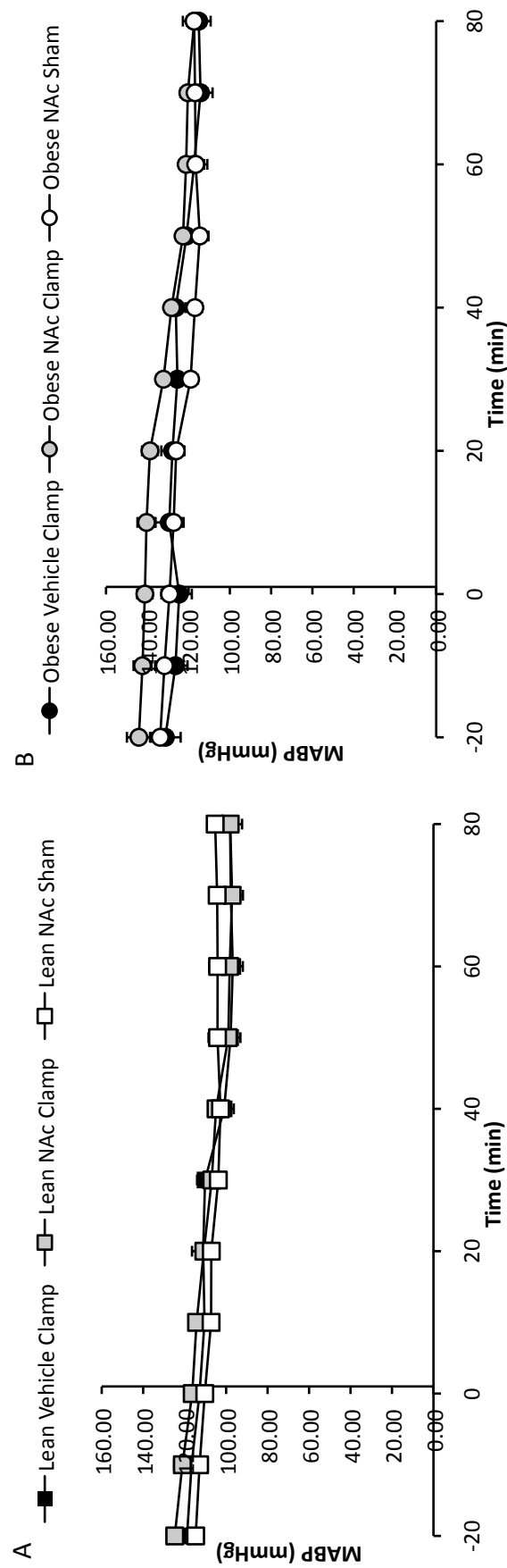


**Figure 4.2 Mean arterial blood pressure for lean and obese Zucker rats during hyperinsulinaemic euglycaemic clamp under different experimental conditions.** Values are mean  $\pm$  SEM. Symbols represent the mean arterial blood pressure for lean vehicle clamp (square black), lean NAc clamp (square grey), lean NAc sham (square white), obese vehicle clamp (spherical black), obese NAc clamp (spherical grey) and obese NAc sham (spherical white). Significances not shown for simplicity, see Table 4.2.

	Time (min)										
	-20	-10	0	10	20	30	40	50	60	70	80
Lean Vehicle Clamp	119 ± 7	117 ± 5	113 ± 5	110 ± 5	111 ± 5	110 ± 4 *	101 ± 5 *	98 ± 4 *	97 ± 2 *	98 ± 1 *	98 ± 3 *
Lean NAc Clamp	125 ± 4	121 ± 4	116 ± 3	114 ± 3	110 ± 2	107 ± 3 *	105 ± 3 *	99 ± 2 *	98 ± 2 *	97 ± 1 *	98 ± 3 *
Lean NAc Sham	115 ± 3	113 ± 2	110 ± 2	107 ± 2	107 ± 1	104 ± 3	103 ± 4	104 ± 4	104 ± 4	104 ± 3	105 ± 3
Obese Vehicle Clamp	131 ± 7	126 ± 6	125 ± 6	129 ± 7	128 ± 5	125 ± 4	126 ± 5	121 ± 5	117 ± 5	114 ± 6	115 ± 6
Obese NAc Clamp	144 ± 6	142 ± 4	141 ± 4	140 ± 4	139 ± 4	132 ± 3	128 ± 3	123 ± 3 *	122 ± 3 *	120 ± 4 *	117 ± 3 *
Obese NAc Sham	134 ± 4	132 ± 5	129 ± 4	127 ± 4	126 ± 4	119 ± 4	117 ± 4	115 ± 4	117 ± 6	117 ± 6	117 ± 5

**Table 4.2 Raw data with significance symbols for mean arterial blood pressure for lean and obese Zucker rats during hyperinsulinaemic euglycaemic clamp under different experimental conditions.** Values are mean ± SEM. Data points correspond to Figure 4.1. \*  $P < 0.05$  Group vs. Group baseline.



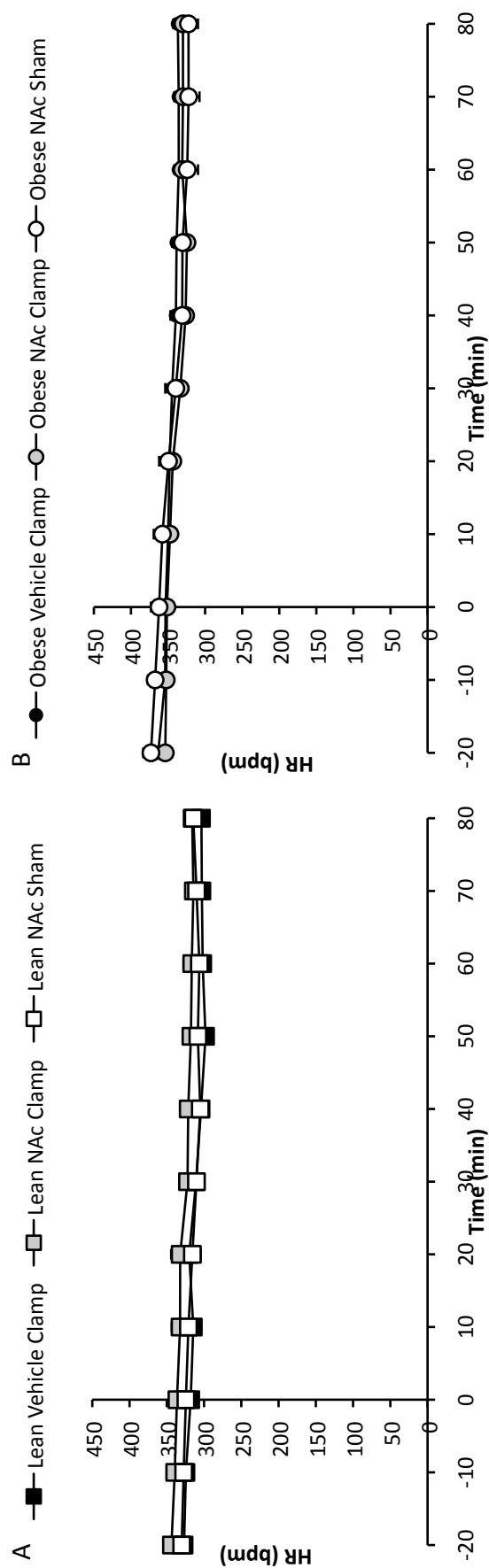


**Figure 4.3 Heart rate for lean and obese Zucker rats during hyperinsulinaemic euglycaemic clamp under different experimental conditions.** Values are mean  $\pm$  SEM. Symbols represent the mean arterial blood pressure for lean vehicle clamp (square black), lean NAc clamp (square grey), lean NAc sham (square white), obese vehicle clamp (spherical black), obese NAc clamp (spherical grey) and obese NAc sham (spherical white). Significances not shown for simplicity, see Table 4.3.

	Time (min)										
	-20	-10	0	10	20	30	40	50	60	70	80
Lean Vehicle Clamp	327 ± 5	324 ± 7	318 ± 7	314 ± 7	320 ± 10	311 ± 10	304 ± 8	298 ± 6	302 ± 9	303 ± 9	304 ± 10
Lean NAc Clamp	344 ± 9	339 ± 10	336 ± 10	332 ± 11	332 ± 12	322 ± 8	321 ± 7	318 ± 11	316 ± 11	314 ± 8	316 ± 7
Lean NAc Sham	330 ± 11	327 ± 12	324 ± 12	321 ± 11	316 ± 11	310 ± 10	305 ± 9	308 ± 7	306 ± 8	310 ± 8	314 ± 8
Obese Vehicle Clamp	363 ± 8	354 ± 8	353 ± 7	350 ± 6	348 ± 5	344 ± 4	339 ± 7	338 ± 6	336 ± 6	336 ± 6	337 ± 6
Obese NAc Clamp	354 ± 8	352 ± 6	351 ± 6	347 ± 5	344 ± 5	333 ± 5	326 ± 6*	324 ± 5*	331 ± 6	330 ± 6	330 ± 6
Obese NAc Sham	373 ± 10	367 ± 10	362 ± 11	358 ± 12	349 ± 13	340 ± 14	331 ± 13	330 ± 14	324 ± 15	322 ± 15	322 ± 13

**Table 4.3 Raw data with significance symbols for heart rate for lean and obese Zucker rats during hyperinsulinaemic euglycaemic clamp under different experimental conditions.** Values are mean ± SEM. Data points correspond to Figure 4.2. \*  $P < 0.05$  Group vs. Group baseline.

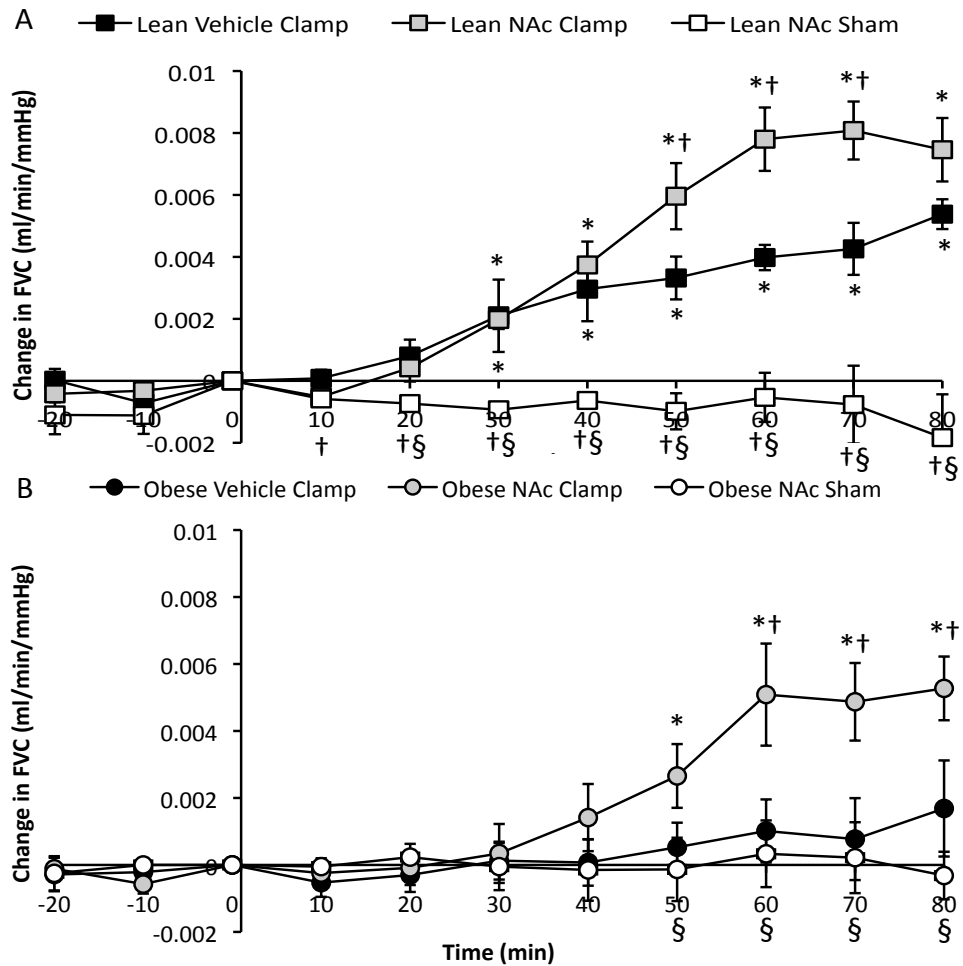


**Figure 4.4 Femoral vascular conductance (FVC) for lean and obese Zucker rats during hyperinsulinaemic euglycaemic clamp under different experimental conditions.** Values are mean  $\pm$  SEM. In graph (A) symbols represent FVC for lean vehicle clamp (square black), lean NAc clamp (square grey) and lean NAc sham (square white). In graph (B) obese vehicle clamp (spherical black), obese NAc clamp (spherical grey) and obese NAc sham (spherical white). \*  $P < 0.05$  Group vs. Group baseline; †  $P < 0.05$  Group vs. Group Vehicle Clamp; §  $P < 0.05$  Group vs. Group NAc Clamp.

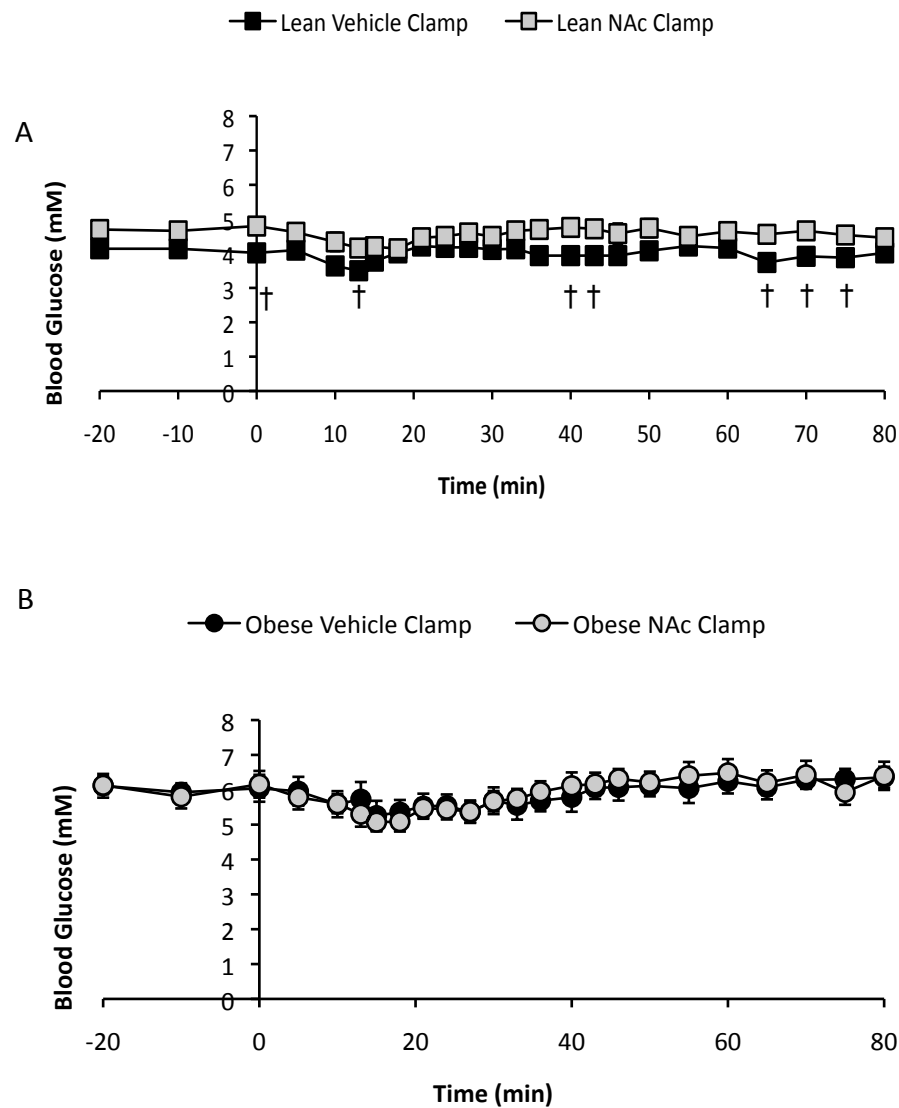


**Figure 4.5 Effect of hyperinsulinaemic euglycaemic clamp with or without nicotinic acid on blood glucose in lean and obese Zucker rats.** Square symbols represent lean animals that have been treated with vehicle (black) or nicotinic acid (grey); spherical symbols represent obese animals that have been treated with vehicle (black) or nicotinic acid (grey). †  $P < 0.05$  Group vs. Group Vehicle Clamp.

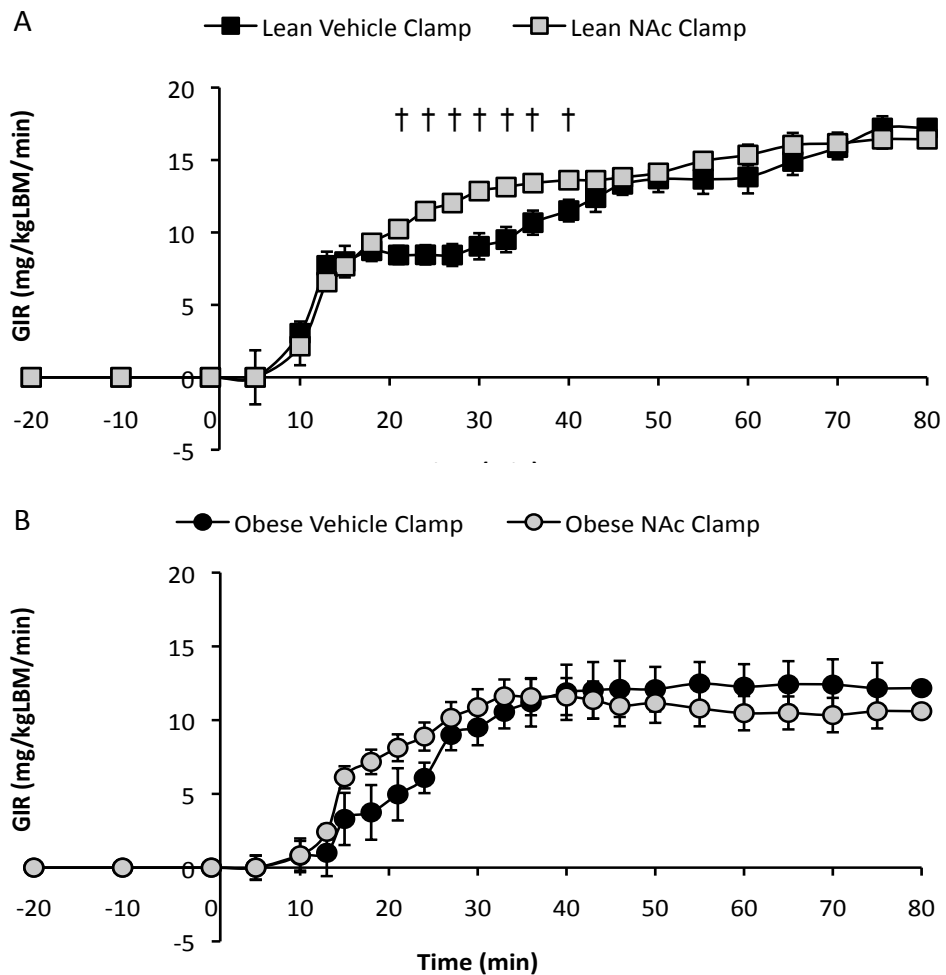


**Figure 4.6 Glucose infusion rate for lean and obese Zucker rats during hyperinsulinaemic euglycaemic clamp with or without nicotinic acid treatment.** Values are mean  $\pm$  SEM. In graph (A) symbols represent glucose infusion rate for lean vehicle clamp (square black) and lean NAc clamp (square grey). In graph (B) symbols represent glucose infusion rate for obese vehicle clamp (spherical black) and obese NAc clamp (spherical grey). †  $P < 0.05$  Group vs. Group Vehicle Clamp.

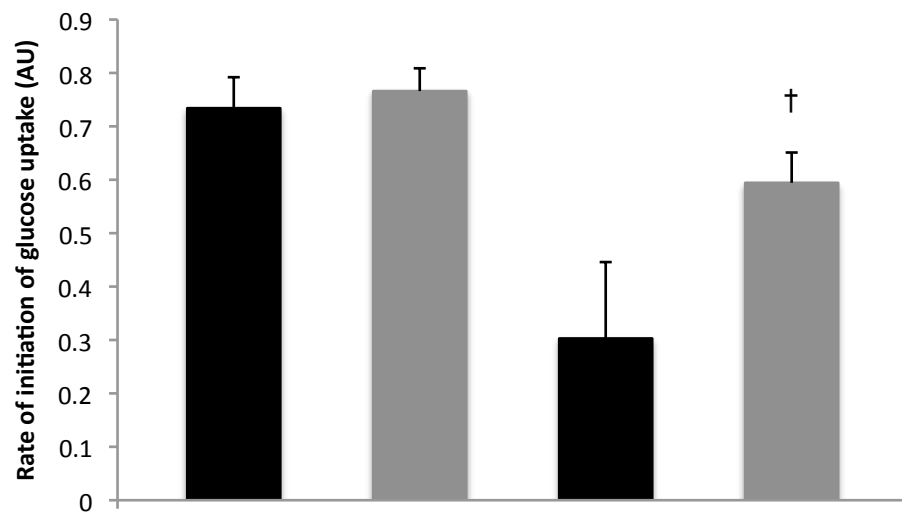
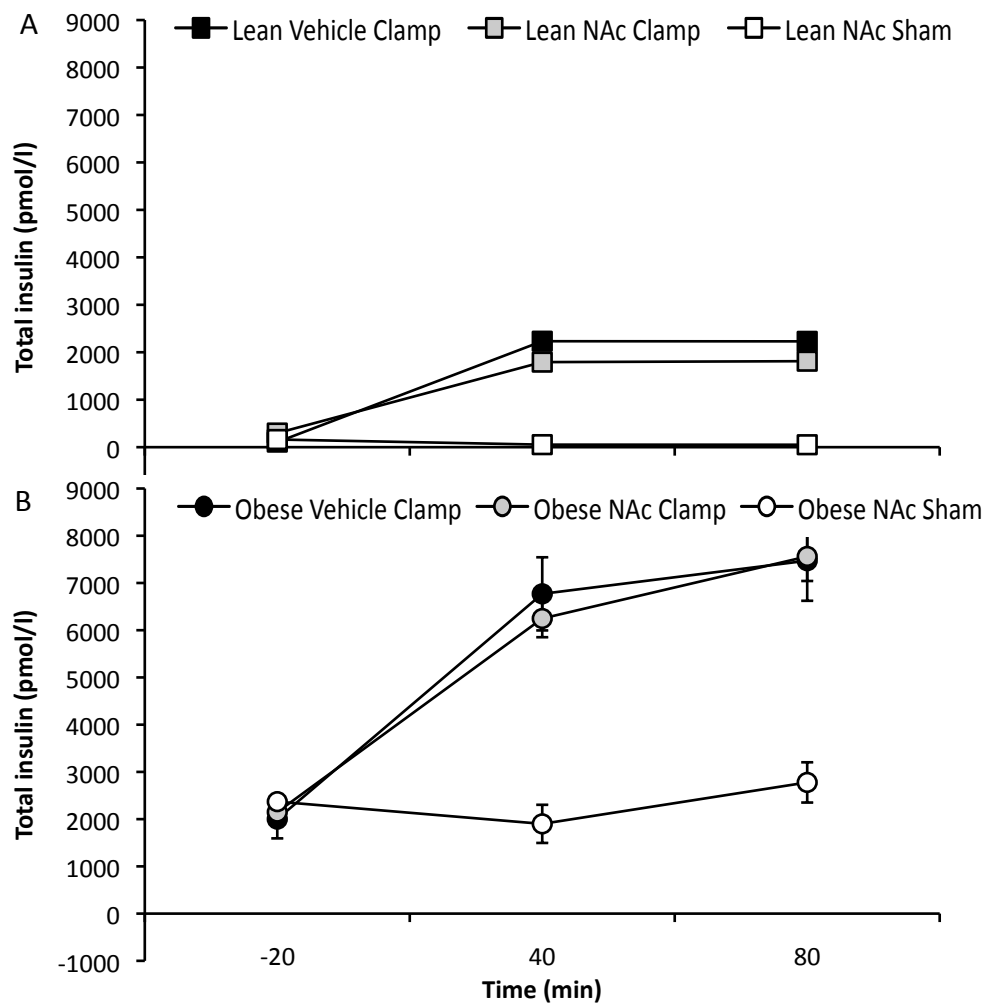


**Figure 4.7 Rate of initiation of glucose uptake for lean and obese Zucker rats during hyperinsulinaemic euglycaemic clamp with or without nicotinic acid treatment.** Values are mean  $\pm$  SEM. Graph represents rate during 5-18 minutes of hyperinsulinaemic euglycaemic clamp for different treatment groups. <sup>†</sup>  $P < 0.05$  Group vs. Group Vehicle Clamp.



Insulin (pmol/L)	-20 min	40 min	80 min
Lean Vehicle Clamp	107.05 ± 11.95	2232.64 ± 136.33 *	2229.76 ± 133.68 *
Lean NAc Clamp	297.29 ± 138.82	1792.43 ± 57.03 *†	1812.04 ± 52.67 *†
Lean NAc Sham	161.55 ± 2.98	53.41 ± 0.25 †	51.49 ± 13.54 †
Obese Vehicle Clamp	2000.81 ± 408.05	6769.88 ± 774.33 *	7472.12 ± 849.27 *
Obese NAc Clamp	2149.29 ± 280.16	6247.96 ± 396.29 *	7562.12 ± 519.86 *
Obese NAc Sham	2370.33 ± 134.69	1899.97 ± 403.82 †	2777.49 ± 426.19 †

**Figure 4.8 Insulin data for lean and obese Zucker rats during hyperinsulinaemic euglycaemic clamp under different experimental conditions.** Values are mean ± SEM. Symbols represent the mean arterial blood pressure for lean vehicle clamp (square black), lean NAc clamp (square grey), lean NAc sham (square white), obese vehicle clamp (spherical black), obese NAc clamp (spherical grey) and obese NAc sham (spherical white). \*  $P < 0.05$  Group vs. Group baseline; †  $P < 0.05$  Group vs. Group Vehicle Clamp.

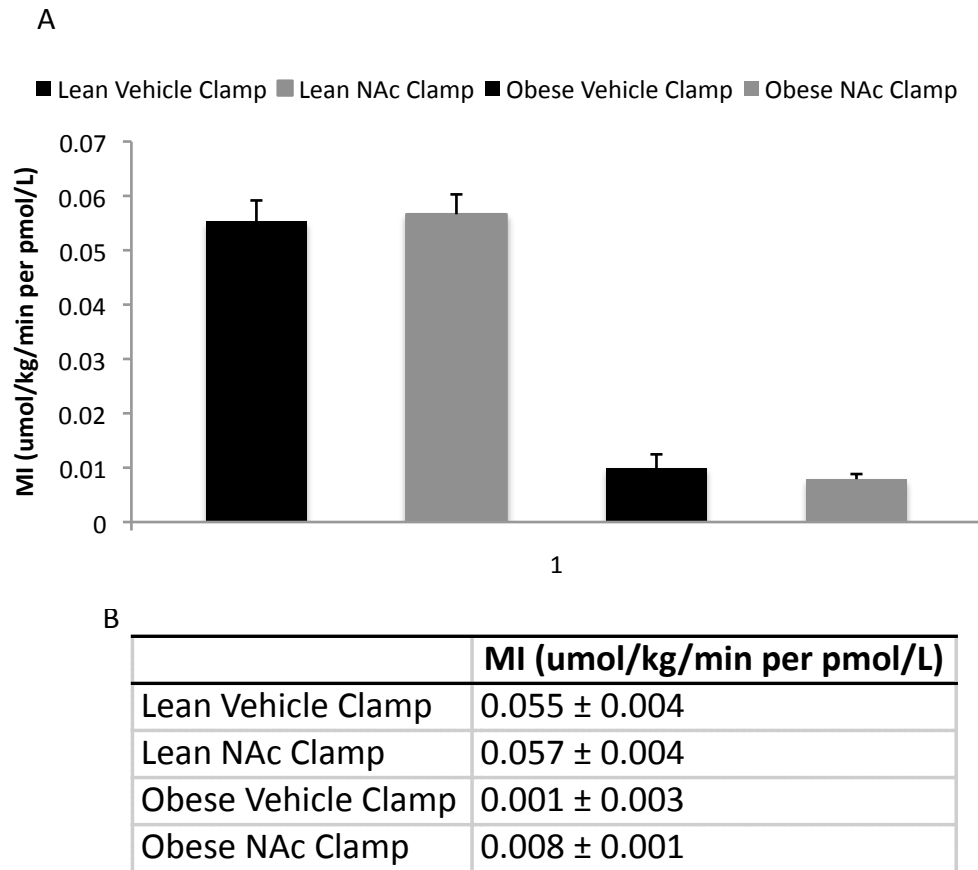
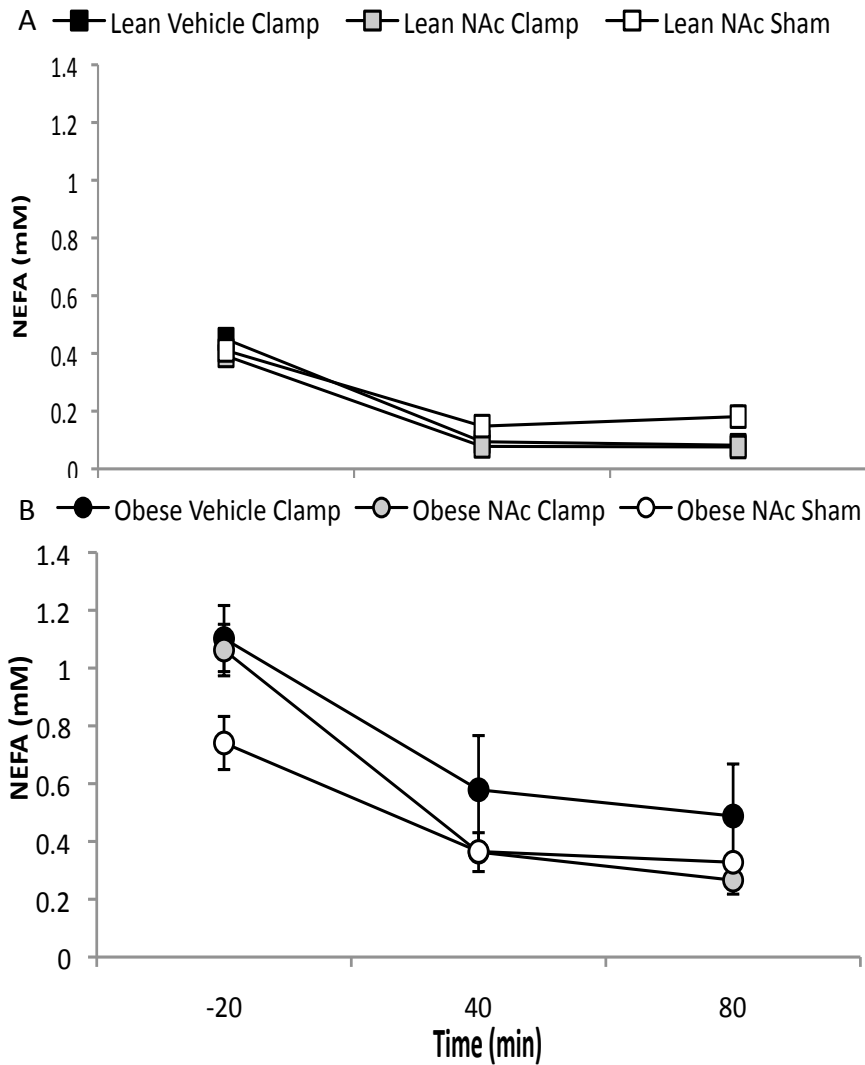


**Figure 4.9 Insulin sensitivity of lean and obese Zucker rats exposed to hyperinsulinaemic euglycaemic clamp with or without nicotinic acid treatment.** Values are mean ± SEM for insulin sensitivity (MI). Graph (A) shows MI for treatment groups lean vehicle clamp (black bar), lean NAc clamp (dark grey bar), obese vehicle clamp (light grey bar) and obese NAc clamp (white bar). Table (B) represents raw data for MI in all groups. \$  $P < 0.05$  vs. Lean.





NEFA (mM)	-20 min	40 min	80 min
Lean Vehicle Clamp	0.45 ± 0.03	0.09 ± 0.01 *	0.08 ± 0.00 *
Lean NAc Clamp	0.40 ± 0.02	0.08 ± 0.00 *	0.08 ± 0.00 *
Lean NAc Sham	0.41 ± 0.02	0.15 ± 0.03 *†§	0.18 ± 0.04 *†§
Obese Vehicle Clamp	1.10 ± 0.11	0.58 ± 0.19	0.49 ± 0.18 *
Obese NAc Clamp	1.06 ± 0.09	0.36 ± 0.07 *	0.27 ± 0.05 *
Obese NAc Sham	0.74 ± 0.09 †§	0.37 ± 0.03 *	0.33 ± 0.03 *

**Figure 4.10 Non-esterified fatty acid data for lean and obese Zucker rats during hyperinsulinaemic euglycaemic clamp under different experimental conditions.** Values are mean ± SEM. Symbols represent the mean arterial blood pressure for lean vehicle clamp (square black), lean NAc clamp (square grey), lean NAc sham (square white), obese vehicle clamp (spherical black), obese NAc clamp (spherical grey) and obese NAc sham (spherical white). \*  $P < 0.05$  Group vs. Group baseline; †  $P < 0.05$  Group vs. Group Vehicle Clamp; §  $P < 0.05$  Group vs. Group NAc Clamp.

## **4.4 Discussion**

The main aim of the present study was to investigate whether acute reduction in plasma NEFA levels by infusion of NAc would improve muscle vasodilatation, glucose uptake and insulin sensitivity during HE clamp in lean and/or obese Zucker rats. However, before these issues are discussed it is important to consider the results obtained during HE clamp per se in the lean and obese Zucker rats in relation to control Wistar rats in studies of previous chapters and to compare lean and obese Zuckers to one another.

### **4.4.1 Responses to HE clamp in lean Zucker rats**

As in experiments of chapters 2 and 3, which were performed on Alfaxan anaesthetized Wistar rats, HR was stable throughout the HE clamp protocol in the lean (Zucker) vehicle clamp rats anaesthetised with pentobarbital, indicating stable anaesthesia throughout. However, in contrast to previous experiments, MABP was significantly decreased below baseline from 30 – 80 minutes in the lean Zucker rats, rather than being maintained constant. This time course closely corresponds to the insulin-induced muscle vasodilatation as FVC was significantly increased from 30 – 80 minutes. It is interesting that this effect of insulin-induced vasodilatation on MABP was not seen in previous studies given that the lean animals in the present chapter received only one third the dose of insulin used in the previous studies. It seems very likely that the difference is due to the use of pentobarbital in the present group of experiments. It has been argued previously that anaesthesia induced with Alfaxan can leave autonomic control of the cardiovascular system intact (see Section 2.1) and that MABP was

maintained during HE clamp by baroreflex effect on sympathetic nervous activity (SNA) and insulin-induced increase in SNA. Thus, it seems likely that in present experiments with pentobarbital anaesthesia, the reflex increase in SNA to the vasculature expected was depressed. This is also consistent with the lack of waning in the FVC response. In the experiments of Chapters 2 and 3, the insulin-induced vasodilatation increased to a maximum at ~ 60 minutes and then waned whereas, in the present experiments, FVC continued to increase throughout HE clamp. It is possible that the lack of a waning of the muscle vasodilatation is due to the lower dose of insulin such that a longer time was required for the development of insulin-induced vasodilatation and that if the clamp was extended a decrease in vasodilatation would have occurred reflecting insulin-induced increase in MSNA. However, it is still the case that the baroreceptor reflex did not buffer the fall in MABP induced by the lower dose of insulin.

Importantly, blood glucose was well maintained in the present study compared to the experiments on lean rats described in previous chapters, particularly at the onset of the HE clamp and GIR was rapidly increased following initiation of the HE clamp. As in studies of previous chapters the increase in FVC seen in the lean Zucker rats was delayed compared to the increase in GIR. GIR was increased almost immediately whereas the increase in FVC did not begin until ~ 30 minutes, suggesting that it was secondary to the increase in GIR, rather than facilitating the increase in GIR.

As expected, plasma insulin concentrations were significantly increased and plasma NEFA concentrations were significantly decreased from basal at 40 and

80 minutes. Thus, the lower concentration (10 mU/kg/min) of insulin used in the HE clamps in lean Zucker rats was sufficient to significantly increase plasma insulin concentrations and to inhibit lipolysis enough to decrease plasma NEFA concentrations.

#### **4.4.2 Responses to HE clamp in obese Zucker rats**

As in the lean vehicle clamp rats, HR was stable throughout the HE clamp protocol in the obese vehicle group. However, in contrast to the lean rats, MABP was not decreased below baseline at any time point and neither did FVC increase.

The fact that blood glucose and plasma insulin concentrations were much higher in the obese vehicle clamp group than lean vehicle clamp rats at baseline indicates, as expected, that insulin sensitivity was much lower in the obese rats. Blood glucose concentrations were successfully maintained at the higher basal concentration throughout the HE clamp in the obese rats. Not surprisingly, plasma insulin concentrations increased during HE clamp and were higher than in the lean group at all time points. Despite this, the requirement of GIR at the plateau phase of HE clamp was much lower in the obese than lean vehicle clamp rats. Rate of initiation of GIR was also much lower in the obese vehicle clamp rats versus lean vehicle clamp rats. Consistent with these findings, NEFA concentrations were decreased during HE clamp from baseline at 80 minutes, but not at 40 minutes suggesting that lipolysis was not as effectively inhibited by insulin in the obese rats.

The results presented in this chapter therefore indicate that the obese Zucker rats were insulin-resistant relative to the lean Zucker rats with regards to the ability of insulin to increase glucose uptake, cause muscle vasodilatation and decrease lipolysis.

#### **4.4.3 Effects of NAc infusion on lean and obese Zucker rat groups**

Patient compliance with NAc is notoriously poor as it is associated with cutaneous flushing (vasodilatation; (Morrow et al., 1992)). One of the reasons for performing sham experiments was to establish whether or not NAc was increasing muscle blood flow. However, there were no changes in MABP, HR, FVC or insulin concentration in response to NAc infusion indicating that it has at most a relatively small dilator effect in the rat. GIR was not measured in these groups, although NEFA concentrations were found to be decreased versus baseline in both lean and obese rats. NAc infusion was not as effective as the HE clamp in decreasing NEFA in lean rats, suggesting that insulin was more effective at inhibiting lipolysis than the dose of NAc used in the present study. In contrast, in obese rats NEFA concentrations were decreased more effectively with NAc than with HE clamp, suggesting that insulin was less effective at inhibiting lipolysis than the dose of NAc used in obese rats. Thus, NAc did not induce significant vasodilatation in muscle even at concentrations at which it decreased NEFA.

#### **4.4.4 Effects of NAc on responses to HE clamp groups**

Plasma insulin concentrations in both the lean and obese NAc clamp rats were increased above basal concentrations by HE clamp, but they were significantly lower in lean NAc clamp rats than in lean vehicle clamp rats at 40 and 80 minutes. This is consistent with an increase in insulin clearance from the plasma and/or a decrease in secretion of endogenous insulin caused by NAc. In fact, Qvigstad et al., (2003) showed that increasing FFA concentration during HE clamp decreased insulin clearance in diabetic humans. Thus, it is most likely that NAc increased insulin clearance in lean Zucker rats. The finding that plasma insulin concentrations were not lowered by NAc during HE clamp in obese Zucker rats may reflect the fact that the plasma insulin concentrations were not different from obese vehicle clamp concentrations. It is possible that the plasma insulin was so high in these animals, a small increase in insulin clearance as a result of NAc action was not enough to affect the prevailing insulin concentrations.

It is perhaps not surprising that such an acute treatment with NAc did not affect insulin sensitivity measured in lean or obese rats during HE clamp, ie. NAc did not increase glucose uptake rates at the end of HE clamp. Although the changes in carbohydrate oxidation exhibited in response to NAc are fast acting (see section 4.1), changes in glycogen synthesis appear to take longer. Thus, Boden and Jadali (1991) showed in healthy subjects exposed to lipid and heparin infusion and therefore increased FFA during HE clamp, that an increase in fat oxidation and decrease in carbohydrate oxidation occurred within one hour whereas a decrease in glucose uptake occurred between two and four hours

later. Further, in healthy subjects under the same experimental conditions around a third of the decrease in glucose uptake occurred as a result of the quicker acting decrease in carbohydrate oxidation. In other words, around two thirds of the decrease in glucose uptake was due to the effects of increased FFA on glycogen synthase activity and took between four and six hours to manifest. Hence it may be that a much longer exposure to NAc would be required to significantly increase the rate of glucose uptake at the plateau of HE clamp and hence the measurement of insulin sensitivity.

Since concomitant NAc treatment with HE clamp did not decrease plasma NEFA concentrations further than HE clamp alone in either lean or obese rats, it is likely that the effects observed on muscle blood flow and rate of onset of the increase in GIR were not NEFA-mediated. Thus, in the lean rats that received NAc with HE clamp, the initiation rate of GIR was not changed relative to HE clamp alone (Figure 4.8) but GIR was significantly greater at 21 - 40 minutes of the clamp. On the other hand, in the obese rats NAc given with HE clamp increased the initiation rate of GIR versus HE clamp alone (Figure 4.7) and tended to produce a left shift in GIR as in the lean animals.

It should be noted that in lean rats, the increase in FBF and FVC evoked by HE clamp occurred earlier when NAc was infused simultaneously and was greater over the period 50 – 70 minutes. Also, in the obese rats, NAc infusion with HE clamp evoked a substantial increase in FBF and FVC from 60 – 80 minutes that did not occur during HE clamp alone. But in both lean and obese rats, the effect of NAc on the increase in GIR in the lean and obese vehicle clamp groups occur

significantly before the increases in FVC, suggesting that the effect on FVC must be secondary to the increase in GIR or to some consequence of it (see discussion below). It is possible that the earlier onset of the increase in GIR in both lean and obese rats reflected improved vasodilatation at the level of terminal arterioles that did not affect gross vascular conductance. But this would need to be tested in future studies.

Hence, in both lean and obese rats, acute NAc infusion facilitated the rate of progression of the increase in GIR. It is possible that the reduction in FFA causes a more rapid insulin dependent tyrosine phosphorylation of IRS in skeletal muscle fibres (see General Introduction) and that this is facilitating the increase in GIR. Alternatively, a possible explanation for this centers around the fact that insulin-induced NO production increases the amount of cGMP in the vascular smooth muscle and B complex vitamins have been shown to increase cGMP at a cellular concentration in rats (Vesely, 1985). Additionally, dietary supplementation of New Zealand white rabbits with niacin was also able to increase tissue cGMP concentrations (Wu et al., 2010). Thus, cGMP provides a possible interaction between the actions of NAc (separate from its ability to decrease NEFA) and the increase in vasodilatation seen in lean and obese rats.

Certainly, it was shown by Young and Leighton (1998) that increased production of cGMP in muscle fibres by NO increased glucose uptake and metabolism. Etgen et al., (1997) also showed in an isolated rat epitochlearis muscle preparation that NO/cGMP stimulated skeletal muscle transport by increasing GLUT4 concentrations at the cell surface. Young and Leighton used incubated soleus



muscle from lean Zucker rats and increased concentrations of cGMP using Zaprinast (a selective inhibitor of phosphodiesterase). This resulted in an increase in lactate production, glycogen and glucose oxidation, which are all markers of increased glucose metabolism. Therefore if NAc acted to increase cGMP concentrations in skeletal muscle fibres then it is possible this contributed to the facilitation of glucose uptake shown in the present chapter.

Although NAc has been used clinically for many years, many aspects of its action are still not understood. A few studies have claimed to show an improvement in endothelial function as a result of NAc action (Thoenes et al., 2007, Warnholtz et al., 2009, Kuvshinov et al., 2002) however these were all chronic treatment protocols and thus, this is unlikely to be the explanation for the present results.

Considering the effects of NAc on FVC in lean and obese rats it is possible that effects are due to products of the metabolic actions of insulin as discussed in Chapter 3. Firstly, lactate production by muscle cells is increased by insulin's action. An increase in lactate production and a decrease in intracellular pH have been associated with increased ATP efflux from skeletal muscle fibres. ATP is converted to adenosine extracellularly and in this way adenosine output and intracellular pH have been shown to be linearly related (Tu et al., 2010b). Hence, an increase in lactate production induced by insulin would be expected to increase the amount of adenosine produced and adenosine is a mechanism by which insulin is thought to cause insulin-induced vasodilatation (see discussion in Section 3.4.1).

Further, the GPR109A receptor, which acts as a receptor for NAc, shares a high degree of sequence homology with GPR109B and GPR81 receptors which form a GPCR subfamily that is activated by hydroxy-carboxylic acid ligands including not only NAc but also 3-hydroxy-octanoate and lactate (Ahmed et al., 2009). If there is a synergistic relationship between the pathways of the GPR109A in response to NAc activation and GPR81 in response to lactate activation then it is possible that this could account for the increased vasodilator effect when both are present.

However, as GIR at the end of HE clamp was not altered, the adenosine hypothesis alone does not explain effects on FVC particularly in obese rats. The effects on redox state may be important in obese. Thus, one hypothesis to explain the effects of NAc on HE-induced dilator responses is that the effects were due to the breakdown products of NAc acting to affect the redox status of the endothelial cells. NAc is metabolised to NAD, nicotinamide adenine dinucleotide phosphate (NADP) and reduced glutathione (GSH) (Ganji et al., 2009). GSH is required to regenerate tetrahydrobiopterin (BH<sub>4</sub>) nonenzymatically. BH<sub>4</sub> is also able to regenerate in the presence of dihydropteridine reductase (DHPR), but in the absence of thiols there is 40-50% less BH<sub>4</sub> production (Stuehr et al., 1990). Thus, NAc may have increased the supply of GSH and BH<sub>4</sub> and therefore facilitated NO synthesis via eNOS possibly enhancing insulin-induced NO synthesis and vasodilatation in obese rats. The estimation of 40-50% reduction in BH<sub>4</sub> without GSH is interesting as in lean animals eNOS and BH<sub>4</sub> are assumed to be functioning normally. Thus, in the present experiments, the 62.5% increase in  $\Delta$ FVC seen in the lean rats when NAc was combined with HE clamp may reflect

the 40-50% increase in BH<sub>4</sub> production seen by Stuehr et al., (1990). Potential effects of NAc on BH<sub>4</sub> and NO synthesis in obese and lean rats would need to be tested in further experiments.

#### **4.4.5 Conclusion**

The present study showed that NAc did not affect NEFA concentrations or insulin sensitivity during HE clamp in either lean or obese Zucker rats. Despite this, there was an increase in rate of onset of the increase in GIR in the obese rats that received NAc versus the obese vehicle group and a significant increase in GIR in the early phase of the clamp in the lean rats that received NAc. Additionally, NAc significantly increased insulin-induced muscle vasodilatation in lean rats and revealed substantial insulin-induced muscle vasodilatation in obese rats.

## CHAPTER 5 - REFINEMENT OF THE MICRODIALYSIS METHOD

### 5.1 Introduction

There are many reasons why assessing insulin sensitivity, in particular muscle insulin sensitivity, by using plasma concentrations of insulin and uptake of glucose in the periphery may not be accurate. Firstly, the plasma insulin concentration required to elicit half-maximal response to systemic glucose disposal rate is significantly higher than that required *in vitro* (Poulin et al., 1994). Secondly, the kinetics for the increase in glucose uptake during HE clamp are markedly delayed compared to the rapid changes in plasma insulin concentration (Castillo et al., 1994). Thirdly, studies have shown in animals and humans that lymphatic insulin concentrations are significantly lower than those in the plasma (Yang et al., 1989), which indicates that the concentration of insulin close to muscle fibres is very different from that measured in plasma.

Interstitial insulin concentrations have been estimated by measuring insulin concentration in lymph as a surrogate measure because ISF drains into the lymph before it re-enters the blood at thoracic duct. As discussed in the General Introduction, several studies have used lymph insulin to assess the movement of insulin into the ISF, for example, in the leg of humans (Castillo et al., 1994) and hindleg or thoracic duct of dogs (Poulin et al., 1994, Yang et al., 1989). Poulin et

al., (1994) also found a good temporal relationship between hind leg lymphatic insulin concentration and glucose uptake and found leg lymph to correlate more strongly than thoracic duct insulin with glucose uptake. Similarly, Castillo et al., (Castillo et al., 1994) found that insulin concentrations in lymph collected from ductules in the foot lagged behind arterial insulin concentration. However, lymph insulin measurements are rarely a direct measure of the ISF insulin concentration in one muscle as they are normally collected across a whole limb and therefore include lymph from skin and adipose tissue as well. Additionally, there is likely to be a time delay between changes occurring in the insulin concentration in the muscle and in lymph drainage from the limb simply because movement of fluid from interstitium to lymph depends on the hydrostatic pressure gradient and may or may not be aided by muscle contraction or gravity.

### **5.1.1 Microdialysis**

Microdialysis is a technique that allows the direct measurement of ISF components in a given tissue (Wentholt et al., 2005). In 1987 Lonnroth et al., performed the first *in vivo* tissue-dialysis technique in the periumbilical subcutaneous tissue of healthy human subjects (Lonnroth et al., 1987).

Microdialysis is now used clinically for continuous glucose monitoring in subcutaneous adipose tissue in diabetes. In combination with an electro-chemical glucose sensor this allows for real-time glucose monitoring (Chaurasia et al., 2007). With further development of the microdialysis technique for the measurement of insulin, an indwelling continuous insulin monitor might provide

a more accurate way of controlling blood glucose concentrations in diabetic patients.

Microdialysis was originally developed for chemical analysis of neuropeptide concentration in the rodent brain using linear probes to access specific areas (Brodin et al., 1983). Since then the technique has been developed for additional purposes. Thus, microdialysis probes are used with a range of molecular weight cutoffs and are made of different materials depending on the substance of interest (Jansson et al., 1993, Niklasson et al., 1998, Rosdahl et al., 2000). Clearly it is important that a probe with the correct characteristics is selected in order to optimize the recovery of the analyte of interest across the membrane.

Whatever its particular purpose, the microdialysis probe consists of two pieces of thin dialysis tubing with an inner diameter of 0.15-0.3 mm converging at a semi permeable membrane (Chaurasia et al., 2007). It acts like an artificial capillary allowing free diffusion across the membrane. Perfusion fluid is passed through the probe using a precision pump at very slow flow rates allowing the substances to diffuse from the tissue into the probe. The slow flow rate allows for equilibration of analytes or solutes across the semipermeable membrane. Samples of perfusion fluid are then collected from the outlet and undergo chemical analysis.

Many studies have found evidence for an arterial-interstitial gradient *in vivo* under hyperinsulinaemic conditions in humans and in rats using microdialysis ((Sjostrand et al., 1999) and (Jansson et al., 1993) respectively).

Recovery of a substance *in vitro* is not a suitable indicator of recovery *in vivo* because of differences in protein binding and diffusion capacity in the interstitial fluid that varies between individual subjects (Lonnroth et al., 1987). The concentration difference between blood and interstitial space depends on factors such as the degree of protein binding, capillary permeability, cellular uptake, degradation and kinetic differences in the various distribution volumes (Lonnroth et al., 1987). It is therefore important that each microdialysis probe is calibrated *in vivo* (Lonnroth and Strindberg, 1995).

The relative recovery describes the ratio between the concentration of a substance in the dialysate and the concentration outside the membrane and is normally expressed as a percentage:

$$RR = [X_{\text{dialysate}}] / [X_{\text{outside the membrane}}]$$

For substances where the concentration outside the membrane is not known, various calibration techniques have been described to calculate this.

Two similar equilibration techniques have been developed for the measurement of substances *in vivo*. However, these are not suitable for the measurement of insulin as they require prolonged periods at steady state concentration. The equilibration method described by Lonnroth et al., (1987) involves the perfusion of the microdialysis probe with different concentrations of the substance of interest; as a linear relationship is established between substance concentration in the inlet tubing and the net change across the membrane, linear regression

analysis can be used to identify the concentration at which there is no net change in substance concentration across the membrane hence identifying the concentration in the tissue. Alternatively, the zero flow model uses different flow rates and extrapolates the recovery data to the recovery at zero flow using nonlinear regression (Jacobson et al., 1985).

A third calibration method was developed by Lonnroth and Strindberg (1995) to avoid the time constraints of the equilibration techniques. The 'hot loss' technique involves infusion of radiolabelled substance of interest in the perfusion fluid and measurement of the recovered radiolabel in the outlet fractions. The fractional efflux of the radiolabelled substance equals the unlabelled influx of the substance and can therefore be used as a measure of relative recovery.

Finally a fourth method, the external reference technique can be used and it is this that is most commonly used for the measurement of insulin in humans and rats. This is more suitable than the hot loss technique when constant monitoring of the ISF concentrations is required over extended periods. The external reference technique involves the infusion of a calibrator with similar diffusion, transport and metabolism properties to solute of interest. Briefly, inulin is usually used when measuring insulin because of its similarities and because it characterizes non specific transcapillary diffusion, and is a well established diffusion marker (Chaurasia et al., 2007). Jansson et al., (1993) demonstrated that the relationship between the recovery of insulin and inulin *in vitro* was similar to the relationship *in vivo*. This led to the assumption that if the *in vitro*



recoveries of two substances could be estimated and a ratio calculated then this ratio could be used to calculate the *in vivo* recovery of the substance of interest from the equilibration substance. The recoveries of a number of different substances (water, urea and sucrose) were shown to be similar *in vivo* and *in vitro* (Deguchi et al., 1991). Inulin is a useful tool as it can be assumed that the concentration of inulin will be the same in the plasma and ISF as it equilibrates rapidly and hence RR can be calculated *in vivo*. In addition to *in vitro* experiments to establish the RR of insulin and inulin it is then possible to calculate the RR of insulin *in vivo* using the following formula:

$$\frac{\text{Recovery of inulin } in vitro}{\text{Recovery of insulin } in vitro} = \frac{\text{Recovery of inulin } in vivo}{\text{Recovery of insulin } in vivo}$$

Experiments described by Holmang et al., (1997) comparing the external reference technique to the equilibration technique confirmed the external reference technique is suitable for use *in vivo*.

### 5.1.2 Variables in the microdialysis method

The variables discussed below need to be considered when using the microdialysis technique to measure interstitial insulin concentrations. In the studies described in the present chapter several elements of the microdialysis technique were assessed and optimized for the recovery of insulin in ISF of skeletal muscle of the rat.

### Pore size

As indicated above, microdialysis probes are now produced in a range of molecular weight cut-offs and are made of different materials depending on the substance of interest (Jansson et al., 1993, Niklasson et al., 1998, Rosdahl et al., 2000). Generally, the pore size must be significantly larger than the molecule of interest in order to allow adequate equilibration across the membrane. A limitation of the microdialysis technique for the measurement of insulin is that dialysis membranes with larger pore size have increased porosity and the internal hydraulic pressure caused by perfusion fluid entering the probe causes some ultrafiltration. This efflux of the perfusion fluid works against the diffusion of insulin into the membrane leading to low recovery rates (Chaurasia et al., 2007). Ultrafiltration also dilutes the microenvironment surrounding the probe leading to potentially underestimating the concentration.

Trickler and Miller (2003) suggested that hydrostatic back pressure on the dialysis membrane could be reduced by lowering the outlet tubing below the level of the subject.

Generally probes with molecular weight cut-offs of 50 (Holmang et al., 1999, Holmang et al., 2001) or 100 kDa (Sjostrand et al., 1999, Gudbjornsdottir et al., 2003) have been used for the measurement of insulin, but it is not clear which is better.

### Perfusion fluid

Perfusion fluid is chosen to maintain fluid balance as well as ion balance across the membrane. This limits the osmotic pressure created by the difference in ion balance across the membrane. Osmotic balancing agents are often added to microdialysis perfusion fluid when using 100 kDa or larger cut-off membranes to prevent excessive ultrafiltration as well as non-specific adsorption onto the materials of the device (Rosdahl et al., 2000). Colloids (such as dextran-70) are commonly included in the perfusate (Rosdahl et al., 2000, Hamrin et al., 2002) as they create an osmotic pressure that offsets the hydrostatic pressure pushing the fluid out of the membrane, initial experiments by Rosdahl et al., (2000) showed that *in vitro* all of the perfusion fluid was lost without the addition of a colloid. The presence of bovine serum albumin (BSA) also creates an osmotic pressure that offsets the hydrostatic pressure pushing the fluid out of the membrane (Trickler and Miller, 2003). BSA concentrations of between 1 (Holmang et al., 1997, Holmang et al., 1999, Holmang et al., 2001, Sjostrand et al., 1999, Sjostrand et al., 2000, Gudbjornsdottir et al., 2003, Gudbjornsdottir et al., 2005) and 5% (Herkner et al., 2003) are commonly used in the microdialysis of insulin. The microdialysis technique when used with a colloid is hence considered to be 'volume neutral' (Chaurasia et al., 2007).

Glucose was also added to the perfusate by Lonnroth et al., (1987) to prevent tissue depletion of glucose into the perfusate. This is now common practice.

### Pump rate

As mentioned above, internal hydraulic pressure is caused by perfusion fluid entering the microdialysis probe and can cause ultrafiltration of the membrane.

This hydraulic pressure increases proportionally as the flow rate is increased hence more fluid is lost from the probe at higher flow rates; this effect is exacerbated in probes with a high molecular weight cut-off (Trickler and Miller, 2003). Reducing the pump rate has been shown to result in a reduction of the error and an increase in the recovery (Lonnroth and Strindberg, 1995). Therefore, insulin and inulin are generally perfused at low flow rates to allow greater exchange between perfusate and interstitial fluid thus flow rates of 2 (Holmang et al., 1998), 2.5 (Jansson et al., 1993) or 1  $\mu\text{l}/\text{min}$  (Holmang et al., 1999, Sjostrand et al., 1999) have been used to measure insulin in the ISF fluid. It will be explored which of these rates is preferential for the measurement of insulin in the rat.

#### Outlet tubing

It is important that the outlet tubing of the microdialysis probe is of a standard length because there is an inevitable time delay in the perfusion fluid travelling from the tissue, along the tubing, to the collection vial. Therefore the length of tubing and its volume is key when trying to calculate temporal changes in the ISF concentration and needs to be evaluated.

#### Calibrator

As discussed above, inulin is commonly used as a calibrator for insulin. In animal studies this often involves the insertion of an osmotic minipump containing  $^{14}\text{C}$  inulin 24 hours before the experiment proper, so that inulin can reach steady state well ahead of the experiment (Holmang et al., 1997).

In experiments on human subjects where 'cold' inulin is used, measurement of the inulin concentration has been performed photometrically using the method described by Waugh (Waugh, 1977). In experiments on human subjects inulin (Inutest®) is often given as an intravenous infusion (commonly preceded by a bolus dose; (Sjostrand et al., 1999)). In experimental animals however, the long time period required for inulin to reach steady state has been considered prohibitive as it significantly prolongs the time over which experimental animals are under anaesthesia before the experiment proper can be started.

The, experiments described in this chapter investigated the possibility of using a 'cold' inulin infusion in experiments on rats, beginning the infusion ~80 minutes before the experimental protocol proper, so as to avoid the need for an additional surgical procedure to implant a minipump.

### Limitations

Limitations in the use of microdialysis technique in small mammals have mainly been the low sensitivity of analytical techniques to measure components in small dialysate samples. Insulin is notoriously difficult to work with as it is adsorbed to infusion materials (Jansson et al., 1993), this typically results in very low recoveries of insulin in the dialysate samples (Lonnroth and Strindberg, 1995). Total microdialysate volumes of a few  $\mu\text{l}$  and analyte concentrations in the pmol/nmol range present enormous challenges to the analytical chemist and must be considered when designing the experiment. Analytical methods may require larger sample volumes for accurate measurements, but as discussed above increasing the flow rate will likely decrease the relative recovery of the

probe. On the other hand, decreasing the flow rate to allow for this may decrease the temporal resolution of the experiment. Thus, there are differences in the methodology used by different groups for the measurement of insulin concentrations in ISF, which can make the results difficult to compare directly. Relative recoveries for insulin *in vivo* are reported to range from 3 to 5.6 % (Holmang et al., 1997, Sjostrand et al., 2000) respectively).

Due to the difficulty of measuring insulin in ISF the majority of microdialysis studies published to date have used different assays for plasma and ISF insulin concentrations, plasma concentration being assayed with techniques that are easy, quick and can be applied to relatively large volumes (Sjostrand et al., 2000, Sjostrand et al., 1999, Gudbjornsdottir et al., 2003, Gudbjornsdottir et al., 2005). Additionally, only one study has been able to measure insulin concentrations in ISF under basal conditions (Herkner et al., 2003). This was achieved by using the time-consuming equilibration technique in humans to establish the concentration. All other studies have measured ISF insulin only when the concentration was raised by infusion of insulin.

Thus, the experiments described in this chapter investigated the possibility of measuring both plasma and ISF insulin reliably with the same assay technique. The possibility of measuring insulin concentrations under basal conditions was also investigated.

Thus, the overall aim of the experiments described in the present chapter was to investigate and optimize all of the variables outlined above in order to be able to

measure ISF insulin concentrations as accurately as possible in hindlimb muscles of anaesthetized rats.

## **5.2 Methods and Results**

All equipment used for microdialysis was purchased from CMA Microdialysis, Sweden via Linton Instrumentation, Norfolk, UK unless otherwise stated.

### **5.2.1 Optimising the conditions for *in vitro* analysis of insulin**

#### **5.2.1.1 Methods**

Factorial experimental design (FED) experiments were performed *in vitro* to determine the best conditions for recovery of insulin. Different combinations of material of collection vial, concentration of bovine serum albumin (BSA), rate of perfusion fluid and sigmacote treatment of equipment were tested against each other.

All probe tubing was cut using a scalpel so as not to crush the lumen of the tubing. Probe inlet and outlet tubing of CMA 20 High cut-off 10 mm probes were cut to ~5 cm and connected to half lengths of FEP tubing using tubing adapters (CMA Microdialysis, Sweden) swollen in 70 % ethanol. 'FEP' tubing was either siliconised using Sigmacote® (Sigma-Aldrich Ltd, UK) or flushed with saline. The lengths of FEP tubing attached to the inlets of the CMA 20 probes were attached with tubing adapters to a 1 ml microsyringe containing perfusion fluid. Perfusion

fluid was prepared using albumin from bovine serum and 20 % (w/v) glucose. A working solution of either 1 or 2 % BSA and 1.5 mmol/L glucose was prepared in 0.9% sodium chloride.

The extended outlet tubings were cut to 45 cm (in order to accommodate a 5 minute time lag in collection). The probes were placed in a CMA 130 *In vitro* stand and the CMA 402 Dual syringe pump was started at either 1, 2 or 2.5 µl/min. The FEP tubing attached to the outlet tubing was fed into a CMA 470 Refrigerated microfraction collector (6°C) and samples were either collected into siliconised glass (Fisher Scientific UK Ltd, Loughborough, UK) or plastic microvials (CMA Microdialysis, Sweden).

Insulin was diluted in 2 % BSA (in 0.9% sodium chloride) to a concentration of 7000 pmol/L and 1 ml of solution was placed in siliconised glass vials. Glass vials were secured in a CMA 130 *In vitro* stand and microdialysis probes were submerged in test solution and secured with the clips provided. Probes were equilibrated for 40 minutes with each new set of conditions. Then a 40 minute sample was collected into the corresponding microvial. Samples were then split, snap frozen and stored at -80°C for later determination of insulin concentration using the Crystal Chem Ultrasensitive Insulin Rat ELISA kit. Each sample was analysed in duplicate.



### 5.2.1.2 Results

Figure 5.3 (A) show the results of the Factorial Experimental Design (FED) experiments. 1 % BSA delivered at 1  $\mu$ l/min consistently provided the highest recovery of insulin in each set of conditions. 2 % BSA at 2.5  $\mu$ l/min consistently provided the lowest recovery in each set of conditions. Optimal conditions for the recovery are sigmacoted glass microvials with sigmacoted FEP tubing using perfusion fluid containing 1 % BSA perfused at 1  $\mu$ l/min. The *in vitro* recovery for insulin under these conditions was 7 %. Thus, these were the conditions used in the remaining microdialysis experiments described in this thesis.

## 5.2.2 Inulin analysis

### 5.2.2.1 Methods

Waugh (1977) presented a method for the colorimetric determination of inulin concentration using a combination of cysteine and tryptophan. Standard curves were produced according to the method presented by Waugh (1977); this is referred to below as the 'Waugh method'. Briefly, cysteine hydrochloride/tryptophan solution was prepared by dissolving 1.30g of L-cysteine hydrochloride monohydrate and 30 mg of DL tryptophan in distilled water to 100ml. Benzoic acid was prepared by dissolving 610mg of benzoic acid and 720mg of sodium benzoate in a final volume of 500 ml with distilled water. Inulin standards were prepared by dissolving inulin (from chicory; Sigma-Aldrich Ltd, UK) in 20 mmol/L benzoic acid solution.

In duplicate series 10 µl of standard was added to 1.5 ml Eppendorf tubes. 10 µl of 1.6mol/liter NaOH was added and mixed using a vortex mixer. The open Eppendorfs were then placed on a heating block at 100 °C for 10 minutes then allowed to cool at room temperature. 100 ul of the dilute sulphuric acid (75% by vol) and 10 ul of the cysteine hydrochloride/tryptophan reagent were then added to the Eppendorfs which were promptly closed and vortexed. The closed Eppendorfs were then placed in a water bath at 56 °C for 25 minutes. Once cooled, samples were read at 515 nm on a spectrophotometer against a matched blank.

#### **5.2.2.2 Results**

Figure 5.4 shows the results obtained using three standard curves of 0 – 100 mg/ml inulin, as suggested for microsamples by the Waugh method. The results are presented separately so that the variability in the data can be viewed. These experiments were repeated and showed similar variability (data not shown) and thus it was decided to proceed with *in vivo* experiments to assess the results from perfusate samples collected *in vivo*.

#### **5.2.3 Preliminary measurements of inulin *in vivo***

##### **5.2.3.1 Methods**

Experiments were performed on three Wistar rats ( $222 \pm 1$  g) to investigate the distribution kinetics of inulin infusion *in vivo*. The rats had been housed in cages

in the Biomedical Services Unit (BMSU) on a controlled 12 hour light-dark cycle. The day before the experiment, animals received a fixed ration of diet of 10 g at 16:00.

Rats were anaesthetised with pentobarbital and prepared as detailed in Chapter 4, except that only three cannulae were inserted into the jugular vein and the femoral artery was not exposed for measurement of femoral blood flow. Following stabilisation the animal received a primed infusion of inulin (Inutest® 25 %; Fresenius Kabi, Graz, Austria; a kind gift from L. Strindberg). These experiments were designed to establish a stable concentration of inulin in plasma as assayed by the Waugh method.

The dosing regimen was based on the Inutest information leaflet provided by personal communication with M. Sjostrand and Murdolo et al., (2008). A baseline plasma sample was taken. Then a 50 mg/kg inulin bolus was given as 0.25 mls over 30 seconds followed immediately with 19 mg/hr/kg as 10 µl/min for 240 minutes. During the inulin infusion, plasma samples were taken every 15 minutes and snap frozen for analysis.

Samples were analysed according to the Waugh method (described above 5.2.2.1) except that samples were deproteinised before processing. To this end, one volume of sample, one volume of distilled water, seven volumes of zinc sulphate heptahydrate solution (14.3 g/L) and one volume of sodium hydroxide solution (0.5 mol/L) were added to Eppendorfs and immediately closed and

agitated. The samples were then centrifuged for five minutes at 14 000 RPM. The supernatant was then removed for analysis.

### **5.2.3.2 Results**

Figure 5.5 (C) shows the results obtained using a standard curve of 0 – 100 mg/ml inulin (Figure 5.5 A) as suggested for microsamples in the Waugh method. The individual data points are shown so that the variability in the data can be viewed. It was considered that the standard curve suggested in the method (0 – 100 mg/ml inulin) might be steepening the standard curve due to its short range of concentrations and therefore distorting results. Therefore, a standard curve of 0 – 1000 mg/ml (Figure 5.5 B) was also used to calculate the results. This decreased the variability in the data and also normalised the values within a tighter range (Figure 5.5 D). Therefore further analysis using the Waugh method in the experiments described in this thesis was calculated using a 0 – 1000 mg/ml standard curve.

However, the duplicates for each animal varied widely (for example: 6 and 45 mg/ml for one sample) and thus it was clear that additional validation of the assay was required in order to use it reliably.

### **5.2.4 Adjustments to the Waugh method**

#### **5.2.4.1 Number of replicates**

As discussed above, changes were required to the assay to improve the reproducibility of the results. In the first instance, the standard curves were repeated in triplicate (as opposed to duplicate) and the mean of the results was presented. Figure 5.6 shows that the standard curve produced when the standard curve was repeated in triplicate was more reliable with less variability. All further analyses using the Waugh method were therefore repeated in triplicate (including samples).

#### **5.2.4.2 Spinning and deproteinisation**

To further decrease the variability of the assay replicates, an additional spin step (45 seconds 14 000 RPM) was added after the addition of each reagent during the assay (after addition of NaOH and of sulphuric acid with cysteine hydrochloride/tryptophan reagent). This was done to ensure that reagents were not only mixed, but also pooled together in the bottom of the Eppendorf. It had previously been observed that without the spin step, small amounts of reagent remained in the lid of the Eppendorf and were therefore not included in the reaction; the additional spin step ensured that this did not happen.

The deproteinisation step was also scrutinized for possible modifications. In the deproteinisation method given by Waugh, samples are diluted 1 in 10 with the reagents. This is a significant dilution given that the concentrations of inulin are reasonably low and results in samples being read off the very bottom of the standard curve. Tests were therefore made of whether the samples could instead be diluted 1 in 5 (one volume of sample, three and a half volumes of zinc sulphate heptahydrate and half a volume of sodium hydroxide) or 2 in 10 (two

volumes of sample, seven volumes of zinc sulphate heptahydrate solution and one volume of sodium hydroxide solution). Hence, the ratio of reagents was kept the same, but the amount of sample was varied. Spiked plasma samples (0, 10, 50, 100, 200 and 500 mg/ml) were tested with the different deproteinisation methods so that recovery of the known concentration could be calculated.

#### **5.2.4.3 Results**

Figure 5.7 (A) shows a standard curve without the additional spin step and in contrast to Figure 5.7 (B) shows the effect of the additional spin step.

Comparison suggests that the standard curves are more reliable with the added spin step than without.

As with the original deproteinisation method, the 1 in 5 method significantly overestimated results at the lowest concentration (10 mg/ml), but to a lesser extent than the original method. Results for higher concentrations (50 – 500 mg/ml) were more accurate than the original method (data not shown). The 2 in 10 method showed a similar pattern of recovery except that the overestimation of the 10 mg/ml was much greater than the other two methods. This complete set of tests was repeated and similar patterns in recovery emerged (data not shown).

An additional deproteinisation method (barium hydroxide) was investigated for use with the Waugh method but was not found to be suitable (data not shown).

Thus, further analysis of inulin made using the Waugh method included additional spin steps, deproteinisation with a 1 in 5 dilution of samples and spiked plasma samples to monitor recovery of the assay.

## **5.2.6 Reassessment of preliminary inulin assays from *in vivo* experiments**

### **5.2.6.1 Methods**

Samples from the experiments described in Section 5.2.3 were reanalyzed using the improved assay technique (see below). There was only enough sample remaining from two of the three original animals to assay. Thus, animals 2 and 3 were reassessed.

Firstly, inulin-spiked plasma samples (0, 10, 50, 100, 200, 500, 1000 mg/ml) were produced using inulin extracted from chicory (Sigma-Aldrich Ltd, UK). Spiked plasma samples and samples were then deproteinised. One volume of sample, three and a half volumes of zinc sulphate heptahydrate solution (14.3 g/L) and a half volume of sodium hydroxide solution (0.5 mol/L) were added to eppendorfs and immediately closed and agitated. The samples were then centrifuged for five minutes at 14 000 RPM. The supernatant was removed for analysis.

Cysteine hydrochloride/tryptophan solution was prepared by dissolving 1.30g of L-cysteine hydrochloride monohydrate and 30 mg of DL tryptophan in distilled water to 100ml. Benzoic acid was prepared by dissolving 610mg of benzoic acid

and 720mg of sodium benzoate in a final volume of 500 ml with distilled water. Standard curves were produced according to the method presented in Waugh et al., (1977). Inulin standards were prepared by dissolving inulin (from chicory; Sigma-Aldrich Ltd, UK) in 20 mmol/L benzoic acid solution. Inulin standards from a previous assay (that had been stored at -80 °C) were also run with this analysis to assess the validity of aliquoting and freezing standards.

In triplicate series, 10 µl of standard or sample was added to 1.5 ml eppendorfs. 10 µl of 1.6mol/liter NaOH was added and mixed using a vortex mixer. Eppendorfs were centrifuged for 45 seconds at 14 000 RPM. Open Eppendorfs were then placed on a heating block at 100 °C for 10 minutes then allowed to cool at room temperature. 100 ul of the dilute sulphuric acid (75% by vol) and 10 ul of the cysteine hydrochloride/tryptophan reagent were then added to the Eppendorfs which were promptly closed, vortexed then centrifuged for 45 seconds at 14 000 RPM. The closed Eppendorfs were then placed in a water bath at 56 °C for 25 minutes. Once cooled samples were read at 515 nm against a matched blank.

#### **5.2.6.2 Results**

Figure 5.8 shows the results of the improved inulin analysis of the inulin infusion experiments from Section 5.2.3. Triplicate analysis greatly improved the reproducibility of the results versus previous analysis (B); error bars on the graph indicate that there was very little variability between replicates of each sample (A). Inulin concentration peaks following a bolus dose of inulin and then



plateaus to steady state of  $\sim 800$  mg/ml at  $\sim 75$  minutes. Values for inulin at steady state were in a similar range for both animals. What is more, the samples were higher up the standard curve than previous analyses, where the recovery values for the assay are more reliable.

Figure 5.8 (B) shows the results from the same analysis run against inulin standards that had been frozen prior to use. It can be seen that the recovery of inulin in these samples is much lower than in Figure 5.8 (A) which confirms that it is not suitable to aliquot and freeze standards for this assay. Therefore in all later experiments fresh standards were made up for each new analysis.

## **5.2.7 The kinetics of inulin infusion *in vivo***

### **5.2.7.1 Methods**

Experiments were performed on three Wistar rats ( $223 \pm 10$  g) to investigate the distribution kinetics of inulin infusion. The rats had been housed in cages in the Biomedical Services Unit (BMSU) on a controlled 12 hour light-dark cycle. The day before the experiment, animals received a fixed ration of rat chow (10 g) at 16:00.

Animals were anaesthetised with pentobarbital and prepared as detailed in Chapter 4 except that only three cannulae were inserted into the jugular vein and the femoral artery was not exposed for measurement of femoral blood flow.

Following stabilization, the rat received a primed infusion of inulin (Inutest® 25 %; Fresenius Kabi, Graz, Austria; a kind gift from L. Strindberg). A baseline

plasma sample was taken, then a 50 mg/kg inulin bolus was given intravenously as 0.25 mls over 30 seconds followed immediately by infusion of inulin 2 mg/kg/min at 10  $\mu$ l/min for 180 minutes. Plasma samples were taken at time points 1, 5 and 15 minutes and for every 15 minutes thereafter. The infusion was stopped at 180 minutes and a final plasma sample was taken at 185 minutes to gain information on clearance. Dosing was based on modeling of the results from Section 5.2.6.2 undertaken by the Pablo Morentin Gutierrez at AstraZeneca, Alderley Park.

Samples were analysed according to the adjusted Waugh method in (see Section 5.2.6.1).

#### **5.2.7.2 Results**

Figure 5.9 shows the results for the 50 mg/kg bolus and 2 mg/kg/min infusion of inulin into anaesthetized Wistar rats. The standard curve and plasma spike values were within the expected ranges. The error bars on the data were very small (except animal 1 at time point 1 minute). Thus, with the adjusted Waugh methodology, the replicates were much more reproducible. The larger error bars for animal 1 at time point 1 are likely due to the fact that the result was higher than the standard curve for the data. It can also be seen in Figure 5.9 that the differences between the animals were much smaller than in the experiments described in Section 5.2.6.2. There was a peak in inulin concentration at 1 minute following inulin infusion but steady state of  $\sim 350$  mg/ml was reached at  $\sim 30$  minutes and maintained throughout the infusion.

## 5.2.8 Microdialysis of inulin *in vivo*

### 5.2.8.1 Methods

In view of the refinements described in Section 5.2.7.2 experiments were performed on four Wistar rats ( $271 \pm 11$  g) to investigate the kinetics of inulin infusion to obtain a steady-state concentration *in vivo*. The rats had been housed in cages in the Biomedical Services Unit (BMSU) on a controlled 12 hour light-dark cycle. The day before the experiment, animals received a fixed ration of chow of 10 g at 16:00 as described in Chapter 4.

All microdialysis probe tubing was cut using a scalpel so as not to crush the lumen of the tubing. Probe inlet and outlet tubing were cut to ~5 cm. 'FEP' tubing was siliconised using Sigmacote® (Sigma-Aldrich Ltd, UK) and cut in half. Half lengths of FEP tubing were attached to the inlet and outlet tubing using tubing adapters (CMA Microdialysis, Sweden) swollen in 70 % ethanol. The lengths of FEP tubing attached to the inlets of the CMA 20 probes were attached with tubing adapters to a 1 ml microsyringe containing perfusion fluid. The extended outlet tubings were cut to 45 cm (in order to accommodate a 5 minute time lag in collection). The probes were placed in a CMA 130 *In vitro* stand and the CMA 402 Dual syringe pump was started at 1  $\mu$ l/min. Once the probes were seen to be patent the animal was prepared.

Animals were anaesthetised with pentobarbital and prepared as detailed in Chapter 4, except that the femoral artery was not exposed for measurement of femoral blood flow. Additionally, a single microdialysis probe (CMA 20 High cut-off 10 mm) was inserted into the left hindlimb muscle by using a guide needle and split tubing (plastic tubing, split along half the length). To this end, a small incision was made in the skin of the left hindlimb, close to the foot and a guide needle and split tubing was inserted through the incision into the Tibialis Anterior muscle at 45° and tunnelled 5mm under the surface. The guide needle was removed from the split tubing and the microdialysis probe inserted into the split tubing and the plastic handles were sutured to the skin. The split tubing was then removed by pulling on either side of the protruding ends leaving the microdialysis probe within the muscle. The FEP tubing attached to the outlet tubing was fed into a CMA 470 Refrigerated microfraction collector (6°C). Samples were collected into siliconised glass microvials then split to be stored at -80°C for later determination of inulin concentration. Probes were checked regularly for patency and flushed at 20 µl/min for ~ 30 seconds if necessary.

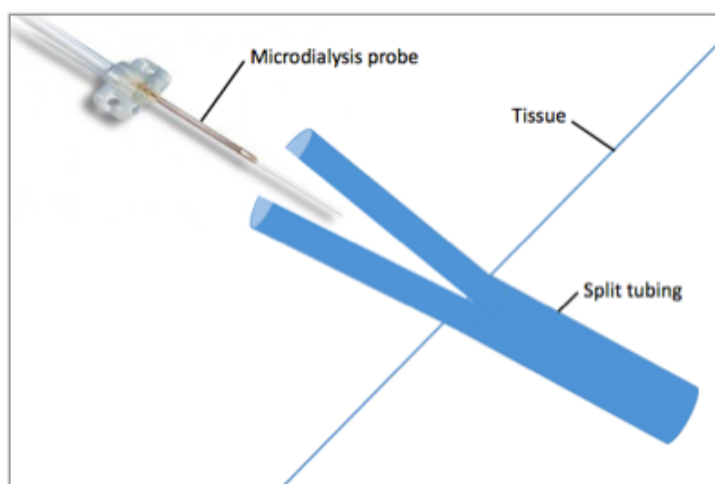


**Figure 5.1 Diagram of microdialysis probe insertion into tissue.**

Split tubing was inserted using a guide needle which was then removed, leaving the split tubing *in situ* (as pictured above). The microdialysis probe was then inserted into the split tubing and sutured to the tissue using the butterfly needle attachment. The split tubing was then removed by pulling the protruding ends apart, leaving the microdialysis probe secured *in situ*.

Following stabilization, animals received a primed infusion of inulin (Inutest® 25 %; Fresenius Kabi, Graz, Austria; a kind gift from L. Strindberg). A baseline plasma sample was taken. Then, a 50 mg/kg inulin bolus was given as 0.25 mls over 30 seconds followed immediately with 1 mg/kg/min inulin at 10 µl/min for 200 minutes as before.

Two animals received only inulin infusion, whereas two animals also underwent HE clamp (10 mU/kg/min insulin). HE clamp was performed as detailed in Chapter 4. Insulin infusion in these experiments began at 80 minutes into the inulin infusion (to ensure that steady state had been reached). Plasma samples time points for inulin analysis therefore corresponded with the plasma samples required for the HE clamp and so were -10, 60, 80, 100, 120, 140, 150 and 160 minutes into the inulin infusion (see Figure 5.2). Microdialysis samples were

taken every 40 minutes from the beginning of the inulin infusion for 200 minutes.

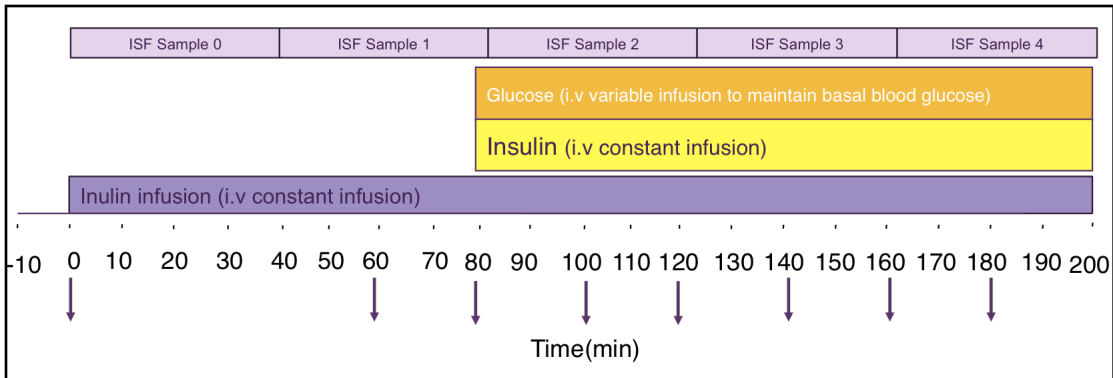


**Figure 5.2 Schematic of protocol for Section 5.2.8.**

Inulin infusion began at 0 minutes and continued for 200 minutes. HE clamp began at 80 minutes and continued for 200 minutes. ISF samples were taken every 40 minutes from 0 minutes onwards. Downward arrows indicate where blood samples were taken.

Samples were analysed for inulin according to the refined Waugh methodology described in Section 5.2.6.1.

**5.2.8.2 Results**

Figure 5.10 (A) shows that results for plasma inulin samples following inulin infusion without (rats 1 and 2) or with (rats 3 and 4) HE clamp. Plasma inulin concentrations were ~ 100 mg/ml in the basal sample and then increased with inulin infusion in all rats to ~ 350 mg/ml. HE clamp did not make any difference to the plasma inulin concentration measured ( $P < 0.54$ ) indicating that insulin does not interact with the inulin assay.

Figure 5.10 (B) shows the results for inulin in ISF samples following inulin infusion without (rats 1 and 2), or with (rats 3 and 4) HE clamp. ISF insulin

concentrations were  $\sim 90$  mg/ml at basal and remained the same during inulin infusion.

These results are concerning for two reasons. Firstly there should be minimal concentrations of inulin in the ISF under basal conditions. Secondly, the inulin concentrations in plasma would be expected to increase greatly with an inulin infusion resulting in plasma inulin concentrations of  $\sim 350$  mg/ml. Further, it is interesting to note that basal plasma inulin concentrations are around the same as those in ISF. This suggests that values are not in fact correct, but did not offer clarity at the lower end of the standard curve for inulin. Therefore, experiments were conducted with double the concentration of inulin to try to bring the sample concentrations onto the linear part of the standard curve.

## **5.2.9 Measurement of insulin and inulin by microdialysis *in vivo***

### **5.2.9.1 Methods**

Experiments were performed on four Wistar rats ( $308 \pm 7$  g) that had been housed in cages in the Biomedical Services Unit (BMSU) on a controlled 12 hour light-dark cycle. The day before the experiment, animals received a fixed ration of chow of 10 g at 16:00. Experiments were carried out under pentobarbital anaesthesia as detailed in Section 5.2.8.1, with a 50 mg/kg inulin bolus being given as 0.25 mls over 30 seconds then followed immediately with 2 mg/kg/min as 10  $\mu$ l/min for 200 minutes (ie. twice the concentration previously used).

Samples were analysed for inulin according to the method described in Section 5.2.6.1. Samples were analysed for insulin concentration on the Crystal Chem Ultrasensitive Insulin Rat ELISA kit as per the protocol provided.

### **5.2.9.2 Results**

Plasma inulin concentrations in this set of experiments were largely undetectable at basal and increased to ~ 650 mg/ml during inulin infusion. As expected, inulin concentrations in ISF were still in the very low part of the standard curve at basal but did not increase enough with inulin infusion to be differentiated from the basal samples. Analysis of the results was repeated to subtract the basal sample from each sample during infusion, but in most cases, this resulted in negative values being calculated. However, the insulin concentrations measured in ISF in these experiments were actually more problematic (see below) so focus was placed on fixing this.

The plasma insulin concentrations measured were as expected for lean animals from previous work (Chapter 4; increasing from ~200 pmol/L to ~ 2000 pmol/L) during HE clamp. However, even basal concentrations of insulin in ISF were off the range of the Crystal Chem Ultrasensitive Insulin Rat ELISA kit ie. > 11, 136 pmol/L. These results were extremely unlikely to be real, given the known difficulty of measuring insulin in the ISF and the fact that the plasma concentrations measured were within the normal range. Thus, extensive investigations were conducted to try to establish why the insulin results were so high.



#### **5.2.10 Investigations into overestimation of ISF insulin**

A number of possibilities were explored to try to explain the high values reported for ISF insulin. Firstly, the samples were run again on the insulin assay with and without deproteinisation. It was hypothesized that a reagent in the deproteinisation step may have reacted with the assay kit to cause saturation of the signal. This was found not to be the case: omitting this step did not reduce the insulin signal.

Interstitial samples were also run on a different assay kit (Mercodia Human and Rat Insulin ELISA kit) to rule out the possibility that it was a kit specific interaction. Again, this was found not to affect the high concentrations of insulin measured.

This kind of interaction had not been previously reported by other groups when measuring ISF insulin concentrations (personal communication with PA. Jansson, Sweden). However, it was noted that for some published studies on rats a lower-molecular weight cut-off probe had been used. Thus, there was a possibility that in rats, the larger probes used in the present study (100 kDa cut-off) allowed other molecules through the membrane (such as IGF-1) that were able to interact with the assay kit, perhaps forming complexes in the wells that were able to saturate the signal. Therefore, lower molecular weight cut-off probes were investigated against the 100 kDa cut-off probe (see below) in conjunction with a commercial assay kit for the measurement of insulin.

### **5.2.11 Use of lower molecular weight cut-off probes and inulin ELISA**

#### **5.2.11.1 Methods**

Preliminary experiments on four Wistar rats using 20 kDa molecular weight cut-off microdialysis probes indicated that they were not suitable for use in lean Wistar rats for the measurement of interstitial insulin and inulin. Recovery of inulin was off the top of the standard curve with the 20 kDa molecular weight cut-off probe, possibly indicating that the probes were ultrafiltrating.

*In vivo* experiments were therefore carried out as detailed in Section 5.2.8.1 except that in two animals 55 kDa cut-off probes were used and in two animals, 100 kDa cut-off probes were used. Additionally, all animals received a 1 mg/ml bolus dose of BioPAL's Inulin for intravenous injection (GFR-GRADE) as 0.125 mls over 30 seconds followed immediately with a 0.08 mg/kg/min infusion at 10 µl/min.

BioPAL's FIT-GFR (Inulin) ELISA kit is provided with inulin for injection but, is also suitable for use with Fresenius' SINISTRIN (Inutest®). To assess the recovery of Inutest® on the BioPAL kit, standard curves of both BioPAL's Inulin for injection (GFR-GRADE) (10 mg/ml) and Inutest® were run on the BioPAL kit. This also allowed comparison with the data provided by the manufacturer. Standards for both types of inulin, diluted in Standard and Sample Diluent, were run at the following concentrations: 0.01, 0.03, 0.1, 0.3, 1, 3 and 10 µg/ml. Spiked

plasma samples of both types of inulin at concentrations of 0.3 and 3 µg/ml (corresponding to the linear part of the standard curve) were also run on the assay.

Experiments were also conducted to investigate whether samples could be refrigerated for more than one week, or whether they needed to be analysed in weekly batches.

#### **5.2.11.2 Results**

The data presented here are from the second group of experiments involving comparison of 55 and 100 kDa probes. As predicted in the standard curves provided by BioPAL, both BioPAL inulin and Inutest® are compatible with the BioPAL ELISA although the standard curves are quite different shapes (Figure 5.11 A and B respectively). The Inutest® curve does not appear to have a clearly defined linear section like the BioPAL inulin curve. The BioPAL comparison curves and to some extent the curve shown in Figure 5.11 B indicate that the Inutest® curve is much flatter at the lower end; this would be expected to result in less differentiation between low concentrations of Inutest®.

The samples taken from the rats of the present study showed that measurement of inulin concentration in the BioPAL spiked plasma samples were overestimated (10.6 for 3 mg/ml and 1.8 for 0.3 mg/ml), whereas the Inutest® spiked plasma samples were more overestimated (18.6 for 3 mg/ml and 8.6 for 0.3 mg/ml).

Thus, it seems that the ELISA performed more reliably with BioPAL inulin rather than with Inutest®.

Given the more desirable shape of the standard curve with the BioPAL inulin and the more accurate recovery in the spiked plasma samples, BioPAL inulin was used for the remaining insulin microdialysis experiments in this thesis.

Recovery of 30 and 15 µg/ml from spiked plasma *in vitro* was more accurate with the 55 versus the 100 kDa cut-off probe (Figure 5.12). However, recovery of plasma inulin *in vivo* was increased with the 100 versus the 55 kDa cut-off probe. Recovery of ISF inulin *in vivo* also increased throughout the protocol with the 100 versus the 55 kDa cut-off probe. Thus, with the 100 kDa cut-off probe inulin concentrations *in vivo* increased throughout the protocol, as expected, whereas with the 55 kDa cut-off probe, inulin concentrations were more variable.

Unlike the experiments performed with Inutest® described in Section 5.2.9, insulin concentrations measured when using BioPAL inulin were within the expected range. Recovery of ISF insulin *in vivo* was similar between 55 and 100 kDa cut-off probes, except that insulin concentrations in the 55 kDa cut-off probes tended to decrease towards the end of clamp, whereas the 100 kDa cut-off probe concentrations did not. ISF insulin concentrations increased throughout the clamp protocol with both probes. Recovery of ISF insulin was however much higher with the 100 kDa cut-off probes versus the 55 kDa cut-off ones (Figure 5.12).

Thus, given that the recovery of insulin and inulin *in vivo* were better with the 100 kDa versus 55 kDa cut-off probe, the 100 kDa probe was used for the remaining experiments described in this thesis.

Experiments to investigate whether or not samples could be kept in the fridge for more than one week showed that after 14 days there was significant loss of inulin concentration versus the results recorded during analysis from the previous week (data not shown).

Further experiments were also completed to determine whether when making plasma spikes, it was preferable to spike given concentrations into plasma or whether to spike in concentrations similar to those found *in vivo* and then dilute them down using the sample diluent. Recovery of the known concentration was much higher when higher concentrations of inulin were diluted using sample diluent (data not shown). Therefore, standards were always made on the morning of the experiment and spiked plasma was made at higher concentrations and diluted down using sample diluent.

#### **5.2.12 Validation of insulin assay for the measurement of ISF samples**

An area of key importance to the measurement of insulin in ISF samples is the accuracy of detection of insulin at very low concentrations. Recent changes in the assay ranges on commercial assays offer improved sensitivity in the measurement of insulin *in vivo*. Hence, Herkner et al., (2003) were able to measure basal concentrations of insulin in their experiments in humans due to

their use of the Mercodia Ultrasensitive Insulin ELISA. Thus, the improved range of the Mercodia Ultrasensitive Rat Insulin ELISA is 0.9 – 120 pmol/L which is much lower than the Mercodia Rat Insulin ELISA (18 – 1,200 pmol/L). However, the limitation of the Mercodia assays, is that the sample volume required is 25  $\mu$ l. Given the chosen flow rate of 1  $\mu$ l/min for these experiments, this would mean only one or two measurements could be made over the course of the experiment (taking into account the need to measure ISF inulin and also the dead space volume). Experiments were therefore conducted to see whether or not the Mercodia Ultrasensitive Rat Insulin ELISA kit could be used by adding 5  $\mu$ l of samples, standards and spikes to the wells instead of the recommended 25  $\mu$ l.

An alternative assay that can be used for the measurement of insulin concentrations in biological samples is the Crystal Chem Rat Ultra Sensitive Insulin ELISA; the range of this assay is 17.4 – 11,136 pmol/L. Although the range is not as low as the Mercodia Ultrasensitive Rat Insulin ELISA it has the major advantage that it only requires a sample volume of 5  $\mu$ l. What is more the assay has been validated by the Analytical Group, CVGI, AstraZeneca, Alderley Park for the measurement of insulin in the range 5.4 – 11,136 pmol/L.

As discussed in Chapter 4, the Mercodia assay cross-reacts with human insulin and thus the results must be calculated using a (given) measure of cross-reactivity in order to accurately measure insulin concentrations when human insulin is infused. For the Crystal Chem assays however, cross-reactivity is not given. Hence, experiments were conducted to investigate the cross-reactivity of human insulin in *in vivo* samples on the Crystal Chem Rat Ultra Sensitive Insulin

ELISA. To this end, samples from previous microdialysis experiments were analysed on the following standard curves: rat standards in assay diluent (provided), human standards in assay diluent and human standards spiked into rat plasma so that the results could be compared.

#### **5.2.12.1 Methods**

The Mercodia Ultrasensitive Insulin ELISA kit was run as detailed in the kit instructions except that 5 µl of standard, QC and sample was added to the well instead of the 25 µl specified in the kit instructions.

The Crystal Chem Ultrasensitive Insulin ELISA was run as detailed in the kit instructions except that several different standard curves were compared. Thus, an extended (5.4 – 11, 136 pmol/L) rat insulin standard curve (provided with the kit) was made up using assay diluent. A standard curve of corresponding human insulin concentrations was also formulated in assay diluent. Finally a standard curve of rat insulin in rat plasma was tested. Samples from previous experiments in this chapter were also run on the assay at the same time so that results could be compared.

#### **5.2.12.2 Results**

The Mercodia Ultrasensitive Insulin ELISA kit was not suitable for use with 5 µl of sample (data not shown).

Measurements of microdialysis samples from previous experiments described in this chapter were made on the following standard curves: rat standards in diluent (provided), human standards in diluent and human standards spiked into rat plasma. These results were then compared. As expected, human insulin has a much higher affinity for the assay than rat insulin and thus human insulin concentrations were over estimated when using the rat standard curve, whereas results measured using the human standard curves were in the range expected. Results from the human standards spiked into rat plasma were more reliable than the results from the human standards in diluent. Thus, recovery of human insulin on this assay was calculated in this way for the remaining experiments described in this thesis.

Despite the fact that the standard curves of human insulin spiked into rat plasma are highly reproducible (Figure 5.13), as the measurement of human insulin on the Crystal Chem kit is so vital to the accurate representation of the data, it was decided that the standard curve of human insulin spiked into rat plasma would be run in conjunction with the provided rat standard curve each time the assay was run. Thus, any variability in the performance of the assay was taken into account. Hence, samples before the initiation of insulin infusion were read off the rat standard curve and samples collected after the initiation of insulin infusion were read off the human standard curve. This allowed for the accurate measurement of concentrations of human insulin on the Crystal Chem assay and validated the recovery of insulin for each repetition of the assay.



### 5.2.13 *In vitro* recovery experiments

Following optimization of the methodology described above, *in vitro* recovery experiments were conducted using the same conditions as those that were used *in vivo* for the remaining experiments described in this thesis.

#### 5.2.13.1 Methods

In order to calculate the recovery of insulin and inulin *in vivo* the following formula was used:

$$\frac{\text{Recovery of inulin } in vitro}{\text{Recovery of insulin } in vitro} = \frac{\text{Recovery of inulin } in vivo}{\text{Recovery of insulin } in vivo}$$

Measurements of the recovery of insulin and inulin using the 100 kDa cut-off probe were required. Thus, experiments were performed as detailed in Section 5.2.1.1 with 1 µl/min flow rate, 1 % BSA and 1.5 mmol/L glucose in the perfusion fluid, siliconised FEP tubing and siliconised glass collection vials. Known concentrations of 3000, 1000 and 300 pmol/L insulin were tested, in conjunction with a known concentration 25 µg/ml of inulin. All concentrations were diluted into 2 % BSA as a representation of the composition of plasma.

Following these experiments, known concentrations of 3000, 1000 and 300 pmol/L insulin were tested and 25 µg/ml of inulin was tested separately as above (also diluted in 2 % BSA).

### 5.2.13.2 Results

Several attempts were made to measure the *in vitro* recovery of insulin and inulin in combination. However, when known concentrations of insulin and inulin were tested together, calculated recoveries were frequently over 100 % (data not shown). This was particularly the case at the lower concentrations of insulin.

Thus, experiments were performed in triplicate to separately analyse the *in vitro* recovery of 3000, 1000 and 300 pmol/L of insulin and 25 µg/ml of inulin (Table 5.1). The recoveries varied with the different concentrations of insulin, suggesting that analysis may need to take into account the concentration of insulin.

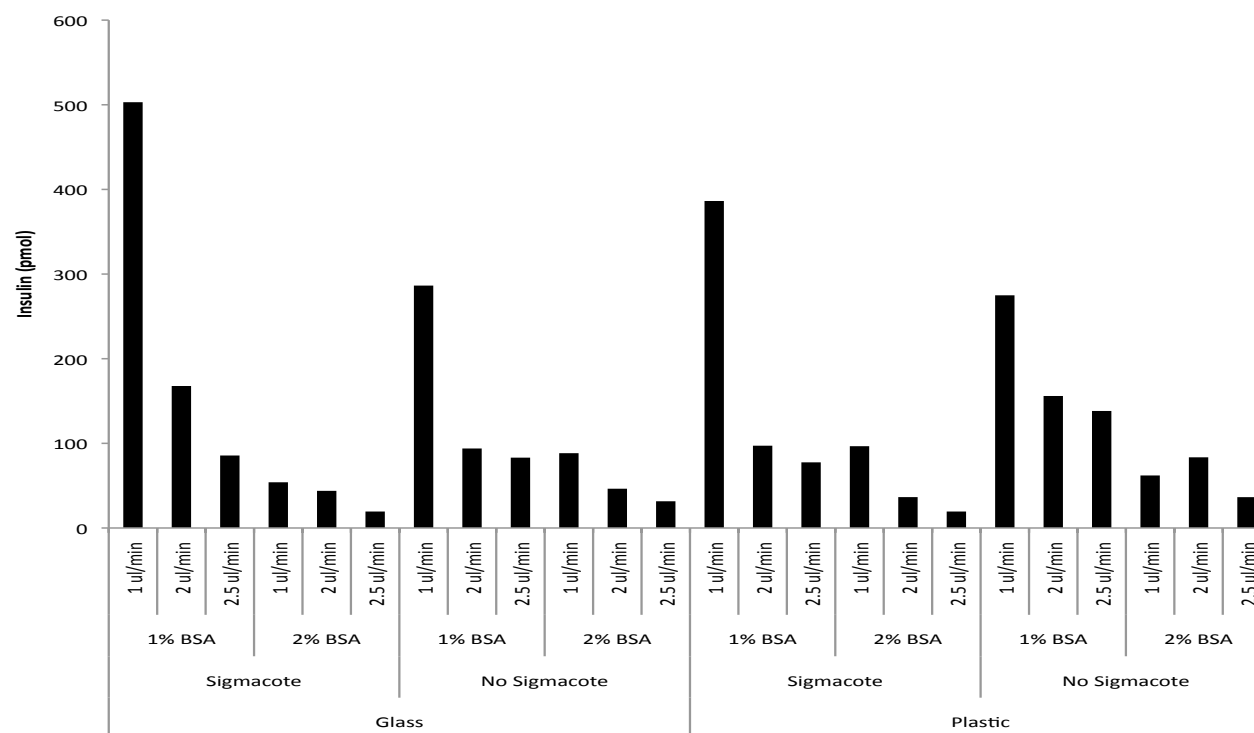


**Figure 5.3 FED analysis of *in vitro* recovery of insulin.** FED analysis was completed to compare material of collection vial (glass or plastic), concentration of bovine serum albumin (1 or 2 % BSA), rate of perfusion fluid (1, 2 or 2.5 ul/min) and sigmacote treatment of equipment or not (Sigmacote / No Sigmacote). Bars represent the mean of two measurements taken under those conditions.

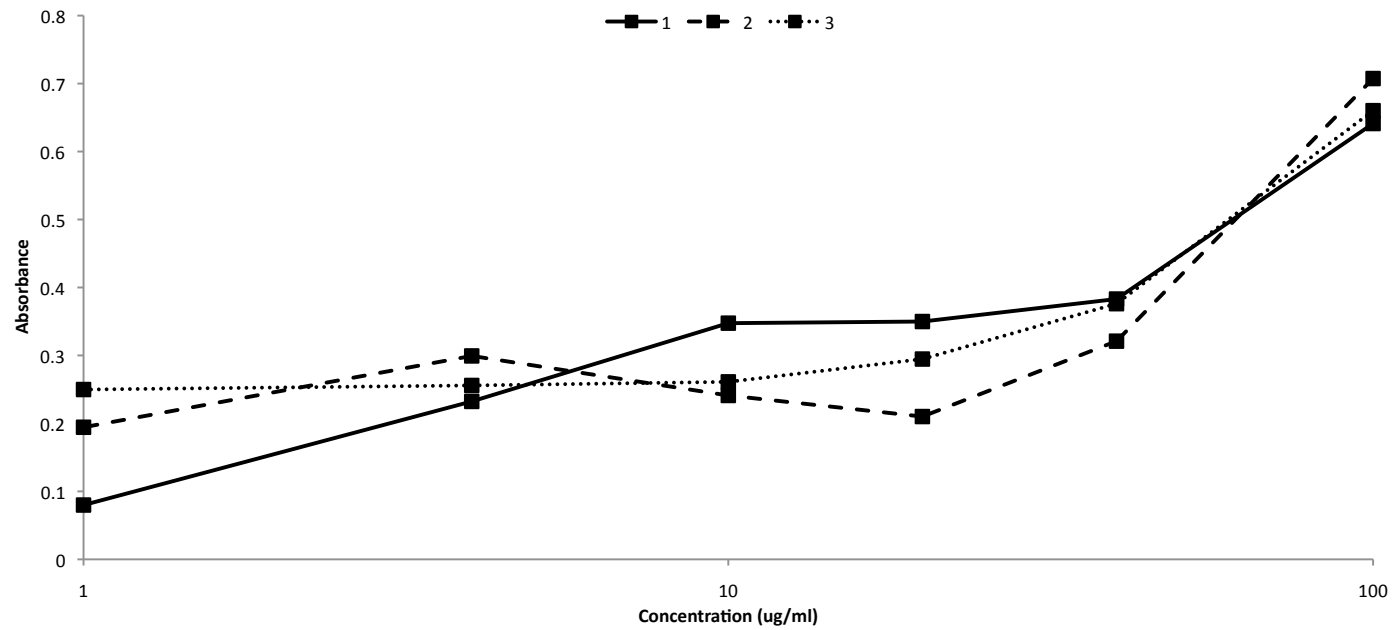


**Figure 5.4 Initial inulin analysis using the Waugh method.** Three standard curves were produced using the Waugh method. Data points represent individual measurements taken so that variability in the data can be viewed.

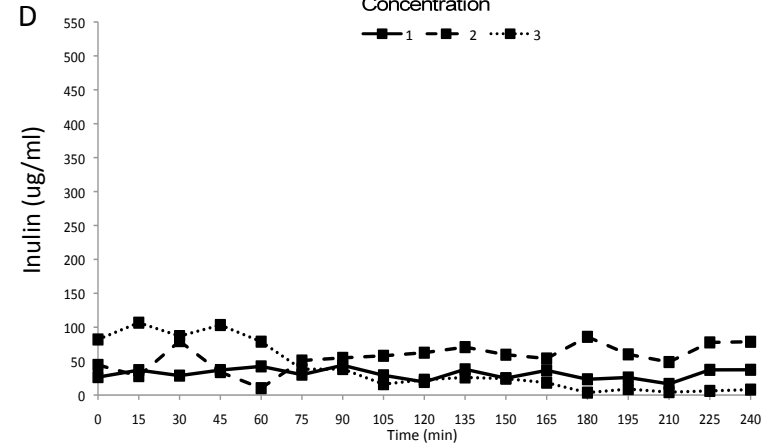
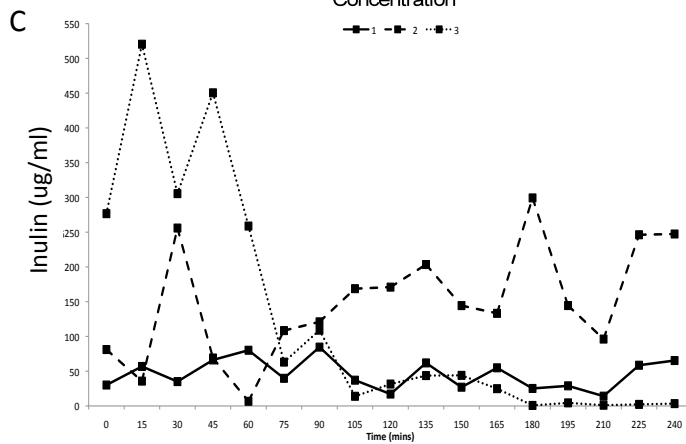
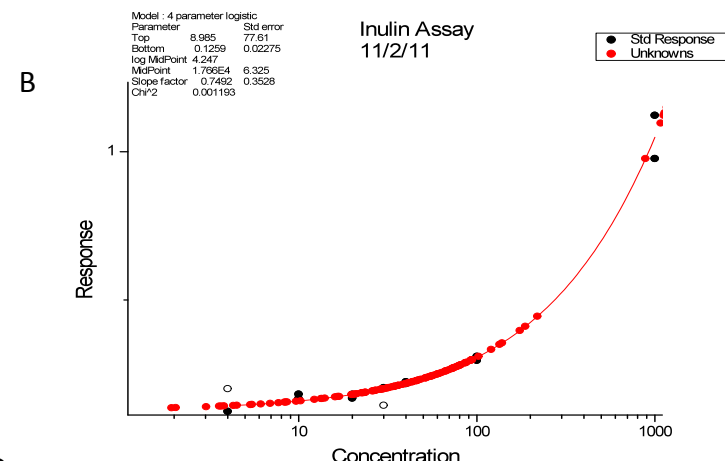
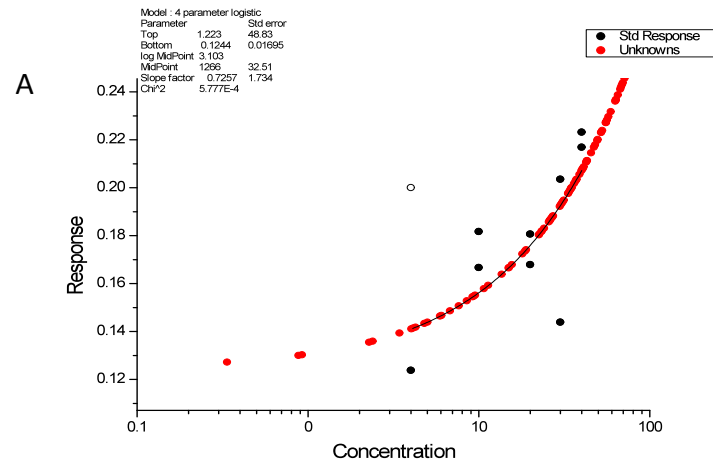


**Figure 5.5 Adjustment of the standard curve used in the Waugh method.** (A) and (B) show the standard curves produced according to the Waugh method using standard curves of 0 – 100 mg/ml and 0 – 1000 mg/ml respectively. (C) and (D) show the results calculated from standard curves (A) and (B) respectively on the same plasma inulin samples. Data points represent individual measurements. Open circles are excluded data points.

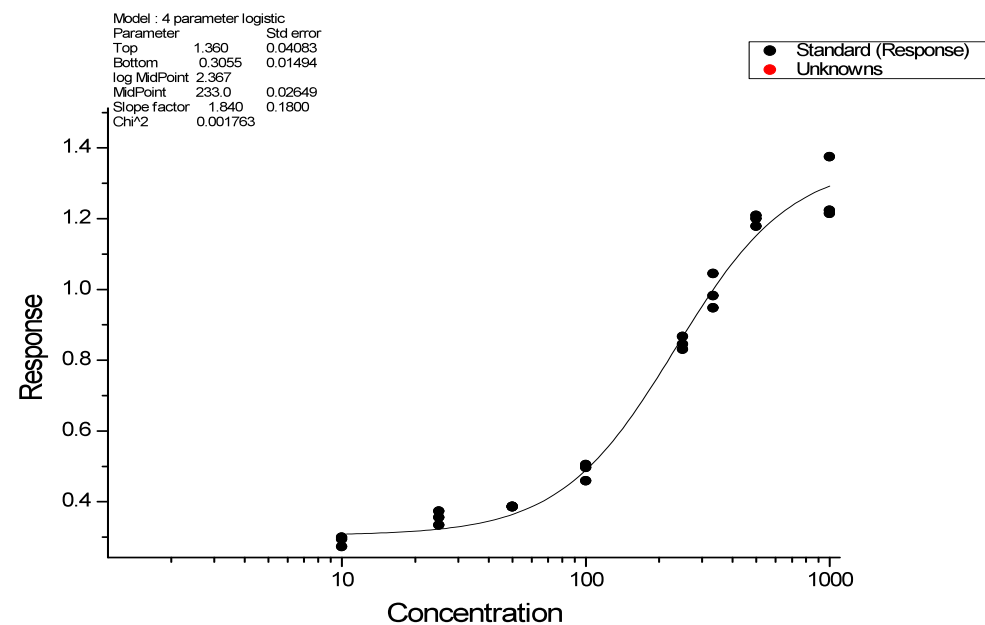


**Figure 5.6 Increased number of replicates using the Waugh method.** A representative standard curve for the Waugh method when standards were repeated in triplicate. Data points represent individual measurements.

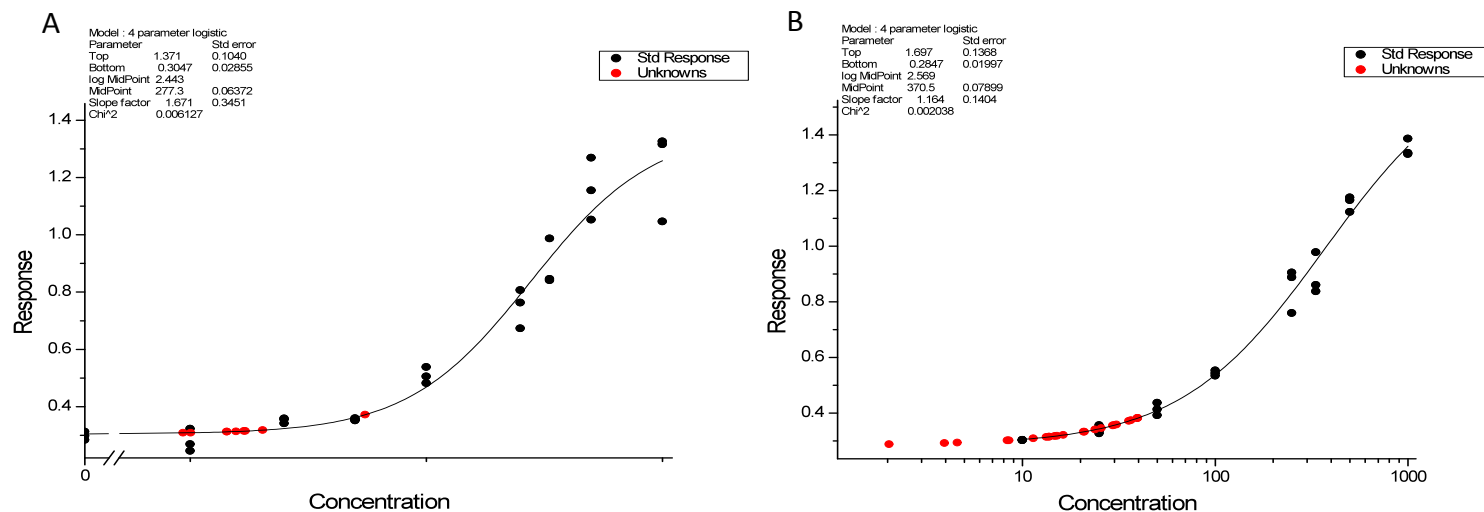


**Figure 5.7 Additional spin steps added to the Waugh method.** (A) represents a standard curve produced without the addition of a spin step to the protocol. (B) represents a standard curve produced with the addition of a spin step to the protocol. Data points represent individual measurements.

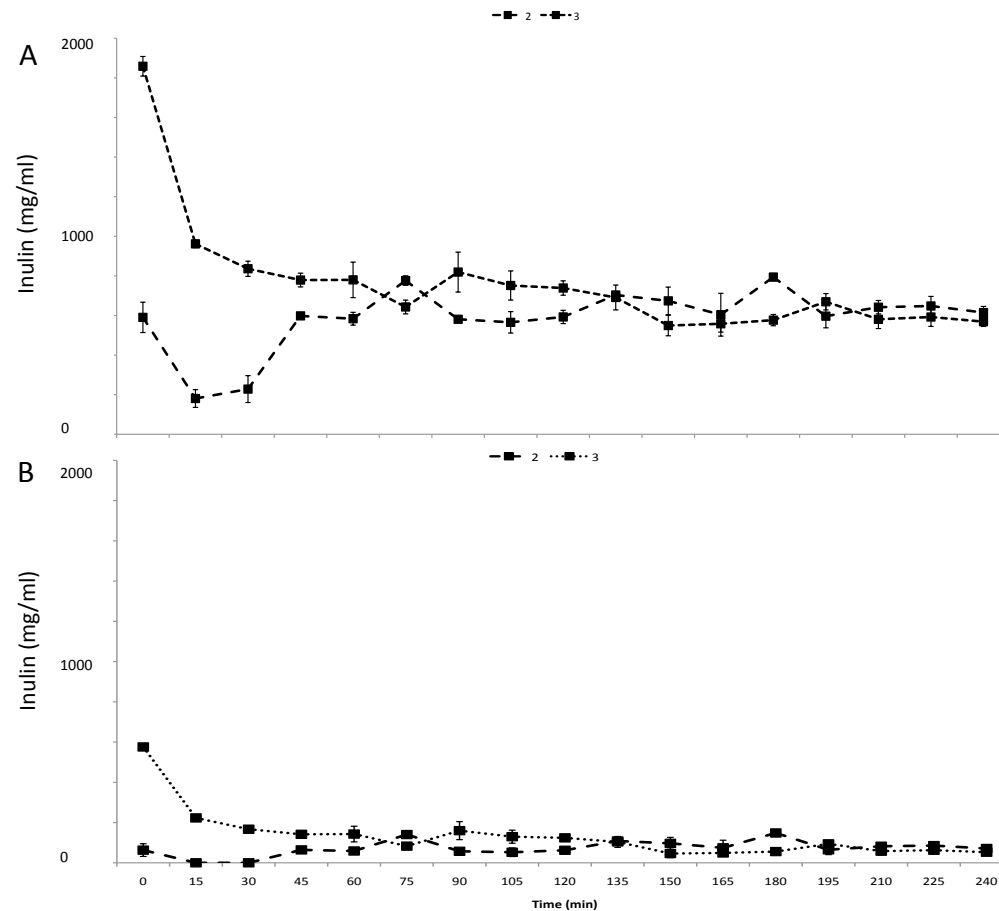


**Figure 5.8 Analysis of *in vivo* samples with the improved Waugh method.** (A) shows re-analysis of samples in Figure 5.6 with the improved Waugh method for the analysis of plasma inulin concentration.(B) shows analysis of the same samples using a standard curve that has been frozen prior to use. Data points are mean  $\pm$  SEM of three measurements.



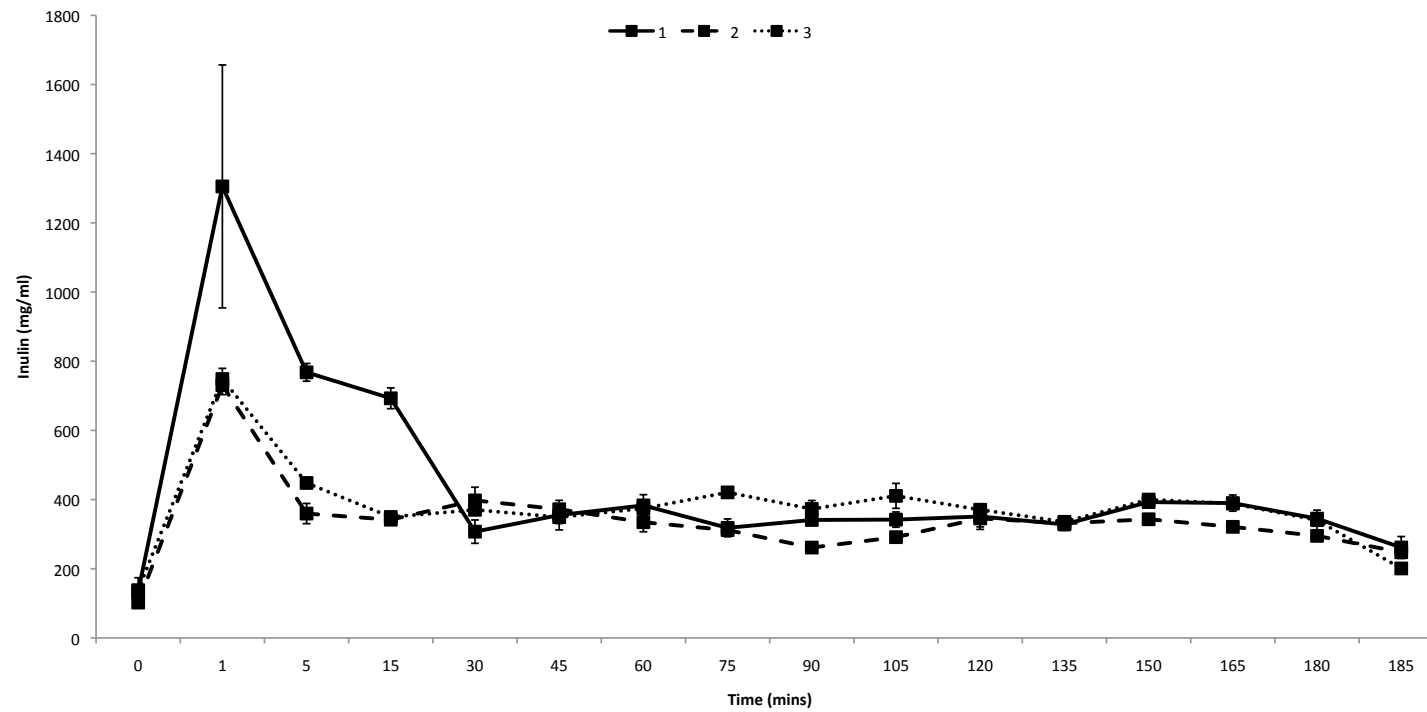


**Figure 5.9 Kinetics of inulin infusion *in vivo*.** Plasma inulin concentrations are shown for three rats in which inulin was infused as a 50 mg/kg bolus followed by a 1 mg/kg/min infusion for 180 minutes. Inulin infusion was ceased at 180 minutes. Data points are mean  $\pm$  SEM of triplicate measurements.

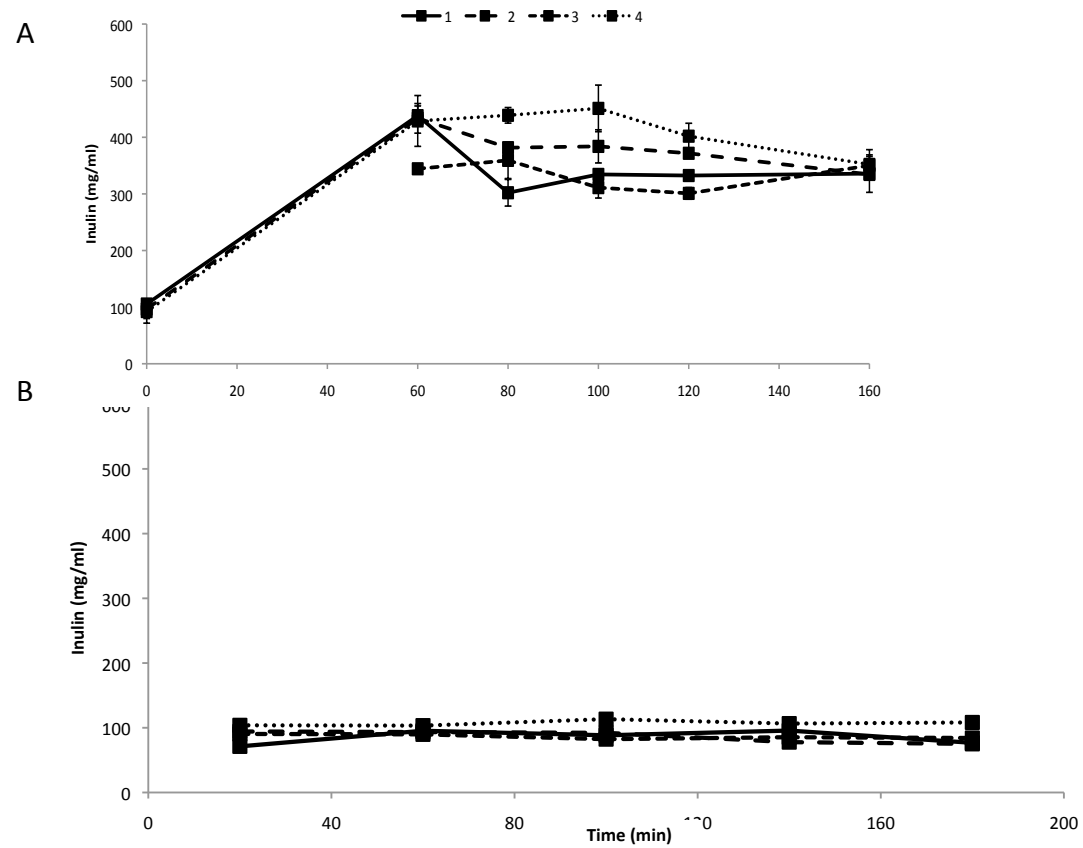


**Figure 5.10 Microdialysis of inulin *in vivo*.** (A) shows results for plasma inulin in rats without (1 and 2) or with (3 and 4) HE clamp. (B) shows results for ISF inulin in rats without (1 and 2) or with (3 and 4) HE clamp. Data points are mean  $\pm$  SEM of triplicate measurements.

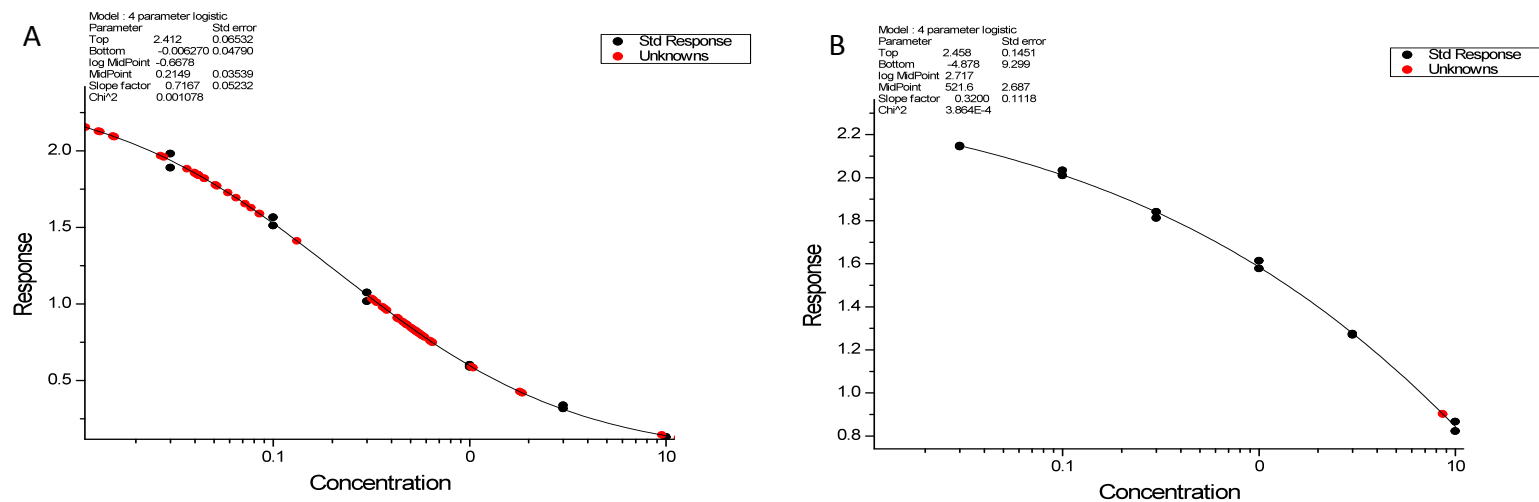


**Figure 5.11 Inulin ELISA with provided BioPAL inulin and Inutest.** Standard curves for BioPAL inulin (A) and Inutest (B) using the BioPAL inulin ELISA. Data points represent individual measurements.

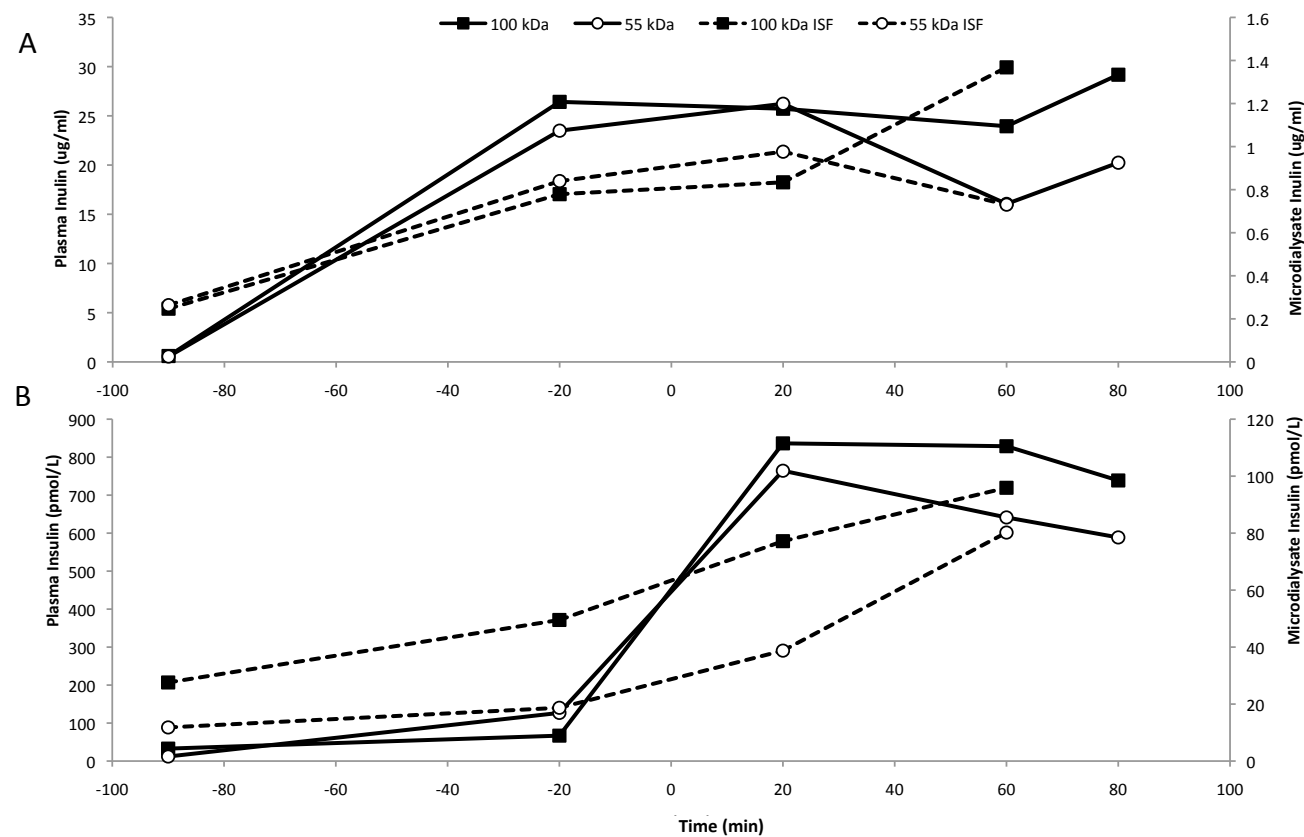


**Figure 5.12 Comparison of 55 and 100 kDa cut-off probes *in vivo*.** (A) shows inulin concentrations with 55 and 100 kDa cut-off probes with plasma inulin on the y axis (solid line) and microdialysate inulin on the additional y axis (broken line). (B) shows insulin concentrations with 55 and 100 kDa cut-off probes with plasma insulin on the y axis (solid line) and microdialysate insulin on the additional y axis (broken line). Data points are mean  $\pm$  SEM for two measurements.

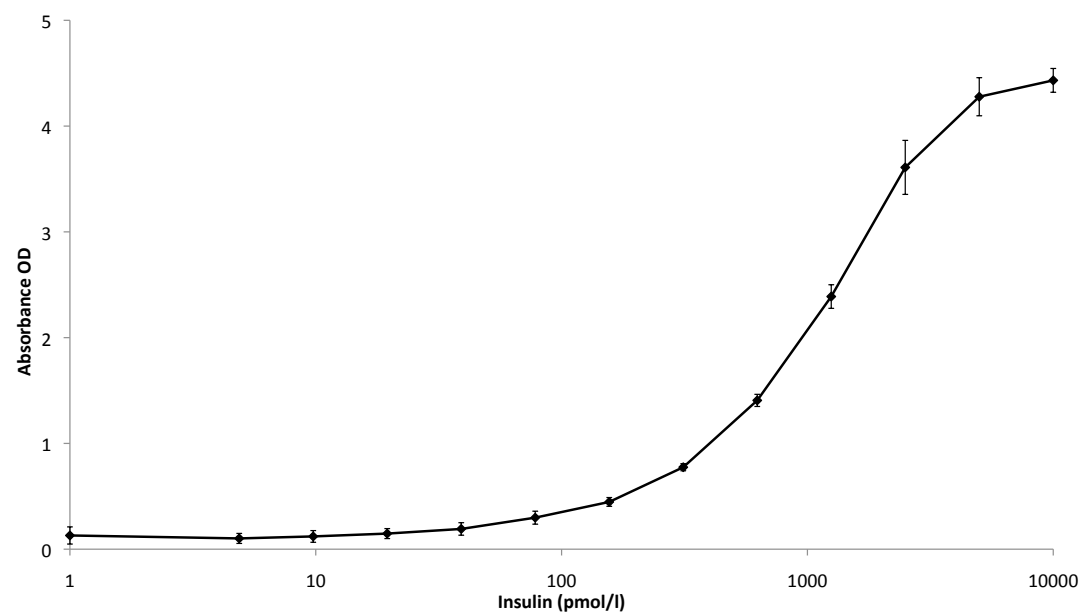


**Figure 5.13 Reproducibility of standard curves of human insulin spikes in rat plasma.** Average standard curve for known concentrations of human insulin spiked into rat plasma run on the Rat Ultrasensitive Crystal Chem kit. Data points are mean  $\pm$  SEM for four repeats.

<b>In vitro recovery</b>	
Insulin concentration (pmol/L)	Recovery (%)
3000	9.4 ± 0.4
1000	14.7 ± 1.8
300	3.2 ± 0.1

<b>In vitro recovery</b>	
Inulin concentration (ug/ml)	Recovery (%)
25	16.7 ± 5.2

**Table 5.1 *In vitro* recoveries for insulin and inulin.** Recoveries are expressed as a per centage of known concentration and are mean ± SEM for three measurements at each concentration. Concentrations were used to correspond to lean and obese basal and HE clamp insulin concentrations, thus, 300 pmol/L for lean animal at basal, 1000 pmol/L for lean animal at clamp and obese animal at clamp and finally 3000 pmol/L for obese animal at clamp.

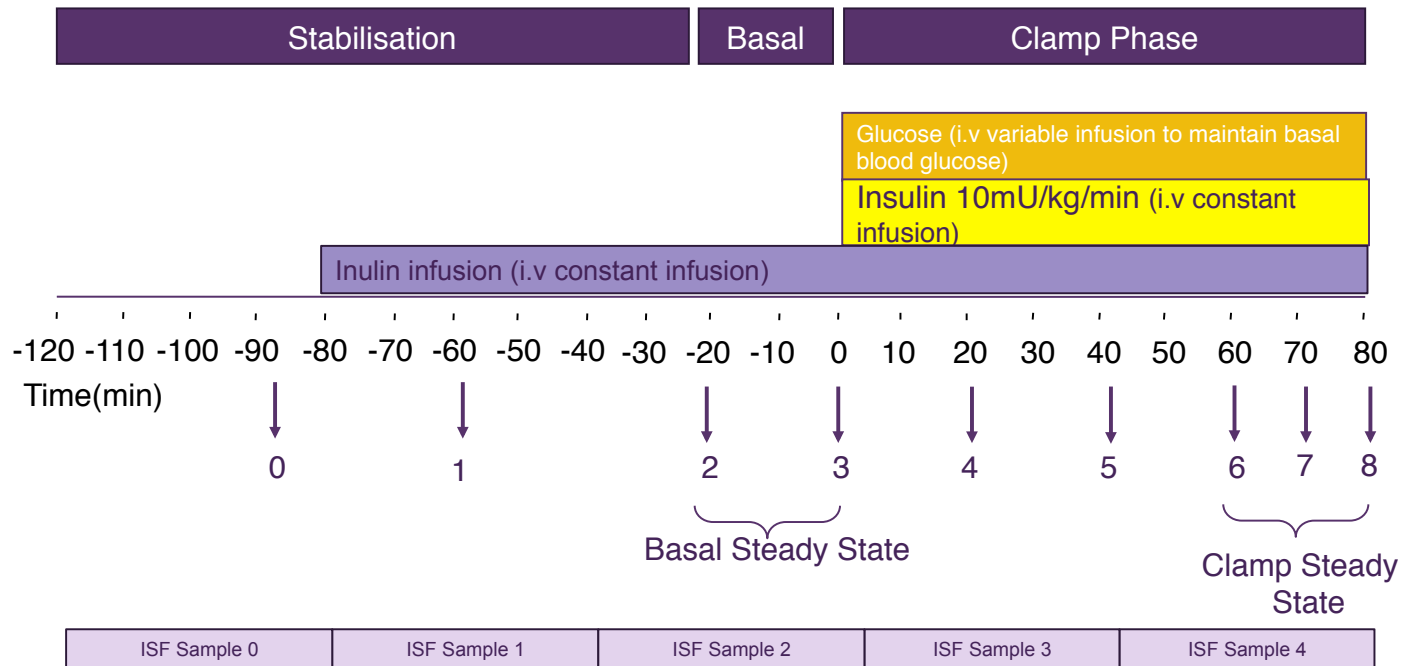


**Figure 5.14 Protocol used for the measurement of insulin with microdialysis during hyperinsulinaemic-euglycaemic clamp.** Probe insertion was at -120 minutes. ISF samples were collected every 40 minutes from -120 minutes. Inulin infusion began at -80 minutes and continued throughout the protocol. HE clamp protocol, as previously described, started at 0 minutes and continued for 80 minutes. Insulin infusion was constant throughout the protocol, glucose infusion was varied in order to maintain blood glucose concentration. Downward arrows represent plasma samples.

### 5.3 Discussion

As discussed in the introduction to this chapter there are several elements of the microdialysis technique that require careful consideration in order to optimize the recovery of a substance of interest. Thus, the amendments made in this chapter offer the opportunity to improve on the methodology presented in the literature.

#### Pore size

Experiments described in Section 5.2.11 showed that the recovery of both insulin and inulin *in vivo* was better with a probe with a molecular weight cut-off of 100 kDa versus 55 kDa. Recovery of both insulin and inulin *in vitro* was higher with the 55 kDa probe, but given that recoveries *in vitro* are generally much higher than *in vivo* it was more important to optimize recovery *in vivo*.

The experiment described in Section 5.2.11 also showed that the 20 kDa probe was not suitable for the measurement of insulin *in vivo* under the present conditions.

#### Perfusion fluid

The experiments of Section 5.2.1 investigated the optimum concentration of BSA in the perfusion fluid. 1 % BSA gave higher recoveries than 2 % BSA, 1 % BSA was therefore chosen for use in all microdialysis experiments. As discussed in the introduction to this chapter, glucose was also added to the perfusate to prevent tissue depletion of glucose (Lonnroth et al., 1987).



### Pump rate

The experiments of Section 5.2.1 tested different pump rates to establish the optimum rate for recovery of insulin. 2.5, 2 and 1  $\mu\text{l}/\text{min}$  were tested. 1  $\mu\text{l}/\text{min}$  was found to give the best recovery of insulin. Therefore, 1  $\mu\text{l}/\text{min}$  was chosen for use in all microdialysis experiments.

### Outlet tubing

Outlet tubing volume was calculated using the internal diameter of the FEP tubing. An outlet tubing length of 45 cm was calculated to have a volume of 5  $\mu\text{l}$  and therefore to correspond to a five minute time delay from tissue to collection vial. The CMA 470 Refrigerated microfraction collector was therefore started five minutes after the inulin infusion and could then be taken to represent real time measurements of tissue concentrations, as the delay in the sample reaching the collection vial is accounted for.

### External calibrator

As discussed in Sections 5.2.2 – 5.2.10, a great deal of work was conducted in an attempt to validate the method for the use of Inutest® and the Waugh method for the measurement of inulin as the calibrator for insulin. However, this proved not to be possible in our hands. Thus, the work described in Section 5.2.11 validated the use of BioPAL's Inulin for injection and BioPAL's FIT-GFR (Inulin) kit for the measurement of inulin *in vivo* and hence, as a calibrator for insulin.

In these experiments, inulin was infused into the animal prior to HE clamp in order to obtain steady-state inulin concentrations prior to HE clamp. Figure 5.11 shows that inulin concentration reaches a steady state at -20 minutes when baseline measurements are taken for the HE clamp. Thus, the inulin dosing protocol only delayed the start of HE clamp by 40 minutes which should not have any effect on the experimental outcomes. Importantly, this protocol avoids the additional surgical procedure and recovery required to insert an osmotic minipump as used in the experiments of (Holmang et al., 1997) on rats, but shortens the time required to reach steady state inulin concentration seen in some studies on humans (Sjostrand et al., 1999).

#### Recovery of insulin

Experiments described in this chapter were performed to try to optimize the recovery of insulin on commercially available assays. It was found that it is not possible to use the Mercodia Ultrasensitive Rat Insulin ELISA with a smaller volume than specified. Therefore, although the sensitivity of the assay is high it was not suitable for use in the present experiments.

The insulin concentrations in plasma and ISF described were always measured using the same insulin assay to ensure that the affinity of insulin to the assay was always the same, thus, making the results directly comparable. This is an important advance as the same assay has not always been used in other experiments described in the literature (Niklasson et al., 1998, Sjostrand et al., 1999, Sjostrand et al., 2000). Additionally, some investigations have used recovery calculations from previous papers to calculate the concentrations of

insulin (Holmang et al., 1999). On the other hand, some investigators have used the same assay to measure insulin in plasma and interstitial samples such as Holmang (2001) but the assay they used (Pharmacia double-antibody radioimmunoassay) had a range similar to that of the Mercodia Rat Insulin ELISA (Hermans et al., 1999) and therefore did not offer clarity at the lower end.

Importantly, the results obtained in the present studies were obtained using a modified standard curve such that human insulin was measured on a human insulin standard curve, rather than on the rat insulin curve provided by the manufacturer. This was shown to be more accurate as analyzing human insulin samples on the rat standard curve was found to overestimate insulin concentrations due to the cross reactivity of the rat insulin antibody with human insulin.

Herkner et al., (2003) measured basal insulin concentrations through their use of the Mercodia Ultrasensitive assay which has a detection limit of  $\sim 0.9$  pmol/L. However this led to large samples being needed due to the required 25  $\mu$ l sample volume. Apart from these measurements, basal insulin concentration has not been recorded in rats and therefore basal concentrations of insulin in ISF of rats is not known. Thus, work was conducted in the studies of this chapter to try to validate a method with the potential to measure basal concentrations of insulin. The Crystal Chem Ultrasensitive Rat Insulin ELISA was used as it has a wide range of detection and has been validated in house for detection down to 5.4 pmol/L (Analytical Group, AstraZeneca, Alderley Park). By running a human

insulin curve in conjunction with the rat insulin curve provided, insulin concentrations could be measured more accurately.

In addition to this, during initial *in vitro* experiments it was noted that the recovery of insulin varied with the plasma concentration of insulin. Therefore it did not seem appropriate to assume a single *in vitro* insulin recovery value for the whole experiment. In order to address this problem three insulin concentrations were tested for their *in vitro* recovery; one that corresponded to the basal phase in lean rats, one that corresponded to the end of the HE clamp in lean rats (as well as basal concentrations in obese rats) and one that corresponded to obese animals at the end of HE clamp. This increased the accuracy of the measurements made using this technique as it separated the recoveries into three broad categories of concentrations.

#### Total volume of sample required

15 µl of ISF sample was required to dilute ISF samples 1 in 10 and to have enough volume to test 50 µl diluted sample in duplicate on BioPAL's FIT-GFR (Inulin) kit. 15 µl of ISF sample was required to test ISF samples neat on the Crystal Chem Rat Ultra Sensitive Insulin ELISA. Therefore to allow for dead space and any small ultrafiltration of samples, microdialysate fractions of 40 minutes were taken in order to ensure that there was enough sample to analyse each fraction.

### 5.3.1 Conclusion

To summarise, each methodological consideration of the microdialysis technique was thoroughly investigated in the present chapter to optimize the recovery and reliability of the microdialysis method in the subsequent chapter. Pore size, perfusion fluid constituents, pump rate, outlet tubing length, external calibrator and measurement of insulin concentrations were all investigated and optimized. Thus, from the range of different experimental variables used in the literature, the best combination was identified in the experiments described in this chapter. Thus, the resultant conditions were as follows: 100 kDa probe with perfusion fluid of 1 % BSA and 1.5 mmol/L glucose, prepared in 0.9% sodium chloride, delivered at 1  $\mu$ l/min. Outlet tubing was 45 cm and collection was into siliconised glass microvials just below the level of the animal. Inulin, as a calibrator, was delivered as a 1 mg/kg bolus and 0.08 mg/kg/min infusion. The protocol is represented in Figure 5.15.

# **CHAPTER 6 - EFFECT OF CHRONIC TETRAHYDROBIOPTERIN TREATMENT ON INSULIN ACCESS TO THE MUSCLE INTERSTITIAL FLUID IN OBESE ZUCKER RATS**

## **6.1 Introduction**

As discussed in the General Introduction, the action of insulin is dependent on its distribution between three body fluid compartments. Thus, it is key to determining insulin sensitivity of skeletal muscle and its mechanism of action that insulin concentration within the bio-available compartment ie. the interstitial fluid, is accurately and reliably determined. As such, the method for the assessment of interstitial insulin concentration by microdialysis was tested and modified for improvement in the *in vitro* and *in vivo* experiments described in the previous chapter.

In the experiments of the present chapter, this improved microdialysis methodology was used to measure interstitial insulin concentration in lean and obese Zucker rats under basal conditions and during HE clamp. Obesity is associated with endothelial dysfunction (Mather et al., 2004) and impaired NO-dependent vasodilatation. Indeed the experiments of Chapter 4 indicated that insulin induced muscle vasodilatation and GIR was impaired in obese Zucker rats compared to lean Zucker rats. Therefore, it was hypothesized that if the availability of NO could be improved experimentally in obese Zucker rats, then

insulin-stimulated vasodilatation and therefore insulin-stimulated glucose uptake may be improved.

Nitric oxide is synthesised by endothelial nitric oxide synthases (eNOS) which use the precursors L-arginine and oxygen ( $O_2$ ) to form NO and L-citrulline. In the presence of L-arginine, electron flow in the eNOS enzyme reduces oxygen, which is used to oxidize L-arginine to NO and citrulline. NO production requires five co-factors. One of the co-factors ( $BH_4$ ) has been found to be the critical determinant in NO synthesis as it determines whether electron flow in the enzyme is directed to L-citrulline by shuttling its electron to L-arginine. Indeed, depletion of  $BH_4$  results in uncoupling of oxygen reduction and arginine oxidation, thereby generating superoxide ( $O_2^{\cdot-}$ ) instead of NO (Vasquez-Vivar et al., 2002). Thus, an increase in  $O_2^{\cdot-}$  such as that seen in diabetes increases the production of peroxynitrite ( $ONOO^{\cdot-}$ ) by reacting with NO.  $ONOO^{\cdot-}$  oxidizes  $BH_4$  and therefore further uncouples eNOS which perpetuates the cycle of vascular oxidative stress (Agrawal et al., 2007). Indeed, Milstein and Katusic showed that peroxynitrite can oxidize  $BH_4$  within several minutes (Milstien and Katusic, 1999).

The amount of  $BH_4$  is measured as  $BH_4$  protein content. Additionally, because  $BH_4$  is oxidized to 7,8-dihydrobiopterin ( $BH_2$ ) and biopterin (B), total biopterin content is often measured as well (Bendall et al., 2005). The ratio of the three components is used as an indication of the amount of active  $BH_4$  available and the amount that has been oxidized and therefore inactivated. For example, mice with streptozotocin-induced diabetes have decreased concentrations of  $BH_4$ , but

normal concentrations of total biopterin, suggesting that BH<sub>4</sub> is oxidized to BH<sub>2</sub> and B (Alp et al., 2003).

There is evidence that the blunting of endothelium-dependent forearm dilatation to acetylcholine seen in subjects with T2D was significantly improved by the concomitant intra-arterial infusion of BH<sub>4</sub> (Heitzer et al., 2000b). This improvement in endothelium-dependent forearm vasodilatation was the result of an increased ability to produce NO as the beneficial effect of BH<sub>4</sub> and was completely blocked by L-NMMA. Further, various studies have assessed the outcomes of BH<sub>4</sub> supplementation in animals. For example, Shinozaki et al., (2000) showed that oral supplementation of fructose-fed rats with BH<sub>4</sub> (10 mg/kg/day) for 8 weeks significantly increased the amount of BH<sub>4</sub> in the aorta and reversed the impairment of endothelial dilator function. BH<sub>4</sub> has also been shown to have more acute effects; relaxation to ACh of aortic rings from streptozotocin-induced diabetes rats was augmented by pre-treatment with BH<sub>4</sub> for 30 minutes (Pieper, 1997). Moreover, with an intermediate length of treatment, Li et al., (2011) showed that when apolipoprotein E<sup>-/-</sup> mice (a genetic model that readily develops atherosclerosis) were given drinking water supplemented with BH<sub>4</sub> for two weeks, this normalised total biopterin and BH<sub>4</sub> concentrations in the left carotid artery. In addition although relaxation to ACh in rings of partially ligated left carotid artery was significantly blunted versus the unligated right carotid artery, BH<sub>4</sub> treatment normalized the peak relaxation to acetylcholine and improved the EC<sub>50</sub>.



Thus, acute and chronic treatment with BH<sub>4</sub> appears to improve endothelial dilator function by increasing the production of NO. This has potential significance in the treatment of T2D not only because of the possible benefits of improving endothelial function in conduit and resistance arterial vessels, but also because the insulin-stimulated production of NO via eNOS is involved in other actions of insulin. Thus, microvascular recruitment in skeletal muscle was found to be dependent on activation of eNOS (Vincent et al., 2003). Therefore an increase in the activity of eNOS due to supplementation with BH<sub>4</sub> could potentially increase microvascular recruitment and therefore the capillary surface area available for the translocation of insulin into muscle ISF. In fact, BH<sub>4</sub> has been shown to improve glucose disposal in patients with T2D without affecting bulk muscle blood flow (Nystrom et al., 2004), as could be explained by an increase in microvascular recruitment and improved access of insulin to the skeletal muscle fibers with a consequent increase in glucose uptake.

A question that has not been thoroughly investigated is how the endothelial barrier affects insulin transport in muscle in diabetes. Thus, Sjostrand et al., (2000) showed by using microdialysis during HE clamp that ISF concentrations of both insulin and glucose were similar in subjects with T2D and controls, but lower than plasma concentrations, despite the 40% lower muscle blood flow in the diabetic state. Later, the same group again reported ISF concentrations of insulin and glucose to be lower than plasma concentrations, in T2D as in control subjects during HE clamp (Gudbjornsdottir et al., 2005). Similarly, as described in the General Introduction, a study involving detailed kinetic analysis of insulin distribution and lymphatic cannulation, indicated that TET in obese subjects is

normal and that the delay in insulin stimulated glucose uptake by muscle lies at the level of the muscle cell (Prager et al., 1986, Castillo et al., 1994).

On the other hand however, it has been reported that during infusion of supraphysiological insulin concentrations in HE clamp experiments, ISF insulin concentration was lower than plasma concentration in normal rats, but equal to plasma concentrations in obese rats. This suggests that the endothelium does not act as a selective barrier in obese rats (Holmang et al., 1997).

Thus, the experiments described in this chapter sought to investigate the endothelial transport of insulin into the ISF in lean and obese Zucker rats by using the microdialysis methodology developed in the experiments of Chapter 5. In addition, obese rats were chronically treated with BH<sub>4</sub> to investigate whether the improvement in endothelial function expected from BH<sub>4</sub> treatment would affect the movement of insulin through the endothelial barrier and into the ISF. It was hypothesized that if the endothelium does not act as a selective barrier in obese rats, as proposed by Holmang et al., (1997); see above), that the rate of access of insulin to the ISF is at least partly responsible for the impaired insulin-stimulated glucose uptake and vasodilatation seen in those rats. Therefore, if endothelial dysfunction in obese Zucker rats, a rat model of T2D in humans, could be rectified by supplementation with BH<sub>4</sub>, then the selective barrier seen in lean Zucker rats would be restored, also restoring the insulin-stimulated glucose uptake and muscle vasodilatation.

## **6.2 Methods**

### **6.2.1 Experimental protocol for HE clamp with microdialysis**

As so many adjustments were made to the methodology described for the experiments of Chapters 2-4 and for particularly Chapter 5, the methods are described in full below.

#### **6.2.1.1 Fasting/Diet Restriction**

Unless otherwise indicated for specific groups of rats below, the day before the experiment, rats received a fixed ration of diet of 16 or 10 g of rat chow (obese and lean respectively) at 16:00. The intention was to provide sufficient food until approximately midnight ensuring that rats were non-absorptive, but not starved during the HE clamp protocol. These amounts were based on previous in house measurements of food consumption in Zucker rats (Cardiovascular and Gastrointestinal Group, AstraZeneca, Alderley Park).

#### **6.2.1.2 Surgical Preparation**

On the morning (09:00) of the experiment, rats were weighed and anaesthetised with an intraperitoneal injection of sodium-thiobutabarbital (Inactin®, Sigma-Aldrich Ltd, UK). Rats received an initial intra-peritoneal dose of 160-190 mg/kg.

The right jugular vein was then isolated for cannulation. Three catheters (PE10 connected to PE50) were placed into the jugular vein for infusions of insulin, glucose, and inulin respectively. A fourth catheter (PE10 connected to PE50) was placed in the same vein for periodic top-up doses and infusions of anaesthetic when required. A fifth catheter (PE10 connected to PE50) was placed in the same vein to ensure a tight seal when the catheters were secured. A tracheotomy was performed using PE240 tubing to facilitate breathing during the experimental procedure. The left carotid artery was isolated, and separated from the vagus nerve for cannulation. One catheter (PE50) was placed into the carotid artery for blood sampling and recording of MABP. All catheters were made from Intramedic™ polyethylene medical grade tubing (Becton, Dickinson and Company, US), and filled with 20mM sodium citrate solution to prevent clotting within catheters. Carotid artery catheter patency was maintained until the conclusion of the experiment by a continuous infusion (10 µl/min) of 20mM sodium citrate solution via the carotid artery catheter using a 5ml Hamilton syringe and digital syringe pump (Model KDS101, KD Scientific Inc, US). Body temperature was monitored and maintained at 37°C using a rectal probe thermo-coupled to a heat blanket (Harvard Apparatus Ltd, UK). A stream of Medical O<sub>2</sub> was directed over the opening of the tracheotomy.

The microdialysis probes were each inserted using a guide needle and split tubing (plastic tubing, split along half the length; for details see Chapter 5). A small incision was made in the skin at the distal ends of each hindlimb and a guide needle and split tubing were inserted through the incision into the tibialis anterior at 45° and tunnelled ~5mm under the surface. The guide needle was

removed from the split tubing and the microdialysis probe inserted into the split tubing and sutured to the skin. The split tubing was then removed by pulling on either side of the protruding ends leaving the microdialysis probe within the muscle. The FEP tubing attached to the outlet tubing was fed into a CMA 470 Refrigerated microfraction collector (6°C) positioned below the level of the rat to avoid back pressure. Samples were collected into siliconised glass microvials then split to be stored at -80°C for later determination of insulin concentration or 5°C for determination of inulin concentration (see below). Probes were checked regularly for patency and flushed at 20 µl/min for ~ 30 seconds if necessary.

Following surgical preparation, the rat was allowed 40 minutes to stabilise from -120 to -80 minutes. During this time, a baseline arterial blood sample was taken (at -90 minute; see Figure 6.1). The rat continued to stabilise until the commencement of the basal phase at time point -20 minutes, but simultaneously at time point -80 minutes the inert inulin infusion was commenced. The microfraction collector was started at -75 minutes and set to collect fractions every 40 minutes. The length of outlet tubing was calculated to correspond to a 5 minute time delay in the transport of the fraction from the rat to the glass vial. Microdialysis fractions could therefore be directly correlated with plasma samples from the same period. An additional arterial blood sample was taken at -60 minutes to correspond with ISF sample 1.

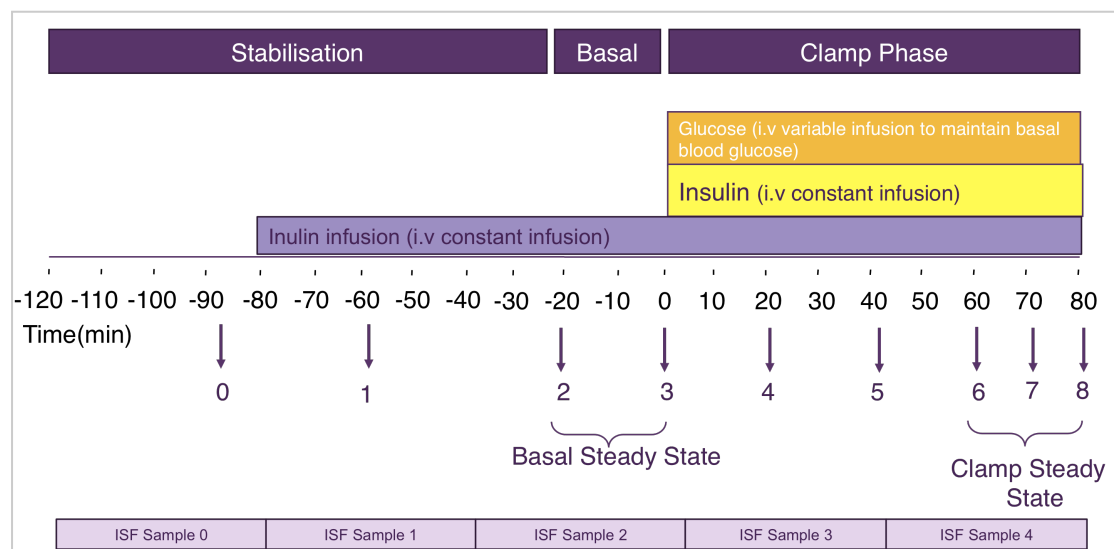


**Figure 6.1 Schematic representation of the hyperinsulinaemic euglycaemic clamp protocol.**

Numbers 0 -8 represent times at which arterial blood samples were taken.

### 6.2.1.3 Hyperinsulinaemic euglycaemic clamp protocol

At -20 minutes the basal phase began and at time 0 minutes, the HE clamp began (see Figure 6.1 ).

#### Basal Phase

Arterial blood samples were collected via the carotid catheter at -20 and 0 min as detailed above. An additional sample was taken at -10 min for determination of blood glucose concentration using a Roche Accu-chek® monitor only. The blood glucose concentrations at -20, -10 and 0 minutes were measured and the average of these values was used as the target blood glucose concentration for the HE clamp. In addition, plasma glucose concentrations at -20 and 0 minutes were used to define plasma glucose concentration and the average of these values was the subsequent plasma glucose concentration for the clamp. Plasma glucose concentration was established during the basal phase of the clamp so that the ratio of plasma to blood glucose concentration could be monitored. If the ratio

changes due to haemodilution or other factors, plasma glucose is a more accurate measure of glucose concentration as it is not affected by the concentration of red blood cells in the sample. In practice however, there was no change in the ratio in any experiment. ISF sample 2 corresponded to the basal phase of the HE clamp.

### HE Clamp Phase

The HE clamp phase began after collection of the 0 min sample. Human insulin was infused via a dedicated jugular vein catheter using a 5 ml Hamilton syringe and digital syringe pump (Model KDS101, KD Scientific Inc, US) at a fixed volume infusion rate of 10  $\mu\text{l}/\text{min}$  to deliver pre-defined final insulin infusion rate of 10 or 20  $\text{mU}/\text{kg}_{\text{LBM}}/\text{min}$  for lean and obese rats respectively. Arterial blood glucose concentration were determined every 3 to 5 min (Roche Accu-chek) using a modified 3-way stop-tap to allow minimal sample volumes (15  $\mu\text{l}/\text{sample}$ ). Blood/plasma glucose was clamped at the basal concentration (see above) with a variable rate infusion of 20% (w/v) glucose via a third jugular vein catheter using a 10 ml Hamilton syringe and digital syringe pump (Model 22, Harvard Apparatus Ltd, UK). The glucose infusion rate was adjusted in response to blood glucose concentrations, such that blood glucose concentration was maintained at the euglycaemic basal concentration. During the HE clamp, additional arterial blood samples for insulin and inulin measurements were taken at 20, 40, 60, 70 and 80 minutes. ISF sample 3 corresponded to the first half of the HE clamp protocol and ISF sample 4 corresponded to the second half of the HE clamp protocol.

At the end of the experimental protocol, rats were humanely killed whilst under anaesthesia by overdose of sodium-thiobutabarbital via the jugular vein, and death confirmed by cervical dislocation. Probe placement was determined by dissection.

#### **6.2.1.4 Reagent Preparation**

All reagents were prepared on the day of study unless otherwise indicated.

##### Inulin infusion

Inulin was given as a primed infusion determined according to lean body mass,  $\text{kg}_{\text{LBM}}$  (estimated from body weight using empirical relationships). Stock solution of 1 mg/kg inulin was diluted in 0.9% sodium chloride to a solution concentration that could deliver both a 1 mg/kg bolus and 0.08 mg/kg/min infusion. The 1 mg/kg bolus dose was given as 0.125 ml bolus over 30 seconds. The infusion pump was then stopped and pump rate adjusted to 10  $\mu\text{l}/\text{min}$  to deliver 0.08 mg/kg/min for the rest of the experiment.

##### Human Insulin for Infusion

The insulin infusate was prepared by diluting human insulin (Actrapid®, Novo Nordisk, Denmark) in 10 ml of Haemaccel®. The volume of stock human insulin solution added to the Haemaccel was determined according to experimental group and lean body mass,  $\text{kg}_{\text{LBM}}$ . The final insulin infusion rate was 20 or 10



mU/kg<sub>LBM</sub>/min for obese and lean rats respectively. The volume infusion rate was fixed in all experiments to 10 µl/min.

#### Microdialysis perfusion fluid

The perfusion fluid was prepared using albumin from bovine serum and 20 % (w/v) glucose. A working solution of 1 % BSA and 1.5 mmol/L glucose was prepared in 0.9% sodium chloride. The volume infusion rate was fixed to 1 µl/min.

#### **6.2.1.5 Microdialysis probe preparation**

All microdialysis equipment was obtained from CMA Microdialysis, Kista, Sweden via Linton Instrumentation, Norfolk, UK unless otherwise stated. Microdialysis equipment was set up and probes were tested for patency before surgical preparation of the rat, so that the probes could be perfused *in vitro* during the surgical preparation. It is critical to ensure that the probe is flowing freely and that there are no air bubbles in the probe before it is inserted. Hence, due to the low flow rate this procedure was begun significantly (> 30 minutes) before the time for probe insertion.

CMA 20 High cut-off (100 kDa) 10 mm probes were used for measurement of interstitial insulin concentration. All probe tubing was cut using a scalpel so as not to crush the lumen of the tubing. Probe inlet and outlet tubing were cut to ~5 cm. 'FEP' tubing was siliconised using Sigmacote® (Sigma-Aldrich Ltd, UK) and

cut in half. Half lengths of FEP tubing were attached to the inlet and outlet tubing using tubing adapters (CMA Microdialysis, Sweden) swollen in 70 % ethanol. The lengths of FEP tubing attached to the inlets of the CMA 20 probes were connected with tubing adapters to a 1 ml microsyringe containing perfusion fluid. The extended outlet tubings were cut to 45 cm (in order to accommodate a 5 minute time lag in collection). The probes were placed in a CMA 130 *In vitro* stand and the CMA 402 Dual syringe pump was started at 1 µl/min.

#### **6.2.1.6 Measurement of glucose, insulin and inulin**

Arterial blood samples (200 µl) were collected from the carotid artery for determination of plasma glucose (using the YSI Clinical Analyser), plasma inulin concentration (using BioPal FIT-GFR kit, BioPal, Worcester, Massachusetts) and plasma insulin concentration (using Crystal Chem Ultrasensitive Rat Insulin ELISA Kit, Crystal Chem, Illinois, USA).

All blood samples were collected into potassium-EDTA coated tubes (Microvette®, Sarstedt Ltd, UK), and were centrifuged (13,000 RPM, 5 min, 4°C) immediately for plasma separation. Plasma glucose concentration was determined using the YSI Clinical Analyser and remaining plasma was aliquoted into 0.5 ml Eppendorf tubes; the samples were split and stored at -20°C for later determination of insulin concentration or 4°C for determination of inulin concentration.

### **6.2.2 Group 1: Preliminary microdialysis experiments**

Experiments were performed on 6 lean and 5 obese Zucker rats (weights  $334.5 \pm 3.9$  and  $470.2 \pm 11.4$  respectively; Charles River France, France) that had been housed in cages on a controlled 12 hour Light/Dark cycle. Experiments were performed exactly as described in Section 6.2.1.

### **6.2.3 Group 2: Preliminary pharmacokinetic studies of BH<sub>4</sub>**

Preliminary pharmacokinetic experiments were performed on 4 lean and 4 obese Zucker rats (weights  $317.5 \pm 6.3$  and  $472.3 \pm 7.6$  respectively; Charles River France, France) that had been housed in pairs on a controlled 12 hour Light/Dark cycle.

Rats were dosed via drinking water for two weeks with either vehicle (0.04% vitamin C) or BH<sub>4</sub> at  $\sim 10$  mg/kg/day diluted in vehicle (Li et al., 2011). Drinking water was changed every 24 hours to minimize the oxidation of BH<sub>4</sub>. This concentration of vitamin C added to the drinking water has previously been shown to prevent oxidation of BH<sub>4</sub> for 24 hours (Li et al., 2011). Water intake and body weight were monitored for one week prior to dosing and daily throughout the two week dosing period. These measurements were used to calculate the required concentration of BH<sub>4</sub> in the drinking water; water intake during the dosing period was used to verify the dose actually given.

Rats were fasted as described in Section 6.2.1.1 and prepared under pentobarbital anaesthesia as described in Section 6.2.1.2. An HE clamp was

performed as detailed in Section 6.2.1.3. At the end of the protocol the animal was perfused to clear the tissues of excess blood. Thus, a thoracotomy was performed and an incision was made into the right ventricle. Animals were then perfused with phosphate-buffered saline (PBS) at a slow flow rate (~10 mls/min) through the carotid artery (40 or 60 mls of PBS for lean and obese rats respectively). Death was confirmed by cervical dislocation. Tissues were snap frozen for analysis by HPLC. Assessment of biopterin concentrations in tissue and plasma samples was performed in collaborations with Professor Keith Channon's Group, Wellcome Trust Centre for Human Genetics, Oxford, UK by Dr Gillian Douglas. Two different HPLC methods were used to determine the concentrations of biopterins in tissue and plasma samples. BH<sub>4</sub>, BH<sub>2</sub> and B concentrations were determined using chemiluminescent and fluorometric detection by HPLC as detailed previously (Bendall et al., 2005).

Samples of drinking water were also taken at 0, 18, 24 and 48 hours after preparation to analyse the stability of BH<sub>4</sub> in the drinking water samples.

#### **6.2.4 Group 3: Modified pharmacokinetic studies of BH<sub>4</sub>**

Following analysis of the results from Section 6.2.3, additional pharmacokinetic studies were performed in order to assess the concentrations of BH<sub>4</sub> in rats that were killed at the end of the dark cycle (during which food and water intake is increased). To this end, acute pharmacokinetic experiments were performed on 4 lean and 4 obese Zucker rats (weights  $334.9 \pm 4.9$  and  $423.7 \pm 7.7$  respectively; Charles River France, France) that had been housed in cages on a controlled 12

hour Light/Dark cycle (6:00 am -18:00 pm). They were dosed via their drinking water for two weeks with either vehicle (0.04% vitamin C) or BH<sub>4</sub> at ~10 mg/kg/day diluted in vehicle as described in Section 6.2.3.1. These rats were not fasted prior to the protocol, but allowed access to food and water overnight *ad lib*. Each rat was then anaesthetised and prepared for experimentation as they came off their dark cycle at 6:00 am.

The right jugular vein was isolated for cannulation and one catheter (PE10 connected to PE50) was placed into the jugular vein for top-up doses of anaesthetic as required. The left carotid artery was isolated, and separated from the vagus nerve for cannulation. One catheter (PE50) was placed into the carotid artery for the perfusion of rats with PBS. All catheters were made from Intramedic™ polyethylene medical grade tubing (Becton, Dickinson and Company, US), and filled with 20mM sodium citrate solution to prevent clotting within catheters. The rat was then immediately perfused as described in Section 6.2.3 so that tissues could be frozen for analysis by HPLC (as described in Section 6.2.3).

Samples of drinking water to which BH<sub>4</sub> had been added were also taken at 0 and 24 hours after preparation, to analyse the stability of BH<sub>4</sub> in the drinking water samples.

### **6.2.5 Group 4: Effects of chronic treatment with BH<sub>4</sub>**

These experiments were performed on 4 lean control, 6 obese control and 6 obese BH<sub>4</sub>-treated Zucker rats (weights  $342.7 \pm 9.9$ ,  $397.2 \pm 7.4$  and  $410.9 \pm 9.8$  g respectively; Charles River France, France) that had been housed in cages on a controlled 12 hour Light/Dark cycle. They were dosed in drinking water for two weeks with either vehicle (0.04% vitamin C) or BH<sub>4</sub> at ~10 mg/kg/day diluted in vehicle as described in Section 6.2.3.1. These rats were given a food ration at 16:00 on the previous day (see 6.2.1.1).

The experimental protocol was performed exactly as described in Section 6.2.1.

### **6.2.6 Calculations**

#### Calculation of Lean Body Mass

Lean body mass (LBM) was estimated from empirical linear regression formulae relating LBM to total body weight (BW). These formulae were derived from body composition analysis of Zucker rats performed at AstraZeneca (Cardiovascular and Gastrointestinal Group, AstraZeneca, Alderley Park).

The equation used for the Obese Zucker rat is:

$$\text{LBM (g)} = 59 + 0.50 \times \text{BW (g)}$$

The equation used for the Lean Zucker rat is:

$$\text{LBM (g)} = 31 + 0.77 \times \text{BW (g)}$$

### Calculation of Insulin Sensitivity

As described in Chapter 4, insulin sensitivity (M/I) was calculated as:

$$\text{M/I } (\mu\text{mol/kg/min per pmol/L}) = \text{GIR } (\mu\text{mol/kg/min}) / \text{Plasma insulin (pmol/L)}$$

Where GIR is the steady state glucose infusion rate at the end of HE clamp and plasma insulin concentrations represent measurements taken at corresponding time points. GIR was corrected for lean body mass, and was calculated and expressed as mg/kg<sub>LBM</sub>/min.

## **6.2.7 Analytical Methods**

### Insulin (Endogenous Rat & Human)

Individual concentrations of insulin in plasma and interstitial samples were determined using the Crystal Chem Ultrasensitive Insulin Rat ELISA kit adapted and validated for this use (see Section 5.2). Briefly, reactivity of the Crystal Chem kit is 100% with rat insulin, however reactivity with human insulin is not given by the manufacturer and thus was determined by using an additional standard curve of known human insulin (Actrapid®) concentrations spiked into rat plasma. Therefore, both standard curves (rat and human insulin) were run on the ELISA plate. Plasma and interstitial samples taken before insulin infusion

commenced (before time 0 minutes) were read against the rat standard curve provided by the manufacturer and samples taken during clamp (after time 0 minutes) were read against the human insulin standard curve.

### Inulin

Inulin concentrations were calculated for plasma and interstitial samples using the BioPal FIT-GFR (Inulin) kit (BioPal, Massachusetts, USA) as described in the manual. Plasma concentrations were measured at 1:50 dilution and interstitial samples at 1:10 dilution.

#### **6.2.8 Recovery of insulin *in vivo***

ISF samples from the microdialysis probes inserted in right and left Tibialis Anterior were analysed separately for recovery of insulin and inulin (see below). ISF concentrations of insulin and inulin obtained from each rat (two microdialysis probes) were then averaged to obtain a mean measure for each rat.

Recovery of insulin *in vivo* was calculated using the external reference technique (Jansson et al., 1993). Briefly, *in vitro* experiments were conducted using known concentrations of insulin and inulin as described in Section 5.2.13 to determine the recovery of both substances *in vitro*. Inulin recovery *in vivo* was calculated from the measured concentrations of plasma and interstitial inulin as inulin equilibrates readily and so the concentrations can be assumed to be the same.

The following formula was used to calculate the recovery of insulin *in vivo*:



Recovery of insulin *in vivo* = Recovery of insulin *in vivo* / (Recovery of insulin *in vitro* / Recovery of insulin *in vitro*)

Interstitial insulin concentration was calculated from the interstitial insulin concentration *in vivo* and the recovery of insulin *in vivo*.

### **6.2.9 Statistical analysis**

Results are expressed as mean  $\pm$  standard error of the mean unless otherwise indicated. Differences between treatment groups were evaluated using an unpaired Student *t* test. Differences from baseline within the group were analysed using a one-way ANOVA with Dunnett's post hoc test.

## **6.3 Results**

### **6.3.1 Group 1: Preliminary microdialysis experiments**

MABP was significantly higher for obese rats throughout the protocol ( $P < 0.05$ ) and was not significantly different from baseline throughout the HE clamp (A). HR was not significantly different between lean and obese rats throughout the protocol ( $P < 0.05$ ) and was not significantly changed from baseline during the HE protocol (B) (see Figure 6.2).

As can be seen in Figure 6.3 blood glucose was significantly higher in obese rats versus lean throughout the protocol ( $P < 0.05$ ); neither group changed from baseline at any time point (A). GIR was significantly different from baseline for lean rats from 24 mins onwards from the onset of the HE clamp and for obese rats from 13 mins onwards ( $P < 0.05$ ). GIR was significantly higher for obese rats from 13 mins onwards (B;  $P < 0.05$ ).

Plasma insulin concentration (Figure 6.4 A) was significantly higher in obese, than lean rats throughout the protocol. Plasma insulin concentrations were significantly higher than their respective baseline at 20 and 40 minutes of the HE clamp in both lean and obese rats (A;  $P < 0.05$ ). M/I was substantially higher in lean rats (Figure 6.5;  $P < 0.05$ ).

There was a tendency for the ISF concentration of insulin to be higher in the obese than lean rats at basal and at the end of HE clamp (Figure 6.4 B;  $P = 0.14$  and  $0.07$  respectively). There was also a trend for ISF insulin to be increased from basal concentrations during HE clamp in the lean rats. However, there was a less obvious trend for the ISF concentration to increase in the obese rats at each time point, the concentrations were more variable. Any changes in ISF insulin during the HE clamp did not reach statistical significance in either lean or obese rats.

### 6.3.2 Group 2: Preliminary pharmacokinetic studies of BH<sub>4</sub>

The main reason for this study was to investigate the tissue concentrations of BH<sub>4</sub>. Therefore the other findings are described very briefly.

The mean data in Figures 6.6 – 6.10 are not presented with error bars as each group comprised only two rats; for this reason, the data were not subjected to statistical analysis. MABP tended to be higher for both groups of obese rats than both groups of lean rats (Figure 6.6); there was no obvious differences between obese rats treated with BH<sub>4</sub> and vehicle (A). HR was similar in all groups of rats (B). Blood glucose tended to be higher for obese rats than the lean rats whereas GIR reached lower levels in obese rats (Figure 6.7 A and B respectively). Again, there was no obvious difference between rats treated with vehicle and BH<sub>4</sub>. Plasma insulin concentrations tended to be higher in obese rats than lean rats at all time points and to be raised above baseline by HE clamp in all groups (Figure 6.8 A). There was no obvious difference in plasma insulin concentration between obese rats treated with vehicle and BH<sub>4</sub> and no obvious changes in M/I with BH<sub>4</sub> treatment in lean or obese rats (Figure 6.8 B).

There was a trend for an increase in FVC in lean rats, but not in obese rats (Figure 6.9 A). There was no obvious change with BH<sub>4</sub> treatment.

BH<sub>4</sub> concentration in drinking water was maintained at 18 and 24 hours after preparation Table 6.1, but there was an obvious large decrease in BH<sub>4</sub> concentration at 48 hours and in the ratio of BH<sub>4</sub>: BH<sub>2</sub> and B.

The, BH<sub>4</sub> concentration in plasma appeared to be lower in the two lean and obese rats treated with BH<sub>4</sub> versus the two lean and obese rats treated with vehicle. Further, with the proviso that there were only two rats in each group, there was a tendency for BH<sub>4</sub> concentration to be greater in the aortas of lean rats that received BH<sub>4</sub> than in those that did not (Figure 6.10). By contrast, BH<sub>4</sub> concentration in aorta of obese rats seemed to be lower in those that received BH<sub>4</sub>. As BH<sub>4</sub> is oxidized to other pterins such as BH<sub>2</sub> and B, a lower BH<sub>4</sub> concentration would be expected to be associated with a decrease in the ratio of BH<sub>4</sub> to BH<sub>2</sub> and B. However, there were no obvious patterns (Figure 6.10 A) except that obese rats appeared to have lower BH<sub>4</sub>: BH<sub>2</sub> + B ratio in plasma than lean rats and these concentrations seemed to be decreased with BH<sub>4</sub> treatment. Further, in the aortas of lean rats, the BH<sub>4</sub>: BH<sub>2</sub> + B ratio in aorta seemed to increase with BH<sub>4</sub> treatment whereas in obese rats the ratio apparently decreased slightly in aorta.

Thus, following surgical preparation and HE clamp these measurements failed to demonstrate either an increase in plasma or blood vessel concentrations of BH<sub>4</sub> in obese rats. Due to the short half-life of BH<sub>4</sub>, these results do not necessarily indicate that levels of BH<sub>4</sub> were not raised during the feeding and drinking phases, particularly during their dark cycle. Therefore, the experiments of Group 3 (below) were designed to take tissue samples immediately following feeding and drinking to limit wash out of BH<sub>4</sub> in order to examine how this affected concentration of BH<sub>4</sub> in plasma and aorta.

### **6.3.3 Group 3: Modified pharmacokinetic studies of BH<sub>4</sub>**

In this group the BH<sub>4</sub> concentration in plasma was greater in both the lean and obese rats that received BH<sub>4</sub> compared to their control, the effect being particularly large in obese rats. Further, in the aortas, there were higher concentrations of BH<sub>4</sub> in both lean and obese rats that were BH<sub>4</sub>-treated, with a larger increase in the lean rats. BH<sub>4</sub> concentration in drinking water was 911.1 µmol/L at 0 hours and 725.8 µmol/L at 24 hours. BH<sub>4</sub> concentration measured in drinking water at 0 and 24 hours shows no significant loss in BH<sub>4</sub> over this time period.

### **6.3.4 Group 4: Effects of chronic treatment with BH<sub>4</sub>**

In the rats who received a fixed amount of chow at 16:00, MABP for lean rats was significantly lower than both control obese and BH<sub>4</sub> treated obese rats at baseline ( $P < 0.05$ ) and until 30 minutes of the HE clamp ( $P < 0.05$ ). Further, MABP did not change from baseline in any group (Figure 6.12 A). HR did not change from baseline in any group and there were no significant differences between the groups (Figure 6.12 B).

Blood glucose was significantly lower in the lean group than in both obese groups at baseline and throughout HE clamp except for at 5, 30, 33 and 70 minutes versus the obese group and at 0, 15, 24, 30 – 40 and 70 minutes versus the obese BH<sub>4</sub> treated group. Blood glucose did not differ between obese rat groups at any time point. Blood glucose in lean rats did not differ from baseline

except for at 13, 15 and 18 minutes (Figure 6.13). Blood glucose was maintained at baseline concentrations throughout the HE clamp in both obese rat groups with only minor fluctuations.

The GIR was significantly higher for lean rats than both obese rat groups at all time points from 13 – 80 minutes ( $P < 0.05$ ). GIR was significantly different from baseline in lean rats from 13 minutes onwards and in obese control rats and obese BH<sub>4</sub>-treated rats from 21 minutes onwards. However, GIR was not significantly different between obese control and obese BH<sub>4</sub>-treated rats at any time point

*In vivo* recoveries for inulin and insulin were  $2.98 \pm 0.17$  and  $1.89 \pm 0.14$  % respectively.

Plasma insulin concentrations were significantly lower in lean rats versus both obese groups at all time points (Figure 6.14 A;  $P < 0.05$ ). Plasma insulin concentrations were significantly increased above baseline by HE clamp in all groups ( $P < 0.05$ ). Plasma insulin was not significantly different between obese control and obese BH<sub>4</sub> group at baseline or at 0 – 40 minutes, but was significantly higher in obese BH<sub>4</sub> rats than obese control rats at 40 – 80 minutes ( $P < 0.05$ ).

Baseline ISF insulin concentrations obtained by using microdialysis was significantly higher in both control obese and BH<sub>4</sub>-treated obese groups than in lean rats (Figure 6.15;  $P < 0.05$ ). ISF insulin concentration tended to be higher in

BH<sub>4</sub> treated rats than vehicle treated obese rats. In lean rats, ISF insulin concentration was increased at 0 – 40 and 40 – 80 minutes relative to baseline (Figure 6.15;  $P < 0.05$ ). By contrast, in obese control and obese BH<sub>4</sub>-treated rats, the ISF insulin concentrations did not differ from baseline at either time point (Figure 6.15).

M/I was significantly higher in lean rats than in both obese rat groups (Figure 6.16;  $P < 0.05$ ): there was no significant difference between obese rats treated with vehicle and BH<sub>4</sub>.

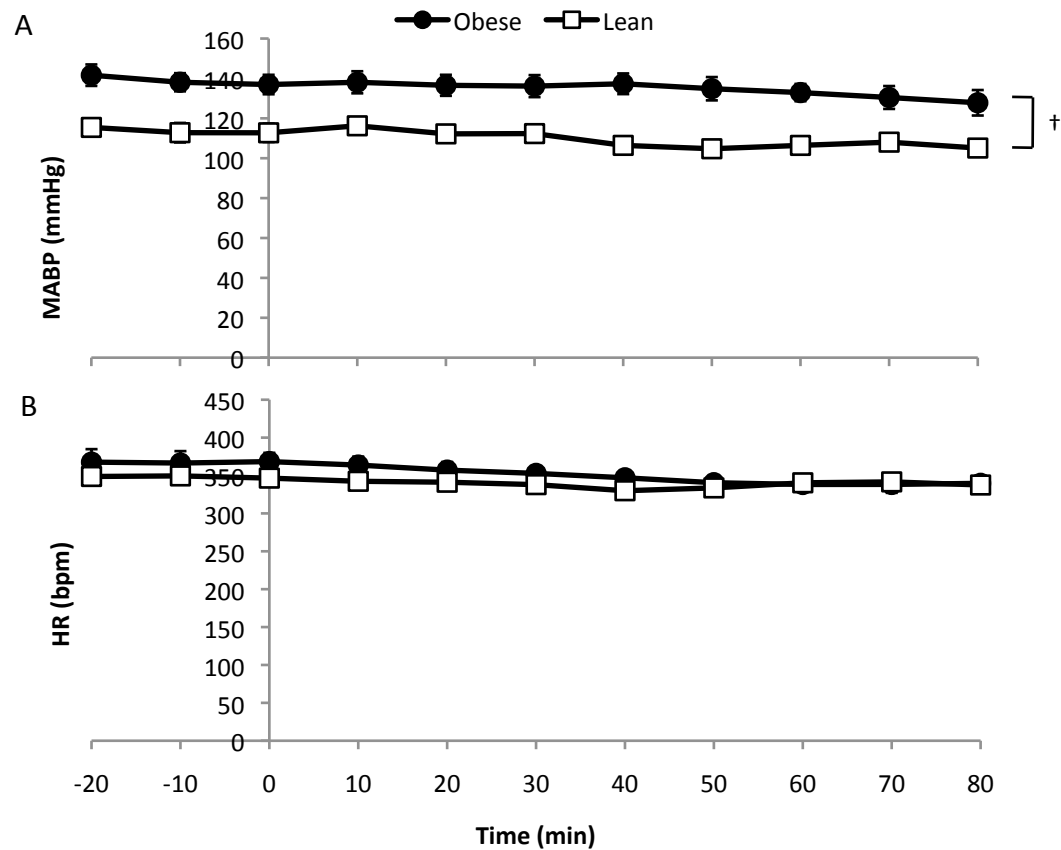


**Figure 6.2 Mean arterial blood pressure and heart rate for lean and obese Zucker rats during hyperinsulinaemic euglycaemic clamp with microdialysis.** Graphs show MABP (A) and HR (B). Symbols represent lean and obese groups (spherical black and square white, respectively). Values are mean  $\pm$  SEM.  $\dagger P < 0.05$  versus lean control group.



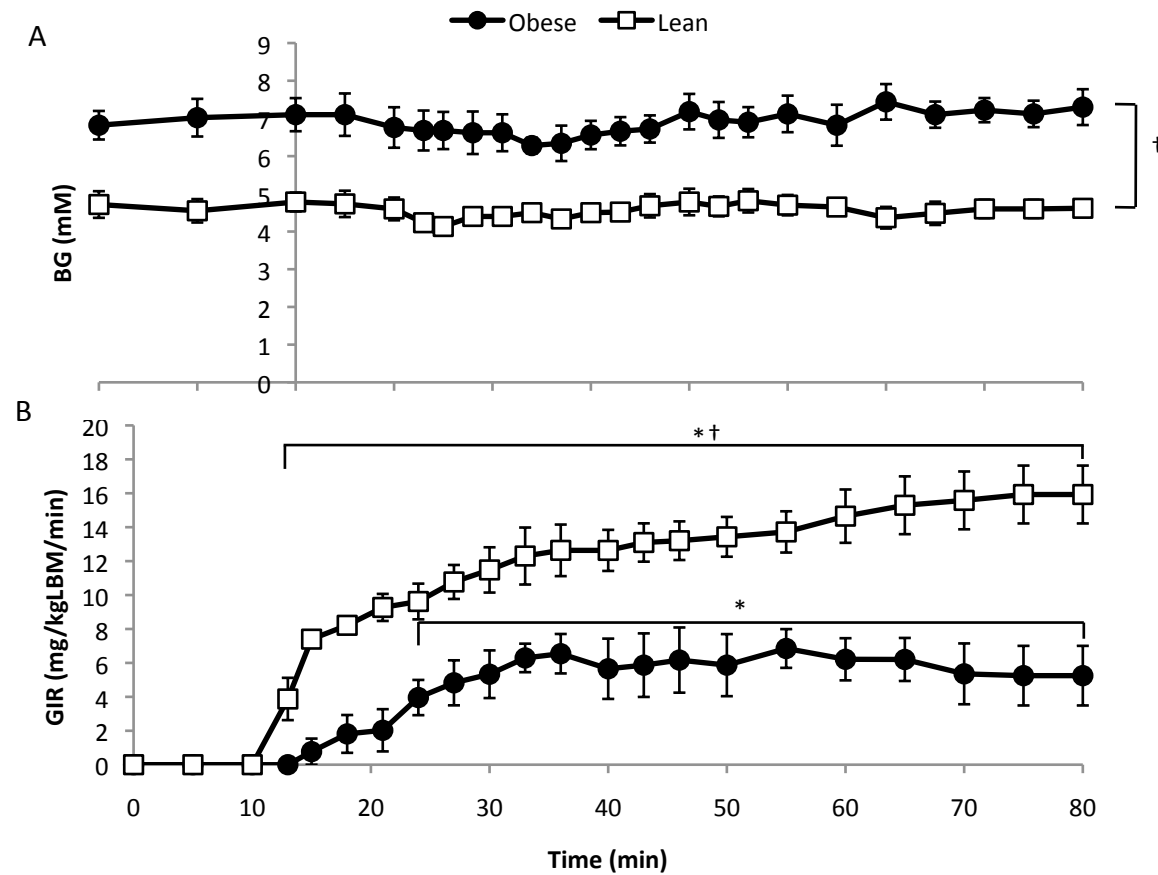


**Figure 6.3 Blood glucose and glucose infusion rate for lean and obese Zucker rats during hyperinsulinaemic euglycaemic clamp with microdialysis.** Graphs show BG (A) and GIR (B). Symbols represent lean and obese groups (spherical black and square white, respectively). Values are mean  $\pm$  SEM. †  $P < 0.05$  obese versus lean control group. \*  $P < 0.05$  versus baseline.

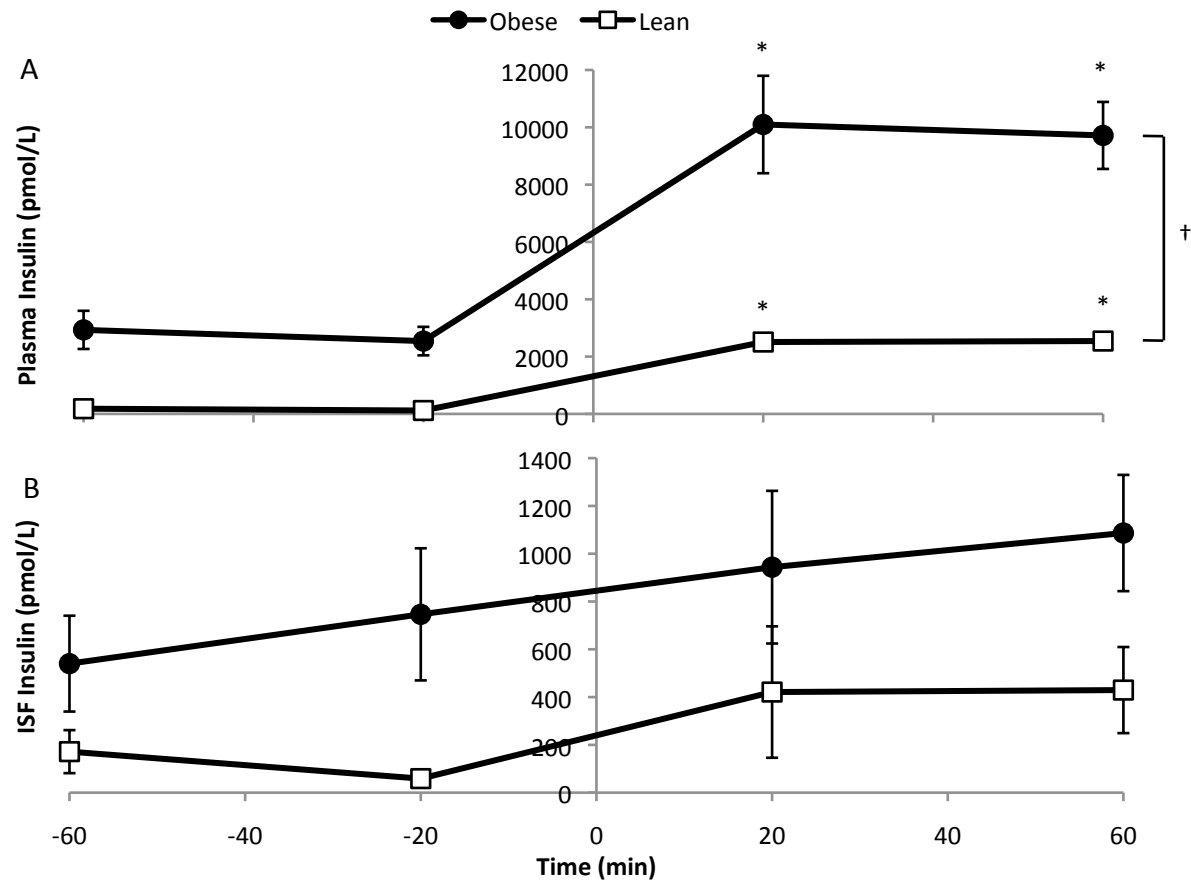


**Figure 6.4 Plasma and interstitial insulin concentrations for lean and obese Zucker rats during hyperinsulinaemic euglycaemic clamp with microdialysis.** Graphs show plasma (A) plasma and ISF (B) insulin concentrations. Symbols represent lean and obese groups (spherical black and square white, respectively). Values are mean  $\pm$  SEM.  $\dagger P < 0.05$  obese versus lean control group.  $* P < 0.05$  versus baseline.

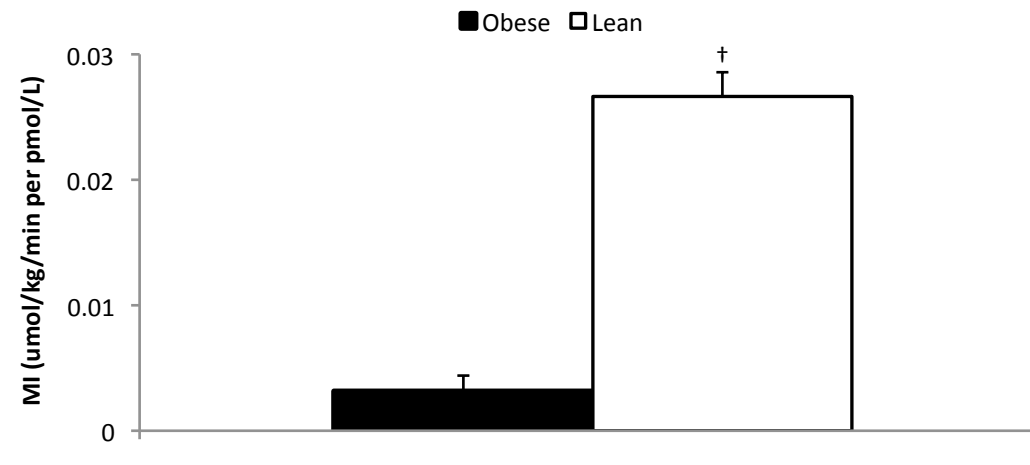


**Figure 6.5 Insulin sensitivity for lean and obese Zucker rats during hyperinsulinaemic euglycaemic clamp with microdialysis.** Symbols represent lean and obese groups (spherical black and square white, respectively). Values are mean  $\pm$  SEM.  $\dagger P < 0.05$  obese vs lean.

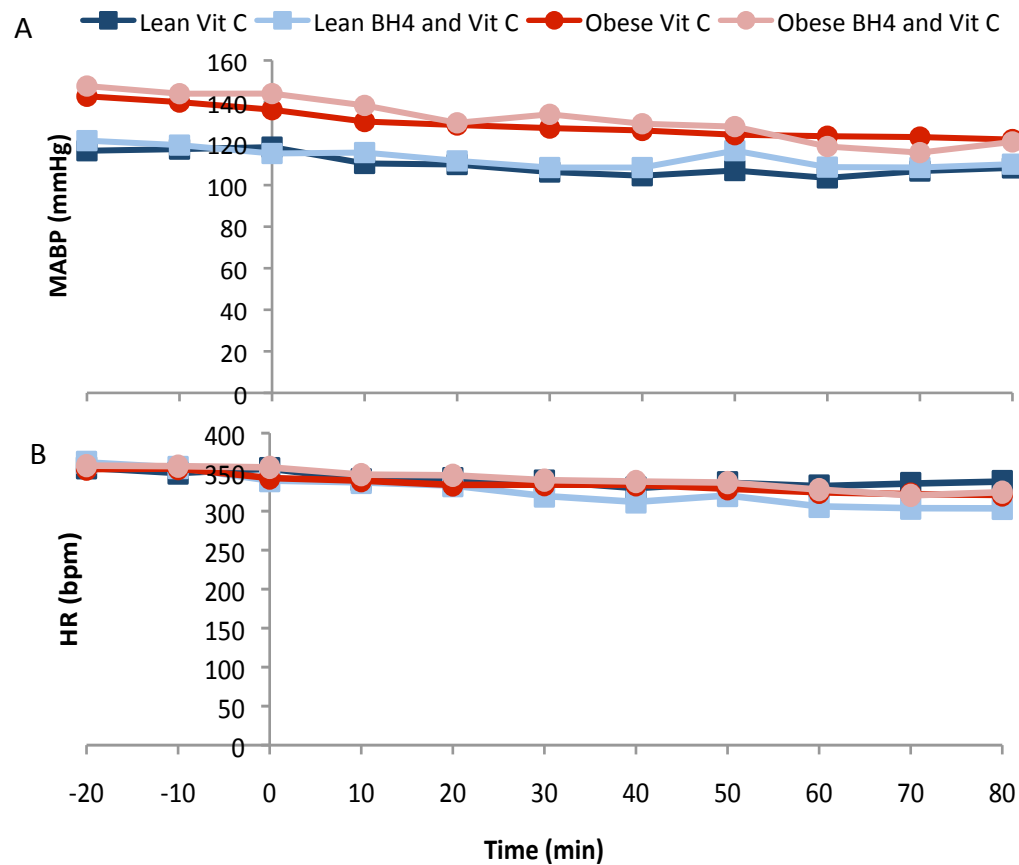


**Figure 6.6 Mean arterial blood pressure and heart rate for lean and obese Zucker rats with or without BH<sub>4</sub> treatment during hyperinsulinaemic euglycaemic clamp.** Graphs show MABP (A) and HR (B). Symbols represent lean vitamin C treated rats (dark blue square), lean BH<sub>4</sub> and vitamin C treated rats (light blue square), obese vitamin C treated rats (red circle) and obese BH<sub>4</sub> and vitamin C treated rats (pink circle). Values are means of two rats and therefore were not tested statistically.

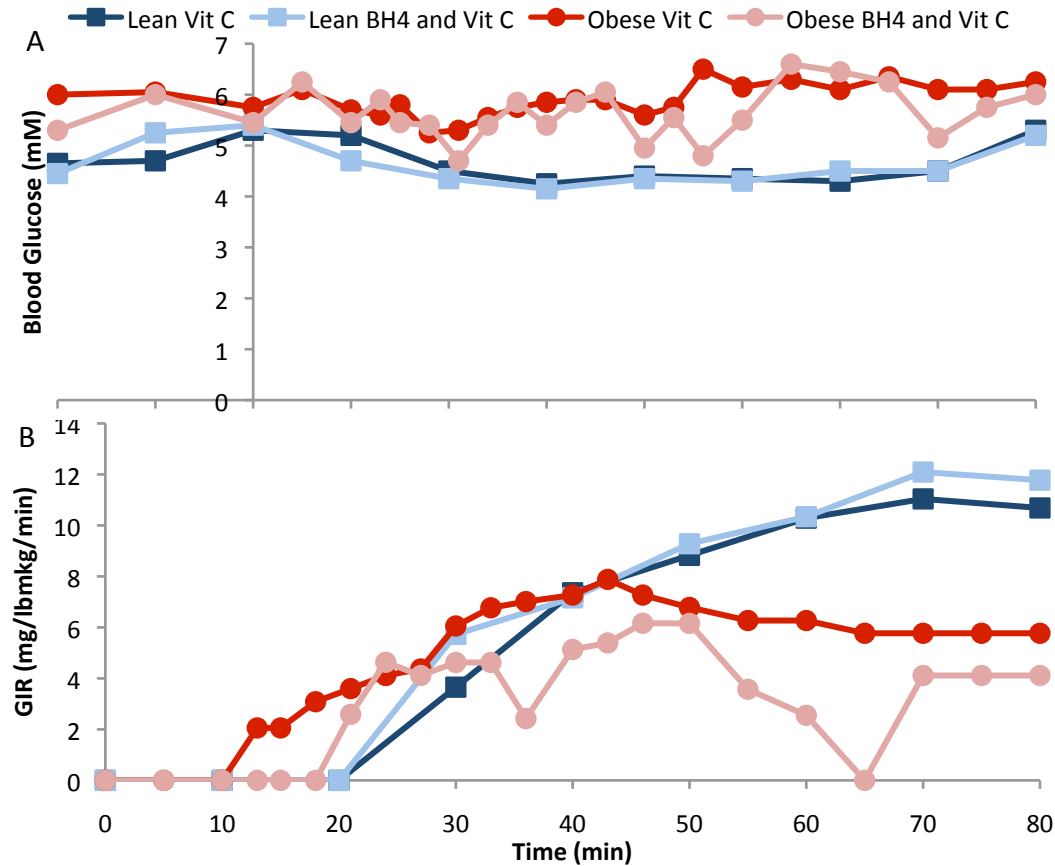


**Figure 6.7 Blood glucose and glucose infusion rate for lean and obese Zucker rats with or without BH<sub>4</sub> treatment during hyperinsulinaemic euglycaemic clamp.** Graphs show blood glucose (A) and glucose infusion rate (B). Symbols represent lean vitamin C treated rats (dark blue square), lean BH<sub>4</sub> and vitamin C treated rats (light blue square), obese vitamin C treated rats (red circle) and obese BH<sub>4</sub> and vitamin C treated rats (pink circle). Values are means of two rats and therefore were not tested statistically.

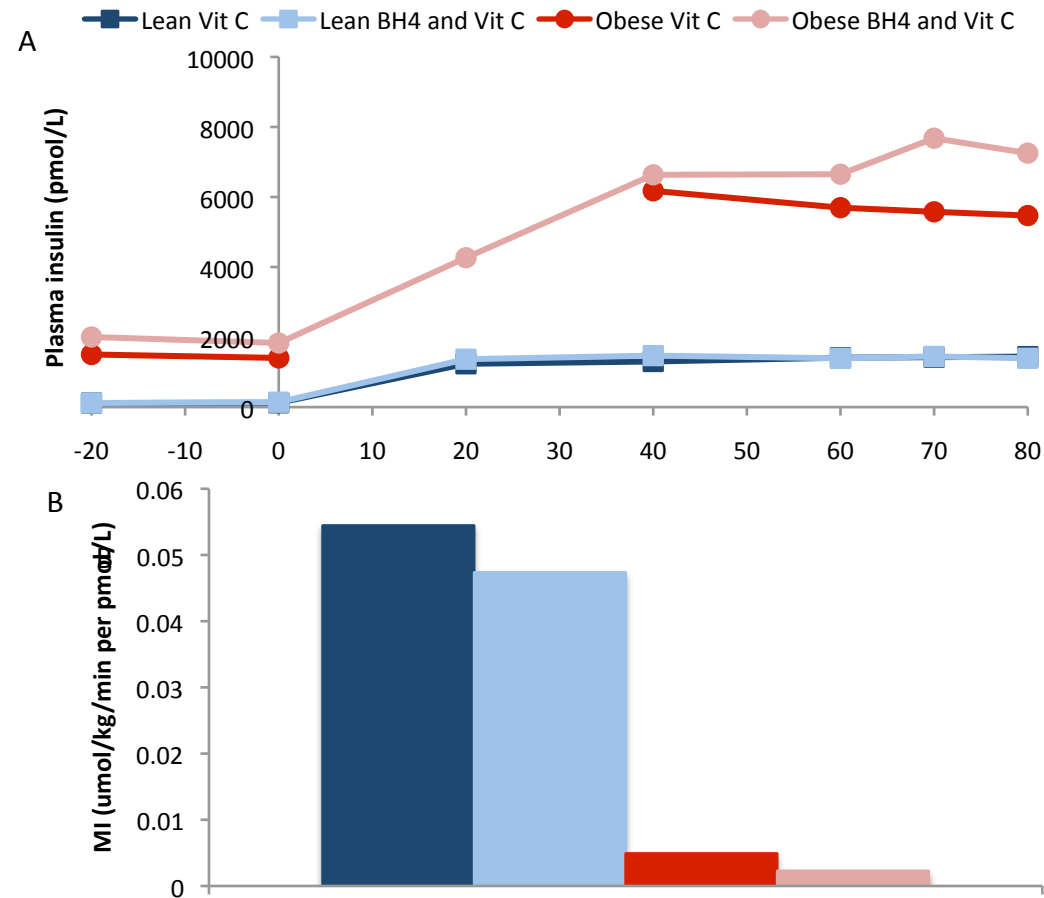


**Figure 6.8 Plasma insulin and insulin sensitivity for lean and obese Zucker rats with or without BH<sub>4</sub> treatment during hyperinsulinaemic euglycaemic clamp.** Graphs show plasma insulin (A) and insulin sensitivity (B). Symbols represent lean vitamin C treated rats (dark blue square), lean BH<sub>4</sub> and vitamin C treated rats (light blue square), obese vitamin C treated rats (red circle) and obese BH<sub>4</sub> and vitamin C treated rats (pink circle). Values are means of two rats and therefore were not tested statistically.

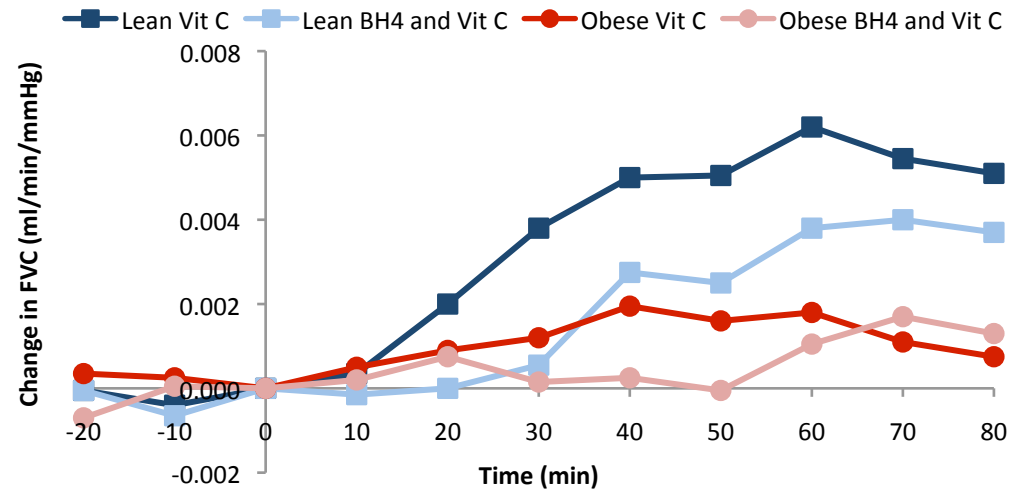


**Figure 6.9 Femoral vascular conductance for lean and obese Zucker rats with or without BH<sub>4</sub> treatment during hyperinsulinaemic euglycaemic clamp.** Symbols represent lean vitamin C treated rats (dark blue square), lean BH<sub>4</sub> and vitamin C treated rats (light blue square), obese vitamin C treated rats (red circle) and obese BH<sub>4</sub> and vitamin C treated rats (pink circle). Values are means of two rats and therefore were not tested statistically.

Time (hr)	BH <sub>4</sub> (umol/L)	Ratio (BH <sub>4</sub> :BH <sub>2</sub> +B)
0	536.6	39.7
18	591.8	48.3
24	496.1	35.2
48	308.3	26.7

**Table 6.1 BH<sub>4</sub> concentration in drinking water at 0, 18, 24 and 48 hours after the solution had been prepared.**  
Drinking water was prepared and left on the bench in order to mimic drinking water being left at room temperature and measure the oxidation of BH<sub>4</sub>.



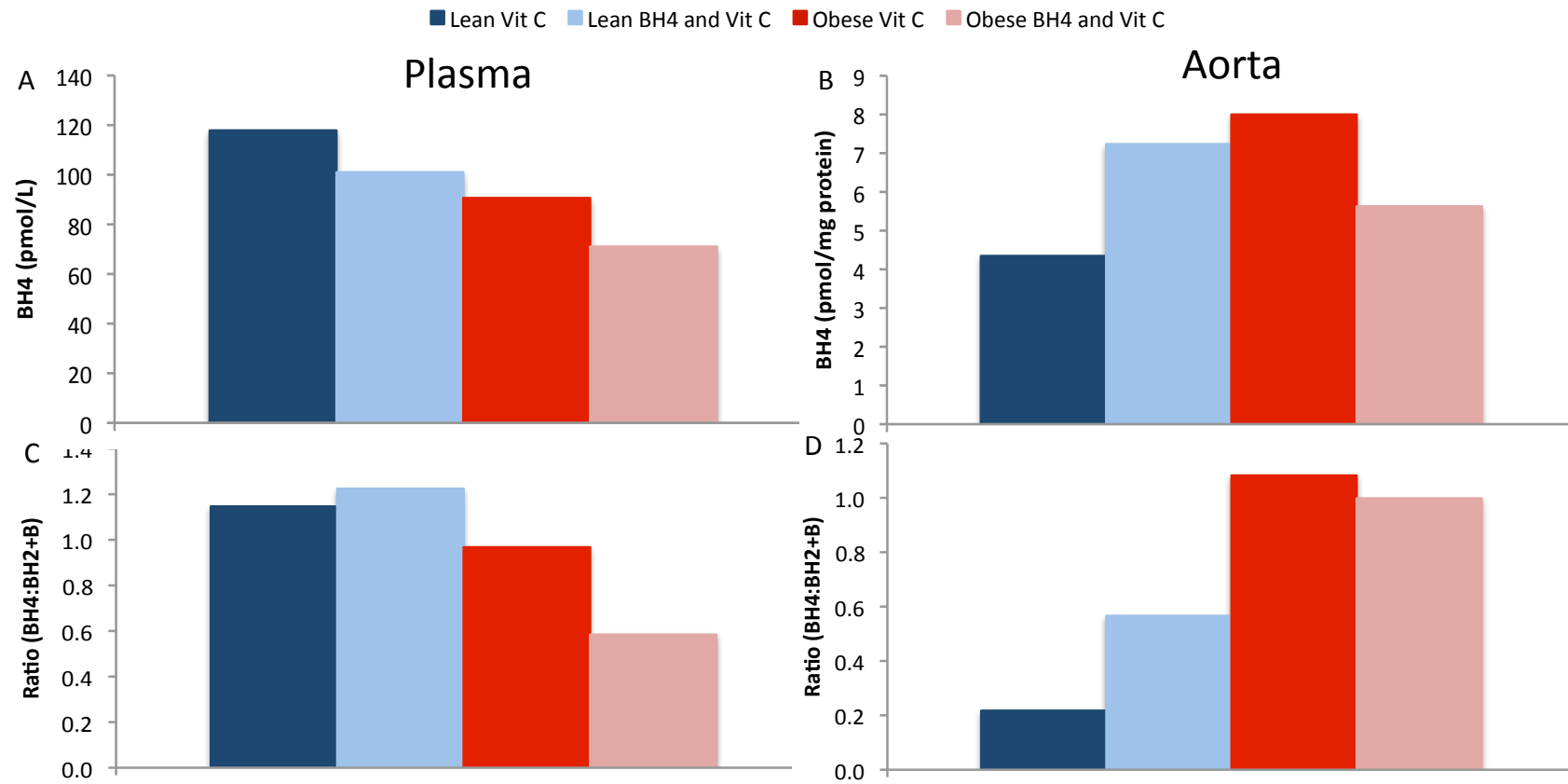


**Figure 6.10 BH<sub>4</sub> concentrations and BH<sub>4</sub>:BH<sub>2</sub>+B ratio in plasma and aorta samples from lean and obese rats with or without BH<sub>4</sub> treatment following HE clamp.** Graphs show the BH<sub>4</sub> concentration in plasma and aorta (A and B respectively) and BH<sub>4</sub>:BH<sub>2</sub>+B ratio in plasma and aorta (C and D respectively) at the end of HE clamp protocol. Bars represent lean vitamin C treated rats (dark blue), lean BH<sub>4</sub> and vitamin C treated rats (light blue), obese vitamin C treated rats (red) and obese BH<sub>4</sub> and vitamin C treated rats (pink). Values are a mean of two animals and therefore were not tested statistically.

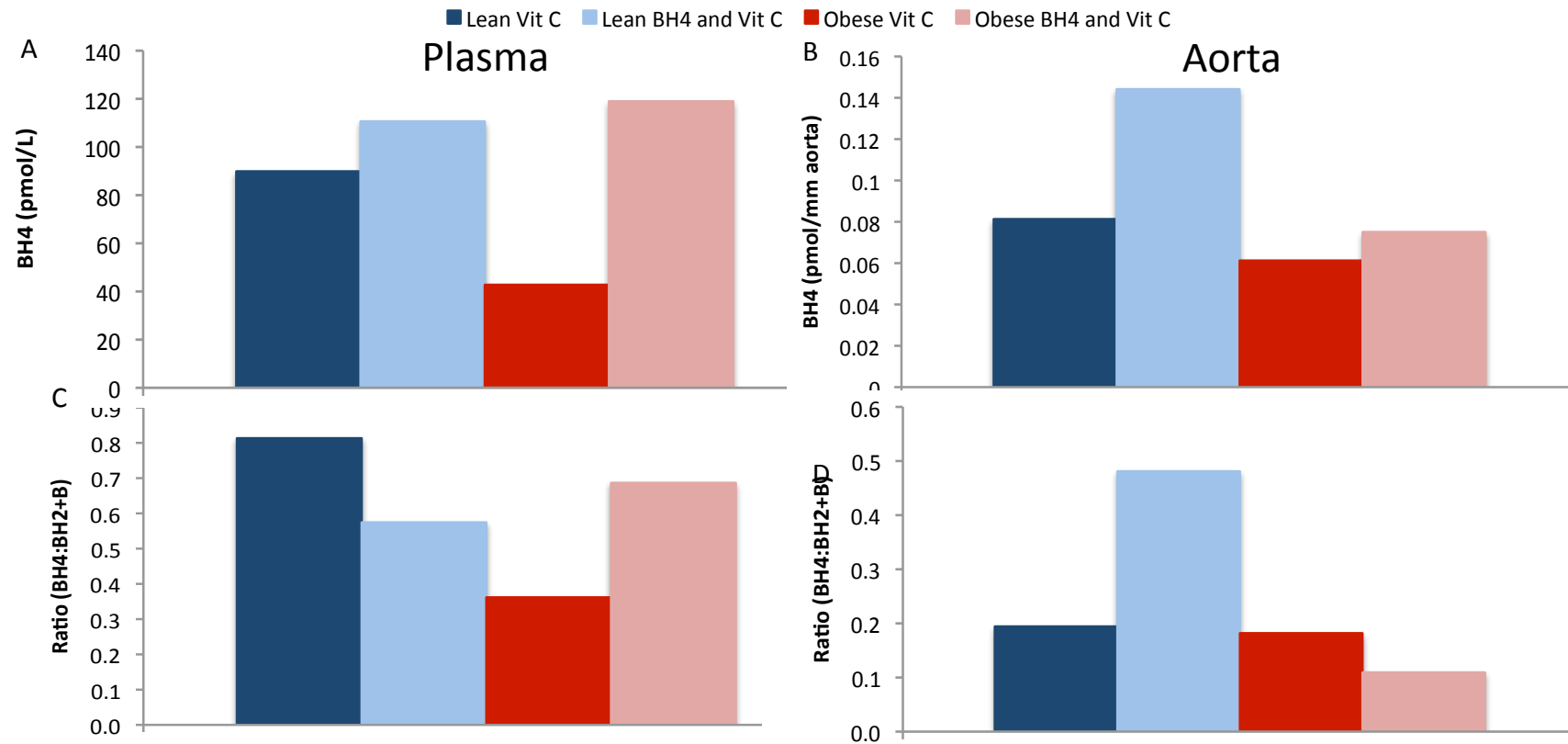


**Figure 6.11 BH<sub>4</sub> concentrations and BH<sub>4</sub>: BH<sub>2</sub> + B ratio in plasma and aorta samples from lean and obese rats with or without BH<sub>4</sub> treatment.** Graphs show the BH<sub>4</sub> concentration in plasma and aorta (A and B respectively) and BH<sub>4</sub>: BH<sub>2</sub> + B ratio in plasma and aorta (C and D respectively) at the end of HE clamp protocol. Bars represent lean vitamin C treated rats (dark blue), lean BH<sub>4</sub> and vitamin C treated rats (light blue), obese vitamin C treated rats (red) and obese BH<sub>4</sub> and vitamin C treated rats (pink). Values are a mean of two animals and therefore were not tested statistically.

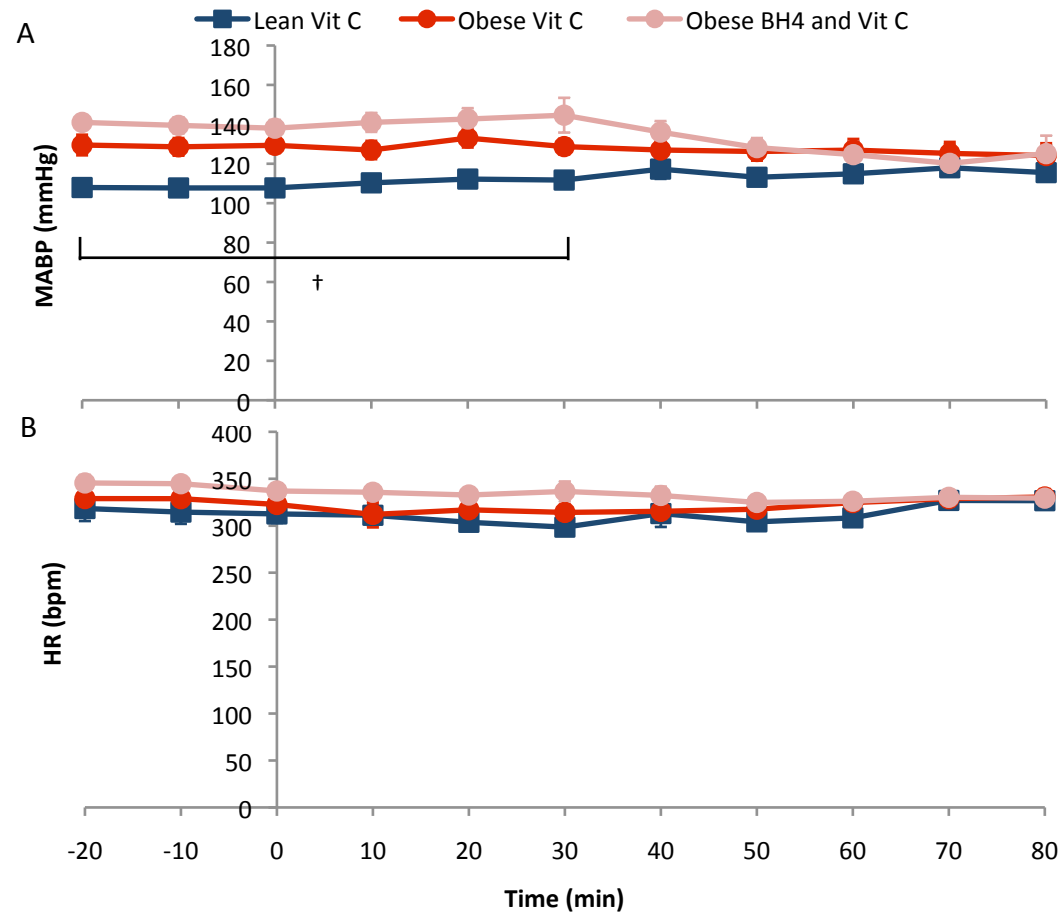


**Figure 6.12 Mean arterial blood pressure and heart rate for lean and obese Zucker rats during hyperinsulinaemic euglycaemic clamp with microdialysis.** Graphs show MABP (A) and HR (B). Symbols represent lean vitamin C treated rats (blue square), obese vitamin C treated rats (red circles) and obese BH<sub>4</sub> treated rats (pink circles). Values are mean  $\pm$  SEM. †  $P < 0.05$  versus lean control group.

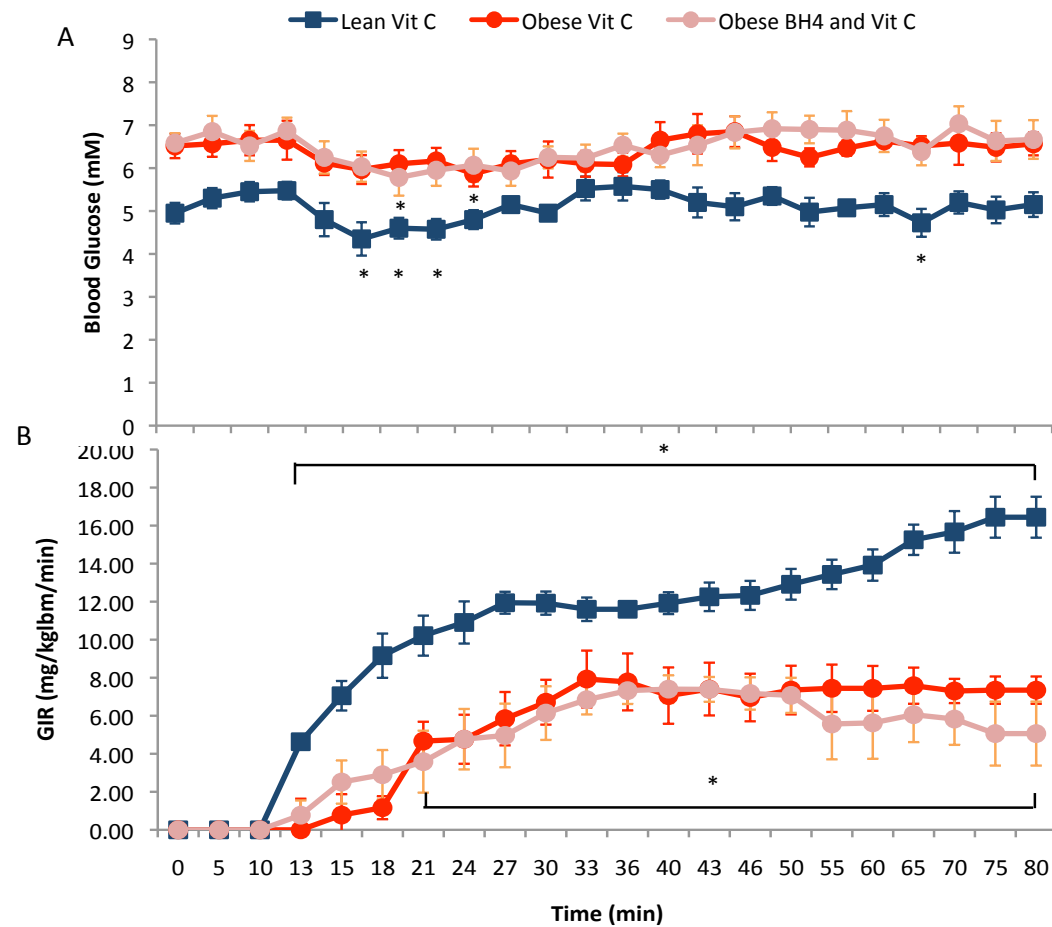


**Figure 6.13 Blood glucose and glucose infusion rate for lean and obese Zucker rats during hyperinsulinaemic euglycaemic clamp with microdialysis.** Graphs show blood glucose (A) and GIR (B). Symbols represent lean vitamin C treated rats (blue square), obese vitamin C treated rats (red circles) and obese BH<sub>4</sub> treated rats (pink circles). Values are mean  $\pm$  SEM. \*  $P < 0.05$  versus baseline.

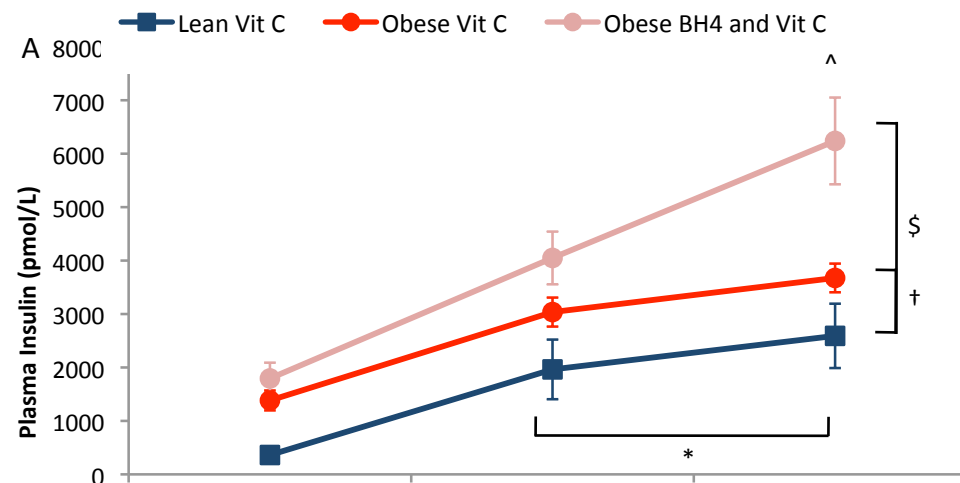


**Figure 6.14 Plasma insulin concentrations for lean and obese Zucker rats during hyperinsulinaemic euglycaemic clamp with microdialysis.** Symbols represent lean vitamin C treated rats (blue square), obese vitamin C treated rats (red circles) and obese BH<sub>4</sub> treated rats (pink circles). Values are mean  $\pm$  SEM. \*  $P < 0.05$  versus baseline. †, \$  $P < 0.05$  for obese vitamin C treated rats and obese BH<sub>4</sub> treated rats versus lean vitamin C treated rats respectively. ^  $P < 0.05$  obese vitamin C treated rats versus obese BH<sub>4</sub> treated rats.

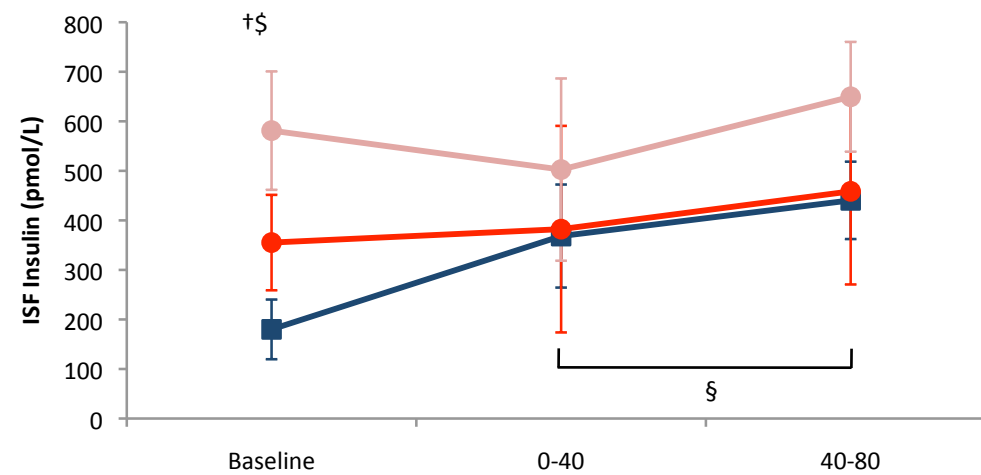


**Figure 6.15 Interstitial insulin concentrations for lean and obese Zucker rats during hyperinsulinaemic euglycaemic clamp with microdialysis.** Symbols represent lean vitamin C treated rats (blue square), obese vitamin C treated rats (red circles) and obese BH<sub>4</sub> treated rats (pink circles). Values are mean  $\pm$  SEM. †, §  $P < 0.05$  for obese vitamin C treated rats and obese BH<sub>4</sub> treated rats versus lean vitamin C treated rats respectively. §  $P < 0.05$  versus baseline for lean vitamin C treated rats.

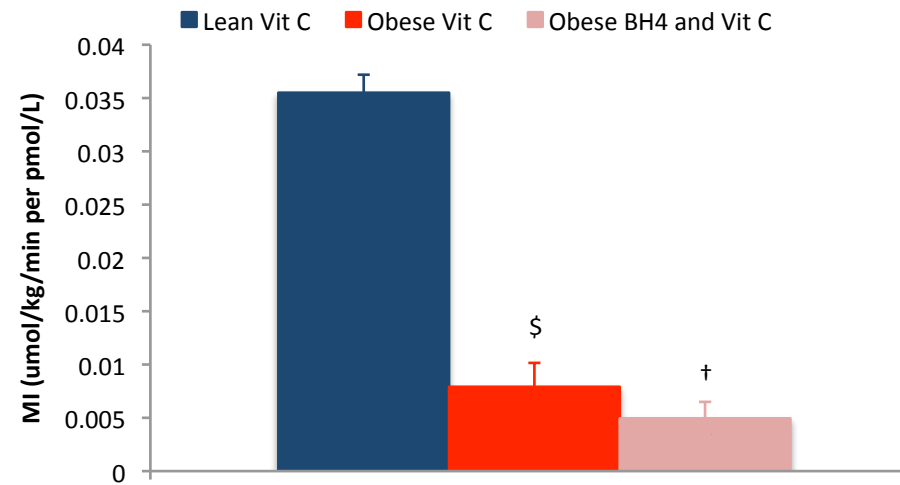


**Figure 6.16 Insulin sensitivity for lean and obese Zucker rats during hyperinsulinaemic euglycaemic clamp with microdialysis.** Bars represent lean vitamin C treated rats (blue), obese vitamin C treated rats (red) and obese BH<sub>4</sub> treated rats (pink). Values are mean  $\pm$  SEM. †, \$  $P < 0.05$  for obese vitamin C treated rats and obese BH<sub>4</sub> treated rats versus lean vitamin C treated rats respectively.

## **6.4 Discussion**

The two major aims of the present study were firstly to use the methodology developed in the experiments of Chapter 5 to obtain measurements of insulin in ISF of muscle in lean and obese Zucker rats before and during HE clamp and secondly, to test the effect of chronic treatment with BH<sub>4</sub> in obese rats. The hypothesis was that in obese Zucker rats, BH<sub>4</sub> would improve NO availability and thereby improve vascular and muscle responsiveness to insulin with an associated change in the transport of insulin to the ISF. However, it became apparent in the preliminary studies that further modifications were necessary to the protocols. Thus, the results and main conclusions that can be drawn from each set of experiments are discussed in turn.

### **6.4.1 Group 1: Preliminary microdialysis experiments**

In group 1 experiments which were performed on six lean and five obese Zucker rats show the effects of HE clamp were very similar in most respects to results presented in Chapter 4. Blood glucose concentrations were lower in the lean rats than in the obese rats and were stable throughout the HE clamp in both groups. GIR increased to higher levels in lean rats than obese rats and the increase from baseline occurred earlier in the lean rats. Further, plasma insulin concentration was significantly lower in the lean than obese rats and during HE clamp particularly in the lean rats so that plasma concentration in the lean rats reached the basal concentration of the obese rats. Thus, insulin sensitivity (M/I) was substantially higher in lean than obese rats.



However, blood glucose and GIR values during the HE clamp in the obese rats of the present chapter were slightly higher than those measured in the obese rats of Chapter 4 although the lean rats of the present chapter were directly comparable to those of Chapter 4. Nevertheless, the insulin sensitivity calculated from plasma insulin and GIR at the end of HE clamp was lower in both lean and obese rats of the present study than in Chapter 4. As there were no differences between the plasma insulin concentrations in the two sets of experiments that could offer an explanation for the differences in insulin sensitivity, it seems that both the lean and obese rats in the present study were less insulin sensitive than those of Chapter 4. A lower insulin sensitivity in the lean rats of the present study may explain why MABP did not fall significantly during the HE clamp, for the increase in FVC which contributed to the fall in MABP in the lean rats of Chapter 4 may have been smaller. As discussed in the General Introduction and Section 6.1, the plasma insulin concentration may not necessarily reflect the concentration of insulin in the muscle ISF and thus access to muscle insulin receptors, highlighting the importance of being able to measure ISF insulin concentrations to accurately assess muscle sensitivity to insulin.

In these preliminary studies, although there were no statistically significant differences, basal concentrations of insulin in ISF tended to be higher in obese rats versus lean ( $P = 0.14$ ). It should be noted that basal insulin concentrations in ISF have not been measured before in ISF of lean or obese rats. It may be that larger group sizes would have allowed statistical significance to be demonstrated (see below). Importantly, it should also be noted that ISF concentrations of insulin were lower than plasma concentrations at all time points, indicating that

the endothelium does act as a barrier to the movement of insulin in both lean and obese rats.

As there was a trend for the ISF insulin concentrations to increase from basal in the lean rats, but not in the obese rats and as ISF insulin concentrations at the end of HE clamp were higher in obese than in lean rats. The present results indicated that differences could be detected with the protocol used and warranted further investigation. An important observation was that ISF insulin concentrations were not different between the two basal time points taken with a 40 minute interval. This indicated that trauma, inducing inflammation introduced by the insertion of the probe had stabilized by the time the HE clamp began. Thus, the first time point was not included in the subsequent analyses of the data so that measurements were taken as long after probe insertion as possible.

#### **6.4.2 Group 2: Preliminary pharmacokinetic studies of tissue BH<sub>4</sub> levels**

The experiments performed on Group 2 were conducted to assess whether or not the BH<sub>4</sub> dosing regimen was effective in increasing plasma and tissue BH<sub>4</sub>. The cardiovascular data, blood glucose and glucose infusion rate data for this small set of lean and obese rats were comparable to those of the groups discussed in previous chapters throughout the protocol.

Importantly, the measurements of the concentration of BH<sub>4</sub> in drinking water established that the BH<sub>4</sub> in the drinking water was not oxidized over 24 hours: in

agreement with the findings of (Li et al., 2011). As the water was changed every 24 hours this meant that rats were receiving BH<sub>4</sub> in drinking water as intended. However, when measured at the end of HE clamp, plasma BH<sub>4</sub> concentrations appeared to be lower in both lean and obese rats who had been dosed with BH<sub>4</sub> treatment. Further, BH<sub>4</sub>: BH<sub>2</sub> + B ratio in plasma of lean rats was unchanged whereas the ratio in the obese rats was slightly lower in the animals that had received BH<sub>4</sub>. Similarly, although there was an apparent tendency for BH<sub>4</sub> concentration in the aorta to be greater in lean rats that received BH<sub>4</sub>, there was a lower concentration in the obese rats that had received BH<sub>4</sub>. Indeed, the BH<sub>4</sub>: BH<sub>2</sub> + B ratio also tended to be lower in obese rats which may indicate more oxidation in the obese rats (Vasquez-Vivar et al., 2002).

Thus, it appeared that dosing the rats with BH<sub>4</sub> did not affect the BH<sub>4</sub> concentration in the plasma or aortas of either lean or obese Zucker rats at least when measured at the end of the HE clamp protocol. It seemed likely this was because animals drank very little water for ~ 16 hours before the tissues were taken: animals were fasted for ~ 8 hours prior to the protocol in which time water intake would also have decreased significantly (in house observations at AstraZeneca, Alderley Park), and obviously they did not drink during surgery or HE clamp. Thus, it is possible that at the time the tissues were taken the BH<sub>4</sub> concentrations may have already fallen due to its short half-life. In other words, these measurements could not be expected to indicate the BH<sub>4</sub> concentration at the time when experiment proper began.

### **6.4.3 Group 3: Modified pharmacokinetic studies of BH<sub>4</sub>**

It was for the reasons discussed above that pharmacokinetic experiments were repeated in which rats were anaesthetized to allow samples to be taken, as soon as they came off their dark cycle and hence after an overnight feed, when the rats had recently been exposed to BH<sub>4</sub> in their drinking water. In these experiments, BH<sub>4</sub> concentration in plasma and aorta of lean BH<sub>4</sub>-treated rats was increased relative to lean control, as was the ratio of BH<sub>4</sub>: BH<sub>2</sub> and B. Further, plasma and aorta concentrations of BH<sub>4</sub> were also increased in BH<sub>4</sub>-treated obese rats, plasma concentrations markedly so. However the ratios of BH<sub>4</sub>: BH<sub>2</sub> and B were increased in lean rats but reduced in both plasma and aorta of obese rats. This very clearly demonstrates an increase in oxidative stress in obese Zucker rats consistent with the ability to reduce BH<sub>4</sub> to BH<sub>2</sub> and B (Vasquez-Vivar et al., 2002). Ratios of BH<sub>4</sub>: BH<sub>2</sub> and B was not decreased in the plasma of obese rats following treatment with BH<sub>4</sub> suggesting that BH<sub>4</sub> in the plasma may be less prone to oxidation than BH<sub>4</sub> in the aorta.

The lower concentrations of BH<sub>4</sub> in obese vehicle-treated rats versus lean vehicle treated rats is in agreement with the observations of Shinozaki et al., that BH<sub>4</sub> was deficient in the condition of endothelial dysfunction associated with fructose feeding. Further, in the obese rats treated with BH<sub>4</sub> the concentration of BH<sub>4</sub> in plasma equaled that of lean rats and that in the aorta increased towards the concentration in the lean vehicle treated rats. This is in agreement with the observation of Li et al., (2011) who showed that supplementation of BH<sub>4</sub> in the

drinking water of apolipoprotein E<sup>-/-</sup> mice for two weeks normalised BH<sub>4</sub> concentrations in the partially ligated left carotid artery. In the latter experiments, samples were taken immediately after the animals were killed, similar to the present modified experiments.

These findings give confidence that rats dosed with BH<sub>4</sub> would have had adequate exposure to BH<sub>4</sub> over a period of two weeks to increase NO availability chronically. However, these results taken together with those obtained in the first set of experiments indicate that BH<sub>4</sub> levels in vascular tissue and aorta must have been falling during the HE clamp protocol.

#### **6.4.4 Group 4: Effects of chronic treatment with BH<sub>4</sub> on responses to HE clamp**

The final set of experiments were performed on rats that probably ceased feeding and drinking some time before the experiment proper began. Therefore, although BH<sub>4</sub> levels were raised chronically over two weeks of dosing, they were likely to be falling during the experiment.

#### **Comparison of lean versus obese control Zucker rats**

Cardiovascular variables for this set of experiments indicate that the rats were stable throughout the protocol. Blood glucose concentrations were maintained throughout the HE clamp protocol with minor fluctuations in lean and obese control groups. Both blood glucose and glucose infusion rates were directly comparable to those of Group 1 in the present chapter and thus the comparison

with control animals in Chapter 4 made in section 6.3.1 is also valid for the groups of the present chapter.

The responses shown by the obese and lean rats of this group were very similar to those just discussed above. Further, insulin sensitivity of lean and obese rats were also similar to those of Group 1 and therefore lower than those calculated in Chapter 4. This probably reflects different batches of animals purchased at different times.

The most important finding of the present study was that the insulin concentration measured in plasma was substantially higher than in ISF in obese rats under basal conditions and during HE clamp and significantly higher in the lean rats at the end of HE clamp. Thus, the present results on lean and obese Zucker rats were consistent with those of Sjostrand et al., (1999) measured insulin with microdialysis in human muscle for the first time and confirmed previous findings in lymph and by microdialysis in the subcutaneous tissue that an arterial-interstitial gradient exists for insulin. However, Holmang et al., (1997) reported that in control Sprague-Dawley rats, plasma and ISF concentrations were the same when plasma insulin was  $< 250$  mU/ml and that ISF was lower than plasma when plasma insulin was  $> 350$  mU/ml. The present results are consistent with this finding in that in the lean control rats insulin concentrations in plasma and ISF were similar under basal conditions ( $\sim 200$  pmol/L) but much lower in the ISF versus the plasma at the end of HE clamp ( $\sim 400$  versus  $\sim 2000$  pmol/L).

The finding that the basal concentration of insulin in the ISF was significantly lower in lean animals than both obese animal groups is new as the only other investigators to measure basal ISF insulin concentrations were Herkner et al., (2003). To achieve this they used the equilibration method in human subjects and a much higher flow rate with an associated higher concentration of BSA. Insulin concentrations at baseline were  $48 \pm 8$  pmol/L in plasma and  $19 \pm 4$  pmol/L in ISF. Mean ISF: plasma ratio at baseline was  $0.48 \pm 0.09$  pmol/L and this ratio was then found to be significantly reduced during HE clamp. They did not however measure the differences between lean and obese subjects as has been done in the experiments in the present chapter.

The finding that there was a significant increase in ISF insulin concentrations throughout the HE clamp in lean rats whereas ISF insulin concentration did not change significantly in obese rats, has not previously been reported. This means that when plasma insulin concentration increases in lean rats during the HE clamp protocol, ISF insulin also correspondingly increased and that this did not happen in obese rats. This seems to suggest that the TET of insulin into the ISF was already maximal at basal concentrations of insulin in the obese rats, perhaps due to the high plasma concentrations of insulin or perhaps to a functional defect in TET. A possible explanation for the present results is that the endothelium in obese rats does not act as a selective barrier or that it is 'leaky'. In support of this proposal, ISF insulin concentrations at the end of HE clamp were very similar for lean and obese vehicle treated rats. For Castillo et al., also showed that insulin TET was normal in healthy obese patients under HE clamp (Castillo et al., 1994). Likewise, during HE clamps in lean and obese subjects Prager et al., showed that

pharmacokinetics were extremely similar between lean and obese humans during HE clamp; showing that differences in access to the ISF couldn't explain the differences in ISGU (Prager et al., 1986). Two studies by Sjostrand et al., on humans (Sjostrand et al., 2000, Gudbjornsdottir et al., 2005) showed that glucose and insulin ISF concentrations in T2D are normal. Thus, all of the above studies indicate that ISF insulin concentration was similar in lean and obese.

Additionally, Holmang et al., (1997) reported that at high supraphysiological insulin concentrations, although a gradient was seen between plasma and ISF insulin concentrations in lean Zucker rats, plasma and ISF concentrations in obese Zuckers were equal. However, equal concentrations of plasma and ISF insulin were not found in the experiments in this chapter. There were many differences between the protocol used in the present study and in the study of Holmang et al., for instance, a minipump was used to deliver insulin as the exogenous calibrator and a smaller (50 kDa) molecular weight cut-off microdialysis probe was used. Additionally, although plasma and ISF insulin were measured on the same assay kit, both human and rat insulin were measured on the same kit with no specified modifications. The insulin concentrations they measured are likely to be less accurate than those measured in the present study where the assay was modified to accurately measure both rat and plasma insulin.

A question raised by the finding that ISF insulin concentrations were significantly higher in obese rats than lean rats at baseline is whether the prevailing high ISF insulin concentrations caused desensitization of the insulin



receptors and contributed to the insulin resistance, or whether delivery of insulin to the ISF was increased in response to poor sensitivity of the muscle cell to insulin. It is almost certainly a contribution of both but requires further investigation now that a method has been established that enables the investigator to assess basal ISF insulin concentrations.

In contrast to the present findings, there has been some speculation that ISF concentrations of insulin may be lower in insulin-resistant muscles (Lillioja and Bogardus, 1988). This proposal of defective endothelial transfer was linked to evidence of a thickened basement membrane (Siemionow and Demir, 2004). The results of the present studies indicate this is not the case, in that ISF insulin concentrations in lean and obese control rats were remarkably similar at HE clamp.

#### **Effects of BH<sub>4</sub> treatment on obese rats**

There were no obvious differences between vehicle and BH<sub>4</sub> treated obese rats at baseline or during HE clamp for MABP, HR, blood glucose or GIR. However, there were some apparent differences in the plasma insulin and ISF insulin concentrations. Notably, plasma insulin concentrations were not significantly different between obese rats treated with BH<sub>4</sub> and those treated with vehicle at basal and 0 – 40 minutes of the HE clamp but at 40 – 80 minutes plasma insulin in the BH<sub>4</sub>-treated obese rats were significantly higher than in the vehicle treated group. This suggests decreased clearance of insulin by non-muscle tissues in the BH<sub>4</sub> treated animals, although it is not possible to determine this from the results of this study. However, it is important to note that the plasma insulin

concentrations in the obese BH<sub>4</sub> treated animals are similar to those in the obese vehicle clamp group in Chapter 4. Thus, in the obese vehicle clamp group the plasma insulin concentrations were ~7500 pmol/L compared to ~6500 pmol/L in the obese BH<sub>4</sub> treated animals. Thus, it may be that it is the vehicle treated obese rats that showed a smaller increase in plasma insulin than might have occurred, rather than that plasma insulin rose to higher levels after BH<sub>4</sub> treatment. This needs to be repeated with rats of the same batch.

The results of the present experiments indicate that BH<sub>4</sub> treatment did not affect cardiovascular variables, blood glucose, glucose infusion rate or basal insulin concentrations in obese Zucker rats. Thus, Figure 6.15 shows M/I was also unaffected by BH<sub>4</sub> treatment, this is in contrast to data presented in the literature. Thus, Nystrom et al., (2004) showed that intra-arterial infusion of BH<sub>4</sub> improved glucose disposal in T2D during HE clamp. Furthermore it was expected that BH<sub>4</sub> treatment might increase M/I as microvascular recruitment has been shown to be dependent on activation of eNOS (Vincent et al., 2003). Therefore an increase in the activation of eNOS due to supplementation of one of its co-factors might have increased microvascular recruitment and therefore the surface area available for the translocation of insulin into the ISF. However this did not seem to be the case in these experiments and may warrant further investigation, for instance by using an acute intravenous infusion of BH<sub>4</sub>. Due to the short half life of BH<sub>4</sub>, an acute infusion of BH<sub>4</sub> given during the HE clamp protocol would help to ensure that high concentrations of BH<sub>4</sub> are maintained throughout; this is particularly important if acute synthesis of NO is required to show effect on variables recorded.

Although the ISF insulin concentrations in obese rats treated with BH<sub>4</sub> were not significantly higher than obese vehicle treated at any time point, there was a tendency for an increase over vehicle treated obese rats. Thus, it is possible that the results are consistent with those of Barrett et al., (2011) that activation of the Akt- eNOS pathway in endothelial cells by insulin increased the transport of insulin through the cell. In other words if NO production was increased in the BH<sub>4</sub> treated rats due to supplementation with BH<sub>4</sub> it may be that the total amount of insulin that moved through the endothelium under basal conditions during HE clamp was increased. This requires further investigation.

A limitation of the microdialysis method is that insertion of microdialysis probes inevitably causes trauma. Investigations have shown however that, changes in local skin circulation return to baseline within 60 minutes (Chaurasia et al., 2007). Further, microdialysis *per se* has been shown not to alter capillary permeability by the demonstration that glucose concentration in the interstitial fluid was identical to that in venous plasma using two of the equilibration methods described in Section 5.1.1 (Lonnroth and Strindberg, 1995). The similarity of the ISF measurements at -60 and -20 indicate little trauma in the present experiments (see Section 6.4.1).

It should be noted that BH<sub>4</sub> can affect endothelium dependent vasodilatation by acting as an antioxidant rather than as a cofactor. However evidence from other groups suggests that this is unlikely to be the case (Li et al., 2011). However,

Heitzer et al., (2000a) showed that another pterin with equal antioxidant potency (tetrahydroneopterin  $\text{NH}_4$ ) to  $\text{BH}_4$  *in vitro* was not able to enhance endothelium-dependent vasodilatation *in vivo*. Futher, Ihlemann et al., (2003) also showed that the inactive stereoisomer of  $\text{BH}_4$  6S-  $\text{BH}_4$  was not able to was not able to protect against experimentally-induced endothelial dysfunction in the same way as  $\text{BH}_4$ , indicating that it is its ability to act as a co-factor for eNOS that is functionally important. Thus, the choice of  $\text{BH}_4$  for the present study as a measure of increasing NO availability was justified.

To further develop the potential of the microdialysis technique it would be desirable, although technically challenging to measure FBF and ISF insulin concentrations at the same time as performing microdialysis. This would enable direct measurement of endothelial function and correlation of the increase in FBF with the changes in ISF insulin concentration. The method development in Chapter 5 was however conducted in rats that were positioned so that the microdialysis probes were inserted into the hindlimb from the dorsal surface. In order to measure FBF the rat ideally needs to be in the supine position with the probe approaching from the ventral surface. Therefore, either the microdialysis probe or the transonic probe would be under the weight of the rat. This could probably be avoided by experimenting with different positions of the limbs and different approaches for the equipment.

Larger group sizes may also be useful due to the variability of the data within each group. To be powered at 0.8 based on the degree of change and variability in the current groups and to achieve significance for the trends observed group

sizes would need to increase to as many as 795 rats per group. For such experiments to be feasible, it seems that further changes to the protocol or conditions need to be made to avoid the use of such large numbers of animals. It may also be noted that in order to be powered at 0.8 based in the variability in the present groups and group size, the magnitude of change in ISF insulin concentration the BH<sub>4</sub> treated rats would need to increase from 581.2 – 649.5 pmol/L in the present experiments to 581.2 – 1106.2 pmol/L.

#### **6.4.5 Conclusion**

The results of the present study show for the first time basal concentrations of insulin in ISF in lean and obese Zucker rats. Basal concentrations of insulin in the lean Zucker were significantly lower than in obese Zucker rats.

Under basal conditions, plasma and ISF insulin concentrations were similar in lean Zucker rats. The ISF insulin concentrations increased substantially during the HE clamp in the lean Zucker rats but despite this, at the end of HE clamp, there was a clear gradient between ISF and plasma concentrations.

In contrast, under basal concentrations in the obese Zucker rats, a gradient was already present between plasma and ISF concentrations of insulin and this was accentuated at the end of HE clamp because ISF concentrations did not significantly increase in the obese Zucker rats during the HE clamp protocol.

BH<sub>4</sub> treatment for two weeks in the obese rats did not affect the cardiovascular variables, blood glucose concentrations, GIR or basal plasma insulin concentrations. Plasma insulin concentrations at the end of HE clamp were greater versus control obese rats but this may have reflected natural variability between obese Zucker rats purchased at different times rather than an effect of BH<sub>4</sub>. There were no significant changes in ISF insulin concentration with BH<sub>4</sub> treatment, but there was a tendency for an increase versus control obese rats at basal and during HE clamp conditions.

## CHAPTER 7 – GENERAL DISCUSSION

The overall aims of this thesis were to use the hyperinsulinaemic euglycaemic (HE) clamp in rats to follow the relationship between insulin-induced muscle vasodilatation and glucose uptake into skeletal muscle. Notably, to examine whether these effects are NO-dependent and whether they are linked to nutritional status. Further, experiments were conducted to investigate the influence of plasma free fatty acids on insulin-induced vasodilatation, glucose uptake and insulin sensitivity using nicotinic acid (NAc) to decrease plasma free fatty acid concentrations.

Since the factors that regulate trans-endothelial transport (TET) are unclear, methodology was developed to enable interstitial concentrations of insulin to be followed during HE clamp by using the technique of microdialysis.

Given that the obese Zucker rat provides a useful model of Type 2 diabetes, comparable experiments were then performed on obese and lean Zuckers to test whether chronic administration of tetrahydrobiopterin, a co-factor for NO synthesis, can improve muscle vasodilatation, transport of insulin into interstitium and glucose uptake.

The initial studies described in this thesis showed that HE clamp with supraphysiological concentrations of insulin did not affect MABP or HR, but caused vasodilatation in the hindlimb muscle of Wistar rats comprising an increase in FVC that was significantly different from baseline from 40 minutes

onwards and maximal at 60 minutes. The GIR required to maintain blood glucose levels at 4.8 mM was also significantly increased from baseline by the HE clamp from 15 minutes onwards and therefore occurred much before the increase in FVC. Administration of L-NAME to inhibit NO synthesis prior to HE clamp completely abolished the insulin-induced increase in FVC, but significantly increased GIR required to maintain blood glucose concentration at 4.8 mM.

The observation of increased GIR during HE clamp in response to L-NAME certainly warrants further investigation as it was unexpected based on evidence in the literature (see Section 2.4). It was suggested in Chapter 2 that the increase in GIR may have reflected an effect of adenosine on glucose transport secondary to an increase in muscle acidosis induced by the lower muscle blood flow after L-NAME. This could be tested by experiments inducing adenosine receptor blockade after L-NAME and by measurements of hydrogen ion efflux. However, it would also be important to establish whether HE clamp continues to increase GIR after L-NAME even when baseline blood flow is restored. This issue is important in another respect. For, although the complete removal of insulin-induced vasodilatation by L-NAME indicates that the response is NO dependent, this result should be interpreted with caution. Thus, NOS inhibition by L-NAME removes the tonic vasodilator effect of NO by decreasing the concentration of cGMP in the vascular smooth muscle as well as by inhibiting any new synthesis of NO. Therefore, not only was baseline MABP raised and baseline FBF decreased after L-NAME, but the concentrations of NO and cGMP that are normally present in the vascular smooth muscle and other cells are removed. Therefore, a clearer examination of the role of NO in insulin-induced vasodilatation could be



obtained if the same experiments were repeated in conjunction with an NO clamp. Concurrent infusion of a NO donor (such as SNP) would re-establish NO and cGMP baselines to normal physiological concentrations whilst inhibiting the production of new NO by eNOS. This would then test whether the insulin-induced increase in FVC is NO-mediated and would demonstrate whether inhibition of new NO-synthesis effects GIR even when tonic levels of NO, cGMP and baseline perfusion are restored.

In Chapter 3, the vasodilator actions of insulin were compared in animals of different nutritional status; HE clamps were conducted in fed and fasted Wistar rats with the animal's blood glucose levels clamped at their own level. Blood glucose concentrations and GIR were significantly higher in the fed rats than in the fasted rats. What is more, fed rats exhibited insulin-induced vasodilatation during HE clamp, that waned from 70 – 100 minutes whereas fasted rats showed no significant change in FVC with a small decrease beginning at ~70 minutes. It therefore seems that the muscle vasodilatation evoked in response to HE clamp may be linked to glucose metabolism, raising the possibility that a metabolic by-product of glucose metabolism may be involved in insulin-induced vasodilatation. This led to further consideration that adenosine may be a common link between the metabolic and vasodilator effects of insulin. It would therefore be interesting to conduct HE clamps in fed rats using an adenosine receptor antagonist such as 8-phenyltheophylline to investigate the role of adenosine in both glucose uptake and insulin-induced vasodilatation in response to HE clamp. If the results suggested a role for adenosine then this could be further explored by using selective A<sub>1</sub> and A<sub>2</sub> receptor antagonists.

It was suggested that the waning of the muscle vasodilatation in the fed rats and the late trend for vasoconstriction in the fasted rats reflected the vasoconstrictor influence of sympathetic nerve activity caused by insulin. It would be interesting to test this by repeating HE clamps after  $\alpha$  receptor antagonists or after denervation of the hindlimb.

Experiments in Chapter 4 were designed to investigate the effects of acute reduction in plasma FFA induced by NAc infusion on insulin-induced vasodilatation and glucose uptake in lean and obese Zucker rats. These experiments were performed using pentobarbital anaesthesia, whereas previous experiments had been performed using Alfaxan which is known to leave the autonomic control of the CVS intact. In these experiments, the lean rats were given lower dose of insulin than in the previous studies on Wistar rats (10 vs. 30 mU/kg/min) and obese rats were given 20 mU/kg/min reflecting the known insulin resistance of obese Zucker rats. During HE clamps on the lean Zucker rats, MABP was significantly decreased below baseline in association with the increase in FVC and the increase in FVC was monophasic; there was no waning during the later phase of the HE clamp. This disparity would be consistent with the proposal that the secondary waning is caused by insulin-induced increase in sympathetic nerve activity for Alfaxan is known to preserve autonomic function better than other anaesthetics. Nevertheless pentobarbital is known to be preferential in studies of glucose metabolism and therefore was deemed to be the more appropriate method of anaesthesia for subsequent experiments

described in this thesis as it allowed comparison with published papers that have mainly used pentobarbital for experiments involving HE clamp in rats.

In the experiments of Chapter 4, NAc treatment was not more effective than NAc treatment in combination with HE clamp and therefore the effects seen can be assumed to not be NEFA mediated.

However, in lean rats, NAc enhanced muscle vasodilator response to HE clamp in that larger change occurred earlier and in obese rats, NAc revealed a muscle vasodilator response to HE clamp: they showed no change in FVC in response to HE clamp alone. NAc infusion alone did not cause an increase in FVC in either lean or obese rats.

GIR required to maintain euglycaemia was much lower in obese, than lean rats and the initiation of the increase in GIR was also much slower in obese than lean rats. NAc infusion during HE clamp increased the development of the increase in GIR in lean rats and increased the 'rate of increase' in obese rats indicating positive effects on GIR in both. However, as expected NAc treatment, did not alter insulin sensitivity measured at the plateau of the HE clamp consistent with the short period of treatment with NAc.

The fact that the increases in GIR occurred earlier in the HE clamp than the increases in FVC in both lean and obese rats seen at the end of HE clamp, again points towards a role for adenosine or some other product of muscle metabolism in insulin-induced vasodilatation. It would therefore be interesting to repeat the

experiments of Chapter 4 using an adenosine receptor antagonist. The ability of NAc to increase cGMP concentrations in skeletal muscle and vascular smooth muscle provides another mechanism by which NAc may have affected the insulin-induced vasodilatation. Thus, repetition of the HE clamp experiments using an inhibitor of cGMP production such as methylene blue would allow investigation of this possibility. It may also be that the ability of NAc to accentuate the early phase of the increase in GIR in both lean and obese rats was related to an increase in cGMP in skeletal muscle fibres.

It would be interesting to undertake longer experiments with NAc particularly to establish whether reducing FFA in obese Zucker rats with chronic administration of NAc (or an analogue of NAc) cannot only facilitate insulin-induced vasodilatation but also improve insulin-sensitivity.

Using the results of experimental Chapters 2, 3 and 4 of this thesis the following diagram (Figure 7.1) is a schematic of the proposed influence of metabolic by-products of glucose (for instance adenosine) on the vasodilator actions of insulin at different levels of the vascular tree.

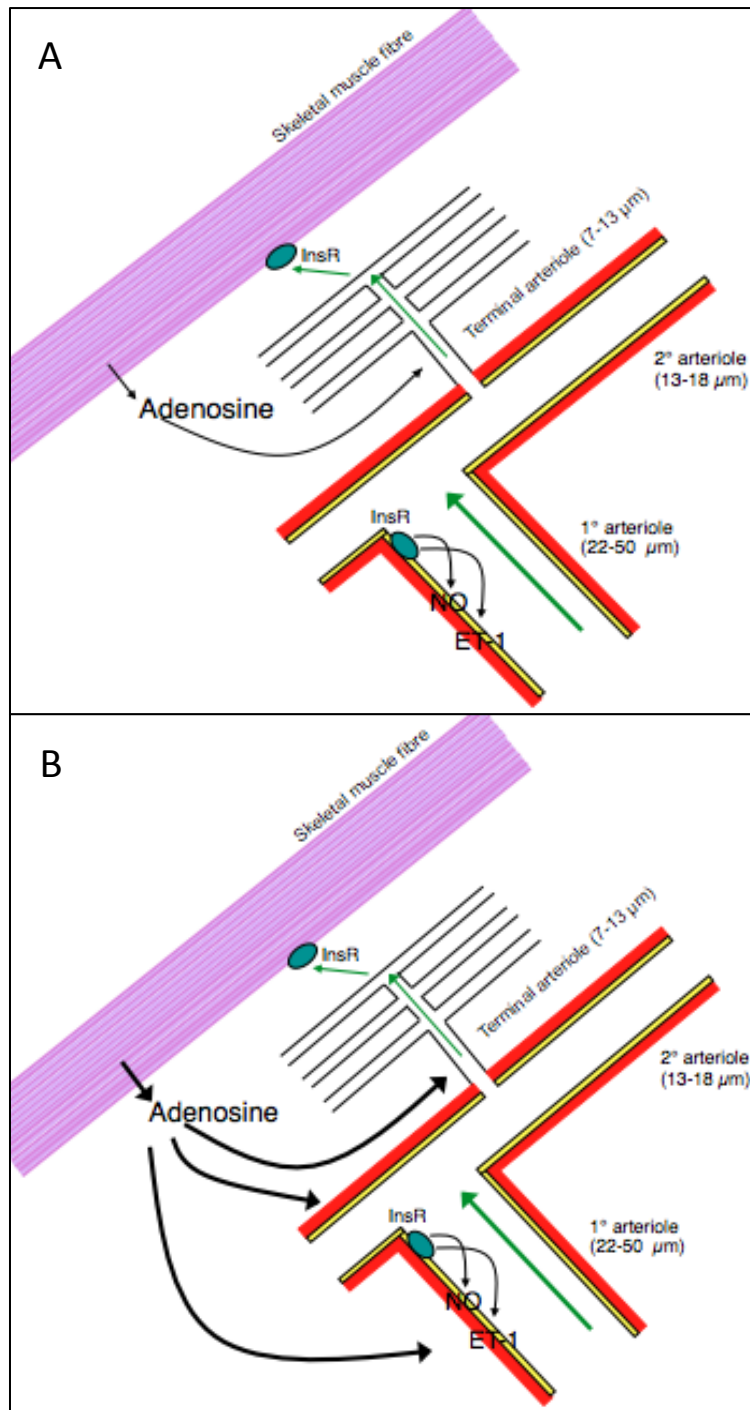


**Figure 7.1 Proposed influence of insulin at different levels of the vascular tree.** In addition to the production of nitric oxide (NO) and endothelin-1 (ET-1) via insulin receptors on the endothelium, stimulation of the insulin receptors on the skeletal muscle results in glucose metabolism and hence the production of metabolic by-products (for instance adenosine). Low insulin concentrations will produce low concentrations of metabolic by-products that are only able to diffuse back and cause terminal arterioles to dilate (A). High insulin concentrations will produce high concentrations of metabolic by-products that are able to dilate higher order vessels (B).

In the experiments of Chapter 5 all elements of the microdialysis technique were examined in order to optimise measurement of insulin. Thus, the following conditions were found to be optimal: 100 kDa probe with perfusion fluid of 1 % BSA and 1.5 mmol/L glucose, prepared in 0.9% sodium chloride and delivered at 1  $\mu$ l/min. Outlet tubing of 45 cm with collection into siliconised glass microvials just below the level of the animal. Inulin, as a calibrator, delivered as a 1 mg/kg bolus and 0.08 mg/kg/min infusion.

In the experiments of Chapter 6 it was confirmed that two weeks dosing of obese Zucker rats with BH<sub>4</sub> in the drinking water was enough to increase the concentration of BH<sub>4</sub> in the plasma and aorta.

Experiments were then performed on lean and obese Zucker control rats and obese Zucker rats that had been treated with BH<sub>4</sub> to measure insulin concentrations in ISF of muscle using the methods for microdialysis developed in the experiments of Chapter 5. Importantly these experiments showed for the first time that basal insulin concentrations in ISF in the lean rats were significantly lower than in obese rats. Insulin concentration in ISF and plasma were similar under basal conditions in lean rats, but when plasma insulin concentrations increased significantly during HE clamp a gradient developed between the ISF and plasma concentrations of insulin such that ISF insulin was significantly lower. In contrast, there was a gradient between ISF and plasma insulin concentrations in obese animals that was also present under basal conditions, the ISF being lower, that tended to increase when the plasma insulin

concentrations were raised significantly by HE clamp; ISF insulin concentrations were not significantly changed by the HE clamp. It is interesting to note that the concentration of insulin in ISF was similar at the end of HE clamp in the lean and obese animals.

It would be interesting in future studies to measure FBF and ISF at the same time in order to study the relationship between the increases in ISF insulin concentrations and blood flow in lean and obese rats. This would be a logical progression but would require some additional validation around the placement of probes when animals are in the supine position for the measurement of FBF.

Additionally, as the results from the first assessment of BH<sub>4</sub> concentrations (following, preparation of animals and then HE clamp) were inconclusive, an acute infusion of BH<sub>4</sub> once animals have been instrumented for recordings may be helpful to maintain BH<sub>4</sub> concentrations during the acute experiment, particularly if acute synthesis of NO via eNOS is required for insulin-induced vasodilatation.

In future experiments it would be important in rats treated with BH<sub>4</sub> to test whether or not endothelium-dependent vasodilatation is improved. This could be carried out by assessing the depressor response or preferably the muscle vasodilator response to acute acetylcholine (ACh) infusion following HE clamp. This would confirm whether or not BH<sub>4</sub> treatment had an effect on endothelial function. Alternatively, the blood vessels could be removed and response to ACh could be measured *ex vivo*.

For all experiments described in this thesis, it would be interesting to repeat them with a measure of microvascular recruitment during the initial phase of the HE clamp, such as CEU (Ross et al., 2008) or intravital microscopy. This would provide information on the time course of insulin-induced vasodilatation in microvessels as to whether it occurs prior to the observed increases in bulk muscle blood flow or ISF insulin concentrations and how it is affected by for example NOS inhibition, NAc or BH<sub>4</sub> treatment. What is more, dose response experiments with various doses of insulin under any given experimental conditions would also help to elucidate the relationship between stimulation of glucose uptake, microvascular recruitment and increases in bulk blood flow to both time and concentration, perhaps in line with the insulin exposure index proposed by (Yki-Jarvinen and Utriainen, 1998).



## References

- ABBINK-ZANDBERGEN, E. J., VERVOORT, G., TACK, C. J. J., LUTTERMAN, J. A., SCHAPER, N. C. & SMITS, P. 1999. The role of adenosine in insulin-induced vasodilation. *Journal of Cardiovascular Pharmacology*, 34, 374-380.
- ABRAMSON, D. I., SCHKLOVEN, N., MARGOLIS, M. N. & MIRSKY, I. A. 1939. Influence of massive doses of insulin on peripheral blood flow in man. *American Journal of Physiology*, 128, 0124-0132.
- AGRAWAL, N. K., MAITI, R., DASH, D. & PANDEY, B. L. 2007. Cilostazol reduces inflammatory burden and oxidative stress in hypertensive type 2 diabetes mellitus patients. *Pharmacological Research*, 56, 118-123.
- AHMED, K., TUNARU, S. & OFFERMANN, S. 2009. GPR109A, GPR109B and GPR81, a family of hydroxy-carboxylic acid receptors. *Trends in Pharmacological Sciences*, 30, 557-562.
- ALP, N. J., MUSSA, S., KHOO, J., CAI, S. J., GUZIK, T., JEFFERSON, A., GOH, N., ROCKETT, K. A. & CHANNON, K. M. 2003. Tetrahydrobiopterin-dependent preservation of nitric oxide-mediated endothelial function in diabetes by targeted transgenic GTP-cyclohydrolase I overexpression. *Journal of Clinical Investigation*, 112, 725-735.
- BAKKER, W., ERINGA, E. C., SIPKEMA, P. & VAN HINSBERGH, V. W. M. 2009. Endothelial dysfunction and diabetes: roles of hyperglycemia, impaired insulin signaling and obesity. *Cell and Tissue Research*, 335, 165-189.
- BALDI, S., NATALI, A., BUZZIGOLI, G., GALVAN, A. Q., SIRONI, A. M. & FERRANNINI, E. 1996. In vivo effect of insulin on intracellular calcium

- concentrations: Relation to insulin resistance. *Metabolism-Clinical and Experimental*, 45, 1402-1407.
- BAR, R. S., BOES, M. & SANDRA, A. 1988. VASCULAR TRANSPORT OF INSULIN TO RAT CARDIAC-MUSCLE - CENTRAL ROLE OF THE CAPILLARY ENDOTHELIUM. *Journal of Clinical Investigation*, 81, 1225-1233.
- BARON, A. D. 1993. CARDIOVASCULAR ACTIONS OF INSULIN IN HUMANS - IMPLICATIONS FOR INSULIN SENSITIVITY AND VASCULAR TONE. *Baillieres Clinical Endocrinology and Metabolism*, 7, 961-987.
- BARON, A. D. 1994. HEMODYNAMIC ACTIONS OF INSULIN. *American Journal of Physiology*, 267, E187-E202.
- BARON, A. D., TARSHOBY, M., HOOK, G., LAZARIDIS, E. N., CRONIN, J., JOHNSON, A. & STEINBERG, H. O. 2000. Interaction between insulin sensitivity and muscle perfusion on glucose uptake in human skeletal muscle - Evidence for capillary recruitment. *Diabetes*, 49, 768-774.
- BARON, A. D., ZHU, J. S., MARSHALL, S., IRSULA, O., BRECHTEL, G. & KEECH, C. 1995. INSULIN-RESISTANCE AFTER HYPERTENSION INDUCED BY THE NITRIC-OXIDE SYNTHESIS INHIBITOR L-NMMA IN RATS. *American Journal of Physiology-Endocrinology and Metabolism*, 269, E709-E715.
- BARRETT, E. J., WANG, H., UPCHURCH, C. T. & LIU, Z. 2011. Insulin regulates its own delivery to skeletal muscle by feed-forward actions on the vasculature. *American Journal of Physiology-Endocrinology and Metabolism*, 301, E252-E263.
- BENDALL, J. K., ALP, N. J., WARRICK, N., CAI, S., ADLAM, D., ROCKETT, K., YOKOYAMA, M., KAWASHIMA, S. & CHANNON, K. M. 2005. Stoichiometric Relationships Between Endothelial Tetrahydrobiopterin, Endothelial NO

- Synthase (eNOS) Activity, and eNOS Coupling in Vivo. *Circulation Research*, 97, 864-871.
- BEVAN, P. 2001. Insulin signalling. *Journal of Cell Science*, 114, 1429-1430.
- BODEN, G., CHEN, X. H., RUIZ, J., WHITE, J. V. & ROSSETTI, L. 1994. MECHANISMS OF FATTY ACID-INDUCED INHIBITION OF GLUCOSE-UPTAKE. *Journal of Clinical Investigation*, 93, 2438-2446.
- BODEN, G. & JADALI, F. 1991. EFFECTS OF LIPID ON BASAL CARBOHYDRATE-METABOLISM IN NORMAL MEN. *Diabetes*, 40, 686-692.
- BONADONNA, R. C., ZYCH, K., BONI, C., FERRANNINI, E. & DEFRONZO, R. A. 1989. TIME-DEPENDENCE OF THE INTERACTION BETWEEN LIPID AND GLUCOSE IN HUMANS. *American Journal of Physiology*, 257, E49-E56.
- BRADLEY, E. A., WILLSON, K. J., CHOI-LUNDBERG, D., CLARK, M. G. & RATTIGAN, S. 2010. Effects of central administration of insulin or l-NMMA on rat skeletal muscle microvascular perfusion. *Diabetes Obesity & Metabolism*, 12, 900-908.
- BRAY, G. A. 1977. ZUCKER-FATTY RAT - REVIEW. *Federation Proceedings*, 36, 148-153.
- BRODIN, E., LINDEFORS, N. & UNGERSTEDT, U. 1983. POTASSIUM EVOKED INVIVO RELEASE OF SUBSTANCE-P IN RAT CAUDATE-NUCLEUS MEASURED USING A NEW TECHNIQUE OF BRAIN DIALYSIS AND AN IMPROVED SUBSTANCE-P-RADIOIMMUNOASSAY. *Acta Physiologica Scandinavica*, 17-20.
- BROWN, G. C. 2001. Regulation of mitochondrial respiration by nitric oxide inhibition of cytochrome c oxidase. *Biochimica et Biophysica Acta (BBA) - Bioenergetics*, 1504, 46-57.

- BRYAN, P. T. & MARSHALL, J. M. 1999. Cellular mechanisms by which adenosine induces vasodilatation in rat skeletal muscle: significance for systemic hypoxia. *Journal of Physiology-London*, 514, 163-175.
- BUSSE, R., POHL, U. & LUCKHOFF, A. 1989. MECHANISMS CONTROLLING THE PRODUCTION OF ENDOTHELIAL AUTACOIDS. *Zeitschrift Fur Kardiologie*, 78, 64-69.
- CARDILLO, C., NAMBI, S. S., KILCOYNE, C. M., CHOUCAIR, W. K., KATZ, A., QUON, M. J. & PANZA, J. A. 1999. Insulin Stimulates Both Endothelin and Nitric Oxide Activity in the Human Forearm. *Circulation*, 100, 820-825.
- CASTILLO, C., BOGARDUS, C., BERGMAN, R., THUILLER, P. & LILLIOJA, S. 1994. INTERSTITIAL INSULIN CONCENTRATIONS DETERMINE GLUCOSE- UPTAKE RATES BUT NOT INSULIN-RESISTANCE IN LEAN AND OBESE MEN. *Journal of Clinical Investigation*, 93, 10-16.
- CHAURASIA, C. S., MUELLER, M., BASHAW, E. D., BENFELDT, E., BOLINDER, J., BULLOCK, R., BUNGAY, P. M., DELANGE, E. C. M., DERENDORF, H., ELMQUIST, W. F., HAMMARLUND-UDENAES, M., JOUKHADAR, C., KELLOGG, D. L., JR., LUNTE, C. E., NORDSTROM, C. H., ROLLEMA, H., SAWCHUK, R. J., CHEUNG, B. W. Y., SHAH, V. P., STAHL, L., UNGERSTEDT, U., WELTY, D. F. & YEO, H. 2007. AAPS-FDA workshop white paper: Microdialysis principles, application and regulatory perspectives. *Pharmaceutical Research*, 24, 1014-1025.
- CHERRINGTON, A. D., LACY, W. W. & CHIASSON, J. L. 1978. EFFECT OF GLUCAGON ON GLUCOSE PRODUCTION DURING INSULIN DEFICIENCY IN DOG. *Journal of Clinical Investigation*, 62, 664-677.

- CHIU, J. D., RICHEY, J. M., HARRISON, L. N., ZUNIGA, E., KOLKA, C. M., KIRKMAN, E., ELLMERER, M. & BERGMAN, R. N. 2008. Direct administration of insulin into skeletal muscle reveals that the transport of insulin across the capillary endothelium limits the time course of insulin to activate glucose disposal. *Diabetes*, 57, 828-835.
- CLARK, A. D. H., BARRETT, E. J., RATTIGAN, S., WALLIS, M. G. & CLARK, M. G. 2001. Insulin stimulates laser Doppler signal by rat muscle in vivo, consistent with nutritive flow recruitment. *Clinical Science*, 100, 283-290.
- CLARKE, K. J., ZHONG, Q., SCHWARTZ, D. D., COLEMAN, E. S., KEMPPAINEN, R. J. & JUDD, R. L. 2003. Regulation of adiponectin secretion by endothelin-1. *Biochemical and Biophysical Research Communications*, 312, 945-949.
- CLELAND, S. J., PETRIE, J. R., UEDA, S., ELLIOTT, H. L. & CONNELL, J. M. C. 1999. Insulin-mediated vasodilation and glucose uptake are functionally linked in humans. *Hypertension*, 33, 554-558.
- CLERK, L. H., RATTIGAN, S. & CLARK, M. G. 2002. Lipid Infusion Impairs Physiologic Insulin-Mediated Capillary Recruitment and Muscle Glucose Uptake In Vivo. *Diabetes*, 51, 1138-1145.
- COLLIER, J. J. & SCOTT, D. K. 2004. Sweet changes: Glucose homeostasis can be altered by manipulating genes controlling hepatic glucose metabolism. *Molecular Endocrinology*, 18, 1051-1063.
- DE JONGH, R. T., SERNE, E. H., IJZERMAN, R. G., DE VRIES, G. & STEHOUWER, C. D. A. 2004. Free fatty acid levels modulate microvascular function - Relevance for obesity-associated insulin resistance, hypertension, and microangiopathy. *Diabetes*, 53, 2873-2882.

- DEFRONZO, R. A., FERRANNINI, E., SATO, Y. & FELIG, P. 1981. SYNERGISTIC INTERACTION BETWEEN EXERCISE AND INSULIN ON PERIPHERAL GLUCOSE-UPTAKE. *Journal of Clinical Investigation*, 68, 1468-1474.
- DEFRONZO, R. A., TOBIN, J. D. & ANDRES, R. 1979. GLUCOSE CLAMP TECHNIQUE - METHOD FOR QUANTIFYING INSULIN-SECRETION AND RESISTANCE. *American Journal of Physiology*, 237, E214-E223.
- DEGUCHI, Y., TERASAKI, T., KAWASAKI, S. & TSUJI, A. 1991. MUSCLE MICRODIALYSIS AS A MODEL STUDY TO RELATE THE DRUG CONCENTRATION IN TISSUE INTERSTITIAL FLUID AND DIALYSATE. *Journal of Pharmacobio-Dynamics*, 14, 483-492.
- DEPARTMENT-FOR-HEALTH 2007.  
[http://www.dh.gov.uk/en/Healthcare/NationalServiceFrameworks/Diabetes/DH\\_074762](http://www.dh.gov.uk/en/Healthcare/NationalServiceFrameworks/Diabetes/DH_074762).
- DERNOVSEK, K. D. & BAR, R. S. 1985. PROCESSING OF CELL-BOUND INSULIN BY CAPILLARY AND MACROVASCULAR ENDOTHELIAL-CELLS IN CULTURE. *American Journal of Physiology*, 248, E244-E251.
- DERNOVSEK, K. D., BAR, R. S., GINSBERG, B. H. & LIOUBIN, M. N. 1984. RAPID-TRANSPORT OF BIOLOGICALLY INTACT INSULIN THROUGH CULTURED ENDOTHELIAL-CELLS. *Journal of Clinical Endocrinology & Metabolism*, 58, 761-763.
- DRESNER, A., LAURENT, D., MARCUCCI, M., GRIFFIN, M. E., DUFOUR, S., CLINE, G. W., SLEZAK, L. A., ANDERSEN, D. K., HUNDAL, R. S., ROTHMAN, D. L., PETERSEN, K. F. & SHULMAN, G. I. 1999. Effects of free fatty acids on glucose transport and IRS-1-associated phosphatidylinositol 3-kinase activity. *The Journal of Clinical Investigation*, 103, 253-259.

- DRUCKER, D. J. & NAUCK, M. A. 2006. The incretin system: glucagon-like peptide-1 receptor agonists and dipeptidyl peptidase-4 inhibitors in type 2 diabetes. *The Lancet*, 368, 1696-1705.
- ETGEN, G. J., FRYBURG, D. A. & GIBBS, E. M. 1997. Nitric oxide stimulates skeletal muscle glucose transport through a calcium/contraction- and phosphatidylinositol-3-kinase-independent pathway. *Diabetes*, 46, 1915-1919.
- FELDMAN, R. D., HRAMIAK, I. M., FINEGOOD, D. T. & BEHME, M. T. 1995. PARALLEL REGULATION OF THE LOCAL VASCULAR AND SYSTEMIC METABOLIC EFFECTS OF INSULIN. *Journal of Clinical Endocrinology & Metabolism*, 80, 1556-1559.
- FOSTER, L. J. & KLIP, A. 2000. Mechanism and regulation of GLUT-4 vesicle fusion in muscle and fat cells. *American Journal of Physiology - Cell Physiology*, 279, C877-C890.
- FREIDENBERG, G. R., SUTER, S., HENRY, R. R., NOLAN, J., REICHART, D. & OLEFSKY, J. M. 1994. DELAYED-ONSET OF INSULIN ACTIVATION OF THE INSULIN-RECEPTOR KINASE IN-VIVO IN HUMAN SKELETAL-MUSCLE. *Diabetes*, 43, 118-126.
- FRISBEE, J. C. & DELP, M. D. 2006. Vascular function in the metabolic syndrome and the effects on skeletal muscle perfusion: lessons from the obese Zucker rat. In: WAGENMAKERS, A. J. M. (ed.) *Essays in Biochemistry, Vol 42: The Biochemical Basis of the Health Effects of Exercise*.
- GANJI, S. H., QIN, S., ZHANG, L., KAMANNA, V. S. & KASHYAP, M. L. 2009. Niacin inhibits vascular oxidative stress, redox-sensitive genes, and monocyte adhesion to human aortic endothelial cells. *Atherosclerosis*, 202, 68-75.

- GILLE, A., BODOR, E. T., AHMED, K. & OFFERMANN, S. 2008. Nicotinic acid: Pharmacological effects and mechanisms of action. *Annual Review of Pharmacology and Toxicology*.
- GRIFFIN, M. E., MARCUCCI, M. J., CLINE, G. W., BELL, K., BARUCCI, N., LEE, D., GOODYEAR, L. J., KRAEGEN, E. W., WHITE, M. F. & SHULMAN, G. I. 1999. Free fatty acid-induced insulin resistance is associated with activation of protein kinase C  $\theta$  and alterations in the insulin signaling cascade. *Diabetes*, 48, 1270-1274.
- GRUNDY, S. M., VEGA, G. L., MCGOVERN, M. E., TULLOCH, B. R., KENDALL, D. M., FITZ-PATRICK, D., GANDA, O. P., ROSENSON, R. S., BUSE, J. B., ROBERTSON, D. D., SHEEHAN, J. P. & DIABETES MULTICENTER RES, G. 2002. Efficacy, safety, and tolerability of once-daily niacin for the treatment of dyslipidemia associated with type 2 diabetes - Results of the assessment of diabetes control and evaluation of the efficacy of niaspan trial. *Archives of Internal Medicine*, 162, 1568-1576.
- GUDBJORNSDOTTIR, S., SJOSTRAND, M., STRINDBERG, L. & LONNROTH, P. 2005. Decreased muscle capillary permeability surface area in type 2 diabetic subjects. *Journal of Clinical Endocrinology & Metabolism*, 90, 1078-1082.
- GUDBJORNSDOTTIR, S., SJOSTRAND, M., STRINDBERG, L., WAHREN, J. & LONNROTH, P. 2003. Direct measurements of the permeability surface area for insulin and glucose in human skeletal muscle. *Journal of Clinical Endocrinology & Metabolism*, 88, 4559-4564.
- HAMRIN, K., ROSDAHL, H., UNGERSTEDT, U. & HENRIKSSON, J. 2002. Microdialysis in human skeletal muscle: effects of adding a colloid to the perfusate. *Journal of Applied Physiology*, 92, 385-393.



- HAN, S. Z., OUCHI, Y., KARAKI, H. & ORIMO, H. 1995. INHIBITORY EFFECTS OF INSULIN ON CYTOSOLIC CA<sup>2+</sup> LEVEL AND CONTRACTION IN THE RAT AORTA - ENDOTHELIUM-DEPENDENT AND ENDOTHELIUM-INDEPENDENT MECHANISMS. *Circulation Research*, 77, 673-678.
- HANSON, J., GILLE, A., ZWYKIEL, S., LUKASOVA, M., CLAUSEN, B. E., AHMED, K., TUNARU, S., WIRTH, A. & OFFERMANN, S. 2010. Nicotinic acid- and monomethyl fumarate-induced flushing involves GPR109A expressed by keratinocytes and COX-2-dependent prostanoid formation in mice. *Journal of Clinical Investigation*, 120, 2910-2919.
- HEITZER, T., BROCKHOFF, C., MAYER, B., WARNHOLTZ, A., MOLLNAU, H., HENNE, S., MEINERTZ, T. & MÜNZEL, T. 2000a. Tetrahydrobiopterin Improves Endothelium-Dependent Vasodilation in Chronic Smokers. *Circulation Research*, 86, e36-e41.
- HEITZER, T., KROHN, K., ALBERS, S. & MEINERTZ, T. 2000b. Tetrahydrobiopterin improves endothelium-dependent vasodilation by increasing nitric oxide activity in patients with Type II diabetes mellitus. *Diabetologia*, 43, 1435-1438.
- HERKNER, H., KLEIN, N., JOUKHADAR, C., LACKNER, E., LANGENBERGER, H., FROSSARD, M., BIEGLMAYER, C., WAGNER, O., RODEN, M. & MULLER, M. 2003. Transcapillary insulin transfer in human skeletal muscle. *European Journal of Clinical Investigation*, 33, 141-146.
- HERMANS, M. P., LEVY, J. C., MORRIS, R. J. & TURNER, R. C. 1999. Comparison of tests of beta-cell function across a range of glucose tolerance from normal to diabetes. *Diabetes*, 48, 1779-1786.

- HOLMANG, A., MIMURA, K., BJORNTORP, P. & LONNROTH, P. 1997. Interstitial muscle insulin and glucose levels in normal and insulin-resistant Zucker rats. *Diabetes*, 46, 1799-1804.
- HOLMANG, A., MULLER, M., ANDERSSON, O. K. & LONNROTH, P. 1998. Minimal influence of blood flow on interstitial glucose and lactate-normal and insulin-resistant muscle. *American Journal of Physiology-Endocrinology and Metabolism*, 274, E446-E452.
- HOLMANG, A., NIKLASON, M., RIPPE, B. & LONNROTH, P. 2001. Insulin insensitivity and delayed transcapillary delivery of insulin in oophorectomized rats treated with testosterone. *Acta Physiologica Scandinavica*, 171, 427-438.
- HOLMANG, A., NILSSON, C., NIKLASSON, M., LARSSON, B. M. & LONROTH, P. 1999. Induction of insulin resistance by glucosamine reduces blood flow but not interstitial levels of either glucose or insulin. *Diabetes*, 48, 106-111.
- IHLEMANN, N., RASK-MADSEN, C., PERNER, A., DOMINGUEZ, H., HERMANN, T., K√ΠBER, L. & TORP-PEDERSEN, C. 2003. Tetrahydrobiopterin restores endothelial dysfunction induced by an oral glucose challenge in healthy subjects. *American Journal of Physiology - Heart and Circulatory Physiology*, 285, H875-H882.
- INTERNATIONAL-DIABETES-FEDERATION 2007. <http://www.eatlas.idf.org>.
- JACOBSON, I., SANDBERG, M. & HAMBERGER, A. 1985. Mass transfer in brain dialysis devices--a new method for the estimation of extracellular amino acids concentration. *Journal of neuroscience methods*, 15, 263-268.

- JANSSON, P. A. E., FOWELIN, J. P., VONSCHENCK, H. P., SMITH, U. P. & LONNROTH, P. N. 1993. MEASUREMENT BY MICRODIALYSIS OF THE INSULIN CONCENTRATION IN SUBCUTANEOUS INTERSTITIAL FLUID - IMPORTANCE OF THE ENDOTHELIAL BARRIER FOR INSULIN. *Diabetes*, 42, 1469-1473.
- JIANG, Z. Y., LIN, Y. W., CLEMONT, A., FEENER, E. P., HEIN, K. D., IGARASHI, M., YAMAUCHI, T., WHITE, M. F. & KING, G. L. 1999. Characterization of selective resistance to insulin signaling in the vasculature of obese Zucker (fa/fa) rats. *Journal of Clinical Investigation*, 104, 447-457.
- KANZAKI, M. 2006. Insulin receptor signals regulating GLUT4 translocation and act in dynamics. *Endocrine Journal*, 53, 267-293.
- KAPUR, S., BÉGIN, S., MARCOTTE, B., CÔTÉ, C. H. & MARETTE, A. 1997. Expression of Nitric Oxide Synthase in Skeletal Muscle: A Novel Role for Nitric Oxide as a Modulator of Insulin Action. *Diabetes*, 46, 1691-1700.
- KIM, F., TYSELING, K. A., RICE, J., PHAM, M., HAJI, L., GALLIS, B. M., BAAS, A. S., PARAMSOTHY, P., GIACHELLI, C. M., CORSON, M. A. & RAINES, E. W. 2005. Free fatty acid impairment of nitric oxide production in endothelial cells is mediated by IKK beta. *Arteriosclerosis Thrombosis and Vascular Biology*, 25, 989-994.
- KIM, J. A., MONTAGNANI, M., KOH, K. K. & QUON, M. J. 2006. Reciprocal relationships between insulin resistance and endothelial dysfunction - Molecular and pathophysiological mechanisms. *Circulation*, 113, 1888-1904.
- KING, G. L. & JOHNSON, S. M. 1985. RECEPTOR-MEDIATED TRANSPORT OF INSULIN ACROSS ENDOTHELIAL-CELLS. *Science*, 227, 1583-1586.

- KLEIN, R. 1995. HYPERGLYCEMIA AND MICROVASCULAR AND MACROVASCULAR DISEASE IN DIABETES. *Diabetes Care*, 18, 258-268.
- KOUBI, H., DUCHAMP, C., GLOVIN, A., FRUMINET, A. & MINAIRE, Y. 1991. Resistance of hepatic glycogen to depletion in obese Zucker rats. *Canadian Journal of Physiology and Pharmacology*, 69, 841-845.
- KRAEGEN, E. W., LAZARUS, L., MELER, H., CAMPBELL, L. & CHIA, Y. O. 1975. CARRIER SOLUTIONS FOR LOW-LEVEL INTRAVENOUS INSULIN INFUSION. *British Medical Journal*, 3, 464-466.
- KUVIN, J. T., RAMET, M. E., PATEL, A. R., PANDIAN, N. G., MENDELSON, M. E. & KARAS, R. H. 2002. A novel mechanism for the beneficial vascular effects of high-density lipoprotein cholesterol: Enhanced vasorelaxation and increased endothelial nitric oxide synthase expression. *American Heart Journal*, 144, 165-172.
- LAAKSO, M., EDELMAN, S. V., BRECHTEL, G. & BARON, A. D. 1990. DECREASED EFFECT OF INSULIN TO STIMULATE SKELETAL-MUSCLE BLOOD-FLOW IN OBESE MAN - A NOVEL MECHANISM FOR INSULIN RESISTANCE. *Journal of Clinical Investigation*, 85, 1844-1852.
- LEMBO, G., IACCARINO, G., RENDINA, V., VOLPE, M. & TRIMARCO, B. 1994. INSULIN BLUNTS SYMPATHETIC VASOCONSTRICTION THROUGH THE ALPHA(2)-ADRENERGIC PATHWAY IN HUMANS. *Hypertension*, 24, 429-438.
- LI, L., CHEN, W., REZVAN, A., JO, H. & HARRISON, D. G. 2011. Tetrahydrobiopterin Deficiency and Nitric Oxide Synthase Uncoupling Contribute to Atherosclerosis Induced by Disturbed Flow. *Arteriosclerosis Thrombosis and Vascular Biology*, 31, 1547-1554.

- LILLIOJA, S. & BOGARDUS, C. 1988. OBESITY AND INSULIN RESISTANCE - LESSONS LEARNED FROM THE PIMA-INDIANS. *Diabetes-Metabolism Reviews*, 4, 517-540.
- LINDSTROM, P. 2007. The physiology of obese-hyperglycemic mice ob/ob mice. *The scientific world journal*, 7, 666-685.
- LIU, Z., LIU, J., JAHN, L. A., FOWLER, D. E. & BARRETT, E. J. 2009. Infusing Lipid Raises Plasma Free Fatty Acids and Induces Insulin Resistance in Muscle Microvasculature. *Journal of Clinical Endocrinology & Metabolism*, 94, 3543-3549.
- LONNROTH, P., JANSSON, P. A. & SMITH, U. 1987. A MICRODIALYSIS METHOD ALLOWING CHARACTERIZATION OF INTERCELLULAR WATER SPACE IN HUMANS. *American Journal of Physiology*, 253, E228-E231.
- LONNROTH, P. & STRINDBERG, L. 1995. VALIDATION OF THE INTERNAL REFERENCE TECHNIQUE FOR CALIBRATING MICRODIALYSIS CATHETERS IN-SITU. *Acta Physiologica Scandinavica*, 153, 375-380.
- LUCKHOFF, A. & BUSSE, R. 1990. ACTIVATORS OF POTASSIUM CHANNELS ENHANCE CALCIUM INFLUX INTO ENDOTHELIAL-CELLS AS A CONSEQUENCE OF POTASSIUM CURRENTS. *Naunyn-Schmiedeberg's Archives of Pharmacology*, 342, 94-99.
- MACDONALD, I. A. & KING, P. 2007. Normal Glucose Metabolism and Responses to Hypoglycaemia. *Hypoglycaemia in Clinical Diabetes*. John Wiley & Sons, Ltd.
- MACIEJEWSKI-LENOIR, D., RICHMAN, J. G., HAKAK, Y., GAIDAROV, I., BEHAN, D. P. & CONNOLLY, D. T. 2006. Langerhans cells release prostaglandin D-2 in

- response to nicotinic acid. *Journal of Investigative Dermatology*, 126, 2637-2646.
- MANLEY, S. E., STRATTON, I. M., CLARK, P. M. & LUZIO, S. D. 2007. Comparison of 11 Human Insulin Assays: Implications for Clinical Investigation and Research. *Clinical Chemistry*, 53, 922-932.
- MARSHALL, J. M. 1987. Analysis of cardiovascular responses evoked following changes in peripheral chemoreceptor activity in the rat. *The Journal of Physiology*, 394, 393-414.
- MASON, R. P., JACOB, R. F., KUBANT, R., WALTER, M. F., BELLAMINE, A., JACOBY, A., MIZUNO, Y. & MALINSKI, T. 2011. Effect of Enhanced Glycemic Control with Saxagliptin on Endothelial Nitric Oxide Release and CD40 Levels in Obese Rats. *Journal of Atherosclerosis and Thrombosis*, 18, 774-783.
- MATHER, K. J., LTEIF, A., STEINBERG, H. O. & BARON, A. D. 2004. Interactions between endothelin and nitric oxide in the regulation of vascular tone in obesity and diabetes. *Diabetes*, 53, 2060-2066.
- MATHIAS, C. J., DACOSTA, D. F., FOSBRAEY, P., CHRISTENSEN, N. J. & BANNISTER, R. 1987. HYPOTENSIVE AND SEDATIVE EFFECTS OF INSULIN IN AUTONOMIC FAILURE. *British Medical Journal*, 295, 161-163.
- MCKAY, M. K. & HESTER, R. L. 1996. Role of nitric oxide, adenosine, and ATP-sensitive potassium channels in insulin-induced vasodilation. *Hypertension*, 28, 202-208.
- MEHARG, J. V., MCGOWANJORDAN, J., CHARLES, A., PARMELEE, J. T., CUTAIA, M. V. & ROUNDS, S. 1993. HYDROGEN-PEROXIDE STIMULATES SODIUM-POTASSIUM PUMP ACTIVITY IN CULTURED PULMONARY ARTERIAL ENDOTHELIAL-CELLS. *American Journal of Physiology*, 265, L613-L621.

- MILES, P. D. G., LEVISETTI, M., REICHART, D., KHOURSHEED, M., MOOSSA, A. R. & OLEFSKY, J. M. 1995. KINETICS OF INSULIN ACTION IN-VIVO - IDENTIFICATION OF RATE-LIMITING STEPS. *Diabetes*, 44, 947-953.
- MILSTIEN, S. & KATUSIC, Z. 1999. Oxidation of tetrahydrobiopterin by peroxynitrite: Implications for vascular endothelial function. *Biochemical and Biophysical Research Communications*, 263, 681-684.
- MORDES, J. P. & ROSSINI, A. A. 1981. Animal models of diabetes. *The American Journal of Medicine*, 70, 353-360.
- MORROW, J. D., AWAD, J. A., OATES, J. A. & ROBERTS, L. J. 1992. IDENTIFICATION OF SKIN AS A MAJOR SITE OF PROSTAGLANDIN-D2 RELEASE FOLLOWING ORAL-ADMINISTRATION OF NIACIN IN HUMANS. *Journal of Investigative Dermatology*, 98, 812-815.
- MUNIYAPPA, R., LEE, S., CHEN, H. & QUON, M. J. 2008. Current approaches for assessing insulin sensitivity and resistance in vivo: advantages, limitations, and appropriate usage. *American Journal of Physiology-Endocrinology and Metabolism*, 294, E15-E26.
- MURDOLO, G., SJÖSTRAND, M., STRINDBERG, L., GUDBJÖRNSDÓTTIR, S., LIND, L., LÖNNROT, P. & JANSSON, P.-A. 2008. Effects of Intrabrachial Metacholine Infusion on Muscle Capillary Recruitment and Forearm Glucose Uptake during Physiological Hyperinsulinemia in Obese, Insulin-Resistant Individuals. *Journal of Clinical Endocrinology & Metabolism*, 93, 2764-2773.
- NATALI, A., BONADONNA, R., SANTORO, D., GALVAN, A. Q., BALDI, S., FRASCERRA, S., PALOMBO, C., GHIONE, S. & FERRANNINI, E. 1994. INSULIN-RESISTANCE AND VASODILATION IN ESSENTIAL-

- HYPERTENSION - STUDIES WITH ADENOSINE. *Journal of Clinical Investigation*, 94, 1570-1576.
- NATALI, A., GALVAN, A. Q., SANTORO, D., PECORI, N., TADDEI, S., SALVETTI, A. & FERRANNINI, E. 1993. RELATIONSHIP BETWEEN INSULIN RELEASE, ANTINATRIURESIS AND HYPOKALEMIA AFTER GLUCOSE-INGESTION IN NORMAL AND HYPERTENSIVE MAN. *Clinical Science*, 85, 327-335.
- NEAHRING, J. M., STEPNIAKOWSKI, K., GREENE, A. S. & EGAN, B. M. 1993. INSULIN DOES NOT REDUCE FOREARM ALPHA-VASOREACTIVITY IN OBESE HYPERTENSIVE OR LEAN NORMOTENSIVE MEN. *Hypertension*, 22, 584-590.
- NELSON, M. T., PATLAK, J. B., WORLEY, J. F. & STANDEN, N. B. 1990. CALCIUM CHANNELS, POTASSIUM CHANNELS, AND VOLTAGE DEPENDENCE OF ARTERIAL SMOOTH-MUSCLE TONE. *American Journal of Physiology*, 259, C3-C18.
- NIKLASSON, M., HOLMANG, A. & LONNROTH, P. 1998. Induction of rat muscle insulin resistance by epinephrine is accompanied by increased interstitial glucose and lactate concentrations. *Diabetologia*, 41, 1467-1473.
- NISWENDER, K. D. & SCHWARTZ, M. W. 2003. Insulin and leptin revisited: adiposity signals with overlapping physiological and intracellular signaling capabilities. *Frontiers in Neuroendocrinology*, 24, 1-10.
- NUTTALL, F. Q., NGO, A. & GANNON, M. C. 2008. Regulation of hepatic glucose production and the role of gluconeogenesis in humans: is the rate of gluconeogenesis constant? *Diabetes-Metabolism Research and Reviews*, 24, 438-458.



- NYSTROM, T., NYGREN, A. & SJOHOLM, A. 2004. Tetrahydrobiopterin increases insulin sensitivity in patients with type 2 diabetes and coronary heart disease. *American Journal of Physiology-Endocrinology and Metabolism*, 287, E919-E925.
- OMATSUKANBE, M. & KITASATO, H. 1990. INSULIN STIMULATES THE TRANSLOCATION OF  $\text{Na}^+/\text{K}^+$ -DEPENDENT ATPASE MOLECULES FROM INTRACELLULAR STORES TO THE PLASMA-MEMBRANE IN FROG SKELETAL-MUSCLE. *Biochemical Journal*, 272, 727-733.
- PALMER, R. M. J., ASHTON, D. S. & MONCADA, S. 1988. VASCULAR ENDOTHELIAL-CELLS SYNTHESIZE NITRIC-OXIDE FROM L-ARGININE. *Nature*, 333, 664-666.
- PIEPER, G. M. 1997. Acute amelioration of diabetic endothelial dysfunction with a derivative of the nitric oxide synthase cofactor, tetrahydrobiopterin. *Journal of Cardiovascular Pharmacology*, 29, 8-15.
- PLAISANCE, E. P., LUKASOVA, M., OFFERMANN, S., ZHANG, Y., CAO, G. & JUDD, R. L. 2009. Niacin stimulates adiponectin secretion through the GPR109A receptor. *American Journal of Physiology-Endocrinology and Metabolism*, 296, E549-E558.
- PLEINER, J., SCHALLER, G., MITTERMAYER, F., BAYERLE-EDER, M., RODEN, M. & WOLZT, M. 2002. FFA-induced endothelial dysfunction can be corrected by vitamin C. *Journal of Clinical Endocrinology & Metabolism*, 87, 2913-2917.
- POULIN, R. A., STEIL, G. M., MOORE, D. M., ADER, M. & BERGMAN, R. N. 1994. DYNAMICS OF GLUCOSE-PRODUCTION AND UPTAKE ARE MORE

- CLOSELY-RELATED TO INSULIN IN HINDLIMB LYMPH THAN IN THORACIC-DUCT LYMPH. *Diabetes*, 43, 180-190.
- PRAGER, R., WALLACE, P. & OLEFSKY, J. M. 1986. INVIVO KINETICS OF INSULIN ACTION ON PERIPHERAL GLUCOSE DISPOSAL AND HEPATIC GLUCOSE OUTPUT IN NORMAL AND OBESE SUBJECTS. *Journal of Clinical Investigation*, 78, 472-481.
- QVIGSTAD, E., MOSTAD, I. L., BJERVE, K. S. & GRILL, V. E. 2003. Acute lowering of circulating fatty acids improves insulin secretion in a subset of type 2 diabetes subjects. *American Journal of Physiology-Endocrinology and Metabolism*, 284, E129-E137.
- RALEVIC, V. & BURNSTOCK, G. 1998. Receptors for Purines and Pyrimidines. *Pharmacological Reviews*, 50, 413-492.
- RANDLE, P. J. 1981. CITATION CLASSIC - THE GLUCOSE FATTY-ACID CYCLE - ITS ROLE IN INSULIN SENSITIVITY AND THE METABOLIC DISTURBANCES OF DIABETES-MELLITUS. *Current Contents/Life Sciences*, 24-24.
- RATTIGAN, S., BARRETT, E. & CLARK, M. 1997. Evidence of capillary recruitment by insulin but not epinephrine in rat skeletal muscle in vivo. *Diabetes*, 46, 332-332.
- RAY, C. J. & MARSHALL, J. M. 2009. Nitric oxide (NO) does not contribute to the generation or action of adenosine during exercise hyperaemia in rat hindlimb. *The Journal of Physiology*, 587, 1579-1591.
- REES, D. A. & ALCOLADO, J. C. 2005. Animal models of diabetes mellitus. *Diabetic Medicine*, 22, 359-370.
- RODEN, M., PERSEGHIN, G., PETERSEN, K. F., HWANG, J. H., CLINE, G. W., GEROW, K., ROTHMAN, D. L. & SHULMAN, G. I. 1996. The roles of insulin and

- glucagon in the regulation of hepatic glycogen synthesis and turnover in humans. *The Journal of Clinical Investigation*, 97, 642-648.
- ROSDAHL, H., HAMRIN, K., UNGERSTEDT, U. & HENRIKSSON, J. 2000. A microdialysis method for the in situ investigation of the action of large peptide molecules in human skeletal muscle: detection of local metabolic effects of insulin. *International Journal of Biological Macromolecules*, 28, 69-73.
- ROSS, R. A., DOWNEY, K., NEWMAN, J. M. B., RICHARDS, S. A., CLARK, M. G. & RATTIGAN, S. 2008. Contrast-enhanced ultrasound measurement of microvascular perfusion relevant to nutrient and hormone delivery in skeletal muscle: A model study in vitro. *Microvascular Research*, 75, 323-329.
- ROSS, R. M., KOLKA, C. M., RATTIGAN, S. & CLARK, M. G. 2007a. Acute blockade by endothelin-1 of haemodynamic insulin action in rats. *Diabetologia*, 50, 443-451.
- ROSS, R. M., WADLEY, G. D., CLARK, M. G., RATTIGAN, S. & MCCONELL, G. K. 2007b. Local Nitric Oxide Synthase Inhibition Reduces Skeletal Muscle Glucose Uptake but Not Capillary Blood Flow During In Situ Muscle Contraction in Rats. *Diabetes*, 56, 2885-2892.
- ROSSETTI, L. & GIACCARI, A. 1990. RELATIVE CONTRIBUTION OF GLYCOGEN-SYNTHESIS AND GLYCOLYSIS TO INSULIN-MEDIATED GLUCOSE-UP TAKE - A DOSE-RESPONSE EUGLYCEMIC CLAMP STUDY IN NORMAL AND DIABETIC RATS. *Journal of Clinical Investigation*, 85, 1785-1792.
- RUDERMAN, N. B. 1975. MUSCLE AMINO-ACID METABOLISM AND GLUCONEOGENESIS. *Annual Review of Medicine*, 26, 245-258.

- SARTORI, C., TRUEB, L., NICOD, P. & SCHERRER, U. 1999. Effects of sympathectomy and nitric oxide synthase inhibition on vascular actions of insulin in humans. *Hypertension*, 34, 586-589.
- SCHERRER, U., RANDIN, D., VOLLENWEIDER, P., VOLLENWEIDER, L. & NICOD, P. 1994. NITRIC-OXIDE RELEASE ACCOUNTS FOR INSULIN'S VASCULAR EFFECTS IN HUMANS. *Journal of Clinical Investigation*, 94, 2511-2515.
- SCHERRER, U., VOLLENWEIDER, P., RANDIN, D., JEQUIER, E., NICOD, P. & TAPPY, L. 1993. SUPPRESSION OF INSULIN-INDUCED SYMPATHETIC ACTIVATION AND VASODILATION BY DEXAMETHASONE IN HUMANS. *Circulation*, 88, 388-394.
- SCHNITZER, J. E., OH, P., PINNEY, E. & ALLARD, J. 1994. FILIPIN-SENSITIVE CAVEOLAE-MEDIATED TRANSPORT IN ENDOTHELIUM - REDUCED TRANSCYTOSIS, SCAVENGER ENDOCYTOSIS, AND CAPILLARY-PERMEABILITY OF SELECT MACROMOLECULES. *Journal of Cell Biology*, 127, 1217-1232.
- SHAFRIR, E. 1996. Development and consequences of insulin resistance: Lessons from animals with hyperinsulinaemia. *Diabetes & Metabolism*, 22, 122-131.
- SHARMA, K., MCCUE, P. & DUNN, S. R. 2003. Diabetic kidney disease in the db/db mouse. *American Journal of Physiology-Renal Physiology*, 284, F1138-F1144.
- SHERWIN, R. S., KRAMER, K. J., TOBIN, J. D., INSEL, P. A., LILJENQUIST, J. E., BERMAN, M. & ANDRES, R. 1974. MODEL OF KINETICS OF INSULIN IN MAN. *Journal of Clinical Investigation*, 53, 1481-1492.

- SHINOZAKI, K., NISHIO, Y., OKAMURA, T., YOSHIDA, Y., MAEGAWA, H., KOJIMA, H., MASADA, M., TODA, N., KIKKAWA, R. & KASHIWAGI, A. 2000. Oral Administration of Tetrahydrobiopterin Prevents Endothelial Dysfunction and Vascular Oxidative Stress in the Aortas of Insulin-Resistant Rats. *Circulation Research*, 87, 566-573.
- SIEMIONOW, M. & DEMIR, Y. 2004. Diabetic neuropathy: Pathogenesis and treatment. A review. *Journal of Reconstructive Microsurgery*, 20, 241-252.
- SJOSTRAND, M., HOLMANG, A. & LONNROTH, P. 1999. Measurement of interstitial insulin in human muscle. *American Journal of Physiology-Endocrinology and Metabolism*, 276, E151-E154.
- SJOSTRAND, M., HOLMANG, A., STRINDBERG, L. & LONNROTH, P. 2000. Estimations of muscle interstitial insulin, glucose, and lactate in type 2 diabetic subjects. *American Journal of Physiology-Endocrinology and Metabolism*, 279, E1097-E1103.
- SOGA, T., KAMOHARA, M., TAKASAKI, J., MATSUMOTO, S., SAITO, T., OHISHI, T., HIYAMA, H., MATSUO, A., MATSUSHIME, H. & FURUICHI, K. 2003. Molecular identification of nicotinic acid receptor. *Biochemical and Biophysical Research Communications*, 303, 364-369.
- SOWERS, J. R. 1996. Effects of insulin and IGF-I on vascular smooth muscle glucose and cation metabolism. *Diabetes*, 45, S47-S51.
- STEELE, R. 1959. INFLUENCES OF GLUCOSE LOADING AND OF INJECTED INSULIN ON HEPATIC GLUCOSE OUTPUT. *Annals of the New York Academy of Sciences*, 82, 420-430.

- STEHOUWER, C. D. A., HENRY, R. M. A. & FERREIRA, I. 2008. Arterial stiffness in diabetes and the metabolic syndrome: a pathway to cardiovascular disease. *Diabetologia*, 51, 527-539.
- STEINBERG, H. O., BRECHTEL, G., JOHNSON, A., FINEBERG, N. & BARON, A. D. 1994. INSULIN-MEDIATED SKELETAL-MUSCLE VASODILATION IS NITRIC-OXIDE DEPENDENT - A NOVEL ACTION OF INSULIN TO INCREASE NITRIC-OXIDE RELEASE. *Journal of Clinical Investigation*, 94, 1172-1179.
- STEINBERG, H. O., PARADISI, G., HOOK, G., CROWDER, K., CRONIN, J. & BARON, A. D. 2000. Free fatty acid elevation impairs insulin-mediated vasodilation and nitric oxide production. *Diabetes*, 49, 1231-1238.
- STEINBERG, H. O., TARSHOBY, M., MONESTEL, R., HOOK, G., CRONIN, J., JOHNSON, A., BAYAZEED, B. & BARON, A. D. 1997. Elevated circulating free fatty acid levels impair endothelium-dependent vasodilation. *Journal of Clinical Investigation*, 100, 1230-1239.
- STORGAARD, H., SONG, X. M., JENSEN, C. B., MADSBAD, S., BJØRNHOLM, M., VAAG, A. & ZIERATH, J. R. 2001. Insulin Signal Transduction in Skeletal Muscle From Glucose-Intolerant Relatives With Type 2 Diabetes. *Diabetes*, 50, 2770-2778.
- STUEHR, D. J., KWON, N. S. & NATHAN, C. F. 1990. FAD AND GSH PARTICIPATE IN MACROPHAGE SYNTHESIS OF NITRIC-OXIDE. *Biochemical and Biophysical Research Communications*, 168, 558-565.
- STUMVOLL, M., GOLDSTEIN, B. J. & VAN HAEFTEN, T. W. 2005. Type 2 diabetes: principles of pathogenesis and therapy. *Lancet*, 365, 1333-1346.

- STUMVOLL, M., MEYER, C., MITRAKOU, A., NADKARNI, V. & GERICH, J. E. 1997.  
Renal glucose production and utilization: New aspects in humans.  
*Diabetologia*, 40, 749-757.
- SZKUDELSKI, T. 2001. The mechanism of alloxan and streptozotocin action in B cells of the rat pancreas. *Physiological research / Academia Scientiarum Bohemoslovaca*, 50, 537-546.
- TACK, C. J. J., LUTTERMAN, J. A., VERVOORT, G., THIEN, T. & SMITS, P. 1996a.  
Activation of the sodium-potassium pump contributes to insulin-induced vasodilation in humans. *Hypertension*, 28, 426-432.
- TACK, C. J. J., SCHEFMAN, A. E. P., WILLEMS, J. L., THIEN, T., LUTTERMAN, J. A. & SMITS, P. 1996b. Direct vasodilator effects of physiological hyperinsulinaemia in human skeletal muscle. *European Journal of Clinical Investigation*, 26, 772-778.
- THOENES, M., OGUCHI, A., NAGAMIA, S., VACCARI, C. S., HAMMOUD, R., UMPIERREZ, G. E. & KHAN, B. V. 2007. The effects of extended-release niacin on carotid intimal media thickness, endothelial function and inflammatory markers in patients with the metabolic syndrome. *International Journal of Clinical Practice*, 61, 1942-1948.
- THONG, F. S. L., LALLY, J. S. V., DYCK, D. J., GREER, F., BONEN, A. & GRAHAM, T. E. 2007. Activation of the A1 adenosine receptor increases insulin-stimulated glucose transport in isolated rat soleus muscle. *Applied Physiology, Nutrition, and Metabolism*, 32, 701-710.
- TOUYZ, R. M., TOLLOCZKO, B. & SCHIFFRIN, E. L. 1994. INSULIN ATTENUATES AGONIST-EVOKED CALCIUM TRANSIENTS IN VASCULAR SMOOTH-MUSCLE CELLS. *Hypertension*, 23, 125-128.

- TRICKLER, W. & MILLER, D. W. 2003. Use of osmotic agents in microdialysis studies to improve the recovery of macromolecules. *Journal of Pharmaceutical Sciences*, 92, 1419-1427.
- TU, J., LE, G. & BALLARD, H. J. 2010a. Involvement of the cystic fibrosis transmembrane conductance regulator in the acidosis-induced efflux of ATP from rat skeletal muscle. *The Journal of Physiology*, 588, 4563-4578.
- TU, J., LE, G. Y. & BALLARD, H. J. 2010b. Involvement of the cystic fibrosis transmembrane conductance regulator in the acidosis-induced efflux of ATP from rat skeletal muscle. *Journal of Physiology-London*, 588, 4563-4578.
- UEDA, S., PETRIE, J. R., CLELAND, S. J., ELLIOTT, H. L. & CONNELL, J. M. C. 1998. The vasodilating effect of insulin is dependent on local glucose uptake: A double blind, placebo-controlled study. *Journal of Clinical Endocrinology & Metabolism*, 83, 2126-2131.
- UTRIAINEN, T., MALMSTROM, R., MAKIMATTILA, S. & YKIJARVINEN, H. 1995. METHODOLOGICAL ASPECTS, DOSE-RESPONSE CHARACTERISTICS AND CAUSES OF INTERINDIVIDUAL VARIATION IN INSULIN STIMULATION OF LIMB BLOOD-FLOW IN NORMAL SUBJECTS. *Diabetologia*, 38, 555-564.
- UTRIAINEN, T., NUUTILA, P., TAKALA, T., VICINI, P., RUOTSALAINEN, U., RONNEMAA, T., TOLVANEN, T., RAITAKARI, M., HAAPARANTA, M., KIRVELA, O., COBELLI, C. & YKIJARVINEN, H. 1997. Intact insulin stimulation of skeletal muscle blood flow, its heterogeneity and redistribution, but not of glucose uptake in non-insulin-dependent diabetes mellitus. *Journal of Clinical Investigation*, 100, 777-785.



- VAN SCHAFTINGEN, E. & GERIN, I. 2002. The glucose-6-phosphatase system. *Biochemical Journal*, 362, 513-532.
- VANHOUTTE, P. M. 2000. Say NO to ET. *Journal of the Autonomic Nervous System*, 81, 271-277.
- VASQUEZ-VIVAR, J., MARTASEK, P., WHITSETT, J., JOSEPH, J. & KALYANARAMAN, B. 2002. The ratio between tetrahydrobiopterin and oxidized tetrahydrobiopterin analogues controls superoxide release from endothelial nitric oxide synthase: an EPR spin trapping study. *Biochemical Journal*, 362, 733-739.
- VESELY, D. L. 1985. B-COMPLEX VITAMINS ACTIVATE RAT GUANYLATE-CYCLASE AND INCREASE CYCLIC-GMP LEVELS. *European Journal of Clinical Investigation*, 15, 258-262.
- VINCENT, M. A., BARRETT, E. J., LINDNER, J. R., CLARK, M. G. & RATTIGAN, S. 2003. Inhibiting NOS blocks microvascular recruitment and blunts muscle glucose uptake in response to insulin. *American Journal of Physiology-Endocrinology and Metabolism*, 285, E123-E129.
- VINCENT, M. A., CLERK, L. H., LINDNER, J. R., KLIBANOV, A. L., CLARK, M. G., RATTIGAN, S. & BARRETT, E. J. 2004. Microvascular recruitment is an early insulin effect that regulates skeletal muscle glucose uptake in vivo. *Diabetes*, 53, 1418-1423.
- VINCENT, M. A., DAWSON, D., CLARK, A. D. H., LINDNER, J. R., RATTIGAN, S., CLARK, M. G. & BARRETT, E. J. 2002. Skeletal muscle microvascular recruitment by physiological hyperinsulinemia precedes increases in total blood flow. *Diabetes*, 51, 42-48.

- VOLLENWEIDER, L., TAPPY, L., OWLYA, R., JEQUIER, E., NICOD, P. & SCHERRER, U. 1995. INSULIN-INDUCED SYMPATHETIC ACTIVATION AND VASODILATION IN SKELETAL-MUSCLE - EFFECTS OF INSULIN-RESISTANCE IN LEAN SUBJECTS. *Diabetes*, 44, 641-645.
- VOLLENWEIDER, P., TAPPY, L., RANDIN, D., SCHNEITER, P., JEQUIER, E., NICOD, P. & SCHERRER, U. 1993. DIFFERENTIAL-EFFECTS OF HYPERINSULINEMIA AND CARBOHYDRATE-METABOLISM ON SYMPATHETIC-NERVE ACTIVITY AND MUSCLE BLOOD-FLOW IN HUMANS. *Journal of Clinical Investigation*, 92, 147-154.
- VON MERING, J. & MINKOWSKI, O. 1890. Diabetes mellitus nach Pankreasextirpation. *Archiv für experimentelle Pathologie und Pharmakologie*, 26, 371-378.
- WAGENMAKERS, A. J. M., VAN RIEL, N. A. W., FRENNEAUX, M. P. & STEWART, P. M. 2006. Integration of the metabolic and cardiovascular effects of exercise. In: WAGENMAKERS, A. J. M. (ed.) *Essays in Biochemistry, Vol 42: The Biochemical Basis of the Health Effects of Exercise*.
- WALLIS, M. G., WHEATLEY, C. M., RATTIGAN, S., BARRETT, E. J., CLARK, A. D. H. & CLARK, M. G. 2002. Insulin-Mediated Hemodynamic Changes Are Impaired in Muscle of Zucker Obese Rats. *Diabetes*, 51, 3492-3498.
- WANG, H., LIU, Z. Q., LI, G. L. & BARRETT, E. J. 2006. The vascular endothelial cell mediates insulin transport into skeletal muscle. *American Journal of Physiology-Endocrinology and Metabolism*, 291, E323-E332.
- WARNHOLTZ, A., WILD, P., OSTAD, M. A., ELSNER, V., STIEBER, F., SCHINZEL, R., WALTER, U., PEETZ, D., LACKNER, K., BLANKENBERG, S. & MUNZEL, T. 2009. Effects of oral niacin on endothelial dysfunction in patients with

- coronary artery disease: Results of the randomized, double-blind, placebo-controlled INEF study. *Atherosclerosis*, 204, 216-221.
- WATSON, R. T., KANZAKI, M. & PESSIN, J. E. 2004. Regulated membrane trafficking of the insulin-responsive glucose transporter 4 in adipocytes. *Endocrine Reviews*, 25, 177-204.
- WATSON, R. T. & PESSIN, J. E. 2006. Bridging the GAP between insulin signaling and GLUT4 translocation. *Trends in Biochemical Sciences*, 31, 215-222.
- WAUGH, W. H. 1977. PHOTOMETRY OF INULIN AND POLYFRUCTOSAN BY USE OF A CYSTEINE-TRYPTOPHAN REACTION. *Clinical Chemistry*, 23, 639-645.
- WENTHOLT, I. M., VOLLEBREGT, M. A., HART, A. A., HOEKSTRA, J. B. & DEVRIES, J. H. 2005. Comparison of a Needle-Type and a Microdialysis Continuous Glucose Monitor in Type 1 Diabetic Patients. *Diabetes Care*, 28, 2871-2876.
- WESTERBACKA, J., WILKINSON, I., COCKCROFT, J., UTRIAINEN, T., VEHKAVAARA, S. & YKI-JARVINEN, H. 1999. Diminished wave reflection in the aorta - A novel physiological action of insulin on large blood vessels. *Hypertension*, 33, 1118-1122.
- WILD, S., ROGLIC, G., GREEN, A., SICREE, R. & KING, H. 2004. Global prevalence of diabetes - Estimates for the year 2000 and projections for 2030. *Diabetes Care*, 27, 1047-1053.
- WILSON, J. R., KAPOOR, S. C. & KRISHNA, G. G. 1994. Contribution of potassium to exercise-induced vasodilation in humans. *Journal of Applied Physiology*, 77, 2552-2557.

- WISE, A., FOORD, S. M., FRASER, N. J., BARNES, A. A., ELSHOUBAGY, N., EILERT, M., IGNAR, D. M., MURDOCK, P. R., STEPLEWSKI, K., GREEN, A., BROWN, A. J., DOWELL, S. J., SZEKERES, P. G., HASSALL, D. G., MARSHALL, F. H., WILSON, S. & PIKE, N. B. 2003. Molecular identification of high and low affinity receptors for nicotinic acid. *Journal of Biological Chemistry*, 278, 9869-9874.
- WIT, C. D., VON BISMARCK, P. & POHL, U. 1994. Synergistic action of vasodilators that increase cGMP and cAMP in the hamster cremaster microcirculation. *Cardiovascular Research*, 28, 1513-1518.
- WU, B. J., YAN, L., CHARLTON, F., WITTING, P., BARTER, P. J. & RYE, K.-A. 2010. Evidence That Niacin Inhibits Acute Vascular Inflammation and Improves Endothelial Dysfunction Independent of Changes in Plasma Lipids. *Arteriosclerosis Thrombosis and Vascular Biology*, 30, 968-U191.
- YANG, Y. J., HOPE, I. D., ADER, M. & BERGMAN, R. N. 1989. INSULIN TRANSPORT ACROSS CAPILLARIES IS RATE LIMITING FOR INSULIN ACTION IN DOGS. *Journal of Clinical Investigation*, 84, 1620-1628.
- YKI-JARVINEN, H. & UTRIAINEN, T. 1998. Insulin-induced vasodilatation: physiology or pharmacology? *Diabetologia*, 41, 369-379.
- YOUD, J. M., RATTIGAN, S. & CLARK, M. G. 2000. Acute impairment of insulin-mediated capillary recruitment and glucose uptake in rat skeletal muscle in vivo by TNF-alpha. *Diabetes*, 49, 1904-1909.
- YOUNG, M. E. & LEIGHTON, B. 1998. Evidence for altered sensitivity of the nitric oxide/cGMP signalling cascade in insulin-resistant skeletal muscle. *Biochemical Journal*, 329, 73-79.

ZACHO, H. D., KRISTENSEN, N. B., HENRIKSEN, J. H. & ABRAHAMSEN, J. 2012.

Validation of <sup>99m</sup>Techneium-labeled mebrofenin hepatic extraction method to quantify meal-induced splanchnic blood flow responses using a porcine model. *Journal of Applied Physiology*, 112, 877-882.

ZEMEL, M. B., JOHNSON, B. A. & AMBROZY, S. A. 1992. INSULIN-STIMULATED VASCULAR RELAXATION - ROLE OF CA(2+)-ATPASE. *American Journal of Hypertension*, 5, 637-641.

ZHANG, L., VINCENT, M. A., RICHARDS, S. M., CLERK, L. H., RATTIGAN, S., CLARK, M. G. & BARRETT, E. J. 2004. Insulin sensitivity of muscle capillary recruitment in vivo. *Diabetes*, 53, 447-453.